# The Combined Effects of Bisphenol A Exposure, Diet, and Physical Activity on the Aging Epigenome

by

Joseph John Kochmanski

A dissertation submitted in partial fulfillment
of the requirements for the degree of
Doctor of Philosophy
(Toxicology)
in the University of Michigan
2018

Doctoral Committee:

Professor Dana C. Dolinoy, Chair
Professor Craig Harris
Professor Karen E. Peterson
Associate Professor Maureen A. Sartor
Professor Peter X.K. Song

Joseph John Kochmanski
jjkoch@umich.edu
ORCID ID: 0000-0002-8472-3032

## Dedication

I dedicate this dissertation to my parents, who taught me to never stop asking questions.

## Acknowledgements

First of all, I would like to acknowledge my dissertation advisor, Dr. Dana Dolinoy, who provided encouragement, guidance, and incredible feedback throughout my doctoral program. It was a pleasure working with Dana for the last six years, and I am so grateful to have her as a mentor. I would also like to thank my dissertation committee of Drs. Craig Harris, Maureen Sartor, Karen Peterson, and Peter Song for their support during my candidacy. Without their guidance, I would still be fumbling around with simple T-tests in Excel.

I would like to acknowledge the Michigan Neonatal Biobank for providing precious neonatal bloodspots for our research purposes. I also thank Dr. Claudia Lalancette at the University of Michigan Epigenomics core for her incredible help generating our next-generation sequencing data and Dr. Raymond Cavalcante for helping me stumble my way through a host of bioinformatics analyses. I also had amazing administrative support from the Environmental Health Sciences staff, including Sue Crawford, Kelsey Hargesheimer, Cecilia Young, Beverly Slane, and Kierstin Fiscus.

I acknowledge all of the members of my PhD cohort and the Dolinoy Lab for their support, both moral and literal, over the years. Specifically, Dr. Jaclyn Goodrich for guiding me through my first two years of lab protocols; she remains a pillar of advice and encouragement. Dr. Chris Faulk for teaching me the importance of aging. Dr. Luke Montrose for excellent scientific conversations. Dr. Pinithi Perera for providing context on all things imprinting. Lisa Marchlewicz for her valuable advice and feedback. Tami Jones for sharing her encyclopedic laboratory knowledge. Matt Savidge for his help processing hundreds of blood samples. And also Ben Roberts, Sheena Martenies, Kate Thompson, and Kari Neier for their support as fellow PhD students and friends.

I also acknowledge the funding sources for my dissertation program – the Environmental Toxicology and Epidemiology Training Grant (ETEP), the Rackham Graduate Program Summer Award, and the University of Michigan School of Public Health Regents' Fellowship Award. Without funding, this dissertation would not have been possible.

I would also like to acknowledge Drs. David Karowe and Raymond Barbehenn for introducing me to scientific research, both in the field and the lab.

Finally, I would like to thank my family and friends for their support over the last four years. Particularly, my parents for their unwavering encouragement, my lovely wife Katie for her love and support, my brother Nick for always being there to talk, and my amazing group of friends in Ann Arbor, MI. Without them, this dissertation never would have happened.

# Table of Contents

# List of Tables

# List of Figures

## List of Abbreviations

5-mC = 5-methylcytosine
5-hmC = 5-hydroxymethylcytosine
AEE = Activity-related Energy Expenditure
ANOVA = Analysis of Variance
BER = Base Excision Repair
BPA = Bisphenol A
BMI = Body Mass Index
BS-seq = Bisulite Sequencing
CLAMS = Comprehensive Laboratory Animal Monitoring System
CpG = Cytosine-phospho-Guanine
DHMR = Differentially Hydroxymethylated Region
DMR/DMC = Differentially Methylated Region/CpG
DNA = Deoxyribonucleic Acid
DOHaD = Developmental Origins of Health and Disease
EDC = Endocrine Disrupting Chemical
ERRBS = Enhanced Reduced Representation Bisulfite Sequencing
FDR = False Discovery Rate
HEI = Healthy Eating Index
HF = Healthy Families
HMeDIP-seq = Hydroxymethylated DNA Immunoprecipitation Sequencing
IAP = Intracisternal A-Particle
ICR = Imprinting Control Region
LINE-1 = Long Interspersed Nuclear Element-1
LME = Linear Mixed Effects
MHFD = Mediterranean High-Fat Diet
MNORC = Michigan Nutrition Obesity Research Center
MVPA = Moderate-to-Vigorous Physical Activity
MZ = Monozygotic
OR = Odds Ratio
OS = Oxidative Stress
OxBS-seq = Oxidative Bisulfite Sequencing
PCR = Polymerase Chain Reaction
PND = Postnatal Day
RNA = Ribonucleic Acid
RMR = Resting Metabolic Rate
RT-qPCR = Reverse Transcriptase Quantitative Polymerase Chain Reaction
TEE = Total Energy Expenditure
WFL = Weight-for-length
WHFD = Western High-Fat Diet

## Abstract

Increasing evidence supports the developmental origins of health and disease (DOHaD) hypothesis, which posits that exposure to environmental factors (e.g. diet, chemicals, stress etc.) during sensitive periods of life (e.g. pre-conception, gestation, infancy, adolescence) alters disease susceptibility later in life by influencing developmental plasticity. As support for DOHaD accumulates, it has been proposed that developmental exposures alter later-life gene regulation and subsequent phenotype through changes in heritable epigenetic marks – e.g. DNA methylation. Both biological aging and environmental exposures are associated with changes in DNA methylation, and it has been shown that developmental exposures can alter the rate of epigenetic aging. Based on these existing data, we defined a new term – environmental deflection – that refers to an environment- or toxicant-mediated shift away from the baseline rate of epigenetic aging within an organism.

For this project, longitudinal animal model and human cohort studies were used to investigate whether developmental exposure to specific environmental factors – bisphenol A (BPA), Western high-fat diet (WHFD), and physical activity – would lead to environmental deflection of the aging epigenome. In the animal model study, matched blood and tail samples were collected from congenic *a/a* Agouti mice perinatally exposed to BPA (50 µg/kg diet) and/or WHFD. Linear mixed effects models were used to test for environmental deflection of epigenetic aging by dietary exposures. In the same mice, we used two next-generation sequencing methods – enhanced reduced representation bisulfite sequencing (ERRBS) and hydroxymethylated DNA

immunoprecipitation sequencing (HMeDIP-seq) – to determine the contributions of 5-methylcytosine (5-mC) and 5-hydroxymethylcytosine (5-hmC) to the aging epigenome. In the Healthy Families Project, a human cohort, we investigated the effects of physical activity and diet quality on age-related methylation in longitudinal blood samples. DNA methylation was measured at obesity-related genes in matched neonatal bloodspot and childhood blood samples (12-24 months old, 3-5 years old, 10-12 years old). In an effort to test the utility of neonatal blood DNA methylation as a biomarker of obesity risk during childhood, we also investigated whether childhood obesity likelihood was associated with neonatal and/or childhood DNA methylation at a number of obesity-related genes.

In both the mouse and human studies, we showed significant, gene-specific age-related DNA methylation. In mice, WHFD, but not BPA exposure, deflected age-related *Esr1* methylation rates away from Control baseline. In the mouse blood sequencing data, we showed a locus-specific contribution of 5-hmC to age-related DNA methylation patterns in mice, and also demonstrated significant effects of BPA exposure on DNA hydroxymethylation in the gene bodies of imprinted loci. In the human cohort, environmental deflection modeling was limited by sample size, but there was some indication of deflection by childhood BMI z-score and physical activity levels. Neonatal bloodspot LINE-1 DNA methylation was significantly associated with obesity likelihood in preschool children, and childhood *PPARA* was also negatively associated with body mass index z-score.

In this dissertation, we showed that both altered diet and physical activity have the potential to alter rates of epigenetic aging. Separately, we found that developmental BPA exposure stably alters DNA hydroxymethylation at murine imprinted genes, and that human neonatal bloodspot DNA methylation may be a useful biomarker for estimating childhood

obesity risk. These results emphasize the importance of longitudinal study design in toxicoepigenetics research, and suggest that environmental factors play a key role in the developmental origins of adult disease.

# Chapter 1

# Introduction

## 1.1 Rationale and Significance

### *Obesity as a disease burden*

Over the past several decades, U.S. adult and childhood obesity rates have steadily increased, reaching 39.8% and 18.5% in 2015-2016, respectively (Hales et al. 2017). As a phenotype, obesity is associated with a number of chronic diseases, including hypertension, various cancers, heart disease, and type 2 diabetes (Dixon 2010). As a result of these negative health impacts, obesity is also a significant economic burden; a recent literature review estimated that the annual medical cost of treating obesity in the U.S. is $149.4 billion in 2014 dollars (Kim and Basu 2016). Public health efforts to improve metabolic health in the U.S. have not been successful, leading to an investment in research examining the biological underpinnings of the obese phenotype. Recent research has shown that childhood obesity or a family history of obesity are the best predictors of adult obesity (Loos and Janssens 2017), indicating that genetics may play a central role in the etiology of obesity. However, a new literature review on this topic showed that BMI-associated genetic variants only explain 0.66-2.70% of BMI variation, suggesting that obesity risk is not reflected in the available genetic information (Loos and Janssens 2017). This inconsistency suggests that there is critical role of the environment – including gene-environment interactions – in shaping obesity risk.

### *Public health significance*

As the rates of both childhood and adult obesity continue to increase across the world, researchers have struggled to identify precise biological mechanisms that explain obesity's rapid rise. The primary goal of this research effort is to identify targets of therapeutic intervention that will either help reverse the rise in obesity or help mitigate the associated negative health impacts of obesity. Right now, therapeutic interventions are able to treat obesity's negative health outcomes, but have not successfully prevented the rising tide of obesity. As such, investigations into the causes of obesity, as well as associated negative health effects, remain necessary. Mounting scientific evidence supports the developmental origins of health and disease (DOHaD) hypothesis, which posits that early-life exposures to environmental factors are linked to the development of disease later in life (Bateson et al. 2004; Heindel et al. 2015). One of the main biological mechanisms thought to regulate this process is the epigenome, which can be defined as mitotically heritable, physical changes to the genome that are unrelated to the dinucleotide sequence. The goal of this dissertation is to determine whether gene-environment interactions, as reflected by exposure-mediated epigenetic changes, are related to the obesity phenotype. Since epigenetic changes are reversible, they represent potential therapeutic targets in treating obesity, and could represent a new avenue to mitigate this growing public health problem.

### *Developmental origins of health and disease*

In the early 1990s, British epidemiologist David Barker proposed a new hypothesis – that the intrauterine environment plays a causal role in the development of adult disease (Barker 1995; Barker et al. 1990). This idea, which went on to be known as the Barker hypothesis, focused on the link between fetal undernutrition and offspring cardiovascular disease risk, thereby introducing the idea of prenatal biological programming. In recent years, this

programming paradigm was expanded beyond fetal nutrition to include developmental chemical exposures, giving birth to the Developmental Origins of Health and Disease (DOHaD) hypothesis (Heindel et al. 2015). This hypothesis states that exposure to nutritional and environmental factors during prenatal and early postnatal periods alters susceptibility to chronic diseases, including obesity, by influencing developmental plasticity (Bateson et al. 2004; Heindel et al. 2015). Given its importance in chronic disease development, DOHaD has become a valuable conceptual framework for investigating the effects of environmental factors on disease outcomes.

## 1.2 Epigenetics

As support for DOHaD accumulates, it has been shown that developmental exposure to environmental factors can alter gene regulation and subsequent phenotype through changes in the epigenome (Waterland and Jirtle 2004; Waterland and Michels 2007). Epigenetics refers to the study of mitotically heritable and potentially reversible changes in gene expression unrelated to the DNA sequence. Epigenetic marks include chromatin remodeling modifications (e.g. histone tail trimethylation), non-coding RNA, and alterations to DNA itself (e.g. DNA methylation, DNA hydroxymethylation) (Bernal and Jirtle 2010; Egger et al. 2004). DNA methylation is a well-characterized epigenetic control mechanism, and is typically defined as the addition of a methyl group to the 5'-carbon of cytosine in a Cytosine-phospho-Guanine (CpG) dinucleotide – 5-methylcytosine (5-mC). In general, DNA methylation is associated with decreased transcription factor binding at promoter/enhancer sites, as well as decreased gene transcription (Medvedeva et al. 2014). Previous work has documented distinct waves of demethylation and de novo methylation that occur during fetal development (Reik et al. 2001; Smallwood and Kelsey

2012), as well as evidence that these waves of epigenetic reprogramming help regulate primordial germ cell proliferation and differentiation (Messerschmidt et al. 2014).

While epigenetic reprogramming events are typically tightly regulated, 5-mC levels have also been shown to change in response to environmental exposures during early development (Anderson et al. 2012; Bernal and Jirtle 2010; Manikkam et al. 2013), adolescence (Essex et al. 2013), and even adulthood (Tellez-Plaza et al. 2014; Wright et al. 2010). Specifically, animal studies have shown that offspring DNA methylation is associated with developmental exposure to a variety of environmental factors, including lead (Pb) (Dosunmu et al. 2012), altered diet (Marco et al. 2014; Vucetic et al. 2010), vinclozolin (Guerrero-Bosagna et al. 2012), arsenic (Reichard and Puga 2010), bisphenol A (BPA) (Kim et al. 2014), trichloroethylene (TCE) (Gilbert et al. 2012), ethanol (EtOH)((Kaminen-Ahola et al. 2010; Laufer et al. 2013; Marjonen et al. 2015), diesel exhaust (DE) (Tachibana et al. 2015), and stress (Dong et al. 2015). While this dissertation focuses mainly on DNA methylation, there is also evidence that environmental factors may influence other epigenetic modifications including posttranslational histone tail modifications (Arita et al. 2012), overall chromatin state (Schick et al. 2015; Veazey et al. 2015), and DNA hydroxymethylation (Tammen et al. 2014). As a result, direct measurements of epigenetic marks like chromatin structure and DNA methylation have become hallmark tools in investigating gene-environment interactions.

## 1.3 Age-Related Methylation and Epigenetic Drift: Two Types of Change over the Life Course

While environmental health sciences studies have focused on the association between toxicological factors and the epigenome in cross-sectional studies and *in utero* exposure models, a number of molecular epidemiology and genomics studies have evaluated DNA methylation

status as a function of age in humans and animal models. The aging epigenome was first described thirty years ago, when early investigations showed that levels of CpG methylation in human fibroblast cells and pooled mouse tissues were inversely related to lifespan (Fairweather et al. 1987; Wilson et al. 1987). More recently, a large number of studies have demonstrated age-dependent changes in DNA methylation, including twin studies (Fraga et al. 2005; Martino et al. 2013), human cohort studies (Alisch et al. 2012; Heyn et al. 2012; Madrigano et al. 2012; Urdinguio et al. 2016; Wang et al. 2012), and animal model studies (Maegawa et al. 2014; Spiers et al. 2016). Among the classically defined epigenetic marks, DNA methylation is most often investigated in epigenetic aging studies because of its stability and the availability of high throughput quantification methods. Studies investigating the aging epigenome show some consistent patterns, including locus-specific increases in DNA methylation with age (Teschendorff et al. 2013), global decreases in DNA methylation with age (Issa 2014; Teschendorff et al. 2013), and bidirectional changes in DNA methylation variability over time (Jones et al. 2015; Shah et al. 2014). To describe the epigenomic changes that occur in conjunction with chronological age, the literature has settled on two terms – age-related methylation and epigenetic drift (Issa 2014; Jung and Pfeifer 2015).

Age-related methylation is traditionally defined as predictable, direction-specific changes in DNA methylation levels that occur with normal aging (Jung and Pfeifer 2015). This concept is closely linked to the "epigenetic clock" proposed by Horvath et al. in 2013, which showed that biological age could be reliably predicted from DNA methylation levels at specific CpG sites across the genome (Horvath 2013). Results from the literature demonstrate that age-related methylation occurs both at specific gene regions (Jung and Pfeifer 2015) and on an epigenome-wide scale (Heyn et al. 2012). Additionally, a recent review of the aging epigenome noted that

the directionality of age-related methylation – hypomethylation or hypermethylation – varies by gene region (Jones et al. 2015). Considered together, these results suggest that age-related methylation is a complex process that can vary by genomic context. Further supporting this idea, age-related methylation has been shown to vary by tissue type. Day et al. looked at methylation array data from four different human tissue types – blood, kidney, brain, and skeletal muscle – and found both tissue-independent and tissue-dependent methylation changes associated with age (Day et al. 2013). These data indicate that age-related methylation is non-random, and may be biologically meaningful.

In contrast to age-related methylation, epigenetic drift refers to stochastic, bidirectional changes in epigenetic (e.g. DNA methylation) variability with age (Jones et al. 2015). These changes, which may alter methylome plasticity, are thought to be a result of methylation maintenance failure during cellular replication (Fraga et al. 2005; Teschendorff et al. 2013). Unlike age-related methylation, epigenetic drift is not a predictable process; instead, it can be conceptualized as the direct result of random inefficiencies in biological machinery that occur with age (Jones et al. 2015; Shah et al. 2014). As such, epigenetic drift is not expected to be consistent across individuals within a population, and cannot be used to predict age. Nevertheless, this concept is critical for describing the epigenetic discordance that arises in monozygotic twins as they age (Fraga et al. 2005), and can also help explain results from cross-sectional studies that show increased epigenetic variability with advanced age (Talens et al. 2012). Baseline levels of epigenetic drift are expected to occur regardless of specific environmental exposures, providing a background rate of increased variability that occurs in tandem with site-specific age-related methylation changes. Supporting this idea, a recent study found an interaction between epigenetic drift and age-related methylation at specific "epigenetic

clock" CpG sites, showing an increased effect of environmental or stochastic influences with increasing age (van Dongen et al. 2016). This suggests that the relative contribution of epigenetic drift to the aging epigenome (i.e. longitudinal DNA methylation) varies across the lifecourse.

### 1.4 Bisphenol A

Bisphenol A (BPA) is a commercial monomer used in the production of polycarbonate plastic and epoxy resins that is found in a variety of consumer products (e.g. metal can linings, receipt paper, etc.). As a result of its presence in common products, BPA has near ubiquitous human exposure across the world (Calafat et al. 2008). BPA is a known endocrine disruptor that can activate a variety of growth-related transcription factors, and has been shown to bind effectively to several nuclear receptors involved in cell maturation (Krüger et al. 2008; Singh and Li 2012; Sui et al. 2012). In addition, BPA exposure has been shown to affect methylation levels across the epigenome (Manikkam et al. 2013; Singh and Li 2012; Wolstenholme et al. 2011; Zhang et al. 2012), and *in utero* doses of BPA in mouse models have been shown to affect both global and gene promoter-specific methylation (Anderson et al. 2012; Singh and Li 2012; Susiarjo et al. 2013). Combined, these results indicate that BPA exposure could alter regulation of gene expression during development, thereby modifying risk for negative health outcomes. The effects of BPA exposure on epigenetic aging have not been previously studied, but based on BPA's documented ability to alter the epigenome, we hypothesized that prenatal BPA exposure would alter rates of age-related methylation.

### 1.5 Western High-Fat Diet

Western High-Fat Diet (WHFD) is characterized by high saturated and omega-6 polyunsaturated fatty acids, reduced omega-3 fatty acid intake, and increased salt and refined sugar intake (Myles 2014). The adoption of the modern Western diet has been implicated in the

rising levels of obesity, diabetes, and immunologic disorders seen in Western countries across the world (Hariharan et al. 2015; Myles 2014). Recent studies in mice indicate that Western diet is associated with short-term increases in oxidative stress and adiposity, and a gradual increase in body fat mass across generations (Heinonen et al. 2014; Massiera et al. 2010). Additional rodent studies indicate that high-fat-diet-induced obesity is associated with altered promoter DNA methylation at genes related to metabolism, including leptin (*Lep*) and peroxisome proliferator-activated receptor-α (*Ppara*) (Ge et al. 2014; Milagro et al. 2009). Genome-wide epigenome studies have also found obesity- and nutrient-sensitive CpG sites throughout the epigenome, suggesting that adiposity or an altered diet can affect specific gene regulation (Parle-McDermott and Ozaki 2011; Xu et al. 2013). Based on these results, it is clear that diet represents an important modifier of DNA methylation, and that it has the potential to affect the epigenome throughout the life course.

### 1.6 Physical Activity and DNA methylation

The physiological benefits of physical activity, which has been shown to alter gene expression levels (Huang et al. 2010; Lesniewski et al. 2013; Lindholm et al. 2014), are well-documented, but the precise mechanism controlling activity-induced changes in gene expression remains relatively elusive. Investigating this idea, several recent studies have shown that physical activity is associated with changes in the epigenome, including gene-specific DNA methylation (Barrès et al. 2012; Rönn et al. 2013). One such study demonstrated that acute physical exertion is associated with decreases in DNA methylation at promoters of skeletal muscle gene promoters (Barrès et al. 2012). A second recent study demonstrated that long-term endurance training, as opposed to short-term physical activity, is associated with significant changes in DNA methylation at enhancer regions across the genome (Lindholm et al. 2014), suggesting that long-

term physical activity may alter gene regulation via the epigenome. Supporting this idea, a third recent study showed that maternal exercise prevents high-fat-diet-induced hypermethylation at the promoter of peroxisome proliferator-activated receptor γ coactivator-1α (Pgc-1α), a master regulator of metabolism (Laker et al. 2014). While it remains unclear how much physical activity is needed to establish these epigenetic effects, it is clear that both acute and long-term physical activity can affect the methylome. As such, physical activity could also be an important modifier of the aging epigenome.

### 1.7 Environmental Deflection of the Aging Epigenome

Of particular interest to the field of toxicology, recent reports indicate that environmental exposure to exogenous environmental factors (e.g. lead (Pb), altered diet) can alter the rate of either age-related methylation (Faulk et al. 2014) or epigenetic drift (Gilbert et al. 2016). These results indicate that an interaction between age and exposure exists, and that investigations into the effects of environmental exposure on DNA methylation should not be limited to cross-sectional analyses. However, while these papers discuss a role of the environment in establishing rates of "epigenetic drift" and/or "age-related methylation," they do not provide a specific mechanism by which the environment could shape the aging epigenome.

In an effort to improve clarity and interpretation of epigenetic studies in both animal models and human cohorts, we introduced a new term for this mechanism – environmental deflection – that refers to an environment- or toxicant-mediated shift away from the baseline rate of age-related methylation or epigenetic drift within an organism (Kochmanski et al. 2017). By altering longitudinal patterns of epigenetic marks, environmental deflection may facilitate long-term changes in gene regulation via specific environmental exposures, showing the greatest effects during sensitive periods of growth and development. As such, environmental deflection

may underlie the apparent delay between developmental exposure and biological effects later in life. This type of long-lived, toxicant-sensitive epigenetic mechanism may also help to explain the growing prevalence of chronic diseases in human populations, demonstrating that longitudinal measures of the epigenome should be considered when designing future toxicoepigenetic and epigenetic epidemiological studies.

***Evidence for environmental deflection***

As a byproduct of their identical genetic background, monozygotic twin pairs are ideal for investigating the role the environment plays in shaping the aging epigenome while controlling for genetic effects. In 2005, a landmark paper by Fraga et al. demonstrated divergence of DNA methylation status with age in separate identical twin populations (Fraga et al. 2005). While this study was not longitudinal, the results suggest that environment and lifestyle, not simply genetics, could be driving age-associated changes in human methylation status. Supporting this idea, a more recent report demonstrated that newborn monozygotic (MZ) twins exhibit distinct patterns of inter-individual DNA methylation variation, indicating that the environment plays a role in determining the neonatal methylome (Ollikainen et al. 2010). Building off these data, another paper found locus-specific increases in within-twin pair methylation discordance across the adult life course (18-49 years old), a pattern that was attributable to the individual's unique environment at most investigated loci (Talens et al. 2012). Extending twin studies to an epigenome-wide scale, several newer studies have shown region-specific hypermethylation with age in adult MZ twins (Bell et al. 2012), high levels of within-pair DNA methylation variability in adolescent twins (Lévesque et al. 2014), and significant interaction between environmental effects and age at 32,234 CpG sites across the epigenome (van Dongen et al. 2016). Combined, the epigenome-wide twin studies support the idea that the

environment plays an integral role in shaping the epigenome throughout human aging. However, by their very nature, twin studies are not able to tease apart the separate effects of environmental factors on epigenetic drift and age-related methylation, and do not examine interactions between specific exposures and the aging epigenome.

Supplementing the available twin studies, a handful of recent non-twin human cohort studies have examined environmental deflection of epigenetic drift or age-related methylation by toxicants and other lifestyle factors. Building off the smaller scale methylation array and global methylation results noted previously, a recent publication using the Illumina 450K BeadChip showed that smoking-associated CpG probes exhibit diminished epigenetic drift, suggesting an environmental deflection of the drift rate by smoking status (Shah et al. 2014). Additionally, another recent publication showed that increased body mass index (BMI) is associated with accelerated age-related methylation at 353 CpG sites in human liver samples, suggesting that nutritionally-induced oxidative stress and metabolic alterations may deflect the rate of age-related methylation (Horvath et al. 2014). These results indicate that environmental deflection of both epigenetic drift and age-related methylation may occur on an epigenome-wide scale in human populations.

A small number of recent animal model studies have investigated the effects of environmental exposures on epigenetic aging. One such study found that perinatal lead (Pb) exposure alters the rate of age-related methylation in the promoter of a murine imprinted gene, *Igf2r*, as well as a metastable epiallele, *CabpIAP* (Faulk et al. 2014). Similarly, examining epigenetic drift, a second study in mice found a trichloroethylene-dependent increase in naïve CD4+ T cell methylation variance at several gene regions, indicating that epigenetic drift can be shifted away from baseline by a chemical exposure (Gilbert et al. 2016). Together, these prior

animal studies provide direct, exposure-specific evidence for environmental deflection of both age-related methylation and epigenetic drift.

***Conceptual model for environmental deflection***

In an effort to establish a clear conceptual framework for environmental deflection, we have utilized a visual bow and arrow metaphor that takes into account exposure timing and age-related methylation (**Figure 1-1**). Time zero in our model represents the period of initial developmental epigenetic programming, the flight of the arrow represents the rate of age-related methylation, and deviations in the flight path represent environmental deflection. Figure 1-1A demonstrates how epigenetic status at a specific locus or global marker can change with age or be deflected by an environmental exposure away from age-related hyper- or hypomethylation. Respectively, these endpoints can be conceptualized as the arrow striking its target and the arrow missing the target by a significant amount. Meanwhile, Figure 1-1B shows environmental deflection of epigenetic drift for a population, with the yellow shaded area representing the normal range of DNA methylation variability for the population. If a subset of the population (dotted circle) is exposed to specific toxicant exposures (vertical dotted arrows) during specific developmental time periods (vertical dotted arrows), the trajectory over time at labile genes could be deflected outside the normal range of variation, depicted by the dotted lines. When firing a real-life arrow, the greatest opportunity to affect the arrow's flight occurs at release. Assuming environmental deflection works in a similar way – as suggested by developmental plasticity theory (Wells 2014) – the greatest opportunity to affect the normal trajectory of age-related methylation and/or epigenetic drift (i.e. the arrow's flight) is early in life (i.e. the release point). However, much like wind or another outside force can alter the path of an arrow after release, environmental deflection can also occur at other points throughout an organism's life

course (**Figure 1-1B**). To test this conceptual model in real populations, longitudinal studies with adequate early life exposure data and repeated epigenetic assessments are recommended to identify epigenetic loci with deflected methylation measurements.

## 1.8 DNA Hydroxymethylation

While much of the available DNA methylation research has focused on 5-mC, recent studies have begun to investigate an oxidized form of the molecule, 5-hydroxymethylcytosine (5-hmC). Previous work in mice and humans have demonstrated low, tissue-specific 5-hmC content that is highest in the brain, but also present in the liver, testes, placenta, colon, and blood, albeit in progressively lower levels (Nestor et al. 2012). While many studies have focused on the role of 5-hmC in DNA demethylation pathways (Ito et al. 2011; Shen and Zhang 2013), other genome-wide studies in humans and mice have shown that 5-hmC is enriched in gene bodies and enhancer regions, suggesting a role in transcriptional control (Johnson et al. 2016; Stroud et al. 2011; Wu et al. 2011). Supporting this idea, additional work has shown that 5-hmC is recognized by a unique binding protein (Mbd3) (Yildirim et al. 2011), that 5-hmC may be maintained across DNA replication via a complex of the DNMT1, Tet, and UHRF1 proteins (Shen and Zhang 2013), and that 5-hmC is enriched at imprinted loci in human tissues (Hernandez Mora et al. 2017). Based on the growing evidence that 5-hmC is a stable epigenetic mark with a unique function, a recent review of the literature concluded that 5-hmC is likely to play an important role in aging and age-related diseases (López et al. 2017). However, due to a lack of studies investigating the role of 5-hmC during normal aging, evidence to support this hypothesis remains scarce. In this dissertation, we tested whether 5-hmC contributes to the aging epigenome through direct, longitudinal measurements of epigenome-wide 5-hmC levels in murine blood samples.

## 1.9 Project Overview

This project uses several environmental factors – chemical, diet, and physical activity – as tools to study the underlying mechanisms of epigenetic aging. The overarching hypotheses for this dissertation are as follows: **1. Developmental exposure to bisphenol A (BPA) will result in altered epigenetic aging, as measured by longitudinal DNA methylation and hydroxymethylation levels in multiple tissues; 2. The rate of epigenetic aging will be mitigated by beneficial environmental cues like exercise and exacerbated by the Western high-fat diet.** To test these central hypotheses, Aim 1 of this project combines an animal model exposure study with target gene pyrosequencing to investigate the effects of developmental BPA exposure, WHFD, and physical activity on age-related methylation. Aim 2 uses next-generation sequencing techniques to examine the effects of BPA exposure on longitudinal epigenome-wide 5-mC and 5-hmC levels from the same developmentally exposed mice. Finally, Aim 3 uses neonatal bloodspots and childhood blood samples to investigate age-related methylation in a childhood obesity cohort. By combining mouse and human data, this dissertation aims to shed light on the contribution of life-course epigenetics to development of the obese phenotype (**Figure 1-2**).

## 1.10 Figures and Tables

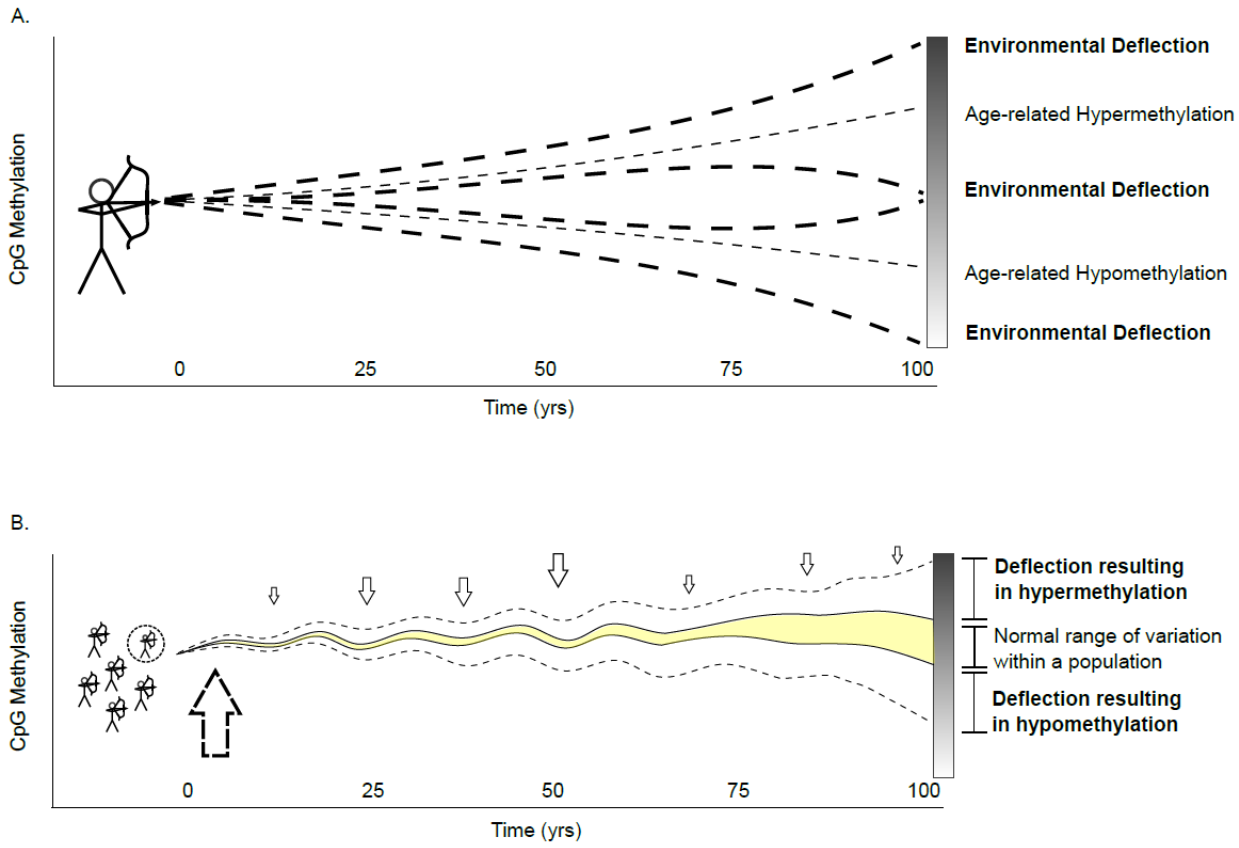


**Figure 1-1: Conceptual framework for environmental deflection of the aging epigenome.** A) Environmental deflection of age-related methylation for an individual; deflection is represented by the altered flight of an arrow fired at a target. The gradient bar on the right shows how epigenetic status at a specific locus or global marker can change with age or be deflected by an environmental exposure away from age-related hyper- or hypomethylation. Respectively, these endpoints can be conceptualized as the arrow striking its target and the arrow missing the target by a significant amount. B) Environmental deflection of epigenetic drift for a population; the vertical arrows represent specific exposures that may affect drift trajectory throughout life. The yellow shaded area is the normal range of DNA methylation variability at a given time point for the population. If a subset of the population (dotted circle) is exposed to a toxicant during the early developmental time period (large vertical dotted arrow), the epigenetic drift trajectory at labile genes could be deflected outside the normal range of variation, depicted by the dotted line.

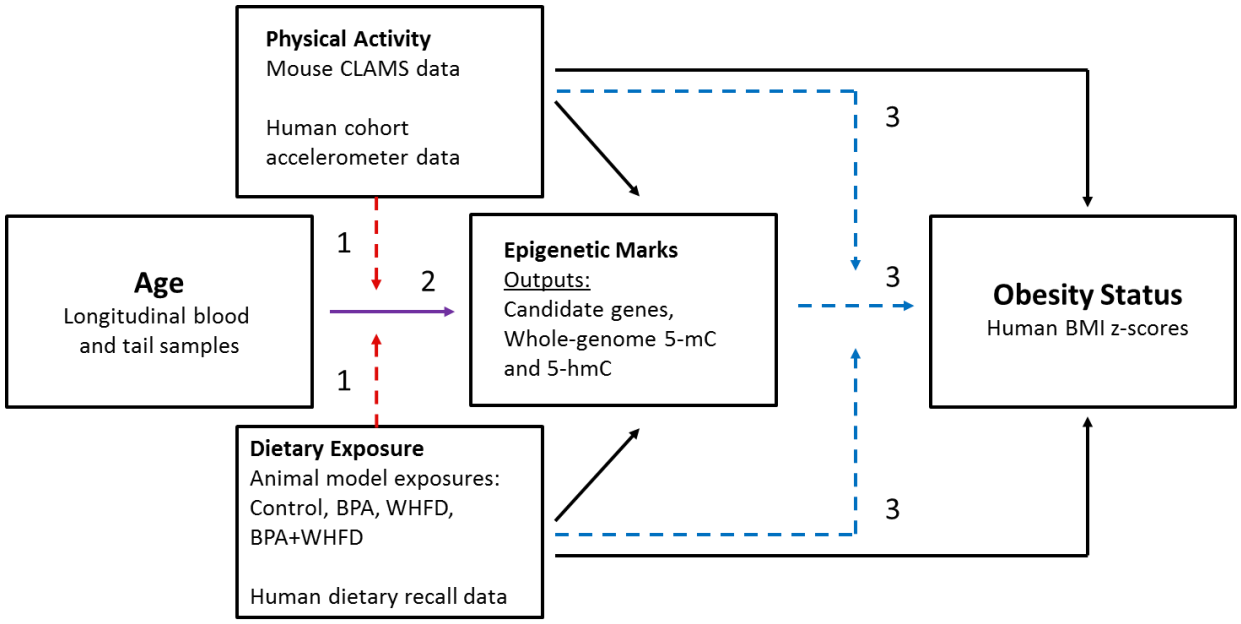


**Figure 1-2: A conceptual model summarizing the dissertation hypotheses.** Questions from the three aims work together to examine the effects of environmental factors on epigenetic aging and obesity. The hypotheses of each aim are indicated by colors (Aim 1 = red, Aim 2 = purple, Aim 3 = blue) and numbers. Variables that were considered in statistical modeling are indicated within the boxes.

## 1.11 References


Alisch RS, Barwick BG, Chopra P, Myrick LK, Satten GA, Conneely KN, et al. 2012. Age-associated DNA methylation in pediatric populations. Genome Res 22:623–632; doi:10.1101/gr.125187.111.

Anderson OS, Nahar MS, Faulk C, Jones TR, Liao C, Kannan K, et al. 2012. Epigenetic responses following maternal dietary exposure to physiologically relevant levels of bisphenol A. Environ. Mol. Mutagen. 53:334–342; doi:10.1002/em.21692.

Arita A, Shamy MY, Chervona Y, Clancy HA, Sun H, Hall MN, et al. 2012. The effect of exposure to carcinogenic metals on histone tail modifications and gene expression in human subjects. J Trace Elem Med Biol 26:174–178; doi:10.1016/j.jtemb.2012.03.012.

Barker DJ. 1995. The fetal and infant origins of disease. Eur. J. Clin. Invest. 25: 457–63.

Barker DJ, Bull AR, Osmond C, Simmonds SJ. 1990. Fetal and placental size and risk of hypertension in adult life. BMJ 301: 259–62.

Barrès R, Yan J, Egan B, Treebak JT, Rasmussen M, Fritz T, et al. 2012. Acute exercise remodels promoter methylation in human skeletal muscle. Cell Metab 15:405–411; doi:10.1016/j.cmet.2012.01.001.

Bateson P, Barker D, Clutton-Brock T, Deb D, D'Udine B, Foley RA, et al. 2004. Developmental plasticity and human health. Nature 430:419–421; doi:10.1038/nature02725.

Bell JT, Tsai PC, Yang TP, Pidsley R, Nisbet J, Glass D, et al. 2012. Epigenome-wide scans identify differentially methylated regions for age and age-related phenotypes in a healthy ageing population. PLoS Genet 8:e1002629; doi:10.1371/journal.pgen.1002629.

Bernal AJ, Jirtle RL. 2010. Epigenomic disruption: the effects of early developmental exposures. Birth Defects Res A Clin Mol Teratol 88:938–944; doi:10.1002/bdra.20685.

Calafat AM, Ye X, Wong LY, Reidy JA, Needham LL. 2008. Exposure of the U.S. population to bisphenol A and 4-tertiary-octylphenol: 2003-2004. Env. Heal. Perspect 116:39–44; doi:10.1289/ehp.10753.

Day K, Waite LL, Thalacker-Mercer A, West A, Bamman MM, Brooks JD, et al. 2013. Differential DNA methylation with age displays both common and dynamic features across human tissues that are influenced by CpG landscape. Genome Biol 14:R102; doi:10.1186/gb-2013-14-9-r102.

Dixon JB. 2010. The effect of obesity on health outcomes. Mol. Cell. Endocrinol. 316:104–108; doi:10.1016/j.mce.2009.07.008.

Dong E, Dzitoyeva SG, Matrisciano F, Tueting P, Grayson DR, Guidotti A. 2015. Brain-derived

neurotrophic factor epigenetic modifications associated with schizophrenia-like phenotype induced by prenatal stress in mice. Biol Psychiatry 77:589–596; doi:10.1016/j.biopsych.2014.08.012.

Dosunmu R, Alashwal H, Zawia NH. 2012. Genome-wide expression and methylation profiling in the aged rodent brain due to early-life Pb exposure and its relevance to aging. Mech Ageing Dev 133:435–443; doi:10.1016/j.mad.2012.05.003.

Egger G, Liang G, Aparicio A, Jones PA. 2004. Epigenetics in human disease and prospects for epigenetic therapy. Nature 429:457–463; doi:10.1038/nature02625.

Essex MJ, Boyce WT, Hertzman C, Lam LL, Armstrong JM, Neumann SM, et al. 2013. Epigenetic vestiges of early developmental adversity: childhood stress exposure and DNA methylation in adolescence. Child Dev 84:58–75; doi:10.1111/j.1467-8624.2011.01641.x.

Fairweather DS, Fox M, Margison GP. 1987. The in vitro lifespan of MRC-5 cells is shortened by 5-azacytidine-induced demethylation. Exp Cell Res 168: 153–159.

Faulk C, Liu K, Barks A, Goodrich JM, Dolinoy DC. 2014. Longitudinal epigenetic drift in mice perinatally exposed to lead. Epigenetics 9:934–941; doi:10.4161/epi.29024.

Fraga MF, Ballestar E, Paz MF, Ropero S, Setien F, Ballestar ML, et al. 2005. Epigenetic differences arise during the lifetime of monozygotic twins. Proc Natl Acad Sci U S A 102:10604–10609; doi:10.1073/pnas.0500398102.

Ge ZJ, Luo SM, Lin F, Liang QX, Huang L, Wei YC, et al. 2014. DNA methylation in oocytes and liver of female mice and their offspring: effects of high-fat-diet-induced obesity. Env. Heal. Perspect 122:159–164; doi:10.1289/ehp.1307047.

Gilbert KM, Blossom SJ, Erickson SW, Reisfeld B, Zurlinden TJ, Broadfoot B, et al. 2016. Chronic exposure to water pollutant trichloroethylene increased epigenetic drift in CD4(+) T cells. Epigenomics 8:633–649; doi:10.2217/epi-2015-0018.

Gilbert KM, Nelson AR, Cooney CA, Reisfeld B, Blossom SJ. 2012. Epigenetic alterations may regulate temporary reversal of CD4(+) T cell activation caused by trichloroethylene exposure. Toxicol Sci 127:169–178; doi:10.1093/toxsci/kfs093.

Guerrero-Bosagna C, Covert TR, Haque MM, Settles M, Nilsson EE, Anway MD, et al. 2012. Epigenetic transgenerational inheritance of vinclozolin induced mouse adult onset disease and associated sperm epigenome biomarkers. Reprod Toxicol 34:694–707; doi:10.1016/j.reprotox.2012.09.005.

Hales CM, Carroll MD, Fryar CD, Ogden CL. 2017. Prevalence of Obesity Among Adults and Youth: United States, 2015–2016 Key findings Data from the National Health and Nutrition Examination Survey. NCHS Data Brief.

Hariharan D, Vellanki K, Kramer H. 2015. The Western diet and chronic kidney disease. Curr Hypertens Rep 17:529; doi:10.1007/s11906-014-0529-6.

Heindel JJ, Balbus J, Birnbaum L, Brune-Drisse MN, Grandjean P, Gray K, et al. 2015. Developmental Origins of Health and Disease: Integrating Environmental Influences. Endocrinology 156:3416–3421; doi:10.1210/EN.2015-1394.

Heinonen I, Rinne P, Ruohonen ST, Ruohonen S, Ahotupa M, Savontaus E. 2014. The effects of equal caloric high fat and western diet on metabolic syndrome, oxidative stress and vascular endothelial function in mice. Acta Physiol 211:515–527; doi:10.1111/apha.12253.

Hernandez Mora JR, Sanchez-Delgado M, Petazzi P, Moran S, Esteller M, Iglesias-Platas I, et al. 2017. Profiling of oxBS-450K 5-hydroxymethylcytosine in human placenta and brain reveals enrichment at imprinted loci. Epigenetics 00–00; doi:10.1080/15592294.2017.1344803.

Heyn H, Li N, Ferreira HJ, Moran S, Pisano DG, Gomez A, et al. 2012. Distinct DNA methylomes of newborns and centenarians. Proc Natl Acad Sci U S A 109:10522–10527; doi:10.1073/pnas.1120658109.

Horvath S. 2013. DNA methylation age of human tissues and cell types. Genome Biol. 14:R115; doi:10.1186/gb-2013-14-10-r115.

Horvath S, Erhart W, Brosch M, Ammerpohl O, von Schonfels W, Ahrens M, et al. 2014. Obesity accelerates epigenetic aging of human liver. Proc. Natl. Acad. Sci. 111:15538–15543; doi:10.1073/pnas.1412759111.

Huang P, Li S, Shao M, Qi Q, Zhao F, You J, et al. 2010. Calorie restriction and endurance exercise share potent anti-inflammatory function in adipose tissues in ameliorating diet-induced obesity and insulin resistance in mice. Nutr Metab 7:59; doi:10.1186/1743-7075-7-59.

Issa JP. 2014. Aging and epigenetic drift: a vicious cycle. J Clin Invest 124:24–29; doi:10.1172/JCI69735.

Ito S, Shen L, Dai Q, Wu SC, Collins LB, Swenberg JA, et al. 2011. Tet proteins can convert 5-methylcytosine to 5-formylcytosine and 5-carboxylcytosine. Science 333:1300–3; doi:10.1126/science.1210597.

Johnson KC, Houseman EA, King JE, von Herrmann KM, Fadul CE, Christensen BC. 2016. 5-Hydroxymethylcytosine localizes to enhancer elements and is associated with survival in glioblastoma patients. Nat. Commun. 7:13177; doi:10.1038/ncomms13177.

Jones MJ, Goodman SJ, Kobor MS. 2015. DNA methylation and healthy human aging. Aging Cell 14:924–932; doi:10.1111/acel.12349.

Jung M, Pfeifer GP. 2015. Aging and DNA methylation. BMC Biol 13:7; doi:10.1186/s12915-015-0118-4.

Kaminen-Ahola N, Ahola A, Maga M, Mallitt KA, Fahey P, Cox TC, et al. 2010. Maternal ethanol consumption alters the epigenotype and the phenotype of offspring in a mouse model. PLoS Genet 6:e1000811; doi:10.1371/journal.pgen.1000811.

Kim DD, Basu A. 2016. Estimating the Medical Care Costs of Obesity in the United States: Systematic Review, Meta-Analysis, and Empirical Analysis. Value Heal. 19:602–613; doi:10.1016/j.jval.2016.02.008.

Kim JH, Sartor MA, Rozek LS, Faulk C, Anderson OS, Jones TR, et al. 2014. Perinatal bisphenol A exposure promotes dose-dependent alterations of the mouse methylome. BMC Genomics 15:30; doi:10.1186/1471-2164-15-30.

Kochmanski J, Montrose L, Goodrich JM, Dolinoy DC. 2017. Environmental Deflection: The Impact of Toxicant Exposures on the Aging Epigenome. Toxicol. Sci. 156:kfx005; doi:10.1093/toxsci/kfx005.

Krüger T, Long M, Bonefeld-Jørgensen EC. 2008. Plastic components affect the activation of the aryl hydrocarbon and the androgen receptor. Toxicology 246:112–123; doi:10.1016/j.tox.2007.12.028.

Laker RC, Lillard TS, Okutsu M, Zhang M, Hoehn KL, Connelly JJ, et al. 2014. Exercise prevents maternal high-fat diet-induced hypermethylation of the Pgc-1α gene and age-dependent metabolic dysfunction in the offspring. Diabetes 63:1605–1611; doi:10.2337/db13-1614.

Laufer BI, Mantha K, Kleiber ML, Diehl EJ, Addison SM, Singh SM. 2013. Long-lasting alterations to DNA methylation and ncRNAs could underlie the effects of fetal alcohol exposure in mice. Dis Model Mech 6:977–992; doi:10.1242/dmm.010975.

Lesniewski LA, Zigler ML, Durrant JR, Nowlan MJ, Folian BJ, Donato AJ, et al. 2013. Aging compounds western diet-associated large artery endothelial dysfunction in mice: prevention by voluntary aerobic exercise. Exp Gerontol 48:1218–1225; doi:10.1016/j.exger.2013.08.001.

Lévesque ML, Casey KF, Szyf M, Ismaylova E, Ly V, Verner M-P, et al. 2014. Genome-wide DNA methylation variability in adolescent monozygotic twins followed since birth. Epigenetics 9:1410–21; doi:10.4161/15592294.2014.970060.

Lindholm ME, Marabita F, Gomez-Cabrero D, Rundqvist H, Ekström TJ, Tegnér J, et al. 2014. An integrative analysis reveals coordinated reprogramming of the epigenome and the transcriptome in human skeletal muscle after training. Epigenetics 9:1557–1569; doi:10.4161/15592294.2014.982445.

Loos RJF, Janssens ACJW. 2017. Predicting Polygenic Obesity Using Genetic Information. Cell Metab. 25:535–543; doi:10.1016/j.cmet.2017.02.013.

López V, Fernández AF, Fraga MF. 2017. The role of 5-hydroxymethylcytosine in development, aging and age-related diseases. Ageing Res. Rev. 37:28–38; doi:10.1016/J.ARR.2017.05.002.

Madrigano J, Baccarelli A, Mittleman MA, Sparrow D, Vokonas PS, Tarantini L, et al. 2012. Aging and epigenetics: longitudinal changes in gene-specific DNA methylation. Epigenetics 7:63–70; doi:10.4161/epi.7.1.18749.

Maegawa S, Gough SM, Watanabe-Okochi N, Lu Y, Zhang N, Castoro RJ, et al. 2014. Age-related epigenetic drift in the pathogenesis of MDS and AML. Genome Res 24:580–591; doi:10.1101/gr.157529.113.

Manikkam M, Tracey R, Guerrero-Bosagna C, Skinner MK. 2013. Plastics derived endocrine disruptors (BPA, DEHP and DBP) induce epigenetic transgenerational inheritance of obesity, reproductive disease and sperm epimutations. PLoS One 8:e55387; doi:10.1371/journal.pone.0055387.

Marco A, Kisliouk T, Tabachnik T, Meiri N, Weller A. 2014. Overweight and CpG methylation of the Pomc promoter in offspring of high-fat-diet-fed dams are not "reprogrammed" by regular chow diet in rats. FASEB J 28:4148–4157; doi:10.1096/fj.14-255620.

Marjonen H, Sierra A, Nyman A, Rogojin V, Gröhn O, Linden AM, et al. 2015. Early maternal alcohol consumption alters hippocampal DNA methylation, gene expression and volume in a mouse model. PLoS One 10:e0124931; doi:10.1371/journal.pone.0124931.

Martino D, Loke YJ, Gordon L, Ollikainen M, Cruickshank MN, Saffery R, et al. 2013. Longitudinal, genome-scale analysis of DNA methylation in twins from birth to 18 months of age reveals rapid epigenetic change in early life and pair-specific effects of discordance. Genome Biol 14:R42; doi:10.1186/gb-2013-14-5-r42.

Massiera F, Barbry P, Guesnet P, Joly A, Luquet S, Moreilhon-Brest C, et al. 2010. A Western-like fat diet is sufficient to induce a gradual enhancement in fat mass over generations. J Lipid Res 51:2352–2361; doi:10.1194/jlr.M006866.

Medvedeva YA, Khamis AM, Kulakovskiy I V, Ba-Alawi W, Bhuyan MS, Kawaji H, et al. 2014. Effects of cytosine methylation on transcription factor binding sites. BMC Genomics 15:119; doi:10.1186/1471-2164-15-119.

Messerschmidt DM, Knowles BB, Solter D. 2014. DNA methylation dynamics during epigenetic reprogramming in the germline and preimplantation embryos. Genes Dev 28:812–828; doi:10.1101/gad.234294.113.

Milagro FI, Campión J, García-Díaz DF, Goyenechea E, Paternain L, Martínez JA. 2009. High

fat diet-induced obesity modifies the methylation pattern of leptin promoter in rats. J Physiol Biochem 65: 1–9.

Myles IA. 2014. Fast food fever: reviewing the impacts of the Western diet on immunity. Nutr J 13:61; doi:10.1186/1475-2891-13-61.

Nestor CE, Ottaviano R, Reddington J, Sproul D, Reinhardt D, Dunican D, et al. 2012. Tissue type is a major modifier of the 5-hydroxymethylcytosine content of human genes. Genome Res. 22:467–77; doi:10.1101/gr.126417.111.

Ollikainen M, Smith KR, Joo EJ, Ng HK, Andronikos R, Novakovic B, et al. 2010. DNA methylation analysis of multiple tissues from newborn twins reveals both genetic and intrauterine components to variation in the human neonatal epigenome. Hum Mol Genet 19:4176–4188; doi:10.1093/hmg/ddq336.

Parle-McDermott A, Ozaki M. 2011. The impact of nutrition on differential methylated regions of the genome. Adv Nutr 2:463–471; doi:10.3945/an.111.001008.

Reichard JF, Puga A. 2010. Effects of arsenic exposure on DNA methylation and epigenetic gene regulation. Epigenomics 2:87–104; doi:10.2217/epi.09.45.

Reik W, Dean W, Walter J. 2001. Epigenetic reprogramming in mammalian development. Science (80-. ). 293:1089–1093; doi:10.1126/science.1063443.

Rönn T, Volkov P, Davegårdh C, Dayeh T, Hall E, Olsson AH, et al. 2013. A six months exercise intervention influences the genome-wide DNA methylation pattern in human adipose tissue. PLoS Genet 9:e1003572; doi:10.1371/journal.pgen.1003572.

Schick S, Fournier D, Thakurela S, Sahu SK, Garding A, Tiwari VK. 2015. Dynamics of chromatin accessibility and epigenetic state in response to UV damage. J Cell Sci 128:4380–4394; doi:10.1242/jcs.173633.

Shah S, McRae AF, Marioni RE, Harris SE, Gibson J, Henders AK, et al. 2014. Genetic and environmental exposures constrain epigenetic drift over the human life course. Genome Res 24:1725–1733; doi:10.1101/gr.176933.114.

Shen L, Zhang Y. 2013. 5-Hydroxymethylcytosine: generation, fate, and genomic distribution. Curr. Opin. Cell Biol. 25:289–96; doi:10.1016/j.ceb.2013.02.017.

Singh S, Li SS. 2012. Epigenetic effects of environmental chemicals bisphenol a and phthalates. Int J Mol Sci 13:10143–10153; doi:10.3390/ijms130810143.

Smallwood SA, Kelsey G. 2012. De novo DNA methylation: a germ cell perspective. Trends Genet 28:33–42; doi:10.1016/j.tig.2011.09.004.

Spiers H, Hannon E, Wells S, Williams B, Fernandes C, Mill J. 2016. Age-associated changes in

DNA methylation across multiple tissues in an inbred mouse model. Mech Ageing Dev 154:20–23; doi:10.1016/j.mad.2016.02.001.

Stroud H, Feng S, Morey Kinney S, Pradhan S, Jacobsen SE. 2011. 5-Hydroxymethylcytosine is associated with enhancers and gene bodies in human embryonic stem cells. Genome Biol 12:R54; doi:10.1186/gb-2011-12-6-r54.

Sui Y, Ai N, Park SH, Rios-Pilier J, Perkins JT, Welsh WJ, et al. 2012. Bisphenol A and its analogues activate human pregnane X receptor. Env. Heal. Perspect 120:399–405; doi:10.1289/ehp.1104426.

Susiarjo M, Sasson I, Mesaros C, Bartolomei MS. 2013. Bisphenol A Exposure Disrupts Genomic Imprinting in the Mouse. G. Kelsey, ed PLoS Genet. 9:e1003401; doi:10.1371/journal.pgen.1003401.

Tachibana K, Takayanagi K, Akimoto A, Ueda K, Shinkai Y, Umezawa M, et al. 2015. Prenatal diesel exhaust exposure disrupts the DNA methylation profile in the brain of mouse offspring. J Toxicol Sci 40:1–11; doi:10.2131/jts.40.1.

Talens RP, Christensen K, Putter H, Willemsen G, Christiansen L, Kremer D, et al. 2012. Epigenetic variation during the adult lifespan: cross-sectional and longitudinal data on monozygotic twin pairs. Aging Cell 11:694–703; doi:10.1111/j.1474-9726.2012.00835.x.

Tammen SA, Dolnikowski GG, Ausman LM, Liu Z, Kim KC, Friso S, et al. 2014. Aging alters hepatic DNA hydroxymethylation, as measured by liquid chromatography/mass spectrometry. J Cancer Prev 19:301–308; doi:10.15430/JCP.2014.19.2.301.

Tellez-Plaza M, Tang WY, Shang Y, Umans JG, Francesconi KA, Goessler W, et al. 2014. Association of global DNA methylation and global DNA hydroxymethylation with metals and other exposures in human blood DNA samples. Env. Heal. Perspect 122:946–954; doi:10.1289/ehp.1306674.

Teschendorff AE, West J, Beck S. 2013. Age-associated epigenetic drift: implications, and a case of epigenetic thrift? Hum Mol Genet 22:R7–R15; doi:10.1093/hmg/ddt375.

Urdinguio RG, Torró MI, Bayón GF, Álvarez-Pitti J, Fernández AF, Redon P, et al. 2016. Longitudinal study of DNA methylation during the first 5 years of life. J. Transl. Med. 14:160; doi:10.1186/s12967-016-0913-x.

van Dongen J, Nivard MG, Willemsen G, Hottenga JJ, Helmer Q, Dolan C V, et al. 2016. Genetic and environmental influences interact with age and sex in shaping the human methylome. Nat Commun 7:11115; doi:10.1038/ncomms11115.

Veazey KJ, Parnell SE, Miranda RC, Golding MC. 2015. Dose-dependent alcohol-induced alterations in chromatin structure persist beyond the window of exposure and correlate with fetal alcohol syndrome birth defects. Epigenetics Chromatin 8:39; doi:10.1186/s13072-015-

0031-7.

Vucetic Z, Kimmel J, Totoki K, Hollenbeck E, Reyes TM. 2010. Maternal high-fat diet alters methylation and gene expression of dopamine and opioid-related genes. Endocrinology 151:4756–4764; doi:10.1210/en.2010-0505.

Wang D, Liu X, Zhou Y, Xie H, Hong X, Tsai HJ, et al. 2012. Individual variation and longitudinal pattern of genome-wide DNA methylation from birth to the first two years of life. Epigenetics 7:594–605; doi:10.4161/epi.20117.

Waterland RA, Jirtle RL. 2004. Early nutrition, epigenetic changes at transposons and imprinted genes, and enhanced susceptibility to adult chronic diseases. Nutrition 20: 63–68.

Waterland RA, Michels KB. 2007. Epigenetic epidemiology of the developmental origins hypothesis. Annu Rev Nutr 27:363–388; doi:10.1146/annurev.nutr.27.061406.093705.

Wells JC. 2014. Adaptive variability in the duration of critical windows of plasticity: Implications for the programming of obesity. Evol Med Public Heal. 2014:109–121; doi:10.1093/emph/eou019.

Wilson VL, Smith RA, Ma S, Cutler RG. 1987. Genomic 5-methyldeoxycytidine decreases with age. J Biol Chem 262: 9948–9951.

Wolstenholme JT, Rissman EF, Connelly JJ. 2011. The role of Bisphenol A in shaping the brain, epigenome and behavior. Horm Behav 59:296–305; doi:10.1016/j.yhbeh.2010.10.001.

Wright RO, Schwartz J, Wright RJ, Bollati V, Tarantini L, Park SK, et al. 2010. Biomarkers of lead exposure and DNA methylation within retrotransposons. Env. Heal. Perspect 118:790–795; doi:10.1289/ehp.0901429.

Wu H, D'Alessio AC, Ito S, Wang Z, Cui K, Zhao K, et al. 2011. Genome-wide analysis of 5-hydroxymethylcytosine distribution reveals its dual function in transcriptional regulation in mouse embryonic stem cells. Genes Dev 25:679–684; doi:10.1101/gad.2036011.

Xu X, Su S, Barnes VA, De Miguel C, Pollock J, Ownby D, et al. 2013. A genome-wide methylation study on obesity. Epigenetics 8:522–533; doi:10.4161/epi.24506.

Yildirim O, Li R, Hung J-H, Chen PB, Dong X, Ee L-S, et al. 2011. Mbd3/NURD Complex Regulates Expression of 5-Hydroxymethylcytosine Marked Genes in Embryonic Stem Cells. Cell 147:1498–1510; doi:10.1016/j.cell.2011.11.054.

Zhang XF, Zhang LJ, Feng YN, Chen B, Feng YM, Liang GJ, et al. 2012. Bisphenol A exposure modifies DNA methylation of imprint genes in mouse fetal germ cells. Mol Biol Rep 39:8621–8628; doi:10.1007/s11033-012-1716-7.

# Chapter 2

## Longitudinal Effects of Developmental Bisphenol A, Variable Diet, and Physical Activity on Age-related Methylation in Mice


### Abstract

Environmental factors, including exogenous exposures and nutritional status, can affect DNA methylation across the epigenome, but effects of exposures on the aging epigenome remain unclear. Here, we tested the hypothesis that early-life exposure to bisphenol A (BPA), variable diet, and/or changes in physical activity result in altered age-related methylation, as measured longitudinally via target loci methylation in matched mouse tail (PND21, 10 months) and blood (2 months, 4 months, 10 months) samples. DNA methylation was quantified at two repetitive elements (LINE-1, IAP), two imprinted genes (*Igf2, H19*), and one non-imprinted gene (*Esr1*) in isogenic *a/a* Agouti mice developmentally exposed to Control, Control+BPA (50 µg/kg diet), Mediterranean high-fat diet (MHFD), Western high-fat diet (WHFD), Mediterranean+BPA, or Western+BPA diets. With age, tail tissue DNA methylation levels significantly ($p<0.05$) decreased at LINE-1, IAP, and *H19*, and significantly increased at *Esr1*. In blood, *Esr1* DNA methylation increased significantly with age, but no other investigated loci showed significant age-related methylation. In the tail tissue, *Igf2* demonstrated WHFD-specific changes in early-life methylation ($p=0.027$), and IAP showed marginal negative environmental deflection in the Western ($p=0.058$) and Western+BPA ($p=0.051$) exposure groups. In blood, *Esr1* showed significant negative environmental deflection by WHFD exposure in females ($p=0.02$). Physical activity, while not significant, showed an opposite, positive effect on age-related *Esr1* methylation in female blood, suggesting that it may abrogate the effects of WHFD on the aging epigenome. Overall, we demonstrated significant age-related DNA methylation in two matched mouse tissues, as well as significant effects of developmental nutritional exposures on age-related methylation patterns.

## 2.1 Introduction

The epigenome is a dynamic regulatory framework that utilizes epigenetic information to govern the response of cells, tissues, and entire organisms to environmental stressors. Epigenetic control mechanisms operate at several levels, including alterations to DNA itself (e.g. DNA methylation), chromatin remodeling (e.g. histone modifications), and non-coding RNA interactions (Bernal and Jirtle 2010; Egger et al. 2004). DNA methylation, which is perhaps the best-studied epigenetic mark, is defined by the addition of a methyl group to the 5'-carbon of cytosine in a cytosine-phospho-guanine (CpG) dinucleotide. Recent evidence indicates that DNA methylation status changes as a function of age in both humans and animal models, and that this change is often gene- or tissue-specific (Florath et al. 2014; Issa 2014; Madrigano et al. 2012; Teschendorff et al. 2013). This process of altered DNA methylation across the life-course is has important implications for gene expression and disease onset throughout the life course (Issa 2014). While this process occurs across all individuals, twin studies have shown that genetically identical individuals can have vast divergence in their epigenetic marks as they age (Fraga et al. 2005). These results suggest that unique environmental exposures throughout life, rather than any inherent genetic predisposition, may lead to a modulation in the rate of age-related DNA methylation.

Mounting evidence indicates that exposure to environmental factors during key developmental windows may alter gene regulation and phenotype through changes in epigenetic marks (Waterland and Jirtle 2004). As such, the epigenome represents a possible mechanism underlying the Developmental Origins of Health and Disease (DOHaD) hypothesis, which states that exposure to nutritional and environmental factors during prenatal and early postnatal periods alters susceptibility to chronic diseases by influencing developmental plasticity (Bateson et al.

2004). In general, methylation of DNA at specific promoter/enhancer sites is associated with decreased transcription factor binding, as well as decreased transcription (Medvedeva et al. 2014). However, gene-specific DNA methyl marks do not accurately predict global 5-methylcytosine levels, which are driven by CpG methylation of non-coding, repetitive DNA elements, including transposons, retrotransposons, and endogenous retroviruses (Nelson et al. 2011; Yang et al. 2004). In contrast to the transcriptional effects seen at gene promoters/enhancers, altered methylation of repetitive elements has the potential to affect genetic stability through increased movement of repetitive elements around the genome (Rodriguez et al. 2006; Ross et al. 2010; Suzuki et al. 2006). Based on the differential regulatory effects of site-specific and global methylation levels, it is important to measure both when investigating the biological effects of epigenetic aging. Recent data also indicate that early life exposure to environmental toxicants has the potential to alter age-related global and gene-specific methylation (Christensen et al. 2009; Huen et al. 2014). Supporting this idea, we recently demonstrated that developmental lead (Pb) exposure in congenic mice altered DNA methylation levels at imprinted genes, and that exposure was associated with alterations in the rate of epigenetic drift throughout the life-course (Faulk et al. 2014).

Endocrine disrupting chemicals (EDCs) are an important class of environmental factors that have been linked to the developmental origins of adult disease (Newbold et al. 2009). One such chemical, bisphenol A (BPA), is a commercial monomer that makes up polycarbonate plastic and epoxy resins. BPA is found in a variety of consumer products (e.g. metal can linings, receipt paper, etc.), and has near ubiquitous and continuous human exposure across the world (Calafat et al. 2008). BPA can directly bind estrogen receptor α, has been shown to activate a variety of growth-related transcription factors, and can also bind effectively to several nuclear

receptors involved in cell maturation (Krüger et al. 2008; Singh and Li 2012; Sui et al. 2012; Watson et al. 2007). BPA exposure has also been shown to affect DNA methylation levels across the epigenome (Manikkam et al. 2013; Singh and Li 2012; Wolstenholme et al. 2011; Zhang et al. 2012). *In utero* doses of BPA in mouse models affect both global and gene promoter-specific methylation, indicating that BPA exposure could alter gene expression during development (Anderson et al. 2012; Kim et al. 2014; Singh and Li 2012). The effects of BPA exposure on age-related methylation in matched samples have not been previously studied, but based on BPA's ability to alter the developing epigenome, BPA exposure has the potential to alter epigenetic aging.

In addition to chemical exposure, maternal diet can also affect offspring DNA methylation levels (Tobi et al. 2018; Waterland and Jirtle 2003). The modern "Western High-Fat Diet" (WHFD) is characterized by high saturated and omega-6 polyunsaturated fatty acids, reduced omega-3 fatty acid intake, and increased salt and refined sugar intake (Myles 2014). Studies in animal models have shown that alterations in maternal diet, specifically levels of methyl donors, can alter gene-specific and global methylation in offspring, indicating that diet can induce long-lasting, inter-generational changes in methylation (Dolinoy et al. 2007; Hollingsworth et al. 2008; Niculescu et al. 2006). Genome-wide studies of the methylome have also noted nutrient-sensitive CpG sites throughout the epigenome, indicating that alterations in diet can affect DNA methylation at specific genomic sites (Parle-McDermott and Ozaki 2011). Based on these results, maternal diet represents an important mediator of the epigenome that has the potential to affect offspring methylation throughout the life course.

Despite increasing investigation of diet- and toxicant-induced epigenetic changes, the role of physical activity in modulating the epigenome has been less extensively studied. Physical

activity is a lifestyle factor with well-documented positive health effects; in mice, exercise training has been shown to increase energy expenditure, offsetting the weight-gain induced by HFD (Sasaki et al. 2014). Physical activity-related energy expenditure (AEE), a measure of physical activity's contribution to metabolic rate, can be calculated in mice using calorimetry data (Hills et al. 2014; Pontzer et al. 2016; Van Klinken et al. 2012). In addition to affecting energy expenditure, exercise/physical activity has also shown associations with gene promoter-specific DNA methylation in mice (Kanzleiter et al. 2015; King-Himmelreich et al. 2016; Nguyen et al. 2016), suggesting that physical activity may also offset the epigenetic effects of HFD. Providing support for this idea, a recent study in mice demonstrated that maternal exercise attenuated HFD-induced *Pgc-1α* promoter hypermethylation in skeletal muscle of offspring (Laker et al. 2014). As such, physical activity is a lifestyle factor that has the potential to not only alter the aging epigenome, but also mitigate the epigenetic effects of HFD exposure.

To investigate the potential combined effects of BPA exposure, Western high-fat diet, and physical activity on the epigenome, DNA methylation was measured in murine target loci regions -- Long Interspersed Nuclear Element-1 (LINE-1) repeats, Intracisternal A-Particle (IAP) repeats, Insulin-like growth factor 2 (*Igf2*) differentially methylated region (DMR) 2 (Faulk et al. 2014; Waterland et al. 2006), *H19* DMR (Faulk et al. 2014; Stouder et al. 2009), and the promoter region of Estrogen receptor α (*Esr1*) (Maegawa et al. 2010). These target gene regions fall into three classes – repetitive elements (LINE-1, IAP), imprinted genes (*Igf2, H19*), and a non-imprinted protein-coding gene (*Esr1*). Target region classes were chosen based on their potential to reflect global methylation levels, their use as frequent biomarkers in environmental epigenetic studies, and their involvement in growth and metabolism, respectively.

Long interspersed nuclear element-1 (LINE-1) is the most common transposable element in the mouse genome, representing more than 20% of the murine sequence (Sookdeo et al. 2013). LINE-1 elements are ancient retrotransposons that replicated in the genome over evolutionary time. Although most LINE-1 elements are no longer active, they have widespread distribution across the genome, making LINE-1 methylation a useful approximation of "global" methylation levels (Nelson et al. 2011; Yang et al. 2004). Intracisternal A-Particle (IAP) retrotransposons are murine, long terminal repeat (LTR)-type genetic elements that also utilize RNA intermediates to retrotranspose around the genome (Horie et al. 2007). With the exception of metastable epialleles like the well-studied viable yellow ($A^{vy}$) IAP element (Dolinoy et al. 2007), most IAPs are tightly regulated, and have lost their ability to retrotranspose (Horie et al. 2007). However, evidence indicates that aging can cause demethylation of IAP promoters, potentially reactivating their retrotransposition competency (Barbot et al. 2002; Horie et al. 2007). The IAP assay in this study utilizes a conserved IAP sequence to measure methylation across all IAP retrotransposons present in the murine genome, thereby providing a second, but more genetically "active" approximation of global methylation.

Along with repetitive elements, several imprinted and non-imprinted genes were also investigated. Imprinted genes display parent-of-origin differential methylation and mono-allelic expression (Sasaki et al. 2000). The imprinted genes included in this study, *Igf2* and *H19*, contain differentially methylated regions (DMRs) that exhibit variability in methylation associated with exposure to diet and/or EDCs (Hoyo et al. 2011; LaRocca et al. 2014; Lee et al. 2014; McKay et al. 2011; Susiarjo et al. 2013; Waterland et al. 2006), making them valuable biomarkers of exposure-induced changes in methylation. In addition to the imprinted genes, we also examined methylation levels at a non-imprinted protein-coding gene – *Esr1*. Estrogen

receptor α is a transcription factor activated by estrogenic ligands, and it mediates estrogen's involvement in the regulation of growth and development (Bondesson et al. 2015). Evidence indicates that methylation of the *Esr1* exon 2 promoter is positively associated with age in unmatched samples of murine small intestine (Maegawa et al. 2010). This fact, combined with *Esr1*'s biological importance throughout life, makes it an ideal non-imprinted candidate gene for assessing the effects of developmental exposure on epigenetic aging.

The described study examines longitudinal changes in absolute mean DNA methylation from paired postnatal day 21 (PND21) and 10 month old mouse tail tissue, as well as matched 2 month, 4 month, and 10 month old blood samples. Matched tail and blood tissues were used due to availability early in life and at sacrifice, and to eliminate inter-individual confounding. This study investigates whether developmental exposure to BPA, altered diet, and/or physical activity levels affects the rate of age-related methylation at five selected genetic loci. We found tissue- and gene-specific changes in absolute mean DNA methylation with age at all measured loci. WHFD exposure had a significant modifying effect on the rate of age-related methylation at the non-imprinted *Esr1* locus in both tail and blood samples. In the blood samples, the effect of WHFD exposure on age-related methylation was sex-specific, showing negative deflection only in female mice. Physical activity had a non-significant positive effect on age-related *Esr1* methylation in female blood. Exposure to WHFD also modified rates of age-related methylation at IAP repeats in tail and blood. Dietary BPA exposure did not have a significant effect on the rate of age-related methylation at any of the investigated loci in either tail or blood. This study demonstrates measurable, gene-specific age-related methylation, as well as diet-dependent alterations in the rate of epigenetic aging at a class of repetitive elements and a non-imprinted locus related to murine growth and development.

## 2.2 Results

### *Litter parameters*

Developmental BPA and/or diet exposure did not significantly alter litter size, sex ratio, or *a/a* to $A^{vy}/a$ genotypic ratio (n=277). Percent survival was significantly lower in the Control+BPA exposed offspring (survival = 73%) compared to Control (survival = 91%, p=0.006) and Mediterranean+BPA (survival = 85%, p=0.007) exposure groups, but was not significantly different in other comparisons. A subset of *a/a* non-agouti wild type mouse pups (n=133) was selected for inclusion in longitudinal follow-up up to 10 months of age, which incorporated collection of matched tail tip and blood samples (**Table 2-1**).

### *Exposure- and diet-dependent changes in cross-sectional DNA methylation*

For all exposure groups, no significant changes in cross-sectional tail DNA methylation were found in the LINE-1, IAP, and *H19* loci across the measured time points. However, several significant differences in PND21 cross-sectional tail DNA methylation were identified at the *Esr1* and *Igf2* loci (**Figure 2-1**). The *Esr1* locus demonstrated significant alterations to PND21 tail methylation when compared to Control, Mediterranean, and Western diets (ANOVA, p = 0.002). Specifically, mice exposed to Western diet showed significantly decreased *Esr1* tail methylation compared to Control (Tukey's test, p= 0.027) and Mediterranean (Tukey's test, p = 0.002), and the Western exposure group demonstrated a significant decrease in *Esr1* tail methylation compared to the Western+BPA group (Student's t-test, p=0.005). The *Igf2* locus demonstrated significant alterations to PND21 tail methylation when comparing BPA, Mediterranean+BPA, and Western+BPA diets (ANOVA, p = 0.020). At PND21, tail *Igf2* methylation in the Western+BPA group was significantly higher than methylation in the BPA group (Tukey's test, p=0.027); a similar, marginally significant increase in tail *Igf2* methylation

was seen when comparing Western+BPA to Mediterranean+BPA (Tukey's test, p=0.073). There were no significant differences in cross-sectional DNA methylation by exposure group in the blood samples.

***DNA methylation changes with age***

DNA methylation at the LINE-1 and IAP repetitive elements, as well as the *Igf2, H19,* and *Esr1* genes, was quantified from paired PND21 and 10 month tail samples (**Table 2-2**). When adjusting for exposure group, sex, age:exposure, and age:sex, LINE-1, IAP, and the *H19* locus demonstrated significant decreases in methylation over time (- 0.94%, p=0.035; -1.32%, p=2.2E-06; -10.44%, p=6.22E-08; respectively). In contrast, the *Igf2* and *Esr1* genes demonstrated increased methylation over time; however, only the increase in the *Esr1* gene was statistically significant (7.60% increase, p=1.44E-12) (**Table 2-2**).

DNA methylation was also quantified from matched 2 month, 4 month, and 10 month blood samples. When adjusting for exposure group, sex, age:exposure, and log(AEE), only the *Esr1* gene demonstrated significant changes over time (β=4.094, p=3.64E-14) (**Table 2-2**). Specifically, *Esr1* showed a significant increase in mean blood DNA methylation from 2 to 10 months of age. Furthermore, the included sex variable showed a significant relationship with mean *Esr1* DNA methylation (β=8.24, p<2E-16), indicating that sex may be modifying the association between age and blood DNA methylation.

***Developmental exposures alter mean DNA methylation***

To examine the effects of exposure on DNA methylation, we first examined whether each exposure group had a direct, significant effect on mean tail DNA methylation compared to Control. LINE-1, IAP, and *H19* showed no significant effects of developmental exposures on mean tail methylation (**Table 2-3**). At the *Igf2* locus, BPA exposure had a marginally significant

negative effect on mean tail methylation compared to Control (β=-3.81, p=0.066); no other exposure groups had a significant effect on tail methylation at this gene. At the *Esr1* gene, Western diet exposure had a significant negative effect on mean tail methylation compared to Control (β= -1.93, p=0.013); this was the only significant exposure effect for the *Esr1* gene in tail tissue (**Table 2-3**).

To follow up on the tail results, we also examined whether BPA and/or WHFD exposure had a significant effect on mean blood DNA methylation compared to Control. IAP, *Igf2*, *H19*, and *Esr1* showed no significant effects of developmental exposures on mean blood methylation (**Table 2-4**). At the LINE-1 repetitive element, WHFD exposed mice showed a significant increase in mean blood methylation compared to Control (β=0.762, p=0.003); no other exposure groups showed a significant change in mean blood methylation at this repetitive element (**Table 2-4**).

***Environmental deflection by exposure***

To further examine the potential effects of exposure on the rate of age-related methylation in tail tissue, an interaction term between age and categorical exposure was included in the linear mixed effects model for each gene (**Table 2-3**). The *Igf2* and *H19* genes showed no significant interaction between age and exposure group, indicating that the relationship between age and tail methylation was not affected by developmental exposures in those genes. On the other hand, at LINE-1 repetitive elements, developmental Western diet exposure had a marginally significant negative effect on the association between age and tail methylation compared to Control (β=-1.05, p=0.069). Similarly, for global IAP, both the Western and Western+BPA diets had marginally significant negative effects on tail age-related methylation relative to Control (β=-0.645, p=0.058; β=-0.0649, p=0.051). At the *Esr1* gene, developmental

Mediterranean+BPA diet exposure had a marginally significant positive effect on tail age-related methylation when compared to Control (β=1.85, p=0.064). Directionality of the interaction between age and exposure was specific to each gene in tail tissue (**Table 2-3, Figure 2-1**).

Given that gene regulation can vary by sex, two additional variables – sex and a sex:age interaction term – were included in the linear mixed model for each gene. Neither sex nor sex:age were significant terms in the mixed models for LINE-1 (p=0.395, p=0.644), IAP (p=0.476, 0.786), *Igf2* (p=0.868, p=0.686), and *H19* (p=0.294, p=0.639) in tail tissue. However, at the *Esr1* gene, while the sex categorical variable did not demonstrate a significant effect on tail methylation, the sex:age interaction term was statistically significant (p=0.003), indicating effect modification of tail age-related methylation by sex.

Following up on the tail results, age:exposure interaction terms were also included in mixed effects models for mouse blood methylation to test for environmental deflection of age-related methylation. There was significant WHFD-induced environmental deflection of age-related blood methylation at LINE-1 (p=0.01), IAP (p=0.04), and *Esr1* (p=0.02) (**Table 2-4**). At these gene regions, WHFD exposed mice had higher % methylation at 2M and lower % methylation at 10M compared to control (**Figure 2-2**). The *Igf2* and *H19* gene loci demonstrated no significant environmental deflection of age-related methylation by exposure.

In the linear mixed model for *Esr1*, the included sex variable showed a significant relationship with mean DNA methylation (β=8.24, p<2E-16), indicating that sex may be having a confounding effect of the association between age and blood DNA methylation. To further examine the effects of sex on this relationship, sex-stratified models of age-related methylation were run for the *Esr1* gene region. These models showed that the effect of age and WHFD exposure on *Esr1* promoter methylation varied by sex in mouse blood. Males showed a

significant increase in *Esr1* methylation with age (β=4.22; p=0.004), but no significant effects of exposure. Meanwhile, females demonstrated both a significant increase in *Esr1* methylation with age (β=2.11, p=0.001) and a significant negative age:WHFD interaction term (β= -1.67, p=0.02). Combined, these data show a WHFD-mediated decrease in the rate of age-related *Esr1* methylation in female mouse blood compared to Control (**Figure 2-3**).

***Environmental deflection by physical activity***

To characterize murine physical activity, spontaneous activity levels were measured using Comprehensive Lab Animal Monitoring System (CLAMS) cages, which used lasers to measure movement in all directions. CLAMS data was collected at 2, 4, and 8 months prior to blood draws. From the CLAMS data, we used penalized spline regression models to calculate activity-related energy expenditure (AEE) values. An age:log(AEE) interaction term was then included in linear mixed models for the *Esr1* gene region, the only gene region in blood with significant age-related methylation. Since the relationship between age and *Esr1* methylation was shown to vary by sex, the age:log(AEE) variable was included in sex stratified models. In the female model, the age:log(AEE) term was non-significant, but positive, showing opposite directionality to the significant negative age:WHFD coefficient (**Table 2-5**). This indicates that AEE may partially offset the significant negative WHFD-mediated environmental deflection in female mice, a result that is apparent in a plot of the female mixed model results (**Figure 2-4**).

## 2.3 Discussion

***BPA exposure***

We did not find any significant effects of developmental BPA exposure on either cross-sectional DNA methylation or age-related methylation at the five investigated genetic loci. These results match our previous work, which showed that the same dose of BPA (50 µg/kg diet) did

not significantly alter LINE-1 repetitive element methylation in liver (Faulk et al. 2016) or *Esr1* methylation in liver (Weinhouse et al. 2015). However, separate studies in our lab have shown that BPA exposure can alter genome-wide and global methylation levels in mouse liver and tail, respectively (Anderson et al. 2012, Kim et al. 2014). Taken together, these contradictory results suggest that the epigenetic effects of BPA may be tissue-, dose-, and gene-specific. Therefore, the lack of significant BPA-related changes in DNA methylation in this study may simply reflect an absence of exposure effects in tail or blood at the selected dose or investigated loci.

***Age-related methylation***

The results from this study indicate that the epigenome is dynamic with age in mouse tail and blood tissues. In tail, age-associated changes in DNA methylation occurred at all measured genetic loci, with statistically significant changes present at *Esr1*, *H19*, LINE-1, and IAP repeats. In blood, only the *Esr1* promoter region demonstrated statistically significant age-related methylation across the 10 month life-course. Consistent with other results in the literature, directionality of age-related methylation was specific to each gene (Christensen et al. 2009; Issa 2014). In blood and tail tissues, the non-imprinted gene promoter, *Esr1*, demonstrated an increase in methylation with age, a result consistent with documented decreases in estrogen receptor α (ERα) expression during aging (Wilson and Westberry 2009). Meanwhile, repetitive element methylation decreased with age in tail, and the investigated imprinted genes either increased or decreased with age in tail depending upon the locus. These results are also consistent with previous reports (Issa 2014; Maegawa et al. 2014; Teschendorff et al. 2013), and indicate that epigenetic aging varies in a region-specific manner.

The effect of age on *Esr1* promoter methylation in blood was also sex-specific, with males showing a more pronounced effect of age compared to females. This may be a reflection

of sex-specific Estrogen receptor α (ERα) regulation during the aging process. Previous work in mouse cortex has shown that adult females have increased ERα protein levels, mRNA expression, and promoter methylation compared to males (Sharma and Thakur 2006; Wilson et al. 2011). As such, females may show decreased effects of age due to a sex-specific requirement for increased ERα expression into adulthood.

The documented region-specific directionality of drift fits a growing hypothesis in the field – that age-related changes in methylation facilitate development of chronic disease (e.g. cancer) via increased genomic instability and altered regulation of genes related to growth and development (Decottignies and d'Adda di Fagagna 2011; Issa 2014; Teschendorff et al. 2010). Decreased DNA methylation of repetitive elements with age has the potential to increase genomic instability through increased transposition of repetitive elements around the genome and dysregulation of expression via cis-chromatin modifying effects (Rodriguez et al. 2006; Ross et al. 2010; Suzuki et al. 2006). Additionally, increased methylation of promoter regions in protein-coding genes is associated with dysregulated transcription (Medvedeva et al. 2014; Varley et al. 2013). Combined, these effects have the potential to produce an epigenetic environment that alters gene expression and may increase the risk of disease states commonly associated with aging.

***Environmental deflection***

Expanding on simply examining the effects of age, we also tested the hypothesis that developmental BPA exposure, high-fat diet, and/or physical activity-related energy expenditure would lead to environmental deflection of age-related methylation rates. In tail tissue, the age:WHFD interaction term demonstrated marginal significance at IAP repeats and the *Esr1* locus, but not at LINE-1, *Igf2*, or *H19*, suggesting that WHFD exposure may lead to

environmental deflection of epigenetic aging. Supporting this idea, the age:WHFD interaction term was also significant at the *Esr1,* IAP, and LINE-1 loci when modeling longitudinal blood methylation. At all three significant loci in blood, WHFD exposed mice had higher % methylation at 2 months and lower % methylation at 10 months, suggesting differential effects of developmental WHFD exposure at distinct life-stages. Although the exact mechanism remains undefined, the apparent delay between WHFD exposure and decreased DNA methylation could be the result of a two phase process: early-life epigenetic programming followed by compensatory changes in regulation of methylation machinery – e.g. Dnmt3a, Tet1. DNA methyltransferase 3a (Dnmt3a) is an enzyme that facilitates the *de novo* addition of methyl groups to CpG sites across the genome (Challen et al. 2011). Meanwhile, ten-eleven translocation methylcytosine dioxygenase 1 (Tet1) is a 5-methylcytosine (5-mC) dioxygenase that facilitates oxidation of 5-mC, thereby tagging methylated CpG sites for active DNA demethylation by base excision repair (BER) (Xu and Wong 2015). Asynchronous alterations in activity of these opposing enzymes may explain the life-stage-specific effects of developmental WHFD exposure.

The two-phase effect of WHFD exposure on the murine epigenome may be the result of oxidative stress (OS) induction. Previous work has demonstrated that Western diet can induce OS in mice (Heinonen et al. 2014), and other work has shown that OS can alter DNA methylation (Yara et al. 2015). For example, research indicates that OS can induce DNA hypermethylation via targeted acceleration of the reaction between cytosine molecules and S-adenyl-methionine (SAM), a methyl group donor (Yara et al. 2015). Research has also shown that oxidative conditions can activate Tet enzymes (Chia et al. 2011; Coulter et al. 2013; Zhao et al. 2014), suggesting that OS may affect active DNA demethylation. These bidirectional effects

of OS on the epigenome fit into a proposed two-phase model for the effects of WHFD on DNA methylation. In the first phase, WHFD-induced OS would increase DNA methylation on a short time scale though direct acceleration of the interaction between SAM and CpG sites across the genome. In the second phase, OS recruits Tet enzymes, leading to hypomethylation at specific promoter regions via targeted oxidation of 5-mC to 5-hydroxymethylcytosine (5-hmC). 5-hmC could then be lost throughout the life-course via active or passive demethylation pathways (Shen et al. 2014). While this model fits well with our results, 5-hydroxymethylcytosine (5-hmC) is not distinguishable from 5-mC in bisulfite-pyrosequencing data (Huang et al. 2010). As a result, there may be an early-life wave of OS-induced 5-mC oxidation to 5-hmC that is not captured in our targeted pyrosequencing data. Additional work is needed to fully characterize the role of OS in WHFD-induced environmental deflection of epigenetic aging in mice.

In contrast to an oxidative stress or environmental mismatch model, the apparent delay between WHFD exposure and age-related hypomethylation may be the result of technical limitations in our methods. The Tet1 enzyme oxidizes 5-mC to 5-hydroxymethylcytosine (5-hmC), but this oxidized form is not distinguishable from 5-mC in bisulfite-pyrosequencing data. As a result, active demethylation would only appear in bisulfite-pyrosequencing data once the oxidized methyl group has been targeted for repair and replaced with an unmethylated cytosine. This means may be an early-life wave of Tet-assisted 5-mC oxidation to 5-hmC that is not captured in our targeted pyrosequencing data. In addition to this technical issue, recent evidence has shown that 5-hmC is a stable epigenetic mark that has a complex role in both positive and negative regulation of transcription (Hahn et al. 2014; Wu et al. 2011). As such, the delay between exposure and *Esr1* hypomethylation could be the result of early-life processing of 5-mC to 5-hmC followed by a gradual loss of 5-hmC during cellular replication.

In addition to WHFD-specific results, female blood also showed opposing effects of WHFD and AEE on longitudinal *Esr1* methylation, suggesting a mitigating effect of life-long physical activity on age-related methylation in WHFD-exposed female mice. Supporting this idea, a recent study in mice showed that maternal exercise attenuated HFD-induced Pgc-1α promoter hypermethylation in skeletal muscle of offspring (Laker et al. 2014). Combined with our results, this suggests that physical activity – whether maternal or life-long – can offset high-fat diet effects on the epigenome. In our study, the opposing effects of WHFD and physical activity on age-related methylation were less clear in male mice, indicating that environmental deflection of age-related *Esr1* methylation may be sex-specific. This may be a reflection of sex-specific regulation of the *Esr1* gene, which is more highly expressed in female mice (Sharma and Thakur 2006). These blood data at the *Esr1* locus demonstrate the importance of considering sex-specific epigenetic effects when studying environmental deflection of epigenetic aging.

For IAP repeats in tail tissue, developmental exposure to the Western and Western+BPA diets was associated with a marginally significant decrease in the rate of age-related methylation. At this global locus, the magnitude of this effect did not differ between the Western and Western+BPA diets, suggesting that exposure to Western diet was driving the age:exposure interaction effect. Given that age-related demethylation of IAP promoters has the potential to reactivate retrotransposition competency (Barbot et al. 2002; Horie et al. 2007), Western HFD, by increasing the rate of age-related methylation loss at IAP elements, may also increase IAP retrotransposition events. This suggests a mechanism by which developmental WHFD influences genomic stability throughout an organism's life.

Although age-related methylation at IAP repetitive elements demonstrated environmental deflection by WHFD in tail tissue, this result was not seen in LINE-1. This suggests that separate

classes of repetitive elements exhibit distinct epigenetic responses to environmental factors. Therefore, when studying the effects of the environment on global DNA methylation – both in cross-section and across the life course – multiple classes of repetitive elements should be included in analysis.

In tail tissue, sex did not significantly alter age-related methylation directionality at LINE-1, IAP, *Igf2,* or *H19.* However, sex did significantly alter age-related methylation at the *Esr1* locus in both tail and blood. Specifically, as age increased from PND21 to 10 months in tail tissue, there was a significant increase in the effect of sex on methylation at the *Esr1* gene. Across all exposures except Med+BPA in tail, male mice demonstrated lower average *Esr1* methylation at PND21, but higher average *Esr1* methylation at 10 months. This trend, combined with a significant age:sex interaction term, suggests a sex-specific change in regulation of the *Esr1* gene during aging. This idea was supported by sex-specific differences in *Esr1* DNA methylation in blood. In blood tissue, males showed greater increases in *Esr1* DNA methylation between 2 months and 10 months of age. Additionally, effects of WHFD on age-related methylation were sex-specific, with a significant environmental deflection only apparent in female mice exposed to developmental WHFD. These data corroborate the fact that the sexes utilize estrogen for very different processes during reproduction and growth, with females of reproductive age demonstrating higher average serum estrogen than males (Bondesson et al. 2015). Therefore, as the animals reach reproductive age, sex-specific effect modification of age-related *Esr1* methylation may occur as a regulatory response to sexually dimorphic estrogen activity.

***Cross-sectional epigenetic effects of exposures***

Given the environmental deflection by WHFD exposure in tail, we also tested the effects of developmental exposure on cross-sectional methylation at PND21 and 10 month tail samples. PND21 tail DNA methylation showed significant changes by exposure group at two candidate regions – *Igf2* and *Esr1*. *Igf2* encodes the Insulin-like growth factor 2 protein, an important regulator of cellular glucose transport during development (Fowden et al. 2006; O'Dell and Day 1998). The cross-sectional WHFD-mediated increase in early-life *Igf2* methylation may be a biological response to an increased simple sugar load, indicating that developmental exposure to WHFD can affect early-life establishment of age-related methylation at a gene related to metabolism and growth. Similarly, at the *Esr1* gene promoter, WHFD had a significant effect on mean methylation, with a decrease in methylation compared to Control at PND21. This suggests that developmental exposure to WHFD alters the epigenetic profile of the *Esr1* locus during development, potentially predisposing animals to increased *Esr1* transcription in anticipation of the Western diet's altered nutritional profile. Given the directionality of this exposure effect, developmental WHFD exposure, which is high in fat and has been linked to obesity, may increase transcription of the Estrogen Receptor α (ERα) early in life. Previous studies have shown that ERα is involved in control of lipid metabolism (Foryst-Ludwig and Kintscher 2010), with ERα knockout mice demonstrating increased adipose tissue deposition with aging (Cooke et al. 2001; Ohlsson et al. 2000). As a result, our results suggest that developmental exposure to WHFD could alter risk for obesity development via epigenetic misregulation of the *Esr1* locus. When a mismatch occurs between the developmental and postnatal environment, there is potential for improper regulation of epigenetic marks and disease development (Bateson et al. 2004; Waterland and Jirtle 2004). The significant effects of exposure on PND21 tail DNA

methylation at the *Igf2* and *Esr1* loci support this idea, indicating that developmental exposure to environmental factors may not only alter the rates of age-related methylation, but also the cross-sectional establishment of DNA methylation at specific genetic loci during development.

At the *Igf2* locus, BPA exposure had a marginally significant effect on mean tail methylation, with Control+BPA exposed mice showing decreased *Igf2* methylation compared to Control at both PND21 and 10 months. This result, which is not present in the Med+BPA or Western+BPA diets, indicates that BPA exposure alone may alter regulation of the *Igf2* gene. A previous study demonstrated decreased *Igf2* methylation and increased *Igf2* expression in developing embryos as a result of early-life 10 mg/kg/day BPA exposure (Susiarjo et al. 2013). Given these past results, the marginally significant effects of 50 µg BPA/kg diet exposure on *Igf2* methylation presented in this report may reflect BPA exposure-mediated alterations in *Igf2* expression, but further investigation is required. The LINE-1, IAP, and *H19* loci did not demonstrate significant cross-sectional effects by BPA exposure, suggesting that these three genetic regions are not sensitive to developmental BPA exposure.

***Effects of mediterranean diet on survival***

Separate from the epigenetic effects, the Mediterranean+BPA diet group had significantly improved PND21 survival rate compared to the Control+BPA diet group. Previous studies have observed that nutritional supplementation counteracts negative epigenetic effects on the epigenome (Bernal et al. 2013; Dolinoy et al. 2007). Furthermore, in multiple longitudinal human birth cohort studies, maternal adherence to a Mediterranean diet was associated with reduced risk of intrauterine growth restriction, low birth weight and low placental weight (Chatzi et al. 2012; Timmermans et al. 2012). Mothers consuming a Mediterranean diet also had higher circulating folate and vitamin B12 concentrations (Timmermans et al. 2012). Folate and vitamin

B12 are critical nutrients in the regeneration of *S*-adenosyl methionine, a major participant in DNA methylation maintenance; this suggests adherence to the Mediterranean diet may impact fetal epigenetic reprogramming. Therefore, it is possible that the developmental Mediterranean diet is providing a protective effect on survival by offsetting BPA-induced changes to epigenetic marks and gene regulation. Future studies should investigate this toxicant-diet interaction more fully.

***Limitations and future directions***

This study demonstrates measurable WHFD-based modifications to the rate of age-related methylation in murine tail and blood, but the potential biological effects of this environmental deflection remain unclear without concurrent, longitudinal measurements of gene expression. Longitudinal measures of gene expression would provide a validation of DNA methylation results, demonstrating whether age- and exposure-related alterations to the epigenome have measurable physiological effects. As such, future studies investigating the effects of early-life toxicant exposure on epigenetic aging could expand the interpretability of their results by examining the effects of exposure and age on longitudinal gene expression, and/or examining DNA methylation and expression levels in other biological tissues of interest including blood – which may be accessed at multiple time points – and target tissues such as liver and brain.

By using matched tail and blood tissues in this longitudinal study, age-related methylation rates reflected defined changes within organisms in the study population rather than changes in time between two separate populations. This matched design, combined with the controlled developmental exposure, isolates the effects of exposure for each organism in the study population, allowing for a direct test of the hypothesis that environmental factors can

modify the rates of epigenetic aging. Despite the longitudinal design, an inherent limitation of this study is the inability of bisulfite sequencing to differentiate between 5-methylcyosine (5-mC) and 5-hydroxymethylcytosine (5-hmC). Although hydroxymethylation is not expected to be a major epigenetic mark in tail or blood tissue, recent study showed that aging affects global hydroxymethylation in healthy hepatic tissue, with a general trend towards increasing 5-hmC levels in older mice (Tammen et al. 2014). This reported increase in global hepatic 5-hmC levels over time is at odds with the previously reported loss of global 5-mC in cancer cells (Issa 2014; Maegawa et al. 2014; Teschendorff et al. 2013), suggesting that these separate epigenetic marks may change in different ways during aging. As a result, future epigenetic aging studies must better characterize the effects of aging on 5-hmC levels at specific CpG sites in the genome, as well as across tissue types.

## 2.4 Conclusion

We measured longitudinal DNA methylation in tail and blood tissue collected from isogenic mice, and then quantified the magnitude of age-related methylation in these samples at five genetic loci – two repetitive elements, two imprinted genes, and one non-imprinted gene. The use of matched tissues from an isogenic mouse colony allowed for strict control of genetic, environmental, and dietary measures, as well as removal of potential confounding. This study demonstrates significant, gene-specific age-related methylation, supporting the growing hypothesis that epigenetic aging plays an important role in the link between aging and cancer (Decottignies and d'Adda di Fagagna 2011; Issa 2014; Teschendorff et al. 2010). In addition, we showed significant WHFD- and sex-dependent environmental deflection of both repetitive elements and a non-imprinted gene. These results indicate that developmental exposure to WHFD can affect the aging epigenome in a mouse model. WHFD-dependent changes in tail

DNA methylation were also evident in two investigated loci at PND21, demonstrating the effect of developmental exposure on early-life establishment of epigenetic marks. Finally, activity-related energy expenditure was shown to attenuate the effects of WHFD on age-related methylation at the *Esr1* locus in blood tissue. To improve the generalizability of these results, the dynamics of epigenetic aging at the studied gene regions should be further evaluated in human cohorts.

## 2.5 Materials and Methods

### *Mouse colony*

Mice were *a/a* offspring sourced from a genetically invariant $A^{vy}/a$ mouse colony maintained in the Dolinoy Lab via sibling mating and forced heterozygosity for more than 220 generations (Waterland 2003). Within this colony, the $A^{vy}$ allele is passed through the heterozygous male line, which has a genetically constant background 93% identical to C57BL/6J strain (Waterland 2003; Weinhouse et al. 2014). Two weeks prior to mate-pairing with $A^{vy}/a$ males, six week old wild type *a/a* dams were placed on one of six experimental diet groups: (1) Control (modified AIN-93G), (2) Control + 50 µg BPA/kg diet, (3) Mediterranean HFD chow, (4) Mediterranean + 50 µg BPA/kg diet, (5) Western HFD chow, and (6) Western HFD + 50 µg BPA/kg diet (**Figure 2-5**). Dietary exposure was continued through pregnancy and lactation, at which point treatment group pups were shifted over to a modified AIN-93G Control diet containing 7% corn oil rather than 7% soybean oil (Harlan Teklad). The 50 µg/kg diet BPA exposure level was chosen based on previous studies, which demonstrated both increased global methylation and sex-specific phenotypic effects at 50 µg/kg BPA (Anderson et al. 2013, 2012). BPA (0.01 g) was mixed with sucrose (9.99 g) in glass containers to achieve a 0.1% BPA mixture. To achieve the 50 µg/kg BPA concentration, 0.1% BPA/sucrose mixture was included

at 0.05 g/kg diet in custom Control/HFD diets by the manufacturer (Harlan Teklad). Western HFD and Mediterranean HFD mixtures were designed based on the U.S. junk food diet and the human Cretan diet, respectively (Block et al. 1985a, 1985b; Kafatos et al. 2000; Trichopoulou et al. 1993). Protein was kept constant between the three base diets, but vitamin levels, lipid ratios, and carbohydrate types were altered to mimic human consumption (**Table 2-6**).

***Exposure and tissue collection***

At postnatal day 21 (PND21), offspring were tail tipped, and collected tail tissue was frozen at -80°C. For each exposure group, a subset of PND 21 *a/a* wild-type pups were maintained until 10 months of age – Control: n = 22, Control+BPA: n=19, Mediterranean (Med): n=23, Mediterranean+BPA: n=24, Western: n=22, Western+BPA: n=23 (**Table 2-1**). At 2, 4, and 8 months of age, offspring were relocated to a new cage outfitted with an integrated open-circuit calorimetry system: Comprehensive Lab Animal Monitoring System (CLAMS, Columbus Instruments); in this context, a host of phenotypic measures were taken, including body weight, oxygen consumption, food intake, and physical activity. After three days in the CLAMS cages, mice were returned to their original cages. During the 2 and 4 month cage transfers, tail vein blood samples were collected from all mice. At 10 months of age, mice were sacrificed; tail and cardiac puncture blood samples were again collected. All animals in this study were stored in polycarbonate-free cages with *ad libitum* access to food and drinking water, and were maintained in accordance with Institute for Laboratory Animal Research (ILAR) guidelines (National Research Council (US) Committee for the Update of the Guide for the Care and Use of Laboratory Animals 2011). The study protocol was approved by the University of Michigan Committee on Use and Care of Animals (UCUCA).

***DNA isolation***

Genomic DNA was isolated from PND21 tail tissue (≤3mm) using a phenol-chloroform-isoamyl alcohol protocol (Sambrook and Russell 2006). Genomic DNA was isolated from 10 month tail tissue (3 mm) using the Maxwell Mouse Tail DNA Purification Kit (Promega, Cat. #AS1120). Genomic DNA was isolated from 2, 4, and 10 month frozen blood using the Qiagen Allprep DNA/RNA Mini Kit (Qiagen, Cat. #80204). Yield and purity of all DNA was measured using a NanoDrop spectrophotometer, and then genomic DNA was bisulfite converted using the Zymo Research 96-well EZ-methylation kit (Zymo Research, Cat. #D5004). Briefly, bisulfite conversion was accomplished through the addition of sodium bisulfite to 0.5-1 µg of genomic DNA, thereby converting unmethylated cytosines to uracil. Bisulfite converted DNA was then amplified using polymerase chain reaction (PCR), which causes uracils to be replaced with thymines. Remaining cytosines in the amplified PCR product are thereby a direct, quantitative measure of DNA methylation (Grunau et al. 2001). PCR amplification was performed on bisulfite converted DNA using HotStarTaq master mix (Qiagen, Cat. #203443), RNAse-free water, forward primer (9 pmol), and biotinylated reverse primer (9 pmol). Total PCR volume was 30-35 µL per sample, and gel electrophoresis was used to verify PCR product identity.

***DNA methylation measurement***

Specific PCR amplification for regions of interest (*Igf2, H19, Esr1,* IAP, and LINE-1) was performed on bisulfite converted DNA with primers designed using the PyroMark Assay Design software 2.0 and mm9 mouse genome. DNA methylation levels were quantified using the PyroMark Q96 MD instrument (Qiagen). Pyrosequencing samples were run in duplicate, and the average of the duplicates provided the final methylation percentages. Sample duplicates with coefficient of variation (%CV) > 10% were discarded and re-run. Pyrosequencing assay

information, including primer sequences, chromosomal location, annealing temperature, and sequences to analyze are available in **Table 2-7**. In an effort to reduce plate-to-plate batch effects, matched samples were run on the same plate for all PCR amplification and pyrosequencing runs. All pyrosequencing plates included 0% and 100% bisulfite converted methylation controls, as well as a no template control, to ensure proper functioning of the instrument and to provide background standards of methylation for each gene.

***Data analysis***

Matched tail tissue was collected at postnatal day 21 and 10 months of age from a total of 133 *a/a* offspring (**Table 2-1**). The effect of developmental BPA/HFD exposure on sex ratio and litter survival rate was determined by Fisher's exact test, with Control as the reference group. Litter number, sex ratio, and litter survival rate were compared between exposure groups using a combined statistical approach involving both 3-way ANOVAs and Independent Student's T-tests. This same approach was used to compare cross-sectional PND21 or 10 month methylation data by exposure group. Separate 3-way ANOVAs were performed to compare Control vs. Mediterranean vs. Western and Control+BPA vs. Med+BPA vs. Western+BPA exposure groups. Separate Student's t-tests were performed to individually compare methylation between base diets and their associated BPA exposure diet (e.g. Control vs. Control+BPA). For all ANOVAs, Tukey's post-hoc test was used to determine the significance of each group-to-group comparison.

In addition to tail, matched blood samples were collected at 2, 4, and 10 months of age from a total of 86 *a*/*a* offspring across four exposure groups – Control: n = 22 (10 female, 12 male), Control+BPA: n=19 (9 female, 10 male), Western: n=22 (11 female, 11 male), Western+BPA: n=23 (12 female, 11 male). Cross-sectional DNA methylation for each target

gene was compared between the Control, Western, Control+BPA, and Western+BPA exposure groups using ANOVA. For all ANOVAs, Tukey's post-hoc test was used to determine the significance of each group-to-group comparison. Physical activity (PA) data on multiple axes of movement -- X ambulatory counts, X total counts, and Z total counts – were measured using CLAMS cages (Columbus Instruments). We summarized physical activity data in a single activity-related energy expenditure (AEE) variable. AEE was calculated from total energy expenditure (TEE; kcal/kg/hour) and resting metabolic rate (RMR; kcal/kg/hour) using the following formula: AEE = 0.9(TEE) – RMR (Hills et al. 2014; Pontzer et al. 2016; Van Klinken et al. 2012). The 0.9 multiplier was based on the thermic effect of food (TEF), which was assumed to be ~10% of TEE (Hills et al. 2014). RMR was calculated from CLAMS data using a three step protocol. First, physical activity data was preprocessed using an optimized power function based on the CLAMS 20 minute sampling interval (Van Klinken et al. 2012). Second, a penalized spline regression model was used to model the time-course relationship between Energy Expenditure and Physical Activity for each mouse. Third, intercepts from the TEE vs. PA models were used to represent the RMR for each mouse. The AEE variable was log-transformed prior to its addition to regression models.

Mixed effect linear models were used to compare absolute methylation levels over time by exposure group. Age, exposure group, and sex were included as explanatory variables in all models. Linear mixed models for each target region also included a random factor to account for matched, within-individual data, as well as a random factor to account for within-litter effects. Environmental deflection of age-related methylation was compared by exposure group via inclusion of an age*exposure interaction term in all mixed models. For tail tissue models, an age*sex interaction term was included in an effort to identify and/or control for potential

modifying effects of sex on age-methylation levels. For blood, age*sex and age*log(AEE) interaction terms were also considered in mixed models; these terms were only included in the final model for *Esr1*, where they demonstrated statistical significance.

Mixed models for tail tissue were fit using the following format: *Methylation ~ Age + Sex + Exposure + Age:Exposure + Age:Sex + [1 | ID] + [1 | Litter]*. For blood, mixed models were fit using the following format: *Methylation ~ Age + Sex + Exposure + log(AEE) + Age:Exposure + Age:Sex + Age:log(AEE) + [1 | ID] + [1 | Litter]*. For all models, the methylation outcome variable was defined as mean methylation across all amplicon CpG sites for two passing replicates. The *lme4* package within the statistical program R was used for all linear mixed models (R version 3.2.3, http://www.r-project.org). Alpha significance levels were set at $p \leq 0.05$ for all statistical comparisons.

## 2.6 Disclosure of Potential Conflicts of Interest

The authors have no conflicts of interest and declare no competing financial interests.

## 2.7 Acknowledgements

This work was supported by the University of Michigan (UM) NIEHS/EPA Children's Environmental Health and Disease Prevention Center P01 (ES022844/RD83543601), the Michigan Lifestage Environmental Exposures and Disease (M-LEEaD) NIEHS Core Center (P30 ES017885), The University of Michigan Nutrition Obesity Research Center (P30 DK089503), as well as the UM NIEHS Institutional Training Grants T32 ES007062 (JJK, EHM), T32 HD079342 (EHM), and F31 ES025101 (EHM).

## 2.8 Figures and Tables

| Developmental Exposure Group | N (litter) | Female | Male | Pups (#) |
|---|---|---|---|---|
| Control | 14 | 10 | 12 | 22 |
| Control+BPA | 25 | 9 | 10 | 19 |
| Med HFD | 20 | 11 | 12 | 23 |
| Western HFD | 21 | 11 | 11 | 22 |
| Med+BPA | 15 | 12 | 12 | 24 |
| Western+BPA | 23 | 12 | 11 | 23 |
| *Total* | *118* | *65* | *68* | *133* |

**Table 2-1: Litter parameters.** A subset of n=133 mouse pups included in longitudinal follow-up. All pups in the longitudinal subset were maintained until sacrifice at 10 months of age.

| Age-Related Methylation in Tail | | | | | |
|---|---|---|---|---|---|
| **Gene** | **N** | **PND21 % Methylation (SE)** | **10M % Methylation (SE)** | **Methylation by Age - Beta coefficient†** | **p-value** |
| LINE-1 | 260 | 65.05 (0.12) | 63.50 (0.11) | -0.943 | ***0.035*** |
| IAP | 222 | 90.31 (0.13) | 88.62 (0.13) | -1.321 | ***2.20E-06*** |
| *Igf2* | 249 | 34.39 (0.78) | 37.87 (0.26) | 3.275 | 0.112 |
| *H19* | 257 | 58.87 (0.62) | 49.31 (0.27) | -10.436 | ***6.22E-08*** |
| *Esr1* | 260 | 4.26 (0.37) | 12.09 (0.26) | 7.604 | ***1.44E-12*** |

| Age-Related Methylation in Blood | | | | | | |
|---|---|---|---|---|---|---|
| **Gene** | **N** | **2M % Methylation (SE)** | **4M % Methylation (SE)** | **10M % Methylation (SE)** | **Methylation by Age - Beta coefficient†** | **p-value** |
| LINE-1 | 252 | 65.85 (0.10) | 65.62 (0.10) | 65.47 (0.10) | 0.085 | 0.542 |
| IAP | 252 | 92.64 (0.09) | 92.80 (0.10) | 92.62 (0.13) | 0.167 | 0.244 |
| *Igf2* | 245 | 46.45 (0.28) | 47.07 (0.22) | 47.05 (0.19) | 0.218 | 0.469 |
| *H19* | 237 | 42.79 (0.19) | 42.87 (0.23) | 43.00 (0.28) | -0.049 | 0.867 |
| *Esr1* | 244 | 50.71 (0.73) | 56.21 (0.62) | 58.69 (0.40) | 4.094 | ***3.64E-14*** |

**Table 2-2: Age-related DNA methylation in mouse tail and blood.** Linear mixed effect models were used to compare absolute methylation levels over time. Age, exposure group, sex, and age:exposure were included as terms in all models. Log(AEE)variable was included for blood variables. Linear mixed models for each gene also included a paired factor to account for matched, within-individual data, as well as a random factor to account for within-litter effects. Separate models were run for each gene; beta coefficients and associated p-values for age predictor from each model are reported. **BOLD** = $p<0.05$; † = Beta coefficient for age predictor in linear mixed effects model.

| Tail Age-related DNA Methylation by Exposure Group | | | | | | | | |
|---|---|---|---|---|---|---|---|---|
| | | | DNA Methylation | | Relative Methylation by Exposure | | Environmental Deflection | |
| **Gene** | **Developmental Exposure Group** | **N** | **PND21 % Methylation (SD)** | **10 Month % Methylation (SD)** | **Methylation by Age Beta Coefficient†** | **p-value** | **Age : Exposure Interaction Beta Coefficient†** | **p-value** |
| LINE-1 | Control | 44 | 64.86 (1.14) | 64.00 (1.40) | (Reference) | n/a | (Reference) | n/a |
| | Control+BPA | 38 | 64.78 (2.18) | 63.32 (1.32) | -0.079 | 0.855 | -0.596 | 0.316 |
| | Med | 44 | 64.81 (1.53) | 63.83 (1.43) | -0.040 | 0.925 | -0.132 | 0.820 |
| | Western | 43 | 65.18 (1.03) | 63.27 (1.13) | 0.331 | 0.431 | -1.052 | **0.069** |
| | Med+BPA | 47 | 65.08 (1.44) | 63.41 (1.29) | 0.232 | 0.568 | -0.818 | 0.147 |
| | Western+BPA | 46 | 64.97 (1.25) | 63.65 (1.09) | 0.122 | 0.766 | -0.450 | 0.426 |
| | | | | | | | | |
| IAP | Control | 38 | 89.98 (1.37) | 88.64 (1.60) | (Reference) | n/a | (Reference) | n/a |
| | Control+BPA | 32 | 90.56 (1.02) | 89.03 (1.19) | 0.560 | 0.279 | -0.358 | 0.299 |
| | Med | 38 | 89.86 (1.15) | 88.29 (1.15) | 0.783 | 0.169 | -0.291 | 0.410 |
| | Western | 34 | 90.34 (1.37) | 88.77 (1.37) | 0.484 | 0.356 | -0.645 | **0.058** |
| | Med+BPA | 42 | 90.74 (1.53) | 88.70 (1.53) | 0.206 | 0.689 | -0.325 | 0.335 |
| | Western+BPA | 38 | 90.37 (1.38) | 88.36 (1.38) | 0.788 | 0.135 | -0.649 | **0.051** |
| | | | | | | | | |
| *Igf2* | Control | 43 | 33.64 (6.23) | 38.07 (2.59) | (Reference) | n/a | (Reference) | n/a |
| | Control+BPA | 37 | 30.65 (8.26) | 37.59 (4.58) | -3.811 | **0.066** | 3.355 | 0.221 |
| | Med | 41 | 32.70 (10.69) | 37.83 (2.05) | -0.513 | 0.804 | 0.338 | 0.900 |
| | Western | 41 | 37.43 (11.04) | 36.99 (1.84) | 2.846 | 0.163 | -3.914 | 0.143 |
| | Med+BPA | 44 | 31.97 (8.02) | 38.61 (1.81) | -2.506 | 0.207 | 2.965 | 0.259 |
| | Western+BPA | 45 | 37.55 (8.26) | 38.25 (3.34) | 3.162 | 0.108 | -2.888 | 0.268 |
| | | | | | | | | |
| *H19* | Control | 38 | 59.77 (7.22) | 48.93 (2.86) | (Reference) | n/a | (Reference) | n/a |
| | Control+BPA | 31 | 58.77 (6.43) | 49.61 (2.29) | -0.830 | 0.650 | 1.588 | 0.521 |
| | Med | 42 | 58.43 (7.31) | 49.51 (3.84) | -1.956 | 0.249 | 2.601 | 0.266 |
| | Western | 42 | 59.75 (8.28) | 50.07 (3.23) | 0.426 | 0.806 | 0.814 | 0.730 |
| | Med+BPA | 42 | 58.43 (6.25) | 48.55 (2.67) | -1.047 | 0.532 | 0.688 | 0.766 |
| | Western+BPA | 37 | 58.02 (7.32) | 49.28 (3.03) | -2.334 | 0.173 | 2.776 | 0.236 |
| | | | | | | | | |
| *Esr1* | Control | 43 | 5.03 (2.25) | 11.90 (1.93) | (Reference) | n/a | (Reference) | n/a |
| | Control+BPA | 38 | 4.45 (1.56) | 12.07 (3.00) | -0.587 | 0.458 | 0.758 | 0.468 |
| | Med | 45 | 4.53 (1.84) | 12.07 (2.01) | -0.523 | 0.489 | 0.669 | 0.504 |
| | Western | 42 | 3.08 (1.12) | 11.48 (1.65) | -1.933 | **0.013*** | 1.620 | 0.112 |
| | Med+BPA | 46 | 3.96 (1.72) | 12.67 (4.95) | -1.089 | 0.150 | 1.851 | **0.064** |
| | Western+BPA | 46 | 4.51 (1.97) | 12.27 (3.14) | -0.604 | 0.424 | 0.988 | 0.321 |
| | | | | | | | | |

**Table 2-3: Tail DNA methylation by exposure group**. Average methylation by age group was compared across exposure groups using a linear mixed effects model. Age, exposure group, sex, age:exposure, and age:sex were included as terms in all models. Linear mixed models included a paired factor to account for matched, within-individual data, as well as a random factor to account for within-litter effects. Separate models were run for each gene; beta coefficients and associated p-values for the exposure categories from each model are reported. Environmental deflection of age-related methylation was tested across all exposure groups via inclusion of an age:exposure interaction term in the model. Control diet was used as the reference exposure in all comparisons. † = Beta coefficient for age predictor in Linear Mixed Model; **BOLD** = $p<0.10$; * = $p<0.05$

| Blood Age-related DNA Methylation by Exposure Group | | | | | | | | | |
|---|---|---|---|---|---|---|---|---|---|
| | | | DNA Methylation | | | Relative Methylation by Exposure | | Environmental Deflection | |
| **Gene** | **Exposure** | **N** | **2M % Methylation (SE)** | **4M % Methylation (SE)** | **10 Month % Methylation (SE)** | **Methylation by Age Beta Coefficient†** | **p-value** | **Age : Exposure Interaction Beta Coefficient†** | **p-value** |
| LINE-1 | Control | 64 | 65.58 (0.24) | 65.39 (0.20) | 65.66 (0.17) | (Reference) | n/a | (Reference) | n/a |
| | BPA | 57 | 65.89 (0.19) | 65.44 (0.23) | 65.52 (0.19) | 0.365 | 0.172 | -0.228 | 0.249 |
| | Western | 66 | 66.24 (0.18) | 65.80 (0.17) | 65.31 (0.26) | 0.762 | **0.003*** | -0.493 | **0.010*** |
| | Western +BPA | 65 | 65.69 (0.16) | 65.84 (0.23) | 65.38 (0.19) | 0.347 | 0.173 | -0.181 | 0.343 |
| | | | | | | | | | |
| IAP | Control | 64 | 92.44 (0.18) | 92.69 (0.12) | 92.78 (0.20) | (Reference) | n/a | (Reference) | n/a |
| | BPA | 57 | 92.60 (0.19) | 92.95 (0.15) | 92.75 (0.32) | 0.228 | 0.430 | -0.099 | 0.626 |
| | Western | 66 | 92.71 (0.14) | 92.84 (0.26) | 92.27 (0.22) | 0.367 | 0.307 | -0.395 | **0.046*** |
| | Western +BPA | 65 | 92.77 (0.17) | 92.73 (0.21) | 92.71 (0.29) | 0.299 | 0.185 | -0.199 | 0.312 |
| | | | | | | | | | |
| *Igf2* | Control | 63 | 46.50 (0.35) | 46.91 (0.39) | 46.92 (0.41) | (Reference) | n/a | (Reference) | n/a |
| | BPA | 55 | 46.43 (0.50) | 47.10 (0.48) | 48.17 (0.65) | -0.270 | 0.676 | 0.636 | 0.138 |
| | Western | 65 | 46.58 (0.33) | 46.97 (0.47) | 46.49 (0.51) | 0.165 | 0.785 | -0.323 | 0.429 |
| | Western +BPA | 62 | 46.29 (0.42) | 47.32 (0.44) | 46.69 (0.59) | -0.004 | 0.994 | -0.033 | 0.937 |
| | | | | | | | | | |
| *H19* | Control | 60 | 43.16 (0.39) | 42.96 (0.44) | 43.06 (0.46) | (Reference) | n/a | (Reference) | n/a |
| | BPA | 56 | 42.44 (0.36) | 42.01 (0.51) | 42.25 (0.72) | -0.739 | 0.256 | -0.095 | 0.816 |
| | Western | 62 | 42.31 (0.27) | 42.47 (0.36) | 42.89 (0.56) | -0.747 | 0.235 | 0.261 | 0.513 |
| | Western +BPA | 59 | 43.32 (0.50) | 43.93 (0.43) | 43.76 (0.52) | 0.307 | 0.631 | 0.264 | 0.518 |
| | | | | | | | | | |
| *Esr1* | Control | 61 | 50.62 (0.90) | 56.36 (1.34) | 59.18 (1.46) | (Reference) | n/a | (Reference) | n/a |
| | BPA | 55 | 50.25 (0.84) | 56.30 (1.35) | 59.58 (1.34) | -0.327 | 0.732 | 0.503 | 0.480 |
| | Western | 63 | 51.48 (0.80) | 56.21 (1.11) | 56.64 (1.57) | 1.417 | 0.114 | -1.489 | **0.029*** |
| | Western +BPA | 65 | 50.41 (0.68) | 56.00 (1.27) | 59.47 (1.42) | 0.139 | 0.876 | 0.389 | 0.565 |
| | | | | | | | | | |

**Table 2-4: Blood DNA methylation by exposure group**. Average methylation by age group was compared across exposure groups using a linear mixed effects model. Age, exposure group, age:exposure, and log(AEE) were included as terms in all models. Linear mixed models included id and litter random factors to account for intra-individual and within-litter effects. Separate models were run for each gene; beta coefficients and associated p-values for the exposure categories from each model are reported. Environmental deflection of age-related methylation was tested across all exposure groups via inclusion of an age:exposure interaction term in the model. Control diet was used as the reference exposure in all comparisons. † = Beta coefficient for age predictor in Linear Mixed Model; **BOLD** = $p<0.10$; * = $p<0.05$.

| Male Esr1 Age-related Methylation in Blood | | | | | Female *Esr1* Age-related Methylation in Blood | | | | |
|---|---|---|---|---|---|---|---|---|---|
| **Variable** | **Estimate** | **SE** | **DF** | **p-value** | **Variable** | **Estimate** | **SE** | **DF** | **p-value** |
| (Intercept) | 53.41 | 0.79 | 109.7 | <2E-16 | (Intercept) | 48.11 | 0.84 | 76.5 | <2E-16 |
| **Age** | **4.22** | **1.42** | **115.7** | **0.004** | **Age** | **2.11** | **0.62** | **93.8** | **0.001** |
| BPA | -0.01 | 1.17 | 109.8 | 0.990 | BPA | -0.76 | 1.25 | 79.8 | 0.544 |
| WHFD | 0.88 | 1.12 | 109.2 | 0.434 | WHFD | 1.70 | 1.15 | 76.2 | 0.144 |
| WHFD + BPA | -0.28 | 1.12 | 109.1 | 0.801 | WHFD + BPA | 0.28 | 1.13 | 76.3 | 0.807 |
| log(AEE) | -2.97 | 1.98 | 85.7 | 0.137 | log(AEE) | -2.91 | 3.29 | 109.0 | 0.379 |
| Age:BPA | 0.17 | 0.86 | 81.9 | 0.846 | Age:BPA | 1.06 | 0.76 | 74.3 | 0.167 |
| Age:WHFD | -0.83 | 0.84 | 81.9 | 0.324 | **Age:WHFD** | **-1.67** | **0.70** | **71.4** | **0.020** |
| Age:WHFD + BPA | 0.80 | 0.88 | 85.7 | 0.362 | Age:WHFD + BPA | 0.74 | 0.70 | 72.1 | 0.293 |
| Age:log(AEE) | 1.59 | 1.22 | 116.0 | 0.193 | Age:log(AEE) | 1.40 | 1.65 | 89.6 | 0.399 |

**Table 2-5: Age-related *Esr1* methylation stratified by sex.** Beta estimates/coefficients for the *Esr1* linear mixed models stratified by sex. Age is a significant predictor in both models, but only female mice show significant negative environmental deflection by WHFD. Age:log(AEE) has a positive, non-significant coefficient in both male and female models.

| Nutrient Content in 3 Base Diets | | | |
|---|---|---|---|
| **Diet Nutrients** | **Control** | **Mediterranean** | **Western** |
| Kcal/g | 3.98 | 4.53 | 4.72 |
| %Calories from Fat | 16% | 42% | 40% |
| PUFE : SFA : MUFA | 1 : 0.2 : 0.5 | 1 : 1.3 : 5.6 | 1 : 1.9 : 1.6 |
| Protein (casein) | 20 | 19 | 19 |
| Carb Content (g/100 g chow) | | | |
| *Cornstarch* | 40 | 23 | 14 |
| *Sucrose* | 10 | 9.2 | 25.5 |
| *Cellulose* | 5 | 8 | 2 |
| Vitamin A (IU) | 4000 | 8000 | 4000 |
| Vitamin C (mg) | 0 | 500 | 0 |
| Vitamin D (IU) | 1000 | 1000 | 400 |
| Vitamin E (IU) | 75 | 75 | 25 |
| Folic Acid (mg) | 2 | 4 | 1 |
| Sodium (mg) | 1039 | 1039 | 7000 |
| Potassium (mg) | 3600 | 8000 | 3600 |
| Magnesium (mg) | 513 | 850 | 513 |

**Table 2-6: Comparison of nutrient content by diet**. Three base diets were included as developmental exposures in this study – Control, Mediterranean HFD, and Western HFD. For all three base diets, protein was kept constant, but vitamin levels, lipid ratios, and carbohydrate types were altered to mimic human consumption. BPA was added to each diet to produce three additional developmental dietary exposure groups – Control+BPA, Med+BPA, and Western+BPA. Apart from BPA addition, nutrient content was not altered from the base diet levels in these three groups.

| Primer/ Sequence to Analyze | *Igf2*[1] | *H19*[1] | LINE-1 | IAP | *Esr1*[2] |
|---|---|---|---|---|---|
| **Location** | chr7:149839707 –149839926 strand = reverse | chr7:149767589-149767843 | Repetitive Element | Repetitive Element | chr10:4712147-4712203 |
| **Forward PCR Primer** | TTTTTTAATA TGATATTTGG AGATAGTT | GGGGGGTTAT AAATGTTATT AGGGGGGTA GG | AAGGGGTTTG TGTTTTAGAT TAGG | GTGTTATTTTT TGATTGGTTGT AGTTT | TTTGGAAGT TGTAGTTTTT GGTTAGT |
| **Reverse PCR Primer** | biotin-CCACATAATT TAATTCACTA ATAATT ACTA | biotin-AACCCCTAAC CTCATAAAAC CCATAACTAT AAAATCA | biotin-AACTCCCCAC CAAATCCTAA AACCTCTA | biotin-ACCAAAAATA TCTTATAACTA CTTATACT | biotin-ACAAAACAC AAATAACCC AACTC |
| **Sequencing Primer** | AATATGATAT TT GGCGATAGTT | GTGTAAAGAT TAGGGTTGT | AGTTTGTTTT TTTATGTATT ATAGT | ATTTTTTGATT GGTTGTAGTTT A | GGAGAGGAG TATGTAAAG |
| **Sequence to Analyze** | YGYGGGAYG T TTGYGTAGAG GTTTGTTTGT TTTTTTGYGT GTTYGTYGGG GTYGT | GYGGTYAGTG AAGTTTYGTA TATYG | TTTAGGTTTY GYGYGATTGG ATTGGGGTAG AYGTTGTGTT TTATTTATTA GAGGTTT | TYGGTYGAGT TGAYGTTAYG GGGAAAGTAG AGTATAAGTA GTTA | TTGGAGAAT T YGGGAGYGT T TGGGTGYGT T TTTTGGAGTT GGGTTATTT G TGTTTT |
| **Amplicon Length (bp)** | 220 | 255 | 132 | 87 | 131 |
| **Annealing Temperature (°C)** | 56 | 55 | 61 | 56 | 55 |
| **Number of Cycles** | 50 | 40 | 44 | 45 | 40 |
| **Number of CpG Sites** | 8 | 4 | 4 | 4 | 3 |

**Table 2-7: Pyrosequencing assay PCR conditions.** Information for each assay, including genomic location, primer sequences (5'-3'), sequence to analyze, amplicon length, annealing temperature, number of cycles, and number of CpG sites measured. [1]Assays from Faulk et al. 2014; [2]Assay adapted from Maegawa et al. 2010.

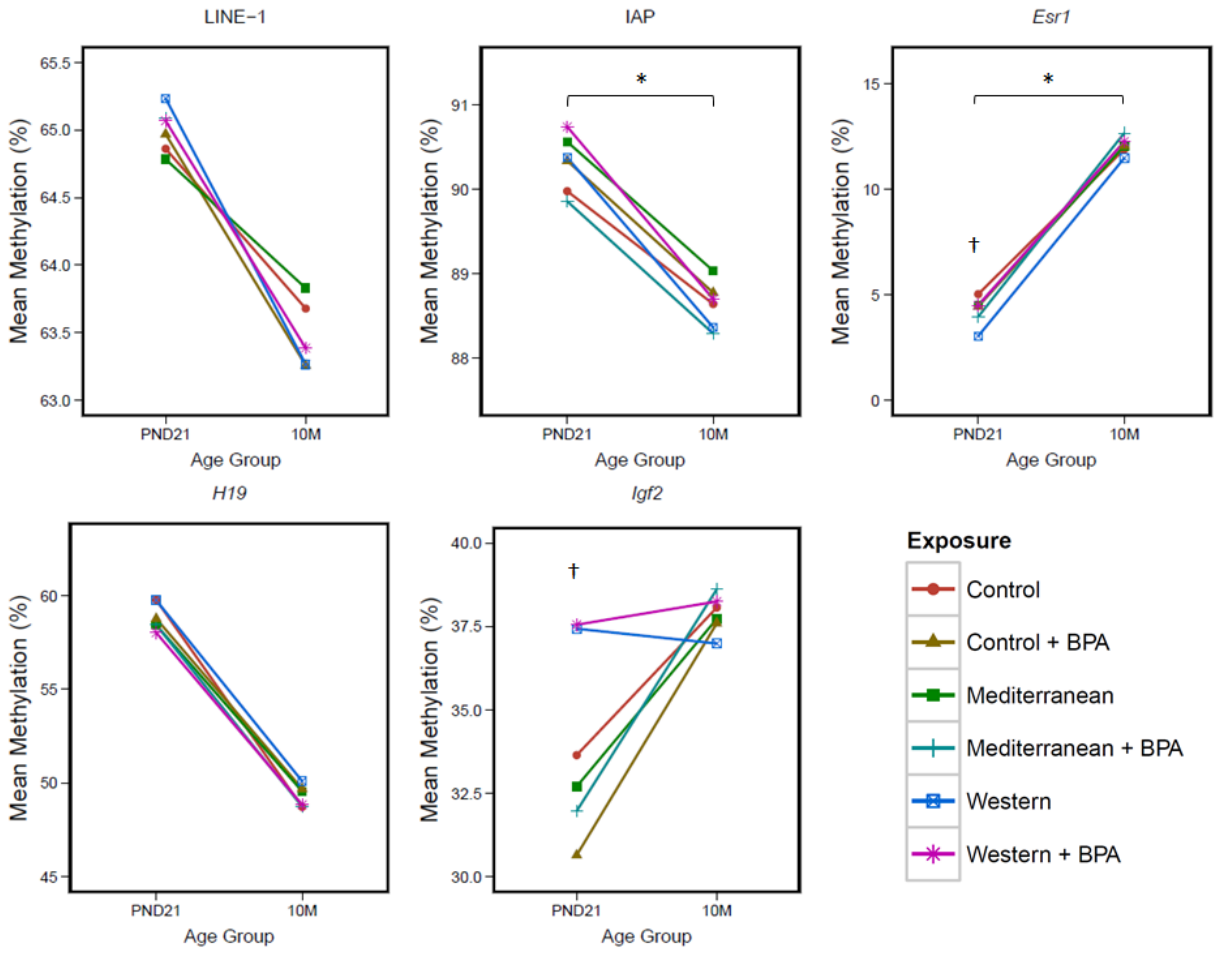


**Figure 2-1: Methylation drift by exposure group.** Visualization of age-related methylation over time at five target loci. LINE-1, H19, and IAP demonstrated a negative association between age and % methylation, while *Esr1* and *Igf2* demonstrated a positive association between age and % methylation. * = age:exposure interaction term p-value <0.10 for at least one exposure group in linear mixed model. † = ANOVA/t-test p-value <0.05 for cross-sectional comparison by exposure group.

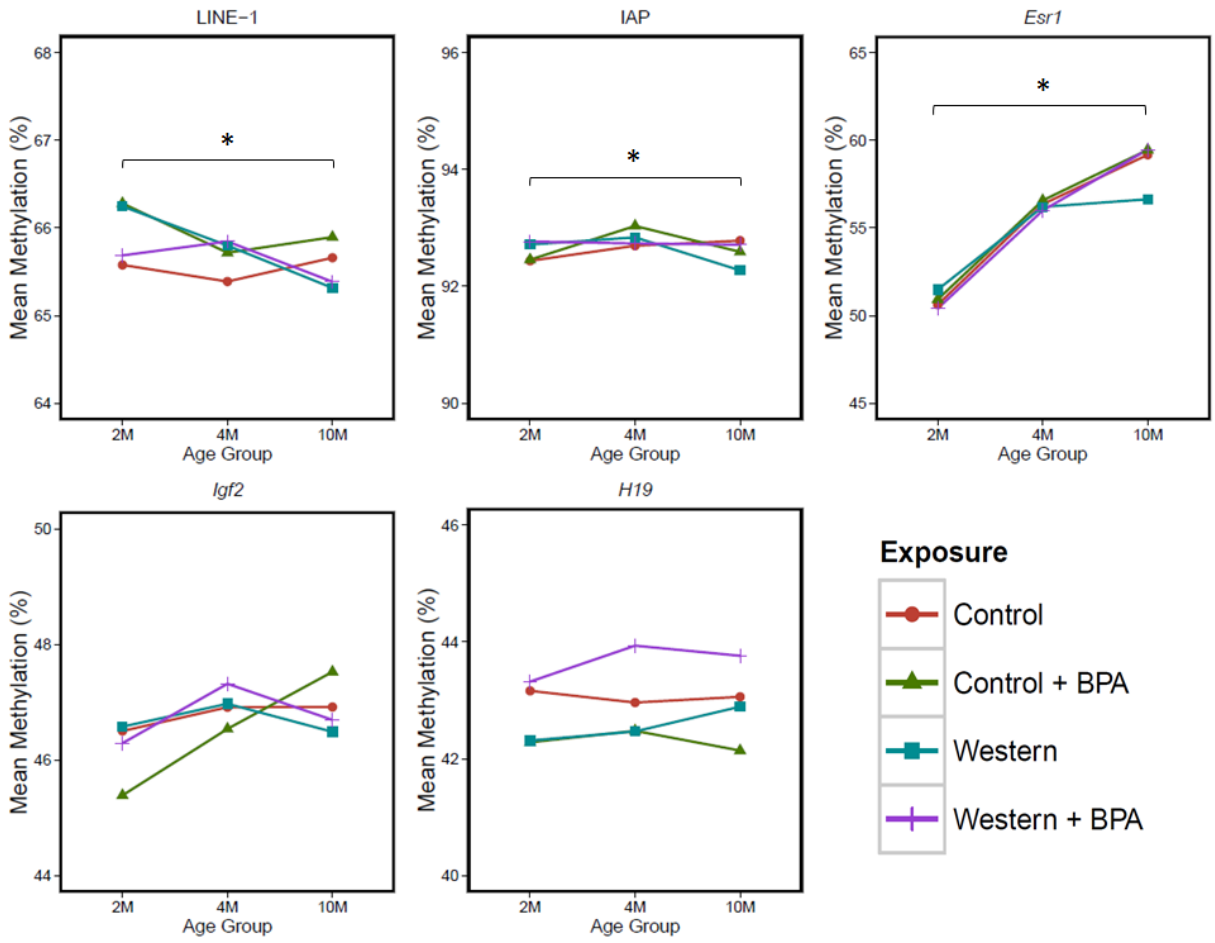


**Figure 2-2: Environmental deflection of age-related methylation by exposure group**. Visualization of environmental deflection by exposure at five target loci. LINE-1, IAP, and *Esr1* demonstrated significant negative deflection of age-related methylation in Western-exposed mice compared to control. Igf2 and H19 did not display environmental deflection by WHFD. * = age:exposure interaction term p-value <0.05 for WHFD exposure group in linear mixed model.

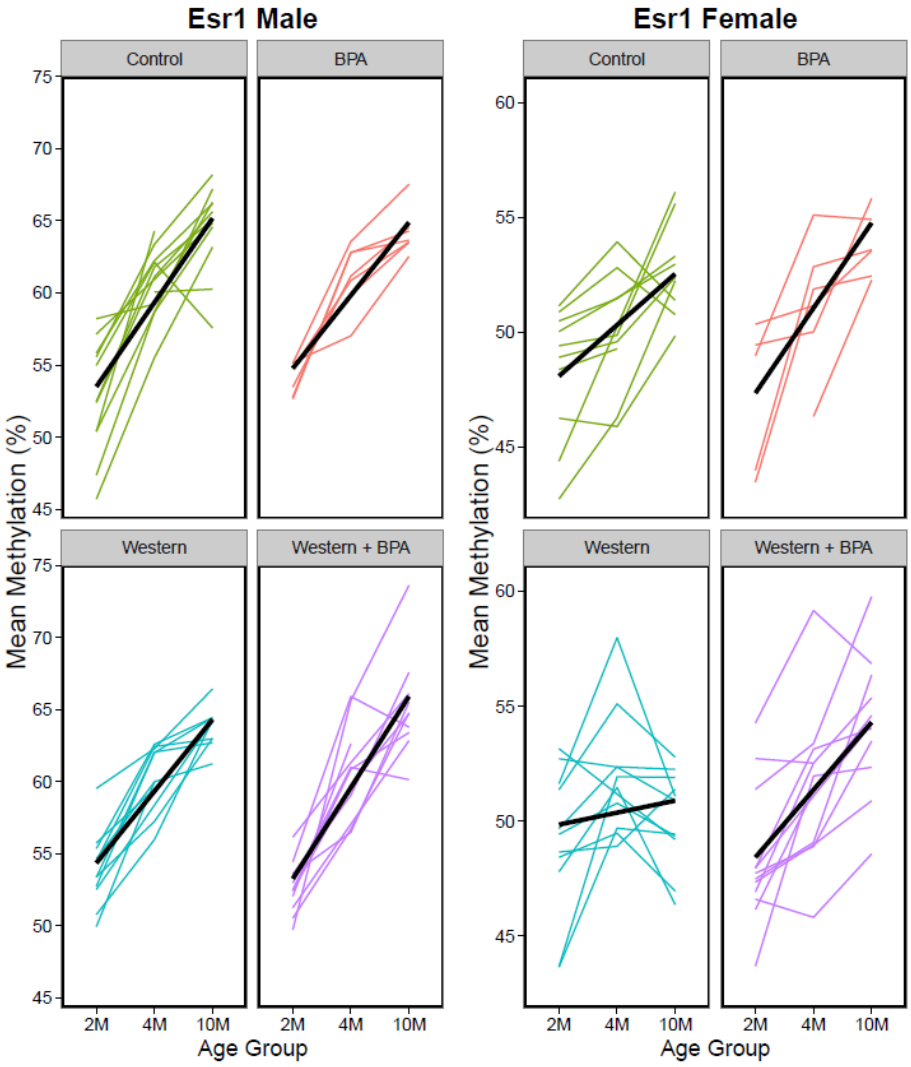


**Figure 2-3: Age-related *Esr1* DNA methylation split by exposure and sex**. Spaghetti plot of age-related *Esr1* methylation as it varies by both exposure and sex. WHFD-exposed female mice had a decreased rate of age-related methylation compared to control (p=0.026). No other group showed a significant interaction between age and DNA methylation.

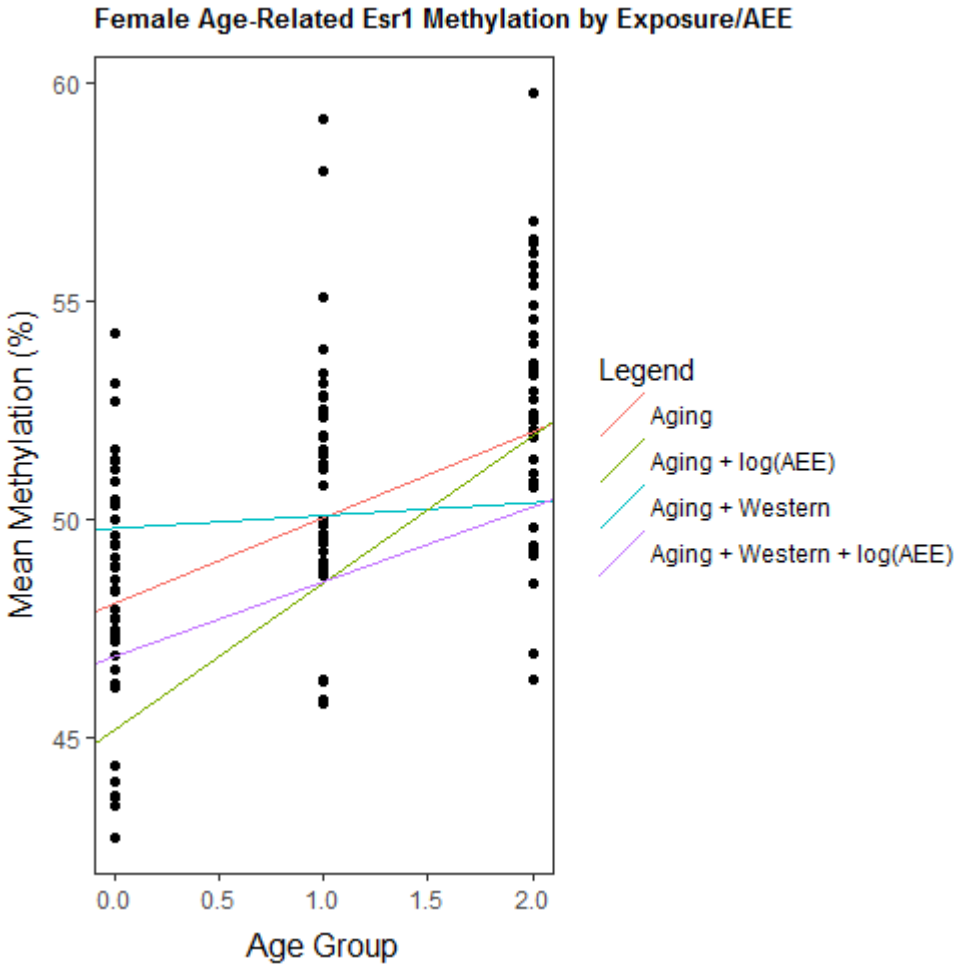


**Figure 2-4: Age-related *Esr1* methylation for female mice**. Slope estimates of the relationship between age and methylation for female mice. Slope estimates are separated based on exposure to Western diet and/or AEE. Slope estimates are based on beta values from the *Esr1* linear mixed model for female mice. In the legend, "aging" refers to the baseline rate of age-related methylation, which is conceptualized as the beta estimate for the age term in the model when AEE and/or WHFD exposure are not considered. The other terms in the legend represent the effect of exposure and/or physical activity beta estimates on the baseline rate of age-related methylation. AEE and WHFD had opposing effects on Esr1 methylation rate in female mouse blood.

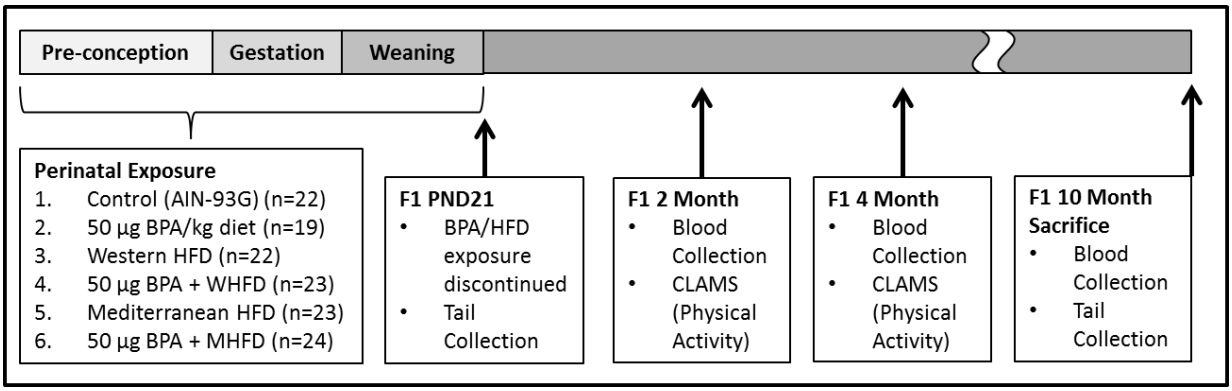


**Figure 2-5: Diagram of exposure timing**. F0 dams were assigned to one of six dietary BPA/HFD exposure groups two weeks prior to mating. Exposure continued throughout conception, gestation, and through lactation until weaning at post-natal day 21 (PND21). After weaning, offspring were transferred to an ad libitum Control diet, which continued until sacrifice at 10 months of age. Matched tail tips were collected at both PND21 and 10 months, and matched blood samples were collected at 2, 4, and 10 months. CLAMS data was collected during animal phenotyping at 2, 4, and 8 months of age.

## 2.9 References


Anderson OS, Nahar MS, Faulk C, Jones TR, Liao C, Kannan K, et al. 2012. Epigenetic responses following maternal dietary exposure to physiologically relevant levels of bisphenol A. Environ. Mol. Mutagen. 53:334–342; doi:10.1002/em.21692.

Anderson OS, Peterson KE, Sanchez BN, Zhang Z, Mancuso P, Dolinoy DC. 2013. Perinatal bisphenol A exposure promotes hyperactivity, lean body composition, and hormonal responses across the murine life course. FASEB J 27:1784–1792; doi:10.1096/fj.12-223545.

Barbot W, Dupressoir A, Lazar V, Heidmann T. 2002. Epigenetic regulation of an IAP retrotransposon in the aging mouse: progressive demethylation and de-silencing of the element by its repetitive induction. Nucleic Acids Res. 30: 2365–73.

Bateson P, Barker D, Clutton-Brock T, Deb D, D'Udine B, Foley RA, et al. 2004. Developmental plasticity and human health. Nature 430:419–421; doi:10.1038/nature02725.

Bernal AJ, Dolinoy DC, Huang D, Skaar DA, Weinhouse C, Jirtle RL. 2013. Adaptive radiation-induced epigenetic alterations mitigated by antioxidants. FASEB J. 27:665–671; doi:10.1096/fj.12-220350.

Bernal AJ, Jirtle RL. 2010. Epigenomic disruption: the effects of early developmental exposures. Birth Defects Res A Clin Mol Teratol 88:938–944; doi:10.1002/bdra.20685.

Block G, Dresser CM, Hartman AM, Carroll MD. 1985a. Nutrient sources in the American diet: quantitative data from the NHANES II survey. I. Vitamins and minerals. Am. J. Epidemiol. 122: 13–26.

Block G, Dresser CM, Hartman AM, Carroll MD. 1985b. Nutrient sources in the American diet: quantitative data from the NHANES II survey. II. Macronutrients and fats. Am. J. Epidemiol. 122: 27–40.

Bondesson M, Hao R, Lin C-Y, Williams C, Gustafsson J-Å. 2015. Estrogen receptor signaling during vertebrate development. Biochim. Biophys. Acta 1849:142–51; doi:10.1016/j.bbagrm.2014.06.005.

Calafat AM, Ye X, Wong LY, Reidy JA, Needham LL. 2008. Exposure of the U.S. population to bisphenol A and 4-tertiary-octylphenol: 2003-2004. Env. Heal. Perspect 116:39–44; doi:10.1289/ehp.10753.

Challen GA, Sun D, Jeong M, Luo M, Jelinek J, Berg JS, et al. 2011. Dnmt3a is essential for hematopoietic stem cell differentiation. Nat Genet 44:23–31; doi:10.1038/ng.1009.

Chatzi L, Mendez M, Garcia R, Roumeliotaki T, Ibarluzea J, Tardón A, et al. 2012. Mediterranean diet adherence during pregnancy and fetal growth: INMA (Spain) and RHEA (Greece) mother–child cohort studies. Br. J. Nutr. 107:135–145;

doi:10.1017/S0007114511002625.

Chia N, Wang L, Lu X, Senut M-C, Brenner C, Ruden DM. 2011. Hypothesis: environmental regulation of 5-hydroxymethylcytosine by oxidative stress. Epigenetics 6: 853–6.

Christensen BC, Houseman EA, Marsit CJ, Zheng S, Wrensch MR, Wiemels JL, et al. 2009. Aging and environmental exposures alter tissue-specific DNA methylation dependent upon CpG island context. PLoS Genet 5:e1000602; doi:10.1371/journal.pgen.1000602.

Cooke PS, Heine PA, Taylor JA, Lubahn DB. 2001. The role of estrogen and estrogen receptor-alpha in male adipose tissue. Mol. Cell. Endocrinol. 178: 147–54.

Coulter JB, O'Driscoll CM, Bressler JP. 2013. Hydroquinone increases 5-hydroxymethylcytosine formation through ten eleven translocation 1 (TET1) 5-methylcytosine dioxygenase. J Biol Chem 288:28792–28800; doi:10.1074/jbc.M113.491365.

Decottignies A, d'Adda di Fagagna F. 2011. Epigenetic alterations associated with cellular senescence: A barrier against tumorigenesis or a red carpet for cancer? Semin. Cancer Biol. 21:360–366; doi:10.1016/j.semcancer.2011.09.003.

Dolinoy DC, Huang D, Jirtle RL. 2007. Maternal nutrient supplementation counteracts bisphenol A-induced DNA hypomethylation in early development. Proc Natl Acad Sci U S A 104:13056–13061; doi:10.1073/pnas.0703739104.

Egger G, Liang G, Aparicio A, Jones PA. 2004. Epigenetics in human disease and prospects for epigenetic therapy. Nature 429:457–463; doi:10.1038/nature02625.

Faulk C, Kim JH, Anderson OS, Nahar MS, Jones TR, Sartor MA, et al. Detection of differential DNA methylation in repetitive DNA of mice and humans perinatally exposed to bisphenol A. Epigenetics. 2016;11:489–500.

Faulk C, Liu K, Barks A, Goodrich JM, Dolinoy DC. 2014. Longitudinal epigenetic drift in mice perinatally exposed to lead. Epigenetics 9:934–941; doi:10.4161/epi.29024.

Florath I, Butterbach K, Müller H, Bewerunge-Hudler M, Brenner H. 2014. Cross-sectional and longitudinal changes in DNA methylation with age: an epigenome-wide analysis revealing over 60 novel age-associated CpG sites. Hum Mol Genet 23:1186–1201; doi:10.1093/hmg/ddt531.

Foryst-Ludwig A, Kintscher U. 2010. Metabolic impact of estrogen signalling through ERalpha and ERbeta. J. Steroid Biochem. Mol. Biol. 122:74–81; doi:10.1016/j.jsbmb.2010.06.012.

Fowden AL, Sibley C, Reik W, Constancia M. 2006. Imprinted Genes, Placental Development and Fetal Growth. Horm. Res. Paediatr. 65:50–58; doi:10.1159/000091506.

Fraga MF, Ballestar E, Paz MF, Ropero S, Setien F, Ballestar ML, et al. 2005. Epigenetic differences arise during the lifetime of monozygotic twins. Proc Natl Acad Sci U S A 102:10604–10609; doi:10.1073/pnas.0500398102.

Grunau C, Clark SJ, Rosenthal A. 2001. Bisulfite genomic sequencing: systematic investigation of critical experimental parameters. Nucleic Acids Res 29: E65-5.

Hahn MA, Szabo PE, Pfeifer GP. 2014. 5-Hydroxymethylcytosine: a stable or transient DNA modification? Genomics 104:314–323; doi:10.1016/j.ygeno.2014.08.015.

Heinonen I, Rinne P, Ruohonen ST, Ruohonen S, Ahotupa M, Savontaus E. 2014. The effects of equal caloric high fat and western diet on metabolic syndrome, oxidative stress and vascular endothelial function in mice. Acta Physiol 211:515–527; doi:10.1111/apha.12253.

Hills AP, Mokhtar N, Byrne NM. 2014. Assessment of Physical Activity and Energy Expenditure: An Overview of Objective Measures. Front. Nutr. 1:5; doi:10.3389/fnut.2014.00005.

Hollingsworth JW, Maruoka S, Boon K, Garantziotis S, Li Z, Tomfohr J, et al. 2008. In utero supplementation with methyl donors enhances allergic airway disease in mice. J Clin Invest 118:3462–3469; doi:10.1172/JCI34378.

Horie K, Saito E-S, Keng VW, Ikeda R, Ishihara H, Takeda J. 2007. Retrotransposons influence the mouse transcriptome: implication for the divergence of genetic traits. Genetics 176:815–27; doi:10.1534/genetics.107.071647.

Hoyo C, Murtha AP, Schildkraut JM, Jirtle RL, Demark-Wahnefried W, Forman MR, et al. 2011. Methylation variation at IGF2 differentially methylated regions and maternal folic acid use before and during pregnancy. Epigenetics 6: 928–36.

Huen K, Yousefi P, Bradman A, Yan L, Harley KG, Kogut K, et al. 2014. Effects of age, sex, and persistent organic pollutants on DNA methylation in children. Environ. Mol. Mutagen. 55:209–222; doi:10.1002/em.21845.

Issa JP. 2014. Aging and epigenetic drift: a vicious cycle. J Clin Invest 124:24–29; doi:10.1172/JCI69735.

Kafatos A, Verhagen H, Moschandreas J, Apostolaki I, Van Westerop JJ. 2000. Mediterranean diet of Crete: foods and nutrient content. J. Am. Diet. Assoc. 100: 1487–93.

Kanzleiter T, Jähnert M, Schulze G, Selbig J, Hallahan N, Schwenk RW, et al. 2015. Exercise training alters DNA methylation patterns in genes related to muscle growth and differentiation in mice. Am J Physiol Endocrinol Metab 308:E912-20; doi:10.1152/ajpendo.00289.2014.

Kim JH, Sartor MA, Rozek LS, Faulk C, Anderson OS, Jones TR, et al. 2014. Perinatal

bisphenol A exposure promotes dose-dependent alterations of the mouse methylome. BMC Genomics 15:30; doi:10.1186/1471-2164-15-30.

King-Himmelreich TS, Schramm S, Wolters MC, Schmetzer J, Möser C V, Knothe C, et al. 2016. The impact of endurance exercise on global and AMPK gene-specific DNA methylation. Biochem Biophys Res Commun 474:284–290; doi:10.1016/j.bbrc.2016.04.078.

Krüger T, Long M, Bonefeld-Jørgensen EC. 2008. Plastic components affect the activation of the aryl hydrocarbon and the androgen receptor. Toxicology 246:112–123; doi:10.1016/j.tox.2007.12.028.

Laker RC, Lillard TS, Okutsu M, Zhang M, Hoehn KL, Connelly JJ, et al. 2014. Exercise prevents maternal high-fat diet-induced hypermethylation of the Pgc-1α gene and age-dependent metabolic dysfunction in the offspring. Diabetes 63:1605–1611; doi:10.2337/db13-1614.

LaRocca J, Binder AM, McElrath TF, Michels KB. 2014. The impact of first trimester phthalate and phenol exposure on IGF2/H19 genomic imprinting and birth outcomes. Environ. Res. 133:396–406; doi:10.1016/j.envres.2014.04.032.

Lee H-S, Barraza-Villarreal A, Biessy C, Duarte-Salles T, Sly PD, Ramakrishnan U, et al. 2014. Dietary supplementation with polyunsaturated fatty acid during pregnancy modulates DNA methylation at *IGF2/H19* imprinted genes and growth of infants. Physiol. Genomics 46:851–857; doi:10.1152/physiolgenomics.00061.2014.

Madrigano J, Baccarelli AA, Mittleman MA, Sparrow D, Vokonas PS, Tarantini L, et al. 2012. Aging and epigenetics: Longitudinal changes in gene-specific DNA methylation. Epigenetics 7:63–70; doi:10.4161/epi.7.1.18749.

Maegawa S, Gough SM, Watanabe-Okochi N, Lu Y, Zhang N, Castoro RJ, et al. 2014. Age-related epigenetic drift in the pathogenesis of MDS and AML. Genome Res 24:580–591; doi:10.1101/gr.157529.113.

Maegawa S, Hinkal G, Kim HS, Shen L, Zhang L, Zhang J, et al. 2010. Widespread and tissue specific age-related DNA methylation changes in mice. Genome Res 20:332–340; doi:10.1101/gr.096826.109.

Manikkam M, Tracey R, Guerrero-Bosagna C, Skinner MK. 2013. Plastics Derived Endocrine Disruptors (BPA, DEHP and DBP) Induce Epigenetic Transgenerational Inheritance of Obesity, Reproductive Disease and Sperm Epimutations. T. Shioda, ed PLoS One 8:e55387; doi:10.1371/journal.pone.0055387.

McKay JA, Xie L, Harris S, Wong YK, Ford D, Mathers JC. 2011. Blood as a surrogate marker for tissue-specific DNA methylation and changes due to folate depletion in post-partum female mice. Mol. Nutr. Food Res. 55:1026–35; doi:10.1002/mnfr.201100008.

Medvedeva YA, Khamis AM, Kulakovskiy I V, Ba-Alawi W, Bhuyan MS, Kawaji H, et al. 2014. Effects of cytosine methylation on transcription factor binding sites. BMC Genomics 15:119; doi:10.1186/1471-2164-15-119.

Myles IA. 2014. Fast food fever: reviewing the impacts of the Western diet on immunity. Nutr J 13:61; doi:10.1186/1475-2891-13-61.

National Research Council (US) Committee for the Update of the Guide for the Care and Use of Laboratory Animals. 2011.In: *Guide for the Care and Use of Laboratory Animals*. National Academies Press (U.S.):Washington, D.C.

Nelson HH, Marsit CJ, Kelsey KT. 2011. Global Methylation in Exposure Biology and Translational Medical Science. Environ. Health Perspect. 119:1528–1533; doi:10.1289/ehp.1103423.

Newbold RR, Padilla-Banks E, Jefferson WN. 2009. Environmental estrogens and obesity. Mol. Cell. Endocrinol. 304:84–9; doi:10.1016/j.mce.2009.02.024.

Nguyen A, Duquette N, Mamarbachi M, Thorin E. 2016. Epigenetic Regulatory Effect of Exercise on Glutathione Peroxidase 1 Expression in the Skeletal Muscle of Severely Dyslipidemic Mice. PLoS One 11:e0151526; doi:10.1371/journal.pone.0151526.

Niculescu MD, Craciunescu CN, Zeisel SH. 2006. Dietary choline deficiency alters global and gene-specific DNA methylation in the developing hippocampus of mouse fetal brains. FASEB J 20:43–49; doi:10.1096/fj.05-4707com.

O'Dell SD, Day IN. 1998. Insulin-like growth factor II (IGF-II). Int. J. Biochem. Cell Biol. 30: 767–71.

Ohlsson C, Hellberg N, Parini P, Vidal O, Bohlooly M, Rudling M, et al. 2000. Obesity and Disturbed Lipoprotein Profile in Estrogen Receptor-α-Deficient Male Mice. Biochem. Biophys. Res. Commun. 278:640–645; doi:10.1006/bbrc.2000.3827.

Parle-McDermott A, Ozaki M. 2011. The impact of nutrition on differential methylated regions of the genome. Adv Nutr 2:463–471; doi:10.3945/an.111.001008.

Pontzer H, Durazo-Arvizu R, Dugas LR, Plange-Rhule J, Bovet P, Forrester TE, et al. 2016. Constrained Total Energy Expenditure and Metabolic Adaptation to Physical Activity in Adult Humans. Curr. Biol. 26:410–7; doi:10.1016/j.cub.2015.12.046.

Rodriguez J, Frigola J, Vendrell E, Risques R-A, Fraga MF, Morales C, et al. 2006. Chromosomal Instability Correlates with Genome-wide DNA Demethylation in Human Primary Colorectal Cancers. Cancer Res. 66:8462–9468; doi:10.1158/0008-5472.CAN-06-0293.

Ross JP, Rand KN, Molloy PL. 2010. Hypomethylation of repeated DNA sequences in cancer. Epigenomics 2:245–269; doi:10.2217/epi.10.2.

Sambrook J, Russell DW. 2006. Purification of Nucleic Acids by Extraction with Phenol:Chloroform. Cold Spring Harb. Protoc. 2006:pdb.prot4455; doi:10.1101/pdb.prot4455.

Sasaki H, Ishihara K, Kato R. 2000. Mechanisms of Igf2/H19 imprinting: DNA methylation, chromatin and long-distance gene regulation. J. Biochem. 127: 711–5.

Sasaki H, Ohtsu T, Ikeda Y, Tsubosaka M, Shibata S. 2014. Combination of meal and exercise timing with a high-fat diet influences energy expenditure and obesity in mice. Chronobiol Int 31:959–975; doi:10.3109/07420528.2014.935785.

Sharma PK, Thakur MK. 2006. Expression of estrogen receptor (ER) alpha and beta in mouse cerebral cortex: effect of age, sex and gonadal steroids. Neurobiol Aging 27:880–887; doi:10.1016/j.neurobiolaging.2005.04.003.

Shen L, Song CX, He C, Zhang Y. 2014. Mechanism and function of oxidative reversal of DNA and RNA methylation. Annu Rev Biochem 83:585–614; doi:10.1146/annurev-biochem-060713-035513.

Singh S, Li SS. 2012. Epigenetic effects of environmental chemicals bisphenol a and phthalates. Int J Mol Sci 13:10143–10153; doi:10.3390/ijms130810143.

Sookdeo A, Hepp CM, McClure MA, Boissinot S. 2013. Revisiting the evolution of mouse LINE-1 in the genomic era. Mob. DNA 4:3; doi:10.1186/1759-8753-4-3.

Stouder C, Deutsch S, Paoloni-Giacobino A. 2009. Superovulation in mice alters the methylation pattern of imprinted genes in the sperm of the offspring. Reprod. Toxicol. 28:536–41; doi:10.1016/j.reprotox.2009.06.009.

Sui Y, Ai N, Park SH, Rios-Pilier J, Perkins JT, Welsh WJ, et al. 2012. Bisphenol A and its analogues activate human pregnane X receptor. Env. Heal. Perspect 120:399–405; doi:10.1289/ehp.1104426.

Susiarjo M, Sasson I, Mesaros C, Bartolomei MS. 2013. Bisphenol A Exposure Disrupts Genomic Imprinting in the Mouse. G. Kelsey, ed PLoS Genet. 9:e1003401; doi:10.1371/journal.pgen.1003401.

Suzuki K, Suzuki I, Leodolter A, Alonso S, Horiuchi S, Yamashita K, et al. 2006. Global DNA demethylation in gastrointestinal cancer is age dependent and precedes genomic damage. Cancer Cell 9:199–207; doi:10.1016/j.ccr.2006.02.016.

Tammen SA, Dolnikowski GG, Ausman LM, Liu Z, Kim KC, Friso S, et al. 2014. Aging alters hepatic DNA hydroxymethylation, as measured by liquid chromatography/mass

spectrometry. J Cancer Prev 19:301–308; doi:10.15430/JCP.2014.19.2.301.

Teschendorff AE, Menon U, Gentry-Maharaj A, Ramus SJ, Weisenberger DJ, Shen H, et al. 2010. Age-dependent DNA methylation of genes that are suppressed in stem cells is a hallmark of cancer. Genome Res. 20:440–446; doi:10.1101/gr.103606.109.

Teschendorff AE, West J, Beck S. 2013. Age-associated epigenetic drift: implications, and a case of epigenetic thrift? Hum Mol Genet 22:R7–R15; doi:10.1093/hmg/ddt375.

Timmermans S, Steegers-Theunissen RP, Vujkovic M, den Breeijen H, Russcher H, Lindemans J, et al. 2012. The Mediterranean diet and fetal size parameters: the Generation R Study. Br. J. Nutr. 108:1399–1409; doi:10.1017/S000711451100691X.

Tobi EW, Slieker RC, Luijk R, Dekkers KF, Stein AD, Xu KM, et al. 2018. DNA methylation as a mediator of the association between prenatal adversity and risk factors for metabolic disease in adulthood. Sci. Adv. 4:eaao4364; doi:10.1126/sciadv.aao4364.

Trichopoulou A, Katsouyanni K, Gnardellis C. 1993. The traditional Greek diet. Eur. J. Clin. Nutr. 47 Suppl 1: S76-81.

Van Klinken JB, van den Berg SAA, Havekes LM, Willems Van Dijk K. 2012. Estimation of Activity Related Energy Expenditure and Resting Metabolic Rate in Freely Moving Mice from Indirect Calorimetry Data. S. Blanc, ed PLoS One 7:e36162; doi:10.1371/journal.pone.0036162.

Varley KE, Gertz J, Bowling KM, Parker SL, Reddy TE, Pauli-Behn F, et al. 2013. Dynamic DNA methylation across diverse human cell lines and tissues. Genome Res. 23:555–567; doi:10.1101/gr.147942.112.

Waterland RA. 2003. Do maternal methyl supplements in mice affect DNA methylation of offspring? J Nutr 133: 238; author reply 239.

Waterland RA, Jirtle RL. 2004. Early nutrition, epigenetic changes at transposons and imprinted genes, and enhanced susceptibility to adult chronic diseases. Nutrition 20: 63–68.

Waterland RA, Jirtle RL. 2003. Transposable elements: targets for early nutritional effects on epigenetic gene regulation. Mol Cell Biol 23: 5293–5300.

Waterland RA, Lin J-R, Smith CA, Jirtle RL. 2006. Post-weaning diet affects genomic imprinting at the insulin-like growth factor 2 (Igf2) locus. Hum. Mol. Genet. 15:705–716; doi:10.1093/hmg/ddi484.

Watson CS, Bulayeva NN, Wozniak AL, Alyea RA. 2007. Xenoestrogens are potent activators of nongenomic estrogenic responses. Steroids 72:124–134; doi:10.1016/j.steroids.2006.11.002.

Weinhouse C, Bergin IL, Harris C, Dolinoy DC. Stat3 is a candidate epigenetic biomarker of perinatal Bisphenol A exposure associated with murine hepatic tumors with implications for human health. Epigenetics. 2015;10:1099–110.

Weinhouse C, Anderson OS, Bergin IL, Vandenbergh DJ, Gyekis JP, Dingman MA, et al. 2014. Dose-Dependent Incidence of Hepatic Tumors in Adult Mice following Perinatal Exposure to Bisphenol A. Environ. Health Perspect.; doi:10.1289/ehp.1307449.

Wilson ME, Westberry JM. 2009. Regulation of Oestrogen Receptor Gene Expression: New Insights and Novel Mechanisms. J. Neuroendocrinol. 21:238–242; doi:10.1111/j.1365-2826.2009.01830.x.

Wilson ME, Westberry JM, Trout AL. 2011. Estrogen receptor-alpha gene expression in the cortex: sex differences during development and in adulthood. Horm Behav 59:353–357; doi:10.1016/j.yhbeh.2010.08.004.

Wolstenholme JT, Rissman EF, Connelly JJ. 2011. The role of Bisphenol A in shaping the brain, epigenome and behavior. Horm Behav 59:296–305; doi:10.1016/j.yhbeh.2010.10.001.

Wu H, D'Alessio AC, Ito S, Wang Z, Cui K, Zhao K, et al. 2011. Genome-wide analysis of 5-hydroxymethylcytosine distribution reveals its dual function in transcriptional regulation in mouse embryonic stem cells. Genes Dev 25:679–684; doi:10.1101/gad.2036011.

Xu G-L, Wong J. 2015. Oxidative DNA demethylation mediated by Tet enzymes. 318–328.

Yang AS, Estécio MRH, Doshi K, Kondo Y, Tajara EH, Issa J-PJ. 2004. A simple method for estimating global DNA methylation using bisulfite PCR of repetitive DNA elements. Nucleic Acids Res. 32:e38; doi:10.1093/nar/gnh032.

Yara S, Lavoie J-C, Levy E. 2015. Oxidative stress and DNA methylation regulation in the metabolic syndrome. Epigenomics 7:283–300; doi:10.2217/epi.14.84.

Zhang XF, Zhang LJ, Feng YN, Chen B, Feng YM, Liang GJ, et al. 2012. Bisphenol A exposure modifies DNA methylation of imprint genes in mouse fetal germ cells. Mol Biol Rep 39:8621–8628; doi:10.1007/s11033-012-1716-7.

Zhao B, Yang Y, Wang X, Chong Z, Yin R, Song S-H, et al. 2014. Redox-active quinones induces genome-wide DNA methylation changes by an iron-mediated and Tet-dependent mechanism. Nucleic Acids Res. 42:1593–1605; doi:10.1093/nar/gkt1090.

# Chapter 3

## Longitudinal Effects of Developmental Bisphenol A Exposure on Epigenome-wide DNA Hydroxymethylation at Imprinted Loci in Mouse Blood


### Abstract

Epigenetic machinery plays an important role in genomic imprinting, a developmental process that establishes parent-of-origin-specific monoallelic gene expression. While a number of studies have investigated the role of 5-methylcytosine in imprinting control, the contribution of 5-hydroxymethylcytosine (5-hmC) to this epigenetic phenomenon remains unclear. Using matched mouse blood samples (2, 4, and 10 months of age), we examined the effects of perinatal bisphenol A (BPA) exposure (50 µg/kg diet) on longitudinal 5-hmC patterns at imprinted regions. We also tested the hypothesis that 5-hmC would show defined patterns at imprinted genes that persist across the life course. Genome-wide 5-hmC content was measured using hydroxymethylated DNA immunoprecipitation sequencing (HMeDIP-seq). Modeling of differential hydroxymethylation by BPA exposure was performed using a pipeline of bioinformatics tools, including the csaw R package.Based on BPA exposure, we identified 5,950 differentially hydroxymethylated regions (DHMRs), including 12 DHMRs that were annotated to murine imprinted genes – *Gnas*, *Grb10*, *Plagl1*, *Klf14*, *Pde10a*, *Snrpn*, *Airn*, *Cmah*, *Ppp1r9a*, *Kcnq1*, *Phactr2*, and *Pde4d*. When visualized, these imprinted gene DHMRs showed clear, consistent patterns of differential 5-hmC by developmental BPA exposure that persisted throughout adulthood. These data show long-term establishment of 5-hmC marks at imprinted loci during development. Further, the effect of perinatal BPA exposure on 5-hmC at specific imprinted loci indicates that developmental exposure to environmental toxicants may alter long-term imprinted gene regulation via an epigenetic mechanism.

## 3.1 Introduction

DNA methylation is an epigenetic mark that typically occurs at cytosines (5-methylctyosine; 5-mC) in cytosine-phosphate-guanine (CpG) dinucleotides. Research has shown that 5-mC plays a role in X chromosome inactivation (Cotton et al. 2015), regulation of gene transcription (Medvedeva et al. 2014), and genomic imprinting (Bartolomei and Ferguson-Smith 2011). In addition to 5-mC, recent studies have shown that the oxidized form of 5-mC – 5-hydroxymethylcyotisine (5-hmC) – is a stable epigenetic mark present in a variety of mammalian tissues (Globisch et al. 2010; Hahn et al. 2014; Wu et al. 2011). Active processing of 5-mC to 5-hmC occurs via a Ten-eleven translocation (TET) methylcytosine dioxygenase-mediated oxidative pathway (Shen et al. 2014), and previous studies show that exposure-induced oxidative stress can alter both TET enzyme expression (Coulter et al. 2013) and global 5-hmC content (Delatte et al. 2015). In addition to these characteristics, 5-hmC has a complex role as both a positive and negative regulator of transcription (Hahn et al. 2014; Wu et al. 2011), suggesting it may represent an important secondary genomic regulator in the methylome.

During early embryonic development, DNA methylation undergoes a distinct wave of demethylation and *de novo* methylation (Reik et al. 2001; Smallwood and Kelsey 2012), processes that assist in the regulation of stem cell proliferation and differentiation (Messerschmidt et al. 2014). After differentiation, there is a second phase of DNA methylation reprogramming that occurs to establish a baseline methylome in primordial germ cells prior to birth (Smallwood and Kelsey 2012). Given these multiple waves of reprogramming during development, DNA methylation has been proposed as a mechanism driving the developmental origins of health and disease (DOHaD) hypothesis. DOHaD posits that exposure to environmental factors (e.g. diet, chemicals, etc.) during sensitive periods of development

influences developmental plasticity, thereby altering disease susceptibility later in life (Bateson et al. 2004; Heindel et al. 2015; Jirtle and Skinner 2007). Of particular interest in the DOHaD field is genomic imprinting, an epigenetic phenomenon by which parent-of-origin-specific monoallelic gene expression is established during development (Bartolomei and Ferguson-Smith 2011; Das et al. 2009). Genomic imprinting is critical for proper placental maturation, embryonic growth and development, and it also plays important roles in post-natal development – especially in parent-offspring interactions (e.g. milk suckling, maternal care) (Plasschaert and Bartolomei 2014). A vast amount of research on genomic imprinting has shown that differential DNA methylation at imprinting control regions (ICRs) plays an important role in establishing genomic imprinting during development, and that these regions are not demethylated during post-fertilization reprogramming (Arnaud 2010; Kelsey and Feil 2012; Kim et al. 2017; Pidsley et al. 2012; Smallwood and Kelsey 2012). Given that imprinted gene expression is controlled via developmentally programmed epigenetic marks, imprinted genes have been investigated as potential targets of developmental environmental exposures in both human and rodent studies (Haycock and Ramsay 2009; Heijmans et al. 2008; Nye et al. 2015; Susiarjo et al. 2013).

However, virtually all of the existing studies on genomic imprinting relied upon sodium bisulfite treatment for generation of DNA methylation levels from biological samples. While bisulfite treatment is a useful quantitative tool for measuring the methylome, it also has an inherent weakness – it does not distinguish between 5-mC and 5-hmC. This is because both 5-mC and 5-hmC are resistant to sodium bisulfite-induced cytosine deamination (Huang et al. 2010). This means that bisulfite treatment-based measurements of the "methylome" actually represent combined 5-mC+5-hmC levels. In recent years, methods to specifically measure 5-hmC, including hydroxymethylated DNA immunoprecipitation sequencing (HMeDIP-seq) (Tan

et al. 2013), have been developed. Despite these recent advances, however, little work has been done to identify the role of 5-hmC in genomic imprinting. One recent study showed enrichment of 5-hmC in imprinted regions in human brain and placenta (Hernandez Mora et al. 2017), but no study has yet investigated the contribution of 5-hmC to imprinting control in animal models. Furthermore, existing animal studies have not investigated effects of the environment on 5-hmC levels at imprinted genes.

Developmental exposure to a number of environmental factors, including endocrine disrupting chemicals (EDCs), has been linked to changes in DNA methylation. Bisphenol A (BPA) is a commercial EDC that is found in a variety of consumer products (e.g. receipt paper, metal can linings, etc.) and has near ubiquitous human exposure across the world (Calafat et al. 2008). BPA can activate growth-related transcription factors, bind nuclear receptors involved in cell growth and maturation, and also alter DNA methylation levels across the epigenome (Krüger et al. 2008; Manikkam et al. 2013; Singh and Li 2012; Sui et al. 2012; Watson et al. 2007; Wolstenholme et al. 2011; Zhang et al. 2012). Developmental BPA exposure in mouse models has been shown to alter the methylome (Anderson et al. 2012; Kim et al. 2014; Singh and Li 2012), including specific effects on DNA methylation at imprinted loci (Susiarjo et al. 2013). Despite these results, however, it remains unclear whether developmental BPA exposure can specifically affect DNA hydroxymethylation.

Here, we used the HMeDIP-seq method to measure epigenome-wide 5-hmC from longitudinal mouse blood samples in an effort to examine DNA hydroxymethylation at imprinted loci throughout murine adulthood. HMeDIP-seq is an antibody-based high-throughput sequencing method that measures the genome-wide distribution of 5-hmC. While this method has some inherent antibody inefficiency and fails to provide base-pair resolution sequencing

data, it does provide cost-effective amplification of high frequency, low signal 5-hmC marks within gene bodies (Skvortsova et al. 2017; Tan et al. 2013). Given the discovery nature of this study and the lack of a priori knowledge regarding 5-hmC levels in mouse blood, HMeDIP-seq was chosen to measure genome-wide 5-hmC from longitudinal blood samples. From this data, we tested the hypothesis that perinatal BPA exposure alters longitudinal 5-hmC content at imprinted genes. We also tested the hypothesis that imprinted genes would show defined 5-hmC peaks that persist across the life course. Our results confirm these hypotheses, showing both BPA-related differential hydroxymethylation and persistent 5-hmC patterning at imprinted genes.

## 3.2 Materials and Methods

### *Study animals and blood collection*

Mice included in longitudinal analysis were *a/a* offspring sourced from a genetically invariant viable yellow agouti $A^{vy}/a$ mouse colony maintained by sibling mating and forced heterozygosity for more than 220 generations (Waterland and Jirtle 2003). Within this colony, the $A^{vy}$ allele is passed through the heterozygous male line, which has a genetically constant background 93% identical to C57BL/6J strain (Waterland and Jirtle 2003; Weinhouse et al. 2014). Two weeks prior to mate-pairing with $A^{vy}/a$ males, eight to ten-week-old wild type *a/a* dams were placed on one of two experimental diet groups: (1) Control (modified, phytoestrogen-free 7% corn oil AIN-93G), (2) Control + 50 µg BPA/kg diet (**Figure 3-1**) (Anderson et al. 2012; Weinhouse et al. 2014). BPA dose was chosen based on a previous dosing study from our lab that showed intake of 50 ug BPA/kg diet produced on average 2.02 ng BPA/g liver (Anderson et al. 2012). This exposure level is within the range of human exposure levels measured in human fetal liver samples (range: non-detect to 96.8 ng BPA/g liver) (Anderson et al. 2012). Dietary

exposure was continued through pregnancy and lactation, at which point BPA-exposed offspring (total n=19; n=6 used for these analyses) were weaned to the modified AIN-93G Control diet and followed along with Control offspring (total n=22; n=6 used for these analyses) until 10 months of age. All diets were provided by Envigo (Indianapolis, IN). At 2 months and 4 months of age, tail vein blood samples were collected from all mice (**Figure 3-1**). At 10 months of age, mice were sacrificed, and blood samples were again collected, this time using cardiac puncture. Six mouse blood samples from each exposure group were selected for inclusion in next-generation sequencing analyses. In accordance with methods established by the NIEHS TaRGET II consortium (Wang et al. 2018), we selected male (n=3) and female (n=3) blood samples collected from six separate litters. All animals were stored in polycarbonate-free cages with ad libitum access to food and drinking water, and were maintained in accordance with Institute for Laboratory Animal Research (ILAR) guidelines (National Research Council (US) Committee for the Update of the Guide for the Care and Use of Laboratory Animals 2011). The study protocol was approved by the University of Michigan Committee on Use and Care of Animals (UCUCA PRO00004797).

***DNA and RNA isolation***

To allow for matched analyses of DNA hydroxymethylation and gene expression from the same set of mice (n=6), genomic DNA and RNA were co-isolated from 2, 4, and 10 month frozen blood using the Qiagen Allprep DNA/RNA/miRNA Universal Kit (Qiagen, Cat. #80224). Yield and purity of all DNA and RNA was measured using a NanoDrop spectrophotometer. All samples were stored at -80°C prior to DNA and RNA isolations.

***Real-time quantitative PCR (RT-qPCR)***

The Bio-Rad iScript cDNA Synthesis Kit (Cat. #1708890) was used to reverse transcribe complementary DNA (cDNA) from 250 ng of RNA for each sample. In preparation for RT-qPCR, cDNA samples were diluted 1:2.5 in RNase-free water, then mixed with 10 µM forward/reverse primers, nuclease-free water, and Bio-Rad iQ SYBR Green Supermix (Cat. #1708880). RT-qPCR was then performed using a Bio-rad CFX96 Real-Time System C1000 Thermal Cycler (Bio-Rad; Hercules, CA). The pre-programmed 2-step PCR+melt curve protocol was used for all qPCR reactions – 95°C for 3 minutes, [95°C for 10 seconds, 55°C for 30 seconds, plate read] x40, 95°C for 10 seconds. The melt curve for each plate was 65°C-95°C; 0.5°C increment for 5 seconds, with plate read at each temperature. RT-qPCR analyses were performed for the *Gnas* genes in triplicate for each cDNA sample. Three housekeeping genes – *Actb*, *18S*, and *Gapdh* – were included as internal controls in all RT-qPCR runs. In addition to housekeeping genes, an inter-plate calibrator control of brain cDNA was included for calculation of relative gene expression across multiple plates. Expression levels were calculated following the $2^{-\Delta\Delta Ct}$ method (Livak and Schmittgen 2001). RT-qPCR primers for the *Gnas* and *Gapdh* genes (**Table 3-1**) were designed using the online Genscript Real-time PCR Primer Design software (https://www.genscript.com/tools/real-time-pcr-tagman-primer-design-tool). The *β-actin* and *18S* gene primer pairs were sourced from the literature (Dolinoy et al. 2010; La Salle et al. 2004). Primer pair specificity for all designed primers was checked using the NCBI Primer-BLAST online tool (https://www.ncbi.nlm.nih.gov/tools/ primer-blast/).

***Next-generation sequencing of 5-hmC***

Epigenome-wide DNA hydroxymethylation was quantified in blood from mice using hydroxymethylated DNA immunoprecipitation sequencing (HMeDIP-seq) (Tan et al. 2013).

Unlike other some other methods, HMeDIP-seq is an antibody-based approach that does not provide base-pair resolution data. This method is also subject to the inherent bias of a multi-step, immunoprecipitation-based sequencing method, including potential for antibody binding inefficiency, as well as library preparation bias, read mapping bias, or PCR amplification bias (Meyer and Liu 2014). Despite these weaknesses, HMeDIP-seq is a cost-effective method to measure genome-wide 5-hmC, including at regions of high frequency weak 5-hmC signal (Tan et al. 2013). Sequencing data were generated by Dr. Claudia Lalancette at the University of Michigan Epigenomics Core Facility for a subset of control (n=6) and BPA-exposed (n=6) mice (**Figure 3-2**). Blood samples from the six mice (3 male, 3 female) in each exposure group were sequenced at three time points across the life-course (2, 4, and 10 months of age), for a total sequencing data sample size of 36 samples. The six mice for each exposure group were selected from different litters to minimize litter effects. Sample quality and quantitation were assessed using the Agilent TapeStation genomic DNA kit (Agilent, Cat. #G2991AA) and Qubit broad range dsDNA (Invitrogen, Cat. #Q32850), respectively. Indexed adapters and PCR primers were synthesized by Integrated DNA Technologies (IDT). Enzymes used for library preparation were sourced from New England BioLabs (NEB).

A total of 1μg of genomic DNA (gDNA) was sheared by adaptive focused acoustics, using the Covaris S220 (Covaris, Cat. #4465653). This sheared DNA was next blunt-ended and phosphorylated. A single adenine nucleotide was then added to the 3'end of the fragments in preparation for ligation of adapter duplex with a thymine overhang. The ligated fragments were cleaned using Qiagen's MinElute PCR purification columns (Qiagen, Cat. #28004). DNA standards for HMeDIP (Diagenode 5-hmC, 5-mC & cytosine DNA standard pack for HMeDIP, Cat. #AF-107-0040) were added to each sample before denaturation. Resuspension was then

performed in ice-cold immunoprecipitation buffer (10 mM Sodium Phosphate pH 7.0, 140 mM NaCl, 0.05% Triton X-100). A 10% volume (input) was retrieved before 2ug of a 5-hmC-specific antibody (Active Motif, Cat # 39791) was added for immunoprecipitation overnight at 4°C with rotation. Dynabeads Protein-G (Invitrogen, Cat. #10003D) was used to pull-down 5-hmC-enriched fragments. The 5-hmC-enriched DNA fragments (IP) were then released from the antibody by digestion with Proteinase K (Ambion, Cat. #AM2548). After cleanup with AMPure XP beads (Beckman Coulter, Prod.# A63880), the percent input enrichment (%input) in the IP was evaluated by qPCR, using hydroxymethylated, methylated, and unmethylated primers for spike-ins. Samples with high % input for the 5-hmC spike-in – typical inclusion threshold was >80% – were then PCR amplified for the final library production, cleaned using AMPure XP beads, and quantified using the Qubit assay (Invitrogen, Cat. #Q32850) and TapeStation High Sensitivity D1000 kit (Agilent, Cat. #G2991AA). Single-end, 50 base pair reads were obtained for each library by sequencing on the HiSeq 4000 system (Illumina). Each HMeDIP-seq sample was run on a single sequencing lane.

***Bioinformatics pipeline for differential 5-hmC***

HMeDIP-seq data for all control and BPA-exposed mice were compared using a suite of bioinformatics tools (**Figure 3-2**). First, the Sartor lab *mint* pipeline was used for data quality control (*FastQC* and *MultiQC*), adapter trimming (*trim_galore*), and alignment (*bowtie2*) (Cavalcante et al. 2017). Based on previous research, we required a minimum overlap of 6bp and minimum quality score of 20 for adapter and quality trimming, respectively (Akalin et al. 2012). Although the default minimum overlap in *trim_galore* is 1 bp, we selected a less stringent minimum overlap of 6 bp in an effort to include all legitimate genomic sequences and improve read depth. Despite these benefits, the less stringent minimum overlap length increases the

possibility for adapter contamination in our data (Krueger 2017). The quality score cut-off is the default in *trim_galore*, and is based on previous research showing an optimal tradeoff between correct read mapping and read survival at quality scores between 20 and 30 (Del Fabbro et al. 2013). Default parameters were used for *bowtie2*.

After data quality check, trimming, and alignment, the *csaw* package was used to test for differential 5-hmC by BPA exposure (Lun and Smyth 2016). Aligned HMeDIP-seq data were read into R using the windowCounts function in *csaw*. When reading in the data, extension was set to 52, window width was set to 100, and sex chromosomes were removed. The data were then filtered twice – by count ( average count >5) and by local enrichment using the filterWindows function (type= "local") – to remove regions of negligible binding. After filtering, normalization factors were calculated for each sample using the normOffsets function on binned data (width=10000). Normalization factors were linked to filtered data using the asDGEList function, and then the estimateDisp function was used to generate dispersion factors based on a multifactorial design matrix. The glmQLFit function was used to fit a model (model design = model.matrix(~ exposure + age + age:exposure + mouse_ID + sex)) for differential 5-hmC binding; an empirical Bayesian method used to stabilize the QL dispersion estimates. Contrast statements were used to extract modeling results for the variable of interest – BPA exposure. To correct for multiple testing, filtered data was clustered using a window length of 500 bp; the combineTests function was then used to compute a combined p-value for each cluster. Multiple testing correction was performed using the Benjamini-Hochberg method (Benjamini and Hochberg 1995, 1997). Differential hydroxymethylated region (DHMR) length cutoff was set at ≥100 bp; significance was set at FDR < 0.10.

After testing for differential hydroxymethylation using *csaw*, the *annotatr* R package was used to annotate all DHMRs to the mm10 genome (Cavalcante and Sartor 2017). The annotate_regions function was used to generate genomic annotations, which include classifications by region class (e.g. intron, exon, promoter, etc.) and annotated gene IDs. A list of mouse imprinted loci was then sourced from the MouseBook online database (Williamson et al. 2013). All available imprinted genes were manually cross-checked with the generated list of BPA-related DHMR annotated gene IDs.

***Sequencing data visualization***

5-hmC peaks were visualized using the *csaw* and *GViz* R packages (Hahne and Ivanek 2016; Lun and Smyth 2016). Using *csaw*, data was first read into R as a GRanges object using the extractReads function. Next, the GeneRegionTrack in the *Gviz* R package was used to define regions of interest for visualization. Separate blue and red genome tracks were used to represent the forward and reverse strand reads, respectively. The plotTracks function was then used to plot 5-hmC peaks for these regions. Reads-per-million was used for the y-axis in all graphs, and scale was adjusted to individual region coverage.

BPA-related DHMRs at imprinted loci were visualized using the *GViz* R package to determine directionality and magnitude of differential 5-hmC. Plots generated in R (R version 3.4.0) were formatted for publication in Adobe Illustrator CS6 (version 16.0.5).

***Pathway analysis***

Pathway analysis for DHMRs was performed using ChIP-enrich (Welch et al. 2014). Within the ChIP-enrich online interface (http://chip-enrich.med.umich.edu/), the gene set filter was set to 2000, peak threshold was set to 1, and adjustment for mappability of gene locus regions was set to false. The genome used for pathway analyses was mm10, and the ChIP-enrich

method was used for enrichment testing. DHMRs were split into hypo- and hyper-hydroxymethylated regions prior to separate analyses. Only regions <5kb from TSS were included in ChIP-enrich analysis. All pathway analyses included GO terms and KEGG pathways. After correcting for multiple testing, only pathways with FDR<0.05 were considered significant.

## 3.3 Results

### *Epigenome-wide differential 5-hmC*

Using the *csaw* R package, multivariate models were constructed to test for differential 5-hmC by perinatal BPA exposure (50 µg/kg diet). Based on the *csaw* models, we identified 5950 differentially hydroxymethylated regions (DHMRs) by BPA exposure (**Table 1**). Comparing the directionality of DHMRs by BPA exposure, we found more hypo-hydroxymethylated regions (n=4247; 71.4%) than hyper-hydroxymethylated regions (n=1559; 26.2%) (**Table 1**). We also identified a small fraction of BPA-related DHMRs (n=144; 2.4%) that showed both hypo- and hyper-hydroxymethylation. Taken together, these epigenome-wide results show that the directionality of differential hydroxymethylation varies by region, with a skew toward decreased 5-hmC by BPA exposure.

### *BPA-related DHMRs at imprinted genes*

Previous research has shown effects of developmental exposures on DNA methylation at imprinted loci (Gallou-Kabani et al. 2010; Susiarjo et al. 2013), but it remains unclear whether exposures can also alter DNA hydroxymethylation at imprinted genes. Further complicating this question, despite recent research in humans showing enrichment of 5-hmC at imprinted loci (Hernandez Mora et al. 2017), the distribution and potential function of 5-hmC at murine imprinted genes remains unknown. In an effort to broadly identify BPA-sensitive regions of 5-hmC at imprinted loci, we cross-checked the BPA-related DHMR annotations with a database of

known murine imprinted genes (Williamson et al. 2013). In total, 12 of the 151 known imprinted genes had annotated BPA-related DHMRs (**Table 3-3**). Five of these twelve genes had increased 5-hmC peaks by BPA exposure – *Grb10*, *Pde10a*, *Pde4d*, *Plagl1*, and *Gnas*. The remaining seven imprinted loci – *Ppp1r9a*, *Phactr2*, *Klf14*, *Kcnq1*, *Cmah*, *Airn*, and *Snrpn* – had decreased 5-hmC peaks by BPA exposure. The number of CpG sites within these DHMRs varied by region, with five of the DHMRs showing zero CpG sites (**Table 3-4**). In an effort to confirm the DHMRs, we visualized the five most significant imprinted gene DHMRs and one DHMR at the well-characterized *Snrpn* gene, showing marked changes in 5-hmC peaks by BPA exposure that persisted across all of the three matched sample ages (**Figure 3-3**). We also showed striking changes in 5-hmC peaks at the remaining six imprinted gene DHMRs, despite their decreased significance (**Figure 3-4**). In an effort to determine whether this was a shared trait at imprinted genes, we visualized 5-hmC peaks at *Igf2* and *H19*, two well-characterized imprinted genes that did not have any annotated DHMRs with FDR < 0.1. Despite their lack of significant DHMRs, *Igf2* and *H19* still had specific 5-hmC peaks that showed non-significant changes by BPA exposure (**Figure 3-5**). Combined, these data suggest that perinatal BPA exposure alters the establishment of 5-hmC marks at specific regions of imprinted genes.

In examining the imprinted loci visually, two of the DHMRs – *Plagl1* and *Gnas* – had 5-hmC peaks that were cut-off by the DHMR boundaries, suggesting larger scale 5-hmC patterns at these genes. To provide a complete picture for these two loci, 5-hmC peaks across the entire gene were visualized. Both *Plagl1* and *Gnas* had widespread 5-hmC peaks along the entire gene-coding region, with only the annotated DHMRs showing apparent modifications by BPA exposure (**Figure 3-6**). Of note, 5-hmC peaks across these two genes were consistent between mice and across time, a pattern that was also observed at the *Igf2* and *H19* imprinted genes

(**Figure 3-5**). Together, these data show that imprinted genes have predictable 5-hmC peaks along the length of their gene bodies.

***RT-qPCR gene expression data***

To follow up on the DHMR annotated to the *Gnas* gene, we performed RT-qPCR on RNA from matched mouse blood samples to examine longitudinal mRNA expression. At the *Gnas* locus, there was a significant increase in mean mRNA expression from 2 to 10 months of age in mice exposed to BPA (p=0.05) (**Figure 3-7**). This increase was not significant in control samples. Additionally, mean *Gnas* expression was significantly lower in control mice than BPA-exposed blood at 10 months of age (p=0.01), a result that reflects a result that reflects the increased *Gnas* 5-hmC peak found in BPA-exposed blood.

***Pathway analysis for DHMRs***

ChIP-enrich pathway analysis was performed on separate lists of hyper- and hypo-methylated DHMRs. In an effort to maximize biological relevance and limit number of comparisons, DHMR datasets were restricted to regions <5kb from the transcription start site. After correction for multiple testing, a small number of GO terms were enriched in hypo- and hyper-hydroxymethylated DHMRs (**Table 3-5**). Of note, enriched pathways showed no overlap between hyper- and hypo-hydroxymethylated DHMRs. In the BPA-related hypo-hydroxymethylated DHMRs, the only two significantly enriched pathways were hippocampus development and spinal cord association neuron differentiation. In the BPA-related hyper-hydroxymethylated DHMRs, the two most significant enriched pathways were L-ascorbic acid binding and oxidoreductase activity. These pathway analysis results indicate that only a few GO terms were enriched in the significant DHMRs, and that enrichment was specific to directionality of BPA-related DHMRs.

## 3.4 Discussion

### *Epigenome-wide differential 5-hmC*

We found statistically significant effects of perinatal BPA exposure on DNA hydroxymethylation across the epigenome. While the exact mechanism driving this relationship is unclear, it is possible that BPA-related DHMRs are a result of BPA-induced oxidative stress (OS) (Gassman 2017). Based on the available literature, free BPA is thought to induce OS via enzymatic formation of BPA phenoxyl radicals (Sakuma et al. 2010), which can then be further processed to other reactive oxygen species (ROS), including superoxides and peroxides (Babu et al. 2013). In addition to potential ROS-induced cytotoxicity (Gassman 2017), the prooxidant activity of BPA also has the potential to modify 5-hmC across the epigenome. Research has shown that Tet enzyme activity is activated under oxidative conditions (Chia et al. 2011; Coulter et al. 2013; Zhao et al. 2014), indicating that active processing of 5-mC to 5-hmC may be affected by ROS production. Further supporting this idea, recent research has shown that OS-inducing exogenous factors – buthionine sulfoximine and $PM_{2.5}$ fine particulate matter – can alter DNA hydroxymethylation levels (Delatte et al. 2015; Wei et al. 2017). These prior results support the hypothesis that BPA exposure could be triggering changes in 5-hmC via induction of oxidative stress. This idea should be further explored in future studies examining the effects of endocrine disrupting chemicals on 5-hmC levels across the epigenome.

### *BPA-related DHMRs at imprinted genes*

In addition to examining the effects of BPA on broad-scale DNA hydroxymethylation, we also specifically investigated whether BPA exposure altered 5-hmC content at murine imprinted genes. Of the 151 interrogated imprinted loci, twelve (7.95%) had annotated DHMRs **(Table 3-3**). As a broad scale comparison, out of the estimated 24,360 known protein-coding

genes in mice (Blake et al. 2017), 1,616 unique gene IDs had annotated DHMRs (6.63%). These results indicate that imprinted genes show slight enrichment for DHMRs compared to all known genes combined. Although none of the twelve imprinted gene BPA-related DHMRs overlapped with known imprinting control regions (ICRs) (**Figure 3-8**), expanded visualization of *Gnas* and *Plagl1* showed widespread hydroxyl across imprinted gene regions. The directionality and magnitude of the imprinted gene DHMRs was also gene-specific. Of note, five of the imprinted gene DHMRs had zero CpG sites (**Table 3-4**), a result that could be driven by several possible scenarios: 1. DNA hydroxymethylation at non-canonical methylation contexts (i.e. CHG sites, where H = A, C, or T); 2. Inexact DHMR definitions due to inherent lack of specificity in pulldown method (HMeDIP-seq); 3. False positives in our data. Supporting the first option, recent work in mice has shown intragenic enrichment of non-CpG methylation at particular domains in clusters of genes related to embryonic development (He et al. 2017). Further fitting with this idea, eight of the twelve imprinted gene DHMRs had at least ten CHG sites within their chromosomal ranges (**Table 3-4**). Nevertheless, it remains difficult to distinguish between the three outlined scenarios using the data available in this project. The most significant imprinted gene DHMR was annotated to the *Gnas* locus, which encodes the G-protein alpha subunit protein, a key component of G-protein coupled signal transduction (Plagge and Kelsey 2006). *Gnas* is an imprinted gene that has a complex expression pattern, four alternative promoters, a number of isoforms, and may be involved in energy homeostasis (Peters and Williamson 2007; Plagge and Kelsey 2006). Given the complexity of transcriptional control at this locus, the identified intronic *Gnas* DHMR may represent a long-range regulatory region. This hypothesis is supported by research demonstrating that 5-hmC is enriched at enhancers (Ehrlich and Ehrlich 2014; Stroud et al. 2011; Sun et al. 2013; Wen et al. 2014), regulatory regions that can be quite

distant from the gene promoters they activate (Pennacchio et al. 2013; Shlyueva et al. 2014). Based on this idea of distant regulatory regions, we hypothesized that the documented increase in intronic *Gnas* 5-hmC would show a corresponding BPA-related change in *Gnas* expression. Using RT-qPCR, we found increased *Gnas* expression by BPA exposure across all three time points, with the magnitude of this increase reaching significance at 10 months of age **(Figure 3-7)**. Given the complex regulation of this locus, the age-specific effect of BPA exposure on *Gnas* expression may be a result of changes in alternative splicing, which is dynamic during the aging process (Li et al. 2017). During aging, *Gnas* splicing could shift toward specific isoforms that are controlled by 5-hmC at the BPA-related DHMR, leading to a late adulthood effect of developmental BPA exposure. Future functional work should explore this idea, as well as test for potential effects of BPA exposure at the human *GNAS* locus.

In addition to *Gnas*, three other imprinted genes – *Grb10, Plagl1*, and *Pde10a* – showed significant increases in 5-hmC by BPA exposure. The first of these additional hyper-hydroxymethylated genes, *Grb10,* encodes the growth factor receptor-bound protein 10 (Grb10). Grb10 is involved in a number of biological processes, including cellular proliferation, apoptosis, and metabolism (Holt and Siddle 2005; Kabir and Kazi 2014; Plasschaert and Bartolomei 2015; Riedel 2004). *Grb10* is maternally expressed in most tissues, but it is paternally expressed in the brain; this complex imprinting pattern is established through tissue-specific alternate promoters (Sanz et al. 2008). The tissue-specific maternal and paternal expression patterns of *Grb10* have been linked to fetal growth and adult social behavior in mice, respectively (Garfield et al. 2011). This complex expression patterning is thought to be controlled via epigenetic modifications (Sanz et al. 2008). Like *Gnas,* the *Grb10* DHMR is intronic, meaning any functional effects of differential 5-hmC at this region would have to be through long-distance contacts. The second

additional gene, *Plagl1*, encodes the pleomorphic adenoma of the salivary gland gene like 1 (Plagl1) protein. Plagl1 is a zinc finger transcription factor that regulates other imprinted loci involved in embryonic growth, including *H19* and *Igf2* (Varrault et al. 2006, 2017). As such, BPA-related alterations in 5-hmC at *Plagl1* have the potential to affect an entire network of imprinted genes. Like *Gnas* and *Grb10*, *Plagl1* has several alternative transcripts in mouse that are controlled by alternate promoters (Iglesias-Platas et al. 2013). The *Plagl1* DHMR overlaps Exon 8 in some *Plagl1* isoforms, but not others, suggesting that this region may play a role in alternative splicing for this gene. The third additional hyper-hydroxymethylated imprinted gene, *Pde10a*, encodes phosphodiesterase 10A (Pde10a). Pde10a is a member of the cyclic nucleotide phosphodiesterases (PDEs), a family of enzymes that regulate intracellular levels of cyclic AMP (cAMP) and cyclic GMP (cGMP), endogenous molecules involved in signal transduction (Bender and Beavo 2006; Soderling et al. 1999). *Pde10a* shows its highest expression levels in the brain, with minimal expression in peripheral tissues (Bender and Beavo 2006; Soderling et al. 1999). Recent research shows that pharmaceutical inhibition of Pde10a leads to increased energy expenditure, decreased food intake, reduced adiposity, and improved insulin sensitivity in mice with high-fat diet-induced obesity (Nawrocki et al. 2014). As such, altered regulation of the *Pde10a* gene has the potential to modify murine energy homeostasis. While we found a *Pde10a* DHMR in blood tissue, where expression is minimal, our developmental BPA exposure occurred throughout tissue differentiation, so it is possible that the BPA-related DHMR annotated to *Pde10a* is present in multiple tissues, including the brain.

We also visualized two hypo-hydroxymethylated DHMRs annotated to imprinted genes – *Klf14* and *Snrpn*. The first of these genes, *Klf14*, encodes the maternally-expressed Krüppel-like factor 14 (Klf14), a member of the Cys2/His2 zinc-finger transcription factors (Small et al. 2011;

Wang et al. 2017). Research shows that *KLF14* acts as master regulator of adipose gene expression in humans (Small et al. 2011), and may be involved in metabolic disease risk. In addition, recent results in mice suggest that Klf14 may interact with peroxisome proliferator-activated receptor-γ coactivator 1α (PGC-1α), a transcription coactivator that regulates a number of metabolic pathways, including hepatic gluconeogenesis (Wang et al. 2017). Based on these prior studies, changes in 5-hmC at *Klf14* have the potential to not only alter murine energy homeostasis, but also modify risk of metabolic disorders. The second imprinted gene to show BPA-related decrease in 5-hmC was *Snrpn*, a paternally expressed gene that encodes the SmN protein, a key component of the spliceosome in the brain (Shemer et al. 1997). *Snrpn* has multiple alternate promoters and splice variants, is directly related to neurological function, and is located in the human Prader-Willi + Angelman syndrome (PWS/AS) imprinted domain (Wu et al. 2012). The PWS/AS imprinted domain is highly complex, containing a large number of C/D box small nucleolar RNAs (snoRNAs) and two imprinting control (IC) regions – PWS-IC and AS-IC (Wu et al. 2012). Research suggests the snoRNAs play a role in the etiology of the murine PWS phenotype (Relkovic and Isles 2013; Skryabin et al. 2007), which is often characterized by weight gain, decreased activity, and impaired attention (Relkovic and Isles 2013). Here, we identified a BPA-related hypo-hydroxymethylated region in an intron of *Snrpn.* While the functional relevance of this region remains unknown, previous work has shown that developmental BPA exposure alters DNA methylation at *SNRPN/Snrpn* (Faulk et al. 2015; Susiarjo et al. 2013), providing support for the idea that BPA can affect the epigenome at this locus. Additionally, the human *SNRPN* domain is enriched for 5-hmC across the expressed allele in brain tissue, indicating that 5-hmC may have a functional role in control of *SNRPN* gene expression (Hernandez Mora et al. 2017). Therefore, it is possible that BPA-related changes in

*Snrpn* 5-hmC could alter gene transcription, thereby modifying risk for PWS, a neurobehavioral disorder.

Remarkably, BPA-related DHMRs at the described imprinted loci persisted throughout adulthood despite BPA exposure ending at postnatal day 21 (PND21). These data indicate that perinatal exposure to BPA can have long-lasting effects on 5-hmC. Given the complex role of 5-hmC in regulating transcription activation (Hahn et al. 2014; Wu et al. 2011), the identified BPA-related DHMRs may reflect programmed changes in gene regulation. Supporting this idea, a number of recent studies have shown that 5-hmC is a stable epigenetic mark that has an important role in gene regulation (reviewed in (López et al. 2017)). Building on the existing data, our results show differential 5-hmC at imprinted genes with complex regulatory patterns, indicating that 5-hmC marks at these genes may play a role in establishment of alternative splicing in response to BPA exposure. Though limited, our RNA expression data support this idea, showing that BPA exposure has long-term functional consequences at the imprinted *Gnas* locus. Based on these results, a new hypothesis has emerged – that differential 5-hmC at imprinted genes could be an important mechanism driving the developmental origins of adult disease.

In addition to the BPA-specific DHMRs, our data separately show that widespread 5-hmC peaks are established across entire imprinted genes during development, and that these patterns persist throughout life. This was apparent at genes with annotated DHMRs – *Gnas* and *Plagl1* – and well-characterized genes without annotated DHMRs – *Igf2* and *H19*. These results match recent research in humans, which showed 5-hmC enrichment at the *H19-IGF2* locus in brain and at *GNAS A/B* in placenta (Hernandez Mora et al. 2017). Combined, the available data indicate that 5-hmC may be involved in imprinting control. As technologies for measuring

genome-wide 5-hmC continue to advance, efforts should be made to further examine the regulatory role of 5-hmC in genomic imprinting.

***Pathway analysis***

GO terms showed specific enrichment based on directionality of differential hydroxymethylation. This suggests that BPA exposure is associated with both up- and down-regulation of several biological processes. In the BPA-related hypo-hydroxymethylated DHMRs, the only two significantly enriched pathways were hippocampus development and spinal cord association neuron differentiation. While it is difficult to interpret these pathways from blood samples, 5-hmC has its highest levels in brain tissue, where it is suspected to play a role in neuron development (Kinde et al. 2015). As such, it's possible that these enriched pathways reflect a pre-differentiation effect of developmental BPA exposure on 5-hmC in stem cells. Previous work has shown that epigenetic marks at imprinted genes are maintained during post-fertilization reprogramming (Plasschaert and Bartolomei 2014), suggesting that the epigenetic effects of developmental exposure could be maintained at imprinted loci during cellular differentiation. Building on this idea, our results indicate that 5-hmC establishment at imprinted genes could be involved in regulating neural plasticity. Additional work in pre-differentiated cells and brain tissue could help determine whether BPA actually alters neuronal differentiation via 5-hmC.

***Limitations***

Little is known about the stability of 5-hmC at imprinted loci across blood cell type proportions, but previous studies have shown that epigenetic marks can vary across blood cell types (Houseman et al. 2012; Skinner 2016). As such, it is possible that the documented effects of BPA on genome-wide 5-hmC in blood are simply a reflection of shifts in blood cell type

proportions. Counter to this idea, however, previous studies have shown that DNA methylation is often conserved across different cell types at imprinted loci (Skinner 2016; Talens et al. 2010), suggesting that investigating differential methylation from whole blood should still be valid at imprinted genes. While this evidence supports the validity our BPA-related DHMRs at imprinted loci, the dynamics of 5-hmC at these imprinted genes across blood cell types remains to be elucidated. To further explore the idea that altered 5-hmC in blood impacts imprinted gene regulation, future studies should also investigate allele-specific expression in individual cell types using new single-cell RNA-seq methods (Santoni et al. 2017). Despite lingering blood cell type questions, the use of matched blood samples allowed for direct measurement of 5-hmC from the same mice over time, reducing the potential confounding of inter-individual variability. Additionally, matched blood samples provide greater translatability to human epigenetics studies, which typically rely on peripheral blood samples.

Due to low RNA yields from the longitudinal blood samples, it was not possible to examine gene expression at all identified imprinted loci with annotated DHMRs. RNA yields were diminished due to the small amount of blood collected during *in vivo* tail vein collection at 2 and 4 months of age. Despite the low amounts of blood RNA available, the use of longitudinal samples allowed for direct measurement of expression at the *Gnas* imprinted locus from the same longitudinal samples used for HMeDIP-seq data generation. As such, BPA-related changes in *Gnas* expression directly coincide with BPA-related alterations in DNA hydroxymethylation at this locus.

DNA hydroxymethylation has only recently become recognized as an important consideration in the field of genomic imprinting, meaning its role in imprinting control is poorly defined. As a result, the exact functional effects of the BPA-related changes shown in this paper

remain undetermined. So far, the available research suggests that 5-hmC can have very different regulatory effects depending upon its genomic context, so the relationship between BPA-related DHMRs and gene expression could vary in a gene-specific manner. Similarly, the phenotypic effects of BPA-related DHMRs remain unclear without additional measures of murine biology throughout the life-course. Despite these limitations in interpretation, we identified a large number of BPA-related DHMRs, indicating that DNA hydroxymethylation is sensitive to environmental factors during development.

## 3.5 Conclusions

We measured 5-hmC in matched blood samples collected from isogenic mice at 2, 4, and 10 months of age, and then examined the effects of BPA on the longitudinal DNA hydroxymethylation. Across the epigenome, we identified a number of exposure-related DHMRs, suggesting that perinatal BPA exposure can alter this DNA modification throughout life. At twelve imprinted loci, including the *Gnas* locus, developmental BPA exposure significantly altered 5-hmC peaks in blood across all three measured ages. Echoing this result, we showed that BPA exposure modified *Gnas* expression throughout murine adulthood. These results suggest that BPA-related increases in *Gnas* hydroxymethylation may have long-lasting effects on gene expression at this complex imprinted locus, possibly through shifts in alternative splicing. In addition to BPA-related DHMRs, we also found stable patterns of 5-hmC along a number of imprinted loci, including *Igf2* and *H19.* Combined, our data indicate that 5-hmC may play an important regulatory role in imprinting control, and that establishment of DNA hydroxymethylation at imprinted loci may be sensitive to developmental BPA exposure. Future studies should examine the contribution of DNA hydroxymethylation to the methylome at

imprinted loci, as well as the impact of additional environmental exposures on this recently rediscovered epigenetic mark.

## 3.6 Acknowledgements

We thank Dr. Claudia Lalancette at the University of Michigan Epigenomics Core for HMeDIP-seq DNA library prep. We also thank the University of Michigan Bioinformatics Core for sequencing data generation and QC.

## 3.7 Figures and Tables

| Gene | Full Name | GenBank Number | Strand | Primers (5' to 3') | Tm (°C) | Amplicon Size |
|---|---|---|---|---|---|---|
| *Gapdh* | Glyceraldehyde 3-phosphate dehydrogenase | NM_008084.3 | FWD | GCCTGCTTCACCACCTTCTT | 59.96 | 98 |
| | | | RVS | CATGGCCTTCCGTGTTCCTA | 59.07 | |
| *Gnas* | GNAS (guanine nucleotide binding protein, alpha stimulating) complex locus | NM_201618.2 | FWD | CTGCCATCATCTTCGTGGTG | 58.99 | 193 |
| | | | RVS | GATTTGCCAGCGAGGACTTT | 58.83 | |

**Table 3-1: RT-qPCR primers for self-designed gene assays.** Forward and reverse primer sequences for the *Gapdh* and *Gnas* RT-qPCR assays are listed, along with melting temperatures and amplicon size. All assays were designed using the online Genscript Real-time PCR Primer Design software (https://www.genscript.com/tools/real-time-pcr-tagman-primer-design-tool).

| Δ5-hmC | BPA-related DHMRs* |
|---|---|
| Hyper-hydroxymethylated | 1559 |
| Hypo-hydroxymethylated | 4247 |
| Both | 144 |
| **Total** | 5950 |

**Table 3-2: Differential 5-hmC in mouse blood by BPA exposure.** The *csaw* R package was used to examine the effect of BPA exposure (50 µg/kg diet) on 5-hmC content across the epigenome. Models included a paired mouse ID variable to account for within-individual effects, as well as a sex variable. Directionality of DHMRs (relative to control) is indicated in separate rows. *DHMR-calling significance threshold was set at FDR < 0.10.

| Chr | Start | End | Gene ID | Gene Name | Location | Direction with BPA exposure | *csaw* score | FDR |
|---|---|---|---|---|---|---|---|---|
| chr2 | 174315451 | 174315750 | 14683 | *Gnas* | intronic | + | 113.4 | <0.001 |
| chr11 | 12004801 | 12005100 | 14783 | *Grb10* | intronic | + | 70.5 | <0.001 |
| chr10 | 13130651 | 13131050 | 22634 | *Plagl1* | exonic | + | 60.7 | <0.001 |
| chr6 | 30957751 | 30958050 | 619665 | *Klf14* | exonic | - | 55.9 | <0.001 |
| chr17 | 8746901 | 8747050 | 23984 | *Pde10a* | intronic | + | 50.1 | <0.001 |
| chr17 | 12828001 | 12828550 | 104103 | *Airn* | intronic | - | 16.2 | 0.02 |
| chr13 | 24335001 | 24335150 | 12763 | *Cmah* | intronic | - | 13.1 | 0.05 |
| chr7 | 60207401 | 60207600 | 20646 | *Snrpn* | intronic | - | 13.0 | 0.05 |
| chr6 | 5079501 | 5079850 | 243725 | *Ppp1r9a* | intronic | - | 12.8 | 0.05 |
| chr7 | 143348051 | 143348350 | 16535 | *Kcnq1* | intronic | - | 11.5 | 0.07 |
| chr10 | 13402051 | 13402250 | 215789 | *Phactr2* | intronic | - | 11.3 | 0.07 |
| chr13 | 108963951 | 108964200 | 238871 | *Pde4d* | intronic | + | 10.1 | 0.10 |

**Table 3-3: Imprinted genetic loci with BPA-related DHMR.** List of imprinted loci with annotated, significant (FDR<0.10) DHMRs generated from *csaw* modeling results. The first four columns show the chromosomal location and entrez gene ID for each annotated imprinted gene. A transformed FDR is used for the *csaw* score, such that score = -10*log10(FDR); higher score indicates a larger degree of significance (lower FDR value). Additionally, direction of effect by BPA exposure is shown, with a (+) indicating increased 5-hmC with BPA exposure, and a (-) indicating decreased 5-hmC with BPA exposure.

| Gene Name | Location | Chr | Start | End | CpG Sites | CHG Sites |
|---|---|---|---|---|---|---|
| *Gnas* | intronic | chr2 | 174315451 | 174315750 | 0 | 21 |
| *Grb10* | intronic | chr11 | 12004801 | 12005100 | 0 | 13 |
| *Plagl1* | exonic | chr10 | 13130651 | 13131050 | 0 | 17 |
| *Klf14* | exonic | chr6 | 30957751 | 30958050 | 23 | 11 |
| *Pde10a* | intronic | chr17 | 8746901 | 8747050 | 1 | 10 |
| *Airn* | intronic | chr17 | 12828001 | 12828550 | 4 | 25 |
| *Cmah* | intronic | chr13 | 24335001 | 24335150 | 0 | 3 |
| *Snrpn* | intronic | chr7 | 60207401 | 60207600 | 0 | 0 |
| *Ppp1r9a* | intronic | chr6 | 5079501 | 5079850 | 1 | 31 |
| *Kcnq1* | intronic | chr7 | 143348051 | 143348350 | 5 | 13 |
| *Phactr2* | intronic | chr10 | 13402051 | 13402250 | 1 | 1 |
| *Pde4d* | intronic | chr13 | 108963951 | 108964200 | 1 | 5 |

**Table 3-4: Number of CpG and CHG sites at imprinted gene DHMRs.** The number of CpG and CHG sites contained within the twelve BPA-related imprinted gene DHMRs were quantified using the mm10 reference genome (https://www.ncbi.nlm.nih.gov/nuccore). The number of CpG sites varied by region, with five of the DHMRs showing zero CpG sites. This unexpected result may be the byproduct of several possible scenarios: 1. DNA hydroxymethylation at non-canonical methylation contexts (i.e. CHG sites); 2. Inexact DHMR definitions due to inherent lack of specificity in pulldown method (HMeDIP-seq); 3. False positives in our data. CpG and CHG sites were counted from the exact chromosomal range that was defined as a BPA-related DHMR.

| Hypo-hydroxymethylated BPA-related DHMR Pathways | | | |
|---|---|---|---|
| **Pathway Type** | **Description** | **FDR** | **Genes** |
| Gene Ontology Biological Process | hippocampus development | 0.007896 | 12568, 12570, 19280, 22062, 22416 |
| Gene Ontology Biological Process | spinal cord association neuron differentiation | 0.013765 | 18505, 21349, 22416 |

| Hyper-hydroxymethylated BPA-related DHMR Pathways | | | |
|---|---|---|---|
| **Pathway Type** | **Description** | **FDR** | **Gene IDs** |
| Gene Ontology Molecular Function | L-ascorbic acid binding | 0.006355 | 18484, 320452 |
| Gene Ontology Molecular Function | oxidoreductase activity, acting on paired donors, with incorporation or reduction of molecular oxygen | 0.006355 | 13105, 18484, 232174, 320452, 60527 |
| Gene Ontology Cellular Component | nucleolar part | 0.02366 | 12578, 68147 |
| Gene Ontology Biological Process | positive regulation of establishment of protein localization to plasma membrane | 0.028313 | 56212, 76686 |
| Gene Ontology Molecular Function | isoprenoid binding | 0.041794 | 225467, 232174 |

**Table 3-5: Enriched BPA-related DHMR pathways.** Pathway analysis for DHMRs was performed using the ChIP-enrich analysis tool (http://chip-enrich.med.umich.edu/). Within the ChIP-enrich tool, the gene set filter was set to 2000, peak threshold was set to 1, and adjustment for mappability of gene locus regions was set to false. The genome used for pathway analyses was mm10, and the ChIP-enrich method was used for enrichment testing. DHMRs were split into hypo- and hyper-methylated regions prior to separate analyses. Only regions <5kb from TSS were included in ChIP-enrich analysis. All pathway analyses included GO terms and KEGG pathways. After correcting for multiple testing, only pathways with FDR<0.05 were considered significant. Significant pathways for hypo- and hyper-methylated DHMRs are listed in separate tables; there was no overlap between significant pathways for these separate analyses. None of the significant pathways included any imprinted genes.

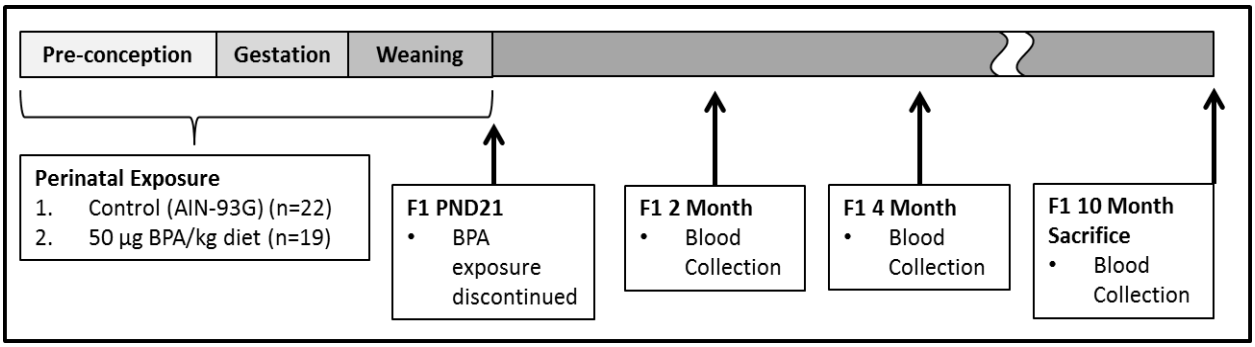


**Figure 3-1: Exposure paradigm and blood collection time points to measure longitudinal 5-hmC patterns.** Two weeks prior to mate-pairing with *Avy/a* males, six week old wild type *a/a* dams were placed on one of two experimental diet groups: (1) Control (modified AIN-93G), (2) Control + 50 µg BPA/kg diet. Exposure continued through pregnancy and lactation, ending for offspring at PND21. Matched blood samples were collected from wildtype a/a offspring at 2 months, 4 months, and 10 months of age.

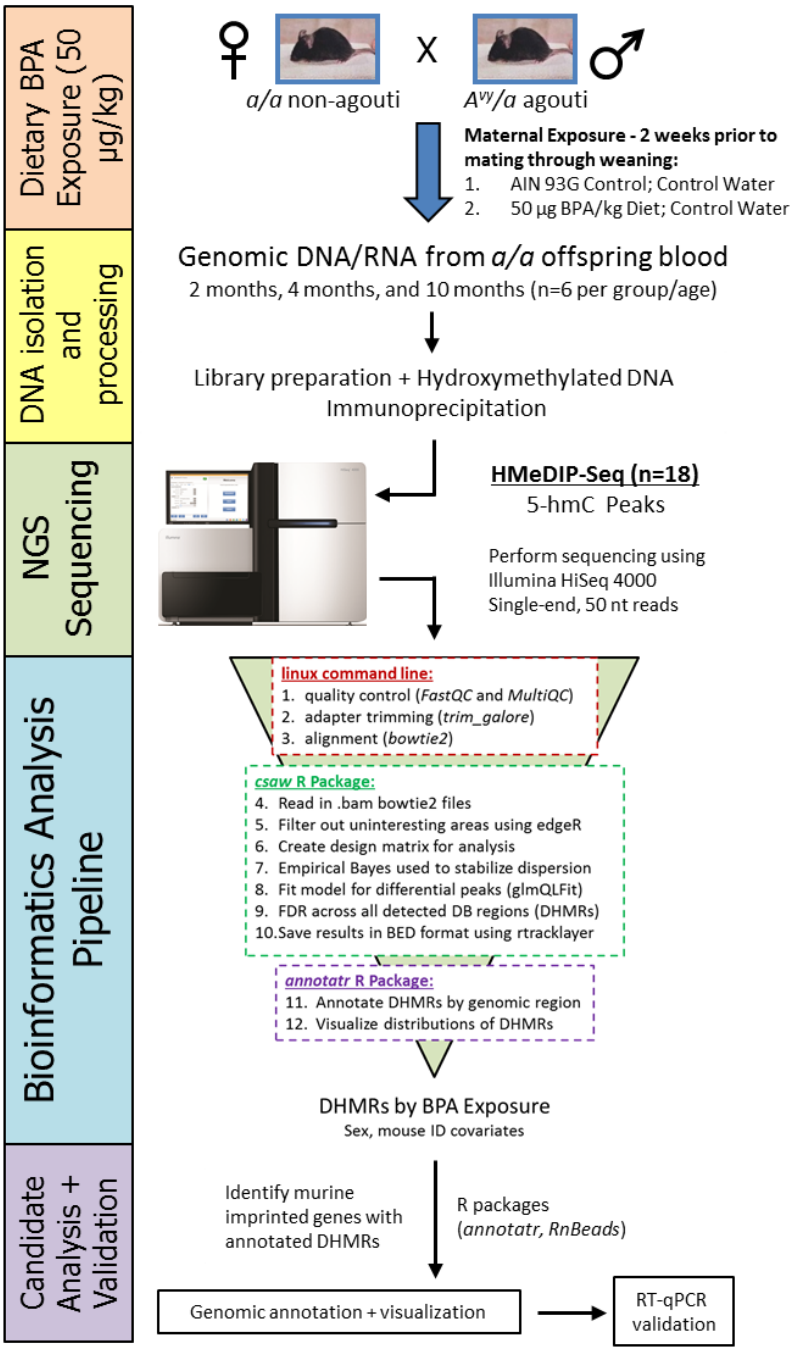


**Figure 3-2: Sequencing data collection and analysis workflow.** Genomic DNA was isolated from matched wild type a/a offspring blood samples at 2 months, 4 months, and 10 months of age. DNA was isolated from a subset of control (n=6 per age group) and BPA-exposed (n=6 per age group) mice, then processed in preparation for HMeDIP-seq. All processed samples were amplified and sequenced on an Illumina HiSeq 4000 sequencer using single-end, 50 nt reads. BPA-related differentially hydroxymethylated regions (DHMRs) were identified and annotated using a bioinformatics pipeline. Annotated DHMRs were then visualized in the genome browser. One target gene region – *Gnas* – was then validated using RT-qPCR on available RNA from the blood samples.

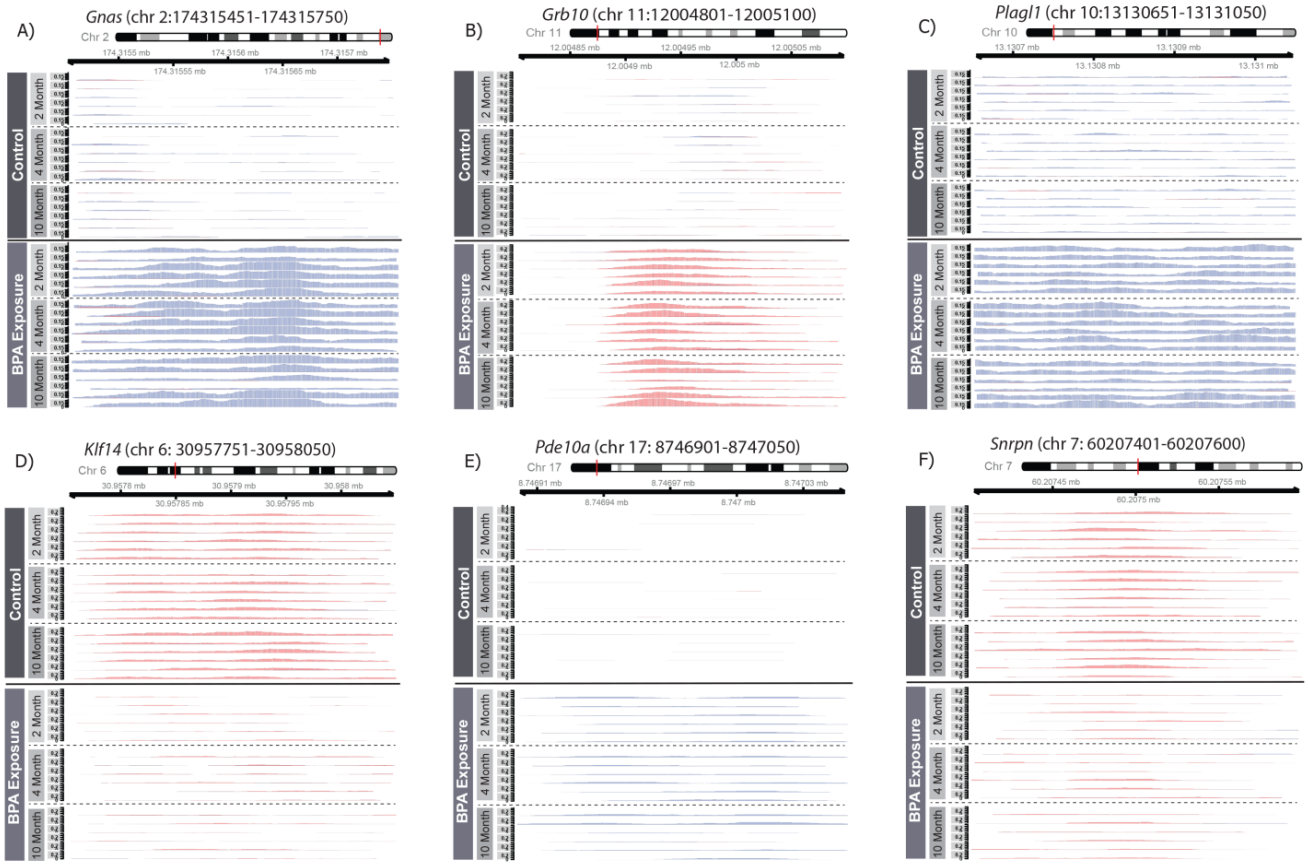


**Figure 3-3: Differential imprinted gene 5-hmC peaks by BPA exposure.** 5-hmC coverage was visualized at six imprinted loci with significant BPA-related DHMRs. 5-hmC peaks are shown for matched 2 month, 4 month, and 10 month blood samples, as indicated by y-axis labels. Blue and red peaks represent forward and reverse strand 5-hmC enrichment, respectively. All six DHMRs showed stable, longitudinal changes in 5-hmC peaks based on perinatal BPA exposure (50 µg/kg diet). A) *Gnas* showed BPA-related enrichment of 5-hmC in an intronic region. B) *Grb10* also showed BPA-related enrichment of 5-hmC in an intronic region. C) *Plagl1* showed BPA-related enrichment of 5-hmC in an exonic region. D) *Klf14* showed BPA-related depletion of 5-hmC in an exonic region. E) *Pde10a* showed subtle BPA-related enrichment of 5-hmC in an intronic region. F) *Snrpn* showed subtle BPA-related depletion of 5-hmC in an intronic region. The degree of 5-hmC enrichment or depletion by perinatal BPA exposure varied by imprinted locus, indicating that BPA has a variable effect on 5-hmC establishment at imprinted genes during development.

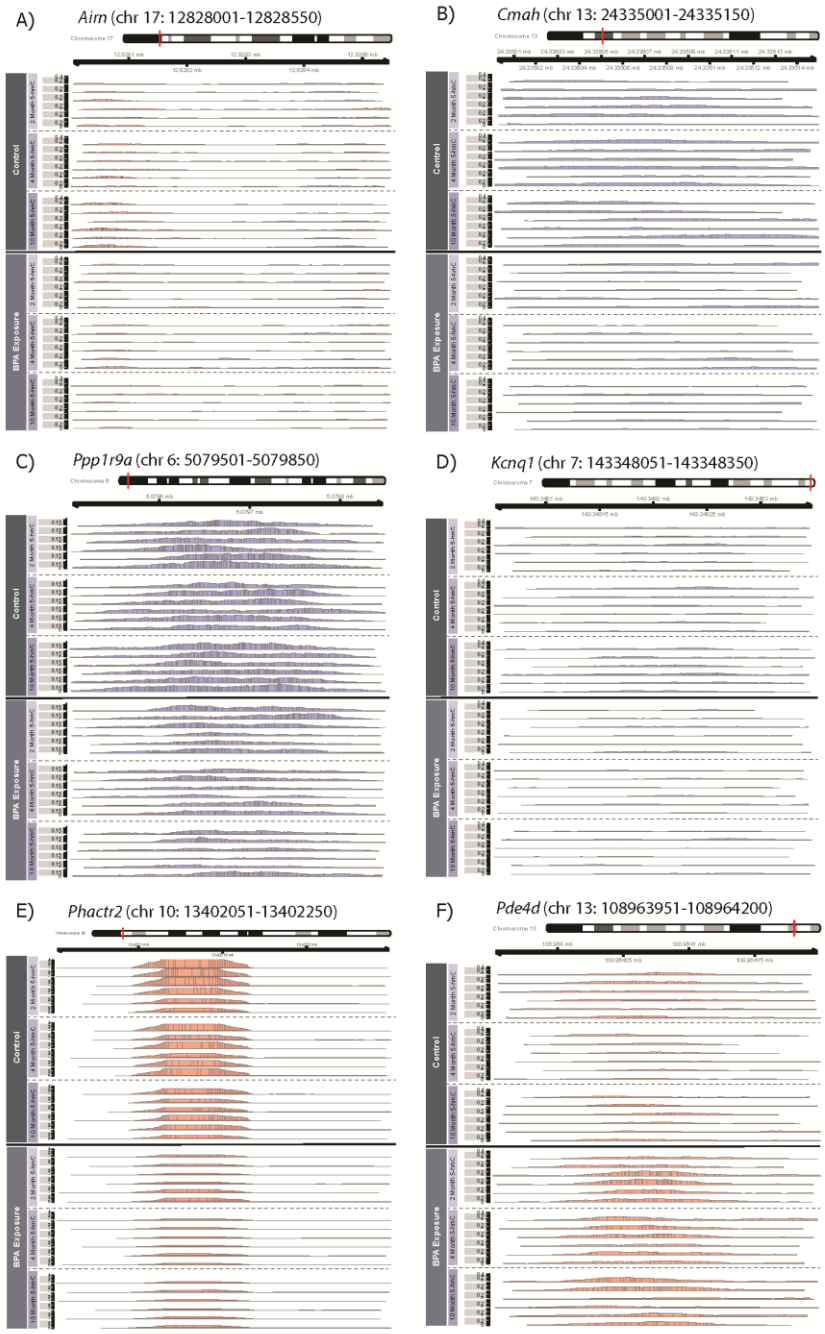


**Figure 3-4: Additional differential imprinted gene 5-hmC peaks by BPA exposure.** 5-hmC coverage was visualized at an additional six imprinted loci with significant BPA-related DHMRs. These six DHMRs also showed stable, longitudinal changes in 5-hmC peaks based on perinatal BPA exposure (50 µg/kg diet). A) *Airn* showed BPA-related depletion of 5-hmC across an intronic region. B) *Cmah* showed BPA-related depletion of 5-hmC in an intronic region. C) *Ppp1r9a* showed BPA-related depletion of 5-hmC in an intronic region. D) *Kcnq1* showed subtle BPA-related depletion of 5-hmC in an intronic region. E) *Phactr2* showed BPA-related depletion of 5-hmC in an intronic region. F) *Pde4d* showed BPA-related enrichment of 5-hmC in an intronic region. The degree of 5-hmC enrichment or depletion by perinatal BPA exposure varied by imprinted locus.

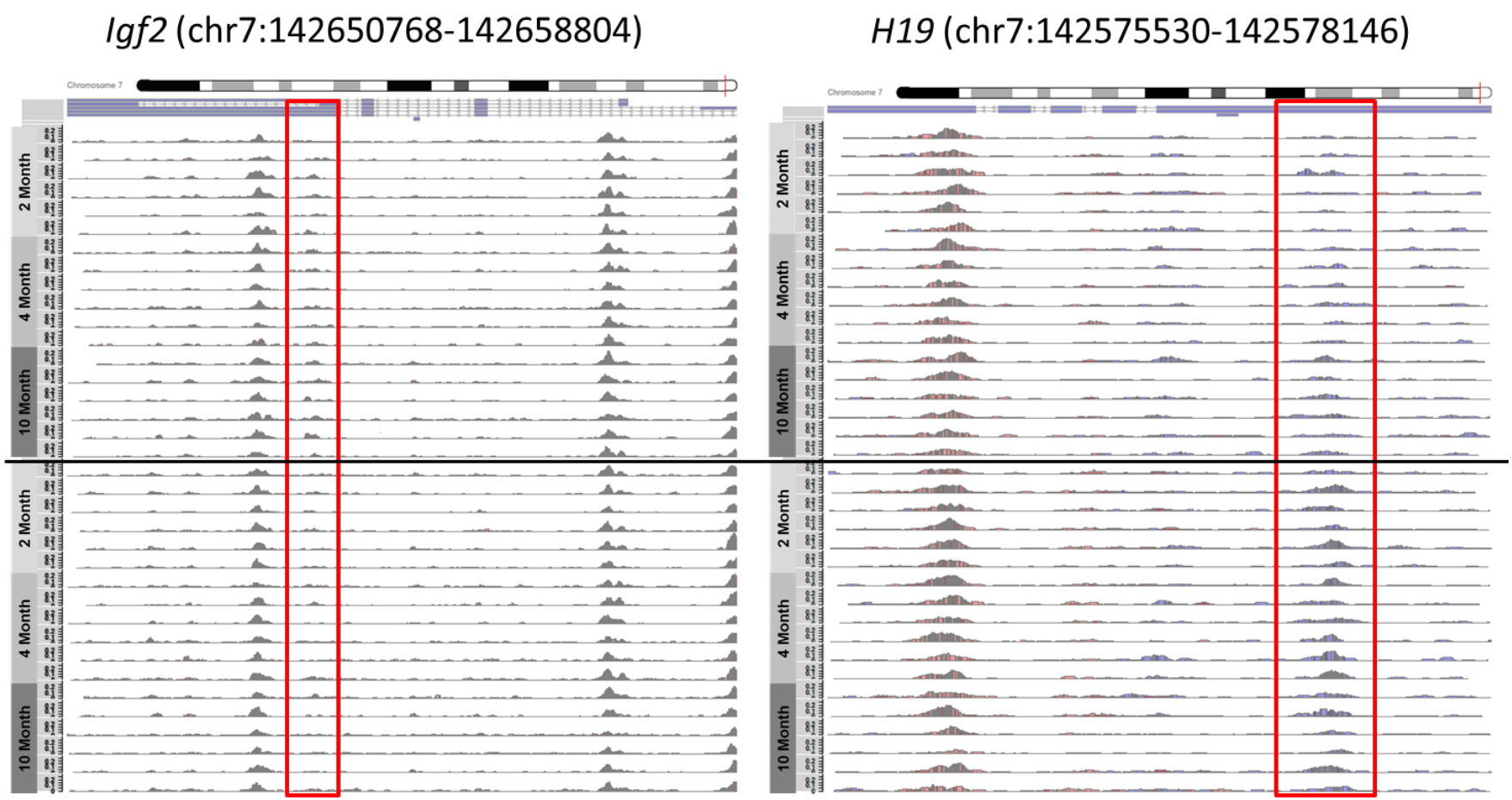


**Figure 3-5: 5-hmC peaks at the *Igf2/H19* imprinted loci.** Based on results at the *Plagl1* locus, which is a regulator of *Igf2* and *H19*, longitudinal 5-hmC patterns across the *Igf2* and *H19* imprinted genes were also visualized. 5-hmC peaks at both loci appear stable across individuals and adulthood stage in longitudinal mouse blood (2, 4, and 10 months old). Regions of non-significant BPA-related differential 5-hmC are indicated in red boxes for both genes. Specifically, *Igf2* shows BPA-related hypo-hydroxymethylation, and *H19* shows BPA-related hyper-hysdroxymethylation. Despite not being detected as significant DHMRs in *csaw*, these BPA-related changes in 5-hmC were stable at all three measured time points.

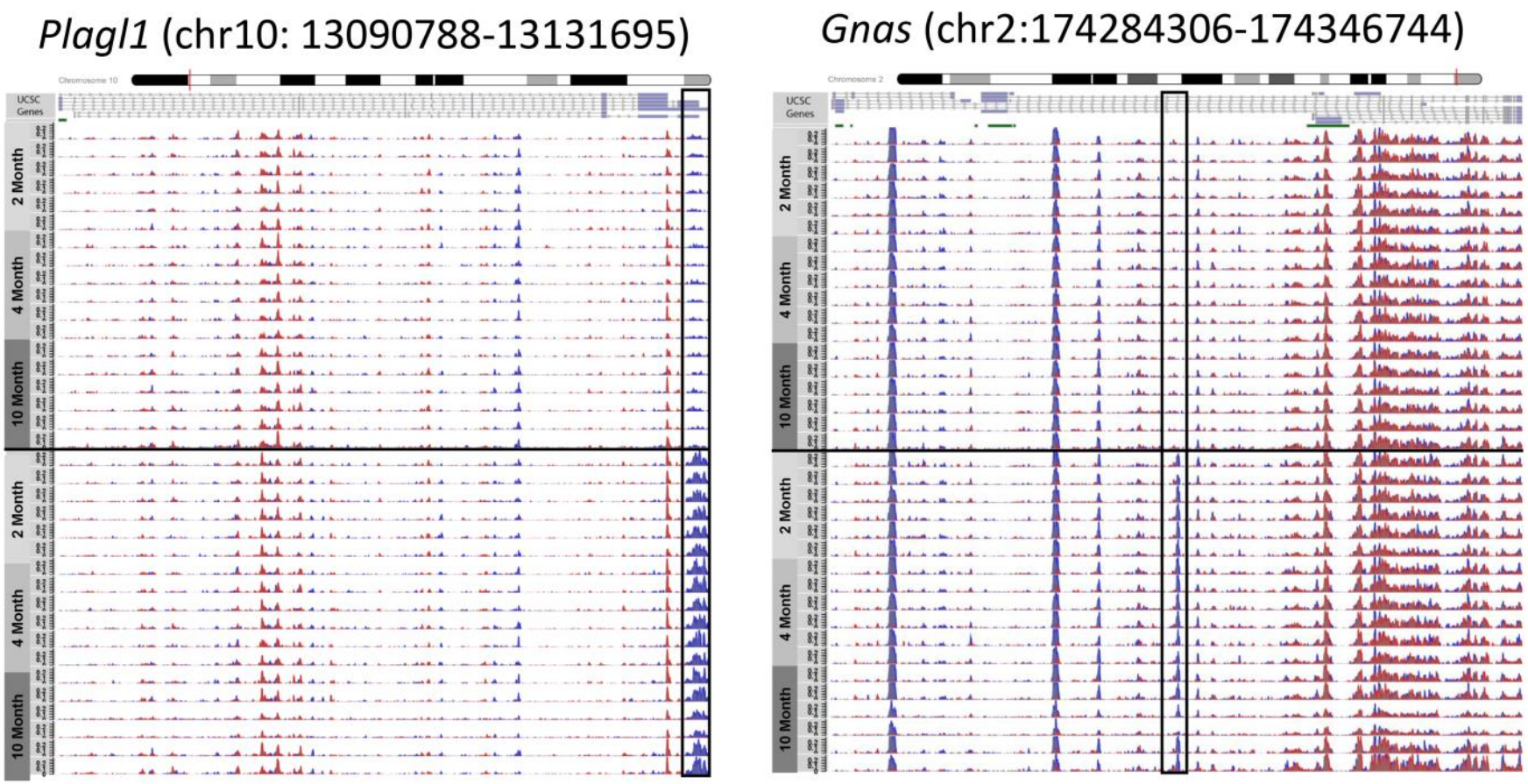


**Figure 3-6: Genomic context of *Gnas* and *Plagl1* DHMRs.** The DHMRs annotated to the *Gnas* and *Plagl1* genes were visualized in the context of their respective imprinted genes using the *csaw* and *Gviz* R packages. 5-hmC peaks across the complete *Gnas* and *Plagl1* imprinted loci are presented, showing distinct 5-hmC peaks along the length of both genes. 5-hmC peaks are shown for matched 2 month, 4 month, and 10 month blood samples, as indicated by y-axis labels. Black boxes indicate significant DHMRs that were identified using *csaw* differential hydroxymethylation models. Blue and red peaks represent forward and reverse strand 5-hmC enrichment, respectively. Green boxes below UCSC gene tracks represent CpG islands.

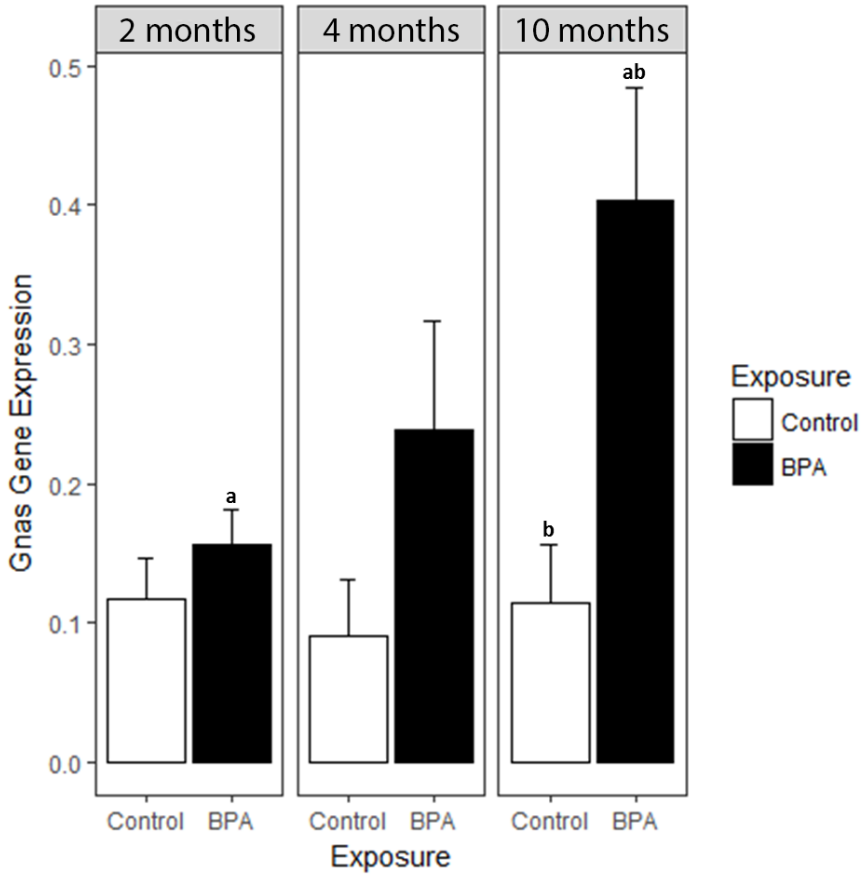


**Figure 3-7: *Gnas* expression by BPA exposure and age.** Based on BPA-related DHMR annotated to the Gnas gene, RT-qPCR was used to investigate longitudinal blood Gnas mRNA expression levels. Three housekeeping genes – *Actb*, *18S*, and *Gapdh* – were included as internal controls in all RT-qPCR runs. In addition to housekeeping genes, an inter-plate calibrator control of brain cDNA was included for calculation of relative gene expression across multiple plates; all expression values are shown relative to this inter-plate calibrator. Expression levels were calculated following the $2^{-\Delta\Delta Ct}$ method. [a]Mean *Gnas* expression in BPA-exposed mouse blood showed a significant increase between 2 and 10 months of age (p=0.05); this pattern was not found in control samples. [b]Mean *Gnas* expression was significantly lower in control blood than BPA-exposed blood at 10 months of age (p=0.01).

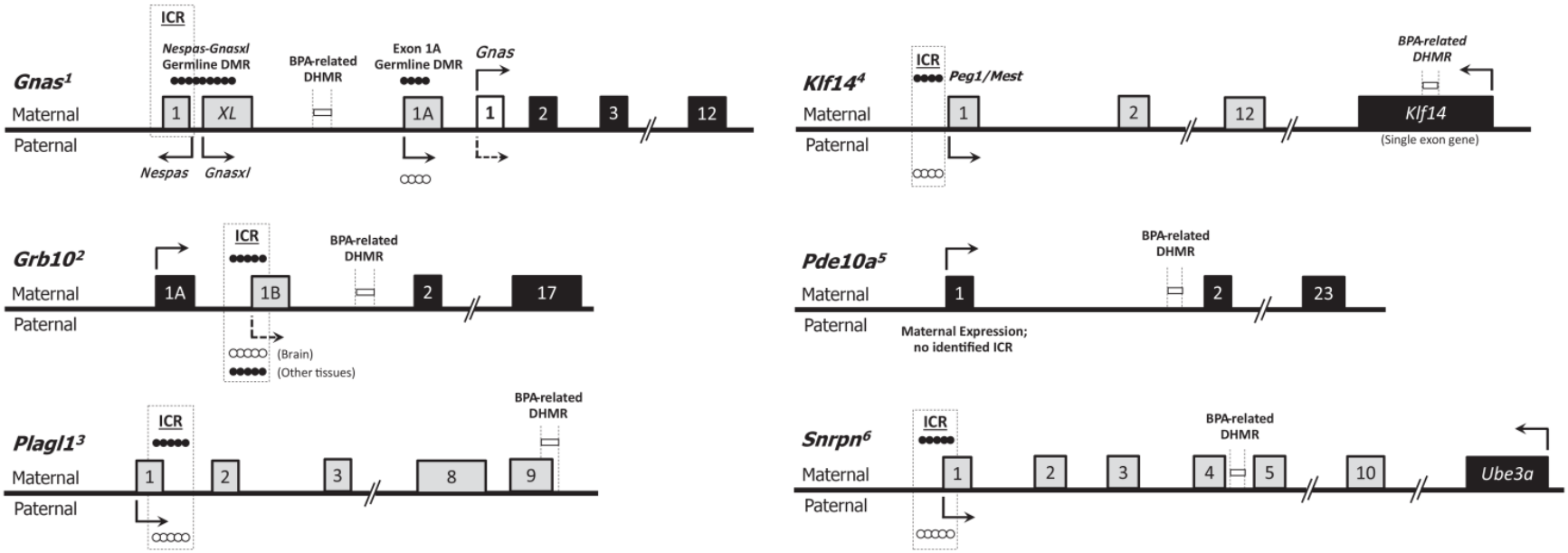


**Figure 3-8: Organization of the *Gnas*, *Grb10*, *Plagl1*, *Klf14*, *Pde10a*, and *Snrpn* imprinted loci.** The thick black mid-line represents the gene sequence. Maternally expressed exons are indicated by black boxes, and paternally expressed exons are indicated by grey boxes. Exon locations for each gene are relative, but not to scale. Exon 1 of the *Gnas* gene is both maternally and paternally expressed, and is therefore indicated by a white box. Arrows show directionality and start sites for transcription. Parental origin-specific expression patterns are represented by location of arrow above or below middle line, and context-specific expression is indicated by dotted arrows. Filled and empty circles represent methylated or unmethylated alleles, respectively. Imprinting control regions (ICRs) are indicated by dotted line boxes, and BPA-related DHMRs are indicated by boxes bordered by dotted vertical lines. None of the identified BPA-related DHMRs are located in known imprinting control regions. [1]Adapted from (Tibbit et al. 2015). [2]Adapted from (Hikichi et al. 2003). [3](Iglesias-Platas et al. 2012; Smith et al. 2002). [4]Adapted from (Parker-Katiraee et al. 2007). [5](Wang et al. 2011). [6](Sanli and Feil 2015; Shemer et al. 1997).

## 3.8 References


Anderson OS, Nahar MS, Faulk C, Jones TR, Liao C, Kannan K, et al. 2012. Epigenetic responses following maternal dietary exposure to physiologically relevant levels of bisphenol A. Env. Mol Mutagen 53:334–342; doi:10.1002/em.21692.

Arnaud P. 2010. Genomic imprinting in germ cells: imprints are under control. Reproduction 140:411–423; doi:10.1530/REP-10-0173.

Babu S, Uppu S, Claville MO, Uppu RM. 2013. Prooxidant actions of bisphenol A (BPA) phenoxyl radicals: implications to BPA-related oxidative stress and toxicity. Toxicol. Mech. Methods 23:273–280; doi:10.3109/15376516.2012.753969.

Bartolomei MS, Ferguson-Smith AC. 2011. Mammalian genomic imprinting. Cold Spring Harb. Perspect. Biol. 3; doi:10.1101/cshperspect.a002592.

Bateson P, Barker D, Clutton-Brock T, Deb D, D'Udine B, Foley RA, et al. 2004. Developmental plasticity and human health. Nature 430:419–421; doi:10.1038/nature02725.

Bender AT, Beavo JA. 2006. Cyclic Nucleotide Phosphodiesterases: Molecular Regulation to Clinical Use. Pharmacol. Rev. 58:488–520; doi:10.1124/pr.58.3.5.

Benjamini Y, Hochberg Y. 1995. Controlling the False Discovery Rate: A Practical and Powerful Approach to Multiple Testing. J. R. Stat. Soc. Ser. B 57:289–300; doi:10.2307/2346101.

Benjamini Y, Hochberg Y. 1997. Multiple Hypotheses Testing with Weights. Scand. J. Stat. 24:407–418; doi:10.1111/1467-9469.00072.

Calafat AM, Ye X, Wong LY, Reidy JA, Needham LL. 2008. Exposure of the U.S. population to bisphenol A and 4-tertiary-octylphenol: 2003-2004. Env. Heal. Perspect 116:39–44; doi:10.1289/ehp.10753.

Cavalcante RG, Patil S, Park Y, Rozek LS, Sartor MA. 2017. Integrating DNA Methylation and Hydroxymethylation Data with the Mint Pipeline. Cancer Res. 77:e27–e30; doi:10.1158/0008-5472.CAN-17-0330.

Cavalcante RG, Sartor MA. 2017. annotatr: genomic regions in context. Bioinformatics 33:2381–2383; doi:10.1093/bioinformatics/btx183.

Chia N, Wang L, Lu X, Senut M-C, Brenner C, Ruden DM. 2011. Hypothesis: environmental regulation of 5-hydroxymethylcytosine by oxidative stress. Epigenetics 6: 853–6.

Cotton AM, Price EM, Jones MJ, Balaton BP, Kobor MS, Brown CJ. 2015. Landscape of DNA methylation on the X chromosome reflects CpG density, functional chromatin state and X-chromosome inactivation. Hum. Mol. Genet. 24:1528–39; doi:10.1093/hmg/ddu564.

Coulter JB, O'Driscoll CM, Bressler JP. 2013. Hydroquinone increases 5-hydroxymethylcytosine formation through ten eleven translocation 1 (TET1) 5-methylcytosine dioxygenase. J Biol Chem 288:28792–28800; doi:10.1074/jbc.M113.491365.

Das R, Hampton DD, Jirtle RL. 2009. Imprinting evolution and human health. Mamm. Genome 20:563–572; doi:10.1007/s00335-009-9229-y.

Delatte B, Jeschke J, Defrance M, Bachman M, Creppe C, Calonne E, et al. 2015. Genome-wide hydroxymethylcytosine pattern changes in response to oxidative stress. Sci Rep 5:12714; doi:10.1038/srep12714.

Dolinoy DC, Weinhouse C, Jones TR, Rozek LS, Jirtle RL. 2010. Variable histone modifications at the A(vy) metastable epiallele. Epigenetics 5:637–44; doi:10.4161/epi.5.7.12892.

Ehrlich M, Ehrlich KC. 2014. DNA cytosine methylation and hydroxymethylation at the borders. Epigenomics 6:563–6; doi:10.2217/epi.14.48.

Faulk C, Kim JH, Jones TR, McEachin RC, Nahar MS, Dolinoy DC, et al. 2015. Bisphenol A-associated alterations in genome-wide DNA methylation and gene expression patterns reveal sequence-dependent and non-monotonic effects in human fetal liver. Environ. epigenetics 1; doi:10.1093/eep/dvv006.

Gallou-Kabani C, Gabory A, Tost J, Karimi M, Mayeur S, Lesage J, et al. 2010. Sex- and Diet-Specific Changes of Imprinted Gene Expression and DNA Methylation in Mouse Placenta under a High-Fat Diet. J. Najbauer, ed PLoS One 5:e14398; doi:10.1371/journal.pone.0014398.

Garfield AS, Cowley M, Smith FM, Moorwood K, Stewart-Cox JE, Gilroy K, et al. 2011. Distinct physiological and behavioural functions for parental alleles of imprinted Grb10. Nature 469:534–538; doi:10.1038/nature09651.

Gassman NR. 2017. Induction of oxidative stress by bisphenol A and its pleiotropic effects. Environ. Mol. Mutagen. 58:60–71; doi:10.1002/em.22072.

Globisch D, Münzel M, Müller M, Michalakis S, Wagner M, Koch S, et al. 2010. Tissue distribution of 5-hydroxymethylcytosine and search for active demethylation intermediates. PLoS One 5:e15367; doi:10.1371/journal.pone.0015367.

Hahn MA, Szabó PE, Pfeifer GP. 2014. 5-Hydroxymethylcytosine: a stable or transient DNA modification? Genomics 104:314–323; doi:10.1016/j.ygeno.2014.08.015.

Hahne F, Ivanek R. 2016. Visualizing Genomic Data Using Gviz and Bioconductor. In: *Methods in molecular biology (Clifton, N.J.)*. Vol. 1418 of. 335–351.

Haycock PC, Ramsay M. 2009. Exposure of Mouse Embryos to Ethanol During Preimplantation

Development: Effect on DNA Methylation in the H19 Imprinting Control Region1. Biol. Reprod. 81:618–627; doi:10.1095/biolreprod.108.074682.

He Y, Hariharan M, Gorkin DU, Dickel DE, Luo C, Castanon RG, et al. 2017. Spatiotemporal DNA Methylome Dynamics of the Developing Mammalian Fetus. bioRxiv 166744; doi:10.1101/166744.

Heijmans BT, Tobi EW, Stein AD, Putter H, Blauw GJ, Susser ES, et al. 2008. Persistent epigenetic differences associated with prenatal exposure to famine in humans. Proc Natl Acad Sci U S A 105:17046–17049; doi:10.1073/pnas.0806560105.

Heindel JJ, Balbus J, Birnbaum L, Brune-Drisse MN, Grandjean P, Gray K, et al. 2015. Developmental Origins of Health and Disease: Integrating Environmental Influences. Endocrinology 156:3416–3421; doi:10.1210/EN.2015-1394.

Hernandez Mora JR, Sanchez-Delgado M, Petazzi P, Moran S, Esteller M, Iglesias-Platas I, et al. 2017. Profiling of oxBS-450K 5-hydroxymethylcytosine in human placenta and brain reveals enrichment at imprinted loci. Epigenetics 00–00; doi:10.1080/15592294.2017.1344803.

Hikichi T, Kohda T, Kaneko-Ishino T, Ishino F. 2003. Imprinting regulation of the murine Meg1/Grb10 and human GRB10 genes; roles of brain-specific promoters and mouse-specific CTCF-binding sites. Nucleic Acids Res. 31: 1398–406.

Holt LJ, Siddle K. 2005. Grb10 and Grb14: enigmatic regulators of insulin action--and more? Biochem. J. 388:393–406; doi:10.1042/BJ20050216.

Huang Y, Pastor WA, Shen Y, Tahiliani M, Liu DR, Rao A. 2010. The Behaviour of 5-Hydroxymethylcytosine in Bisulfite Sequencing. J. Liu, ed PLoS One 5:e8888; doi:10.1371/journal.pone.0008888.

Iglesias-Platas I, Court F, Camprubi C, Sparago A, Guillaumet-Adkins A, Martin-Trujillo A, et al. 2013. Imprinting at the PLAGL1 domain is contained within a 70-kb CTCF/cohesin-mediated non-allelic chromatin loop. Nucleic Acids Res. 41:2171–9; doi:10.1093/nar/gks1355.

Iglesias-Platas I, Martin-Trujillo A, Cirillo D, Court F, Guillaumet-Adkins A, Camprubi C, et al. 2012. Characterization of Novel Paternal ncRNAs at the Plagl1 Locus, Including Hymai, Predicted to Interact with Regulators of Active Chromatin. E.E. Schmidt, ed PLoS One 7:e38907; doi:10.1371/journal.pone.0038907.

Jirtle RL, Skinner MK. 2007. Environmental epigenomics and disease susceptibility. Nat. Rev. Genet. 8:253–262; doi:10.1038/nrg2045.

Kabir NN, Kazi JU. 2014. Grb10 is a dual regulator of receptor tyrosine kinase signaling. Mol. Biol. Rep. 41:1985–1992; doi:10.1007/s11033-014-3046-4.

Kelsey G, Feil R. 2012. New insights into establishment and maintenance of DNA methylation imprints in mammals. Philos. Trans. R. Soc. B Biol. Sci. 368:20110336–20110336; doi:10.1098/rstb.2011.0336.

Kim J, He H, Kim H. 2017. Inversion of the imprinting control region of the Peg3 domain. Y. Yu, ed PLoS One 12:e0181591; doi:10.1371/journal.pone.0181591.

Kim JH, Sartor MA, Rozek LS, Faulk C, Anderson OS, Jones TR, et al. 2014. Perinatal bisphenol A exposure promotes dose-dependent alterations of the mouse methylome. BMC Genomics 15:30; doi:10.1186/1471-2164-15-30.

Kinde B, Gabel HW, Gilbert CS, Griffith EC, Greenberg ME. 2015. Reading the unique DNA methylation landscape of the brain: Non-CpG methylation, hydroxymethylation, and MeCP2. Proc. Natl. Acad. Sci. U. S. A. 112:6800–6; doi:10.1073/pnas.1411269112.

Krüger T, Long M, Bonefeld-Jørgensen EC. 2008. Plastic components affect the activation of the aryl hydrocarbon and the androgen receptor. Toxicology 246:112–123; doi:10.1016/j.tox.2007.12.028.

La Salle S, Mertineit C, Taketo T, Moens PB, Bestor TH, Trasler JM. 2004. Windows for sex-specific methylation marked by DNA methyltransferase expression profiles in mouse germ cells. Dev. Biol. 268:403–415; doi:10.1016/j.ydbio.2003.12.031.

Li H, Wang Z, Ma T, Wei G, Ni T. 2017. Alternative splicing in aging and age-related diseases. Transl. Med. Aging; doi:10.1016/J.TMA.2017.09.005.

Livak KJ, Schmittgen TD. 2001. Analysis of Relative Gene Expression Data Using Real-Time Quantitative PCR and the 2−ΔΔCT Method. Methods 25:402–408; doi:10.1006/meth.2001.1262.

López V, Fernández AF, Fraga MF. 2017. The role of 5-hydroxymethylcytosine in development, aging and age-related diseases. Ageing Res. Rev. 37:28–38; doi:10.1016/J.ARR.2017.05.002.

Lun ATL, Smyth GK. 2016. csaw: a Bioconductor package for differential binding analysis of ChIP-seq data using sliding windows. Nucleic Acids Res. 44:e45–e45; doi:10.1093/nar/gkv1191.

Manikkam M, Tracey R, Guerrero-Bosagna C, Skinner MK. 2013. Plastics derived endocrine disruptors (BPA, DEHP and DBP) induce epigenetic transgenerational inheritance of obesity, reproductive disease and sperm epimutations. PLoS One 8:e55387; doi:10.1371/journal.pone.0055387.

Medvedeva YA, Khamis AM, Kulakovskiy I V, Ba-Alawi W, Bhuyan MS, Kawaji H, et al. 2014. Effects of cytosine methylation on transcription factor binding sites. BMC Genomics

15:119; doi:10.1186/1471-2164-15-119.

Messerschmidt DM, Knowles BB, Solter D. 2014. DNA methylation dynamics during epigenetic reprogramming in the germline and preimplantation embryos. Genes Dev 28:812–828; doi:10.1101/gad.234294.113.

National Research Council (US) Committee for the Update of the Guide for the Care and Use of Laboratory Animals. 2011.In: *Guide for the Care and Use of Laboratory Animals*. National Academies Press (U.S.):Washington, D.C.

Nawrocki AR, Rodriguez CG, Toolan DM, Price O, Henry M, Forrest G, et al. 2014. Genetic deletion and pharmacological inhibition of phosphodiesterase 10A protects mice from diet-induced obesity and insulin resistance. Diabetes 63:300–11; doi:10.2337/db13-0247.

Nye MD, Hoyo C, Murphy SK. 2015. In vitro lead exposure changes DNA methylation and expression of IGF2 and PEG1/MEST. Toxicol. In Vitro 29:544–50; doi:10.1016/j.tiv.2015.01.002.

Parker-Katiraee L, Carson AR, Yamada T, Arnaud P, Feil R, Abu-Amero SN, et al. 2007. Identification of the Imprinted KLF14 Transcription Factor Undergoing Human-Specific Accelerated Evolution. PLoS Genet. 3:e65; doi:10.1371/journal.pgen.0030065.

Pennacchio LA, Bickmore W, Dean A, Nobrega MA, Bejerano G. 2013. Enhancers: five essential questions. Nat. Rev. Genet. 14:288–95; doi:10.1038/nrg3458.

Peters J, Williamson CM. 2007. Control of Imprinting at the Gnas Cluster. EpigeneticsEpigenetics 244:207–213; doi:10.4161/epi.2.4.5380doi.org/10.4161/epi.2.4.5380.

Pidsley R, Fernandes C, Viana J, Paya-Cano JL, Liu L, Smith RG, et al. 2012. DNA methylation at the Igf2/H19 imprinting control region is associated with cerebellum mass in outbred mice. Mol. Brain 5:42; doi:10.1186/1756-6606-5-42.

Plagge A, Kelsey G. 2006. Imprinting the <i>Gnas</i> locus. Cytogenet. Genome Res. 113:178–187; doi:10.1159/000090830.

Plasschaert RN, Bartolomei MS. 2014. Genomic imprinting in development, growth, behavior and stem cells. Development 141:1805–1813; doi:10.1242/dev.101428.

Plasschaert RN, Bartolomei MS. 2015. Tissue-specific regulation and function of Grb10 during growth and neuronal commitment. Proc. Natl. Acad. Sci. 112:6841–6847; doi:10.1073/pnas.1411254111.

Reik W, Dean W, Walter J. 2001. Epigenetic reprogramming in mammalian development. Science (80-. ). 293:1089–1093; doi:10.1126/science.1063443.

Relkovic D, Isles AR. 2013. Behavioural and cognitive profiles of mouse models for Prader–Willi syndrome. Brain Res. Bull. 92:41–48; doi:10.1016/J.BRAINRESBULL.2011.09.009.

Riedel H. 2004. Grb10 exceeding the boundaries of a common signaling adapter. Front. Biosci. 9: 603–18.

Sakuma S, Nakanishi M, Morinaga K, Fujitake M, Wada S, Fujimoto Y. 2010. Bisphenol A 3,4-quinone induces the conversion of xanthine dehydrogenase into oxidase in vitro. Food Chem. Toxicol. 48:2217–2222; doi:10.1016/j.fct.2010.05.051.

Sanli I, Feil R. 2015. Chromatin mechanisms in the developmental control of imprinted gene expression. Int. J. Biochem. Cell Biol. 67:139–147; doi:10.1016/J.BIOCEL.2015.04.004.

Sanz LA, Chamberlain S, Sabourin J-C, Henckel A, Magnuson T, Hugnot J-P, et al. 2008. A mono-allelic bivalent chromatin domain controls tissue-specific imprinting at Grb10. EMBO J. 27:2523–32; doi:10.1038/emboj.2008.142.

Shemer R, Birger Y, Riggs AD, Razin A. 1997. Structure of the imprinted mouse Snrpn gene and establishment of its parental-specific methylation pattern. Proc. Natl. Acad. Sci. U. S. A. 94: 10267–72.

Shen L, Song CX, He C, Zhang Y. 2014. Mechanism and function of oxidative reversal of DNA and RNA methylation. Annu Rev Biochem 83:585–614; doi:10.1146/annurev-biochem-060713-035513.

Shlyueva D, Stampfel G, Stark A. 2014. Transcriptional enhancers: from properties to genome-wide predictions. Nat. Rev. Genet. 15:272–286; doi:10.1038/nrg3682.

Singh S, Li SS. 2012. Epigenetic effects of environmental chemicals bisphenol a and phthalates. Int J Mol Sci 13:10143–10153; doi:10.3390/ijms130810143.

Skryabin B V., Gubar L V., Seeger B, Pfeiffer J, Handel S, Robeck T, et al. 2007. Deletion of the MBII-85 snoRNA Gene Cluster in Mice Results in Postnatal Growth Retardation. PLoS Genet. 3:e235; doi:10.1371/journal.pgen.0030235.

Small KS, Hedman AK, Grundberg E, Nica AC, Thorleifsson G, Kong A, et al. 2011. Identification of an imprinted master trans regulator at the KLF14 locus related to multiple metabolic phenotypes. Nat. Genet. 43:561–4; doi:10.1038/ng.833.

Smallwood SA, Kelsey G. 2012. De novo DNA methylation: a germ cell perspective. Trends Genet 28:33–42; doi:10.1016/j.tig.2011.09.004.

Smith RJ, Arnaud P, Konfortova G, Dean WL, Beechey C V., Kelsey G. 2002. The mouse Zac1 locus: basis for imprinting and comparison with human ZAC. Gene 292:101–112; doi:10.1016/S0378-1119(02)00666-2.

Soderling SH, Bayuga SJ, Beavo JA. 1999. Isolation and characterization of a dual-substrate phosphodiesterase gene family: PDE10A. Proc. Natl. Acad. Sci. U. S. A. 96: 7071–6.

Stroud H, Feng S, Kinney SM, Pradhan S, Jacobsen SE. 2011. 5-Hydroxymethylcytosine is associated with enhancers and gene bodies in human embryonic stem cells. Genome Biol. 12:R54; doi:10.1186/gb-2011-12-6-r54.

Sui Y, Ai N, Park SH, Rios-Pilier J, Perkins JT, Welsh WJ, et al. 2012. Bisphenol A and its analogues activate human pregnane X receptor. Env. Heal. Perspect 120:399–405; doi:10.1289/ehp.1104426.

Sun Z, Terragni J, Borgaro JG, Liu Y, Yu L, Guan S, et al. 2013. High-Resolution Enzymatic Mapping of Genomic 5-Hydroxymethylcytosine in Mouse Embryonic Stem Cells. Cell Rep. 3:567–576; doi:10.1016/J.CELREP.2013.01.001.

Susiarjo M, Sasson I, Mesaros C, Bartolomei MS. 2013. Bisphenol A Exposure Disrupts Genomic Imprinting in the Mouse. G. Kelsey, ed PLoS Genet. 9:e1003401; doi:10.1371/journal.pgen.1003401.

Tan L, Xiong L, Xu W, Wu F, Huang N, Xu Y, et al. 2013. Genome-wide comparison of DNA hydroxymethylation in mouse embryonic stem cells and neural progenitor cells by a new comparative hMeDIP-seq method. Nucleic Acids Res 41:e84; doi:10.1093/nar/gkt091.

Tibbit C, Williamson C, Mehta S, Ball S, Chotalia M, Nottingham W, et al. 2015. Antisense Activity across the Nesp Promoter is Required for Nespas-Mediated Silencing in the Imprinted Gnas Cluster. Non-Coding RNA 1:246–265; doi:10.3390/ncrna1030246.

Varrault A, Dantec C, Le Digarcher A, Chotard L, Bilanges B, Parrinello H, et al. 2017. Identification of Plagl1/Zac1 binding sites and target genes establishes its role in the regulation of extracellular matrix genes and the imprinted gene network. Nucleic Acids Res. 45:10466–10480; doi:10.1093/nar/gkx672.

Varrault A, Gueydan C, Delalbre A, Bellmann A, Houssami S, Aknin C, et al. 2006. Zac1 Regulates an Imprinted Gene Network Critically Involved in the Control of Embryonic Growth. Dev. Cell 11:711–722; doi:10.1016/j.devcel.2006.09.003.

Wang L, Tong X, Gu F, Zhang L, Chen W, Cheng X, et al. 2017. The KLF14 transcription factor regulates hepatic gluconeogenesis in mice. J. Biol. Chem. jbc.RA117.000184; doi:10.1074/jbc.RA117.000184.

Wang X, Soloway PD, Clark AG. 2011. A survey for novel imprinted genes in the mouse placenta by mRNA-seq. Genetics 189:109–22; doi:10.1534/genetics.111.130088.

Waterland RA, Jirtle RL. 2003. Transposable elements: targets for early nutritional effects on epigenetic gene regulation. Mol Cell Biol 23: 5293–5300.

Watson CS, Bulayeva NN, Wozniak AL, Alyea RA. 2007. Xenoestrogens are potent activators of nongenomic estrogenic responses. Steroids 72:124–134; doi:10.1016/j.steroids.2006.11.002.

Wei H, Feng Y, Liang F, Cheng W, Wu X, Zhou R, et al. 2017. Role of oxidative stress and DNA hydroxymethylation in the neurotoxicity of fine particulate matter. Toxicology 380:94–103; doi:10.1016/j.tox.2017.01.017.

Weinhouse C, Anderson OS, Bergin IL, Vandenbergh DJ, Gyekis JP, Dingman MA, et al. 2014. Dose-dependent incidence of hepatic tumors in adult mice following perinatal exposure to bisphenol A. Env. Heal. Perspect 122:485–491; doi:10.1289/ehp.1307449.

Welch RP, Lee C, Imbriano PM, Patil S, Weymouth TE, Smith RA, et al. 2014. ChIP-Enrich: gene set enrichment testing for ChIP-seq data. Nucleic Acids Res. 42:e105–e105; doi:10.1093/nar/gku463.

Wen L, Li X, Yan L, Tan Y, Li R, Zhao Y, et al. 2014. Whole-genome analysis of 5-hydroxymethylcytosine and 5-methylcytosine at base resolution in the human brain. Genome Biol. 15:R49; doi:10.1186/gb-2014-15-3-r49.

Williamson C, Blake A, Thomas S, Beechey C, Hancock J, Cattanach B, et al. 2013. World Wide Web Site - Mouse Imprinting Data and References. MRC Harwell, Oxfordsh. Available: http://www.har.mrc.ac.uk/research/genomic_imprinting/.

Wolstenholme JT, Rissman EF, Connelly JJ. 2011. The role of Bisphenol A in shaping the brain, epigenome and behavior. Horm Behav 59:296–305; doi:10.1016/j.yhbeh.2010.10.001.

Wu H, D'Alessio AC, Ito S, Wang Z, Cui K, Zhao K, et al. 2011. Genome-wide analysis of 5-hydroxymethylcytosine distribution reveals its dual function in transcriptional regulation in mouse embryonic stem cells. Genes Dev 25:679–684; doi:10.1101/gad.2036011.

Wu M-Y, Jiang M, Zhai X, Beaudet AL, Wu R-C. 2012. An unexpected function of the Prader-Willi syndrome imprinting center in maternal imprinting in mice. PLoS One 7:e34348; doi:10.1371/journal.pone.0034348.

Zhang XF, Zhang LJ, Feng YN, Chen B, Feng YM, Liang GJ, et al. 2012. Bisphenol A exposure modifies DNA methylation of imprint genes in mouse fetal germ cells. Mol Biol Rep 39:8621–8628; doi:10.1007/s11033-012-1716-7.

Zhao B, Yang Y, Wang X, Chong Z, Yin R, Song S-H, et al. 2014. Redox-active quinones induces genome-wide DNA methylation changes by an iron-mediated and Tet-dependent mechanism. Nucleic Acids Res. 42:1593–1605; doi:10.1093/nar/gkt1090.

# Chapter 4

# Age-related Epigenome-wide DNA Methylation and Hydroxymethylation in Longitudinal Mouse Blood


## Abstract

DNA methylation status at cytosine-phosphate-guanine (CpG) dinucleotides changes as a function of age in humans and animal models, a process that may contribute to chronic disease development. Recent studies have begun to investigate the role of an oxidized form of DNA methylation – 5-hydroxymethylcyotisine (5-hmC) – in the epigenome, but its role in age-related DNA methylation remains unclear. We tested the hypothesis that 5-hmC changes with age, but in a direction opposite to 5-methylctosine (5-mC), thereby playing a distinct role in epigenetic aging. To characterize whether epigenetic aging is driven by changes in 5-mC or 5-hmC, DNA modifications were measured in longitudinal blood samples (2, 4, and 10 months of age) from isogenic mice. Genome-wide 5-mC and 5-hmC levels were measured using two sequencing methods – enhanced reduced representation bisulfite sequencing (ERRBS) and hydroxymethylated DNA immunoprecipitation sequencing (HMeDIP-seq). Examining the epigenome by age, we identified 38,300 unique differentially methylated CpGs (DMCs) and 8,613 differentially hydroxymethylated regions (DHMRs). Comparing age-related DMCs and DHMRs, 1,854 annotated genes showed both differential 5-mC and 5-hmC, including one gene – Nfic – at five CpGs in the exact same chromosomal region. At this shared region, 5-mC and 5-hmC levels both decreased with age. Reflecting these age-related epigenetic changes, Nfic RNA expression in blood decreased with age, suggesting that age-related regulation of this gene may be driven by 5-hmC, not canonical DNA methylation. Combined, our genome-wide results show age-related differential 5-mC and 5-hmC, as well as some indication that changes in 5-hmC may drive age-related DNA methylation and gene expression.

## 4.1 Introduction

Epigenetics refers to the study of heritable and potentially reversible changes in gene expression unrelated to the DNA sequence. Epigenetic marks include alterations to DNA itself (e.g. DNA methylation), chromatin modifications (e.g. histone tail trimethylation), and non-coding RNAs (Bernal and Jirtle 2010; Egger et al. 2004). DNA methylation, which is the focus of this study, is typically defined as the addition of a methyl group to the 5'-carbon of cytosine in a Cytosine-phosphate-Guanine (CpG) dinucleotide; in simpler terms, it is termed 5-methylctyosine (5-mC). Previous work has shown that increased promoter DNA methylation is associated with decreased transcription factor binding and decreased gene transcription (Medvedeva et al. 2014). During development, the methylome undergoes discrete waves of demethylation and *de novo* methylation (Reik et al. 2001; Smallwood and Kelsey 2012), processes that help regulate both somatic cell differentiation and primordial germ cell proliferation (Messerschmidt et al. 2014).

Despite their establishment during development and maintenance through cellular replication, DNA methylation levels demonstrate clear changes with age. Predictable, unidirectional changes in DNA methylation that occur with age are referred to as "age-related methylation" (Jung and Pfeifer 2015; Kochmanski et al. 2017). Separate from these predictable changes, there are also stochastic, bidirectional alterations in epigenetic variability that occur with age; these are referred to as "epigenetic drift" (Jones et al. 2015; Kochmanski et al. 2017). Combined, these two processes represent "epigenetic aging," a phenotype of age-associated changes in the epigenome. These age-related changes in DNA methylation have important implications for transcriptional control and protein expression throughout life, and may underlie later-life disease development.

Separate from 5-mC, recent studies have begun to investigate the role of an oxidized form of DNA methylation – 5-hydroxymethylcyotisine (5-hmC) – in the epigenome. Hydroxylation of 5-mC to 5-hmC occurs via the Ten-eleven translocation (TET) dioxygenase enzymes, and 5-hmC is an intermediate on the active demethylation pathway (Shen et al. 2014). Beyond its role in demethylation, however, recent evidence suggests that 5-hmC is a secondary epigenetic mark that has a complex role as a regulator of transcription (Hahn et al. 2014; Wu et al. 2011). Previous studies have shown that 5-hmC is specifically recognized by DNA-binding proteins (Mellén et al. 2012; Spruijt et al. 2013), and that 5-hmC enrichment varies by tissue and genic region in mouse and human tissues (Globisch et al. 2010; Hernandez Mora et al. 2017; Nestor et al. 2012; Wen et al. 2014). Despite the increased interest in 5-hmC as an epigenetic mark, traditional bisulfite treatment sequencing methods do not distinguish between 5-mC and 5-hmC (Huang et al. 2010), so it remains unclear whether 5-hmC contributes to epigenetic aging. Here, we tested the hypothesis that 5-hmC would change with age, but in a direction opposite to 5-mC, thereby playing a distinct role in the aging epigenome.

## 4.2 Results

### *ERRBS – epigenome-wide differential 5-mC+5-hmC*

Enhanced reduced representation bisulfite sequencing (ERRBS) is a bisulfite treatment-based sequencing method that measures epigenome-wide 5-mC and 5-hmC at the same time. Despite this, to remain consistent with previous studies, we refer to all ERRBS data using the catch-all terms "methylation" or "5-mC." Using the *DSS* R package, multifactorial models were used to test for differential methylation by age in matched ERRBS data from blood samples collected at three time points – 2 months old (n=6), 4 months old (n=6), and 10 months old (n=6) (**Figure 4-1**). In total, we identified 20 differentially methylated regions (DMRs) and 28196

differentially methylated CpGs (DMCs) by age (**Table 4-1**). Comparing the directionality of DMRs by age, we found slightly more hypomethylated DMRs (n=11; 55.0%) than hypermethylated DMRs (n=9; 45.0%). Conversely, we found more hypermethylated DMCs (n=17460; 61.9%) than hypomethylated DMCs (n=10736; 38.1%) by age (**Table 4-1**). Using the *annotatr* R package, all DMRs and DMCs were annotated to the mm10 genome. Comparing to a random distribution generated from the ERRBS libraries, age-related DMCs showed variable patterns of enrichment and depletion depending on the genomic annotation. Of note, age-related DMCs were enriched at promoters, CpG islands, CpG shores, CpG shelves, promoters, 5' UTRs, and exons, but were depleted at interCGI regions. (**Figure 4-2**).

***HMeDIP-Seq – epigenome-wide differential 5-hmC***

Unlike ERRBS, HMeDIP-seq is an immunoprecipitation-based method that measures only 5-hmC; therefore, we refer to HMeDIP-seq data as "hydroxymethylation" or "5-hmC." For the HMeDIP-seq data, multivariate models were constructed in the *csaw* R package to test for differential 5-hmC by age. Based on the *csaw* models, we identified 8613 DHMRs by age (**Table 4-1**). Comparing the directionality of DHMRs by age, almost all DHMRs were hypo-hydroxymethylated (n=8446; 98.1%) compared to hyper-hydroxymethylated (n=160; 1.9%). We also identified a small fraction of age-related DHMRs that showed both hypo- and hyper-hydroxymethylation (n=7; 0.001%). Using the *annotatr* R package, age-related DHMRs were annotated to the mm10 genome. Comparing to a random distribution, age-related DHMRs showed moderate enrichment at CpG shores, CpG shelves, promoters, 3'-UTRs, 5'-UTRs, exons, and introns, as well as mild depletion at interCGI regions and CpG islands (**Figure 4-2).** On a broad scale, our data showed decreased epigenome-wide 5-hmC with age.

***Comparison of epigenome-wide differential 5-mC and 5-hmC***

Due to inherent bias in the ERRBS method, the measured 5-mC levels have incomplete coverage across the genome, making direct comparison to the genome-wide HMeDIP-seq data imperfect. Despite this limitation, we used the bedtools intersect function to directly compare annotated DMRs/DMCs and DHMRs by chromosomal location across the epigenome. For age-related DMCs and DHMRs, we found 65 CpGs that intersected by chromosomal location (**Figure 4-3**). However, when comparing age-related DMRs and DHMRs, we found zero regions matched by chromosomal location. For the age-related DMC and DHMR overlap sites, there were 40 unique annotated gene IDs. Of these 40 genes, three had multiple DMCs that overlapped a DHMR – *Fbln1*, *Ldlrad3I*, and *Nfic*. At the *Nfic* locus, we identified five age-related DMCs overlapping a single DHMR. These five sites are located in a CpG shelf 2588-2639 bp upstream of the *Nfic* gene (**Figure 4-4**).

Building on our previous research in mouse tail and blood samples from this colony (Kochmanski et al. 2016, 2018), we checked for age-related DMRs, DHMRs, and DMCs annotated to the *Esr1* gene. While we did not find any age-related DHMRs or DMRs annotated to the *Esr1* gene, it did have seven annotated age-related DMCs (**Table 4-2**). Examining the age-related *Esr1* DMCs, four of the sites had increased methylation with age, including two CpGs annotated to the promoter region. The other three age-related *Esr1* DMCs -- one exonic and two intronic – showed decreased methylation with age. Given the large number of DMCs annotated to *Esr1*, we interrogated the HMeDIP-seq data at the *Esr1* gene, pulling out a large region that contained all annotated DMCs. On this broad scale, we did not see any obvious differences in 5-hmC by age, but we did find stable 5-hmC peaks across the *Esr1* genic region (**Figure 4-5**). This suggests that 5-hmC levels at the *Esr1* locus are stable during adulthood in mouse blood.

***RT-qPCR expression data***

To further investigate the functional effects of age-related epigenetic results at the *Nfic* and *Esr1* genes, we performed RT-qPCR using RNA from the same matched mouse blood samples (primers available in **Table 4-3**). We found a significant decrease in *Nfic* expression between 2 and 10 months of age in blood samples (p=0.04), but no significant change in *Esr1* expression with age (**Figure 4-6**). The significant decrease in *Nfic* expression with age echoes the observed age-related decrease in 5-hmC upstream of the *Nfic* gene. Conversely, the lack of an observed difference in *Esr1* expression with age is consistent with the stable 5-hmC levels at *Esr1* across adulthood.

***Pathway analysis***

ChIP-enrich pathway analysis was performed on separate lists of hyper- and hypo-methylated age-related DMCs and DHMRs. DMC and DHMR datasets were both restricted to sites and regions <5kb from the transcription start site. Due to the large number of significant CpGs, DMC datasets were further limited to sites annotated to a gene promoter. After correction for multiple testing, a number of molecular function and biological process GO terms were enriched in hypo- and hyper-methylated age-related DMCs and DHMRs. Of note, enriched pathways showed very little overlap between hypo- and hypermethylated sites or regions, showing specific enrichment based on directionality of differential methylation or hydroxymethylation. DHMR pathways were particularly discordant, showing no overlap between hyper- and hypo-methylated regions for age-related DHMRs. The hypo-hydroxymethylated DHMRs showed enrichment for T cell activation pathways, while hyper-hydroxymethylated DHMRs showed enrichment for B cell activation pathways. Unlike the discordance found in the DHMRs, there was some overlap in enriched pathways between hyper-

and hypo-methylated DMCs. Specifically, for the age-related DMCs, both hyper- and hypo-methylated sites showed enrichment for development of primary sexual characteristics.

## 4.3 Discussion

The results from this study indicate that both 5-mC and 5-hmC are dynamic with age in mouse blood. We identified statistically significant age-related DNA methylation and hydroxymethylation on an epigenome-wide scale, indicating that both epigenetic marks are altered during murine aging. To our knowledge, this is the first study to examine age-related 5-hmC levels in a longitudinal model. Given the lack of available research on this topic, the biological effects of age-related changes in DNA hydroxymethylation remain poorly characterized. However, we found moderate enrichment of age-related DHMRs at CpG shores, CpG shelves, promoters, 5'-UTRs, exons, introns, and 3'-UTRs compared to a random distribution (**Figure 4-2)**. While this enrichment of DHMRs at specific genomic locations was subtle, DHMRs also showed a clear bias toward hypo-hydroxymethylation with age (**Table 4-1**), a pattern supported by human studies showing decreased 5-hmC levels in blood with age (Truong et al. 2015; Xiong et al. 2015). Combined, these data suggest that age-related changes in 5-hmC are non-random, and that DNA hydroxymethylation could play an important role in the aging process. Future studies should examine whether longitudinal 5-hmC levels can be used to accurately predict biological age, as has been shown in DNA methylation (Horvath 2013).

Contrary to our original hypothesis, there was little overlap between sites or regions of age-related methylation and regions of age-related hydroxymethylation. It's possible that this lack of overlap reflects differences in the effects of aging on 5-hmC and 5-mC, with age-related changes in these separate epigenetic marks occurring at disparate genomic regions. This idea is supported by recent evidence showing that 5-hmC is a stable epigenetic mark with its own

distinct genomic distribution (Hahn et al. 2014; López et al. 2017; Stroud et al. 2011). Alternatively, this lack of overlap could be due to the limited genomic coverage of the ERRBS method; a more complete comparison of 5-mC and 5-hmC could be achieved using whole-genome bisulfite sequencing. Using the available data, only 65 age-related DMCs overlapped the annotated DHMRs by chromosomal location. After annotating these 65 CpG sites to the mm10 genome, we identified one gene – *Nfic* – with five age-related DMCs overlapping a single DHMR. These five sites are 2588-2639 bp upstream of the *Nfic* gene, a locus that encodes the nuclear factor I-C (NFI-C) protein (**Figure 4-4)**. NFI-C is a member of the nuclear factor I (NFI) transcription factors, a class of proteins involved in stem cell differentiation and maintenance during development and adulthood, respectively (Harris et al. 2015). While NFI proteins are expressed in most adult tissues (Chaudhry et al. 1997; Gronostajski 2000), the limited available research on NFI-C shows that it plays an important role in hepatocyte proliferation during liver regeneration (Edelmann et al. 2015) and odontoblast and osteoblast differentiation (Lee et al. 2014; Roh and Park 2017). As a result, age-related changes in *Nfic* regulation could have important consequences on tissue maintenance with age. This idea is supported by the fact that *Nfic*$^{-/-}$ mice exhibit an age-related osteoporosis-like phenotype (Lee et al. 2014). In our longitudinal data, we found simultaneous age-related decreases in combined 5-mC+5-hmC levels (ERRBS) and 5-hmC peaks (HMeDIP-seq) upstream of the *Nfic* gene. This overlap suggests that age-related decreases in DNA methylation at this region may be at least partially driven by decreases in 5-hmC levels. Given that 5-hmC has shown localization to enhancers and positive associations with gene expression (Ehrlich and Ehrlich 2014; Greco et al. 2016; Sérandour et al. 2012; Wen et al. 2014), we predicted that *Nfic* expression would decrease with age in concordance with 5-hmC levels. Matching our expectation, *Nfic* expression decreased with age

in blood (**Figure 4-6**), supporting the idea that 5-hmC, not 5-mC, may be driving age-related changes in the methylome upstream of the *Nfic* gene. This result, while only from a single gene, highlights the importance of considering 5-hmC when examining age-related methylation patterns. Without measuring 5-hmC, the documented age-related decreases in 5-mC and *Nfic* expression would have been difficult to reconcile with the classic view that DNA methylation is a repressive epigenetic mark. As a result, it is important for future studies investigating epigenetic aging to consider the contribution of DNA hydroxymethylation.

In a previous study, we found age-related DNA methylation changes at the *Esr1* gene promoter (chr10:4712147-4712203) in matched mouse tail and blood tissues (Kochmanski et al. 2016, 2018). To follow up on these results, we interrogated our sequencing data for age-related DMCs annotated to the *Esr1* locus. In total, we found seven age-related DMCs annotated to *Esr1;* four of these sites had increased methylation with age, including two CpGs in the promoter region (**Table 4-2**). This result matches our prior results, which showed increased promoter *Esr1* methylation with age in murine tail and blood (Kochmanski et al. 2016, 2018). Upon locating the seven DMCs annotated to *Esr1*, we also examined the HMeDIP-seq data at the *Esr1* gene, visualizing a region containing all of the annotated *Esr1* DMCs. We did not find any significant differences in *Esr1* 5-hmC by age; instead, there were a number of 5-hmC peaks along the *Esr1* gene body that were stable across individuals and time (**Figure 4-5**). This suggests that 5-hmC content at the *Esr1* locus is tightly regulated, and may not contribute to the documented age-related methylation patterns at this locus.

Enriched age-related GO terms were discordant between hypo- and hypermethylated sites and regions, showing specific enrichment based on directionality of differential methylation or hydroxymethylation. This suggests that age is associated with up- or down-regulation of various

biological processes. In the age-related DHMRs, hypo-hydroxymethylated regions showed enrichment for T cell activation pathways and hyper-hydroxymethylated regions showed enrichment for B cell activation pathways. Reports have shown age-related changes in T cell and B cell function and generation (Cancro et al. 2009; Moro-García et al. 2013), so these differences in enriched pathways may reflect distinct epigenetic changes that occur in T cell and B cell populations with age. Related to this idea, it is possible that many of the age-related enriched pathways are actually a result of shifting blood cell populations, not defined changes in biological regulation. This possibility should be further investigated in additional longitudinal studies of the mouse and/or human blood epigenome.

DNA methylation and hydroxymethylation levels vary by tissue (Globisch et al. 2010; Lokk et al. 2014; Maegawa et al. 2010), so it remains to be seen whether the documented epigenetic aging in blood would be consistent in other murine tissues – e.g. liver, kidney, brain. Despite this uncertainty, blood samples have some distinct advantages over other murine target tissues. First, we were able to collect blood samples from the same mice over time, allowing for direct measurement of intra-individual age-related methylation during adulthood. Second, the use of tail vein puncture at 2 and 4 months of age meant that blood collection was minimally invasive and did not disrupt mouse health. Third, the use of blood allows for greater translatability to human epigenetics studies, which often use peripheral blood samples collected in the field or clinic. For these reasons, we chose to use blood samples as our tissue of interest; however, future studies should examine whether our results carry over to other target tissues.

As stated previously, the number of significant age-related DMRs identified in the ERRBS data was relatively small compared to the number of age -related DMCs. This result is likely the byproduct of two combined factors – inherent limitations of the ERRBS method and

our variable of interest (aging). ERRBS is not a whole-genome sequencing method, rather relying on MspI (C^CGG) restriction enzyme digestion to enrich for GC-rich regions prior to amplification and sequencing (Garrett-Bakelman et al. 2015). CpG-dense regions are often found in regulatory regions (e.g. promoters), and may be under tight biological control, limiting 5-mC variability. Additionally, these well-regulated regions may not be sensitive to a variable like age, which shows lower magnitude epigenetic effects than distinct disease states like cancer. Supporting this idea, previous literature shows that age-related methylation occurs at high rates in repetitive elements and intragenic regions (Zampieri et al. 2015), genetic locations that are not well covered by ERRBS. The genomic bias inherent in ERRBS data may also partially explain the low number of overlapping DMCs and DHMRs in our data. Specifically, we noted a number of DHMRs that did not have coverage in ERRBS data, a constraint that weakened our comparative analyses.

In addition to coverage inconsistencies, data from the two sequencing methods were also analyzed using different statistical methods. For the ERRBS data, an analysis pipeline was created based on the *DSS* R package, which uses a Bayesian hierarchical model to estimate and shrink gene- or CpG site-specific dispersions, then detects differential expression/methylation using a Wald statistical test. This is appropriate for the ERRBS data, which provides read coverage for discrete CpG sites. Meanwhile, for the HMeDIP-seq data, we used the *csaw* R package, which uses sliding windows to identify differences in binding patterns for 5-hydroxymethylcytosine across the genome. This is appropriate for the HMeDIP-seq data structure because it provides read coverage across regions. While these analysis methods are appropriate for their respective sequencing data types, their differences in resolutions and statistical methods make it difficult to directly compare called DMRs/DMCs and DHMRs. To

avoid these limitations, future studies could use similar methods – e.g. whole genome bisulfite sequencing (WGBS) and oxidative bisulfite sequencing (oxBS-seq) – to measure epigenome-wide site-specific 5-mC and 5-hmC. While expensive, WGBS provides genomic coverage far greater than ERRBS (Ziller et al. 2014), and simultaneous oxBS-seq sequencing would allow for a direct comparison of 5-mC and 5-hmC at the base pair level (Booth et al. 2013). In this way, it would be possible to probe for additional genomic regions where epigenetic aging is driven by changes in 5-hmC.

## 4.4 Conclusion

We measured DNA methylation and hydroxymethylation in matched blood samples collected from isogenic mice at 2, 4, and 10 months of age, then examined the effects of age on the longitudinal methylome. The use of matched blood allows for greater translatability to bioavailable specimens in human populations. On an epigenome-wide scale, we identified a number of age-related DMCs, DMRs, and DHMRs, suggesting that age alters both 5-mC and 5-hmC levels throughout the murine life course. Examining the age-related DMCs and DHMRs, we found a small number of DMC/DHMR overlap regions, including one upstream of the *Nfic* gene. At this region, both 5-mC and 5-hmC decreased with age, patterns that were reflected in decreased *Nfic* mRNA expression. This result suggests that age-related methylation patterns at some genes can be at least partially driven by changes in DNA hydroxymethylation, an important consideration for future epigenetic aging studies.

## 4.5 Materials and Methods

### *Study animals and blood collection*

Mice included in longitudinal analyses (n=6) were *a/a* offspring sourced from a genetically invariant $A^{vy}/a$ mouse colony maintained by sibling mating and forced heterozygosity

for more than 220 generations (Waterland and Jirtle 2003). Within this colony, the $A^{vy}$ allele is passed through the heterozygous male line, which has a genetically constant background 93% identical to C57BL/6J strain (Waterland and Jirtle 2003; Weinhouse et al. 2014). At 2 months and 4 months of age, tail vein blood samples were collected from all mice (**Figure 4-1**). At 10 months of age, mice were sacrificed, and blood samples were collected using cardiac puncture. All animals were stored in polycarbonate-free cages with ad libitum access to food and drinking water, and were maintained in accordance with Institute for Laboratory Animal Research (ILAR) guidelines (National Research Council (US) Committee for the Update of the Guide for the Care and Use of Laboratory Animals 2011). Mice were fed a modified AIN-93G standard chow with 7% corn oil substituted for 7% soybean oil (Harlan Teklad). The study protocol was approved by the University of Michigan Committee on Use and Care of Animals (UCUCA).

***DNA and RNA isolation***

Genomic DNA and RNA were isolated from matched 2 month (n=6), 4 month (n=6), and 10 month (n=6) frozen blood using the Qiagen Allprep DNA/RNA/miRNA Universal Kit (Qiagen, Cat. #80224). All isolates were stored at -80°C.

***Next-generation sequencing of 5-mC and 5-hmC***

Epigenome-wide DNA hydroxymethylation and methylation levels were quantified in blood from mouse blood using two sequencing methods -- hydroxymethylated DNA immunoprecipitation sequencing (HMeDIP-seq) and enhanced reduced representation bisulfite sequencing (ERRBS) (Garrett-Bakelman et al. 2015; Tan et al. 2013). Standard bisulfite sequencing methods, including ERRBS, do not distinguish between 5-mC and 5-hmC, so HMeDIP-seq data was generated in parallel to ERRBS to specifically measure epigenome-wide 5-hmC. Sequencing data were generated for a subset of colony mice (n=6) with longitudinal

blood collection (**Figure 4-1**). Blood samples from the six mice (3 male, 3 female) were sequenced at three time points across the life-course (2, 4, and 10 months of age), giving a total sequencing data sample size of 18 samples for each method. The six mice included in longitudinal analyses were selected from different litters to minimize potential batch effects.

ERRBS was performed at the University of Michigan Epigenomics Core as described (Akalin et al. 2012; Garrett-Bakelman et al. 2015). Briefly, 75 ng of genomic DNA was digested using MspI, a restriction enzyme that preferentially cuts CG-rich sites. The digested DNA was then purified using phenol:chloroform extraction and ethanol precipitation in the presence of glycogen, before blunt-ending and phosphorylation. A single adenine nucleotide was next added to the 3'end of the fragments in preparation for ligation of adapter duplex with a thymine overhang. The ligated fragments were cleaned, and processed for size selection on agarose gel. Selected fragments were treated with sodium bisulfite to convert unmethylated cytosines to uracils, which are then replaced with thymines during PCR amplification. After cleanup with AMPure XP beads (Beckman Coulter, Prod.# A63880), libraries were quantified using the Agilent TapeStation genomic DNA kit (Agilent, Cat. #G2991AA) and Qubit broad range dsDNA (Invitrogen, Cat. #Q32850). Single-end, 50 base pair reads were obtained for each library by sequencing on the HiSeq 4000 system (Illumina). ERRBS samples were multiplexed, with three samples per sequencing lane.

For HMeDIP-seq, a total of 1μg of genomic DNA (gDNA) was sheared by adaptive focused acoustics, using the Covaris S220 (Covaris, Cat. #4465653). This sheared DNA was next blunt-ended and phosphorylated. A single adenine nucleotide was then added to the 3'end of the fragments in preparation for ligation of adapter duplex with a thymine overhang. The ligated fragments were cleaned using Qiagen's MinElute PCR purification columns (Qiagen,

Cat. #28004). DNA standards for HMeDIP (Diagenode 5-hmC, 5-mC & cytosine DNA standard pack for HMeDIP, Cat. #AF-107-0040) were added to each sample before denaturation. Resuspension was then performed in ice-cold immunoprecipitation buffer (10 mM Sodium Phosphate pH 7.0, 140 mM NaCl, 0.05% Triton X-100). A 10% volume (input) was retrieved before 2ug of a 5hmC-specific antibody (Active Motif, Cat # 39791) was added for immunoprecipitation overnight at 4°C with rotation. Dynabeads Protein-G (Invitrogen, Cat. #10003D) was used to pull-down of 5hmC-enriched fragments. The 5hmC-enriched DNA fragments (IP) were then released from the antibody by digestion with Proteinase K (Ambion, Cat. #AM2548). After cleanup with AMPure XP beads (Beckman Coulter, Prod.# A63880), the percent input enrichment (%input) in the IP was evaluated by qPCR, using primers for spike-ins. Samples with high % input for the 5-hmC spike-in – typical inclusion threshold was >80% – were then PCR amplified for the final library production, cleaned using AMPure XP beads, and quantified using the Qubit assay (Invitrogen, Cat. #Q32850) and TapeStation High Sensitivity D1000 kit (Agilent, Cat. #G2991AA). Single-end, 50 base pair reads were obtained for each library by sequencing on the HiSeq 4000 system (Illumina). Each HMeDIP-seq sample was run on a single sequencing lane.

***Bioinformatics pipeline for differential 5-mC and 5-hmC***

Sequencing results for all three ages were compared using a number of bioinformatics tools (**Figure 4-1**). The *mint* pipeline was used for data quality control (*FastQC* and *MultiQC*), adapter trimming (*trim_galore*), and alignment (*bismark* and *bowtie2*) (Cavalcante et al. 2017). For quality and adapter trimming, we required a minimum overlap of 6bp and minimum quality score of 20 in conjunction with special ERRBS trimming of 2bp from the 3’ end. For *bismark*

methylation extractor, the minimum threshold to consider a CpG site in analysis was 5 reads. Default parameters were used for *bowtie2*.

The *DSS* R package was used to test for differential 5-mC in ERRBS data by age (Feng et al. 2014; Park and Wu 2016; Wu et al. 2013, 2015). Within the *DSS* package, the DMLfit.multiFactor function was used to test for differential methylation by age using a multifactorial modeling approach, with matched mouse ID and sex included as covariates. As such, modeling was performed according to the following formula: ~age + mouseID + sex. The DMLtest.multiFactor function was used to test the null hypothesis that the age coefficient was equal to 0. Differentially methylated CpG sites (DMCs) were then sorted and filtered according to a false discovery rate (FDR) cutoff < 0.05. The callDMR function in *DSS* was for DMR calling. DMRs were called at a p-value < 0.05 and absolute methylation difference ≥ 5%.

The *csaw* package was used to test for differential 5-hmC by age (Lun and Smyth 2016). Aligned HMeDIP-seq data were read into R using the windowCounts function in *csaw*. When reading in the data, extension was set to 52, window width was set to 100, and sex chromosomes were removed. Next, the data were filtered twice – by count (average count >5) and by local enrichment using the filterWindows function (type= "local") – to remove regions of negligible binding. After filtering, normalization factors were calculated for each sample using the normOffsets function on binned data (width=10000). Normalization factors were linked to filtered data using the asDGEList function, and then the estimateDisp function was used to generate dispersion factors based on a multifactorial design matrix identical to that used for ERRBS data. The glmQLFit function was used to fit a model for differential 5hmC binding by age; an empirical Bayesian method used to stabilize the QL dispersion estimates. A contrast statement was used to extract modeling results for the age variable. To correct for multiple

testing, filtered data were clustered using a window length of 500 bp; the combineTests function was then used to compute a combined p-value for each cluster. The Benjamini-Hochberg method was then used to control the FDR in all clusters (Benjamini and Hochberg 1995, 1997). DHMRs were called using an FDR < 0.10.

After testing for differential 5-mC and 5-hmC, the *annotatr* R package was used to annotate all DMCs, DMRs, and DHMRs to the mm10 genome (Cavalcante and Sartor 2017). The annotate_regions function was used to generate annotations, including gene IDs and genomic context (e.g. intron, exon, promoter, etc.). Within *annotatr*, the randomize_regions function was used to create a secondary, random distribution of annotated sites or regions from the complete ERRBS or HMeDIP-seq data, respectively. Distributions of DMCs and DHMRs by genomic annotation were plotted against the random distribution using the plot_categorical and plot_annotation functions, respectively. Lists of chromosomal locations were compared using the bedtools (version 2.26.0) intersect function to determine overlap between DMCs and DHMRs.

***Sequencing data visualization***

5-mC levels were visualized using the *RnBeads* R package (Assenov et al. 2014). Within this package, the rnb.execute.import function was first used to import the aligned ERRBS data. Next, the rnb.sample.groups function was used to group samples by age. The rnb.plot.locus.profile function was then used to plot relative 5-mC level in a heat map output for defined regions of the genome. A custom set of nine red colors were chosen from RColorBrewer for the heat map gradient.

5-hmC levels were visualized using the *csaw* and *GViz* R packages (Hahne and Ivanek 2016; Lun and Smyth 2016). Data were read into R as a GRanges object using the extractReads function. Next, the GeneRegionTrack in the *Gviz* R package was used to define regions of

interest for visualization. Separate blue and red genome tracks were used to represent the forward and reverse strand reads, respectively. The plotTracks function was then used to plot 5-hmC levels for these regions. Reads-per-million was used for the y-axis in all graphs, and scale was adjusted to individual region coverage.

Plots generated in R (R version 3.4.0) were formatted for publication in Adobe Illustrator CS6 (version 16.0.5).

***Real-time quantitative PCR (RT-qPCR)***

The Bio-Rad iScript cDNA Synthesis Kit (Cat. #1708890) was used to reverse transcribe complementary DNA (cDNA) from 250 ng of RNA for each blood sample (n=6 per age). In preparation for RT-qPCR, cDNA samples were diluted 1:2.5 in RNase-free water, then mixed with 10 µM forward/reverse primers, nuclease-free water, and Bio-Rad iQ SYBR Green Supermix (Cat. #1708880). RT-qPCR was then performed using a Bio-rad CFX96 Real-Time System C1000 Thermal Cycler (Bio-Rad; Hercules, CA). The pre-programmed 2-step PCR+melt curve protocol was used for all qPCR reactions – 95°C for 3 minutes, [95°C for 10 seconds, 55°C for 30 seconds, plate read] x40, 95°C for 10 seconds. The melt curve for each plate was 65°C-95°C; 0.5°C increment for 5 seconds, with plate read at each temperature. RT-qPCR analyses were performed for the *Nfic* and *Esr1* gene in triplicate for each cDNA sample. Three housekeeping genes – *Actb*, *18S*, and *Gapdh* – were included as internal controls in all RT-qPCR runs. In addition to housekeeping genes, an inter-plate calibrator control of brain cDNA was included for calculation of relative gene expression across multiple plates. Expression levels were calculated following the $2^{-\Delta\Delta Ct}$ method (Livak and Schmittgen 2001). RT-qPCR primers for the *Nfic*, *Esr1*, and *Gapdh* genes (**Table 4-3**) were designed using the online Genscript Real-time PCR Primer Design software (https://www.genscript.com/tools/real-time-pcr-tagman-primer-

design-tool). The *Actb* and *18S* gene primer pairs were sourced from the literature (Dolinoy et al. 2010; La Salle et al. 2004)**.** Primer pair specificity for all designed primers was checked using the NCBI Primer-BLAST online tool (https://www.ncbi.nlm.nih.gov/tools/ primer-blast/).

***Pathway analysis***

Pathway analyses for DMCs and DHMRs were performed using the ChIP-enrich analysis tool (Welch et al. 2014). In the ChIP-enrich online interface (http://chip-enrich.med.umich.edu/), the gene set filter was set to 2000, peak threshold was set to 1, and adjustment for mappability of gene locus regions was set to false. The ChIP-enrich method was used for GO term and KEGG pathway enrichment testing against the mm10 reference genome. Both DMCs and DHMRs were split into hypo- and hyper-methylated sites/regions prior to separate analyses. For DHMRs and DMCs, only peaks <5kb from TSS were included in ChIP-enrich analysis. Due to the large number of significant DMCs, DMC pathway analyses were restricted to CpGs annotated to promoter regions. After correcting for multiple testing, pathways with FDR<0.05 were considered significant.

## 4.6 Funding

This work was supported by the University of Michigan (UM) NIEHS/EPA Children's Environmental Health and Disease Prevention Center P01 ES022844/RD83543601, the Michigan Lifestage Environmental Exposures and Disease (M-LEEaD) NIEHS Core Center (P30 ES017885), as well as the UM NIEHS Institutional Training Grant T32 ES007062 (JJK, EHM), UM NICHD Institutional Training Grant T32 079342 (EHM), NSRA F31 ES025101 (EHM), and the University of Michigan School of Public Health Regents' Fellowship (JJK). The authors have no conflicts of interest and declare no competing financial interests.

## 4.7 Acknowledgements

We thank Dr. Claudia Lalancette at the University of Michigan Epigenomics Core for ERRBS and HMeDIP-seq DNA library preparation. We also thank the University of Michigan Bioinformatics Core for sequencing data generation and quality control.

## 4.8 Figures and Tables

| Δ5-mC/5-hmC | Age | | |
|---|---|---|---|
| | DMRs† | DMCs* | DHMRs‡ |
| Hyper- | 9 | 17460 | 160 |
| Hypo- | 11 | 10736 | 8446 |
| Both | 0 | 0 | 7 |
| **Total** | 20 | 28196 | 8613 |

**Table 4-1: Differential 5-mC and 5-hmC in mouse blood by age.** The *DSS* and *csaw* R packages were used to examine the effect of age on 5-mC and 5-hmC levels across the epigenome. For all models, effect of age was defined as 10 months old relative to 2 months old (baseline). Models also included a paired mouse ID variable to account for within-individual effects, as well as a sex variable. Directionality of DMRs, DMCs, and DHMRs are indicated in separate rows; direction is relative to 2 month old samples. DMR, DMC, and DHMR calling thresholds are indicated -- †DMRs = $\Delta > 0.05$ and p-value $< 0.05$; *DMCs = $\Delta > 0.05$ and FDR $< 0.05$; ‡DHMRs = FDR $< 0.10$.

| Chr | Start | End | Strand | Location | Δ % Methylation* |
|---|---|---|---|---|---|
| chr10 | 4666894 | 4666894 | + | intron | -25.7% |
| chr10 | 4709922 | 4709922 | + | promoter | 10.0% |
| chr10 | 4712221 | 4712221 | + | promoter | 41.2% |
| chr10 | 4712716 | 4712716 | + | exon | -25.4% |
| chr10 | 4932943 | 4932943 | + | 1 to 5kb | 30.4% |
| chr10 | 4971465 | 4971465 | + | intron | 36.2% |
| chr10 | 4972470 | 4972470 | + | intron | -14.9% |

**Table 4-2: Age-related DMCs annotated to the *Esr1* locus.** List of significant *DSS* modeling DMCs annotated to the *Esr1* locus. *Change in % methylation is defined as 10 month old level relative to 2 month old level.

| Gene | Full Name | GenBank Number | Strand | Primers (5' to 3') | Tm (°C) | Amplicon Size |
|---|---|---|---|---|---|---|
| *Gapdh* | Glyceraldehyde 3-phosphate dehydrogenase | NM_008084.3 | FWD | GCCTGCTTCACCACCTTCTT | 59.96 | 98 |
| | | | RVS | CATGGCCTTCCGTGTTCCTA | 59.07 | |
| *Nfic* | Nuclear factor I-C | AF111265.1 | FWD | CGAGAAGCGCATGTCCAAGG | 58.83 | 168 |
| | | | RVS | GCCTTCTTGCCAGTCACAGC | 58.95 | |
| *Esr1* | Estrogen Receptor 1 (Alpha) | NM_007956 | FWD | AACCGGAGGAAGAGTTGCCA | 58.40 | 76 |
| | | | RVS | TCCGTATGCCGCCTTTCATCA | 59.05 | |

**Table 4-3: RT-qPCR primers for self-designed gene assays.** Forward and reverse primer sequences for the *Gapdh*, *Nfic*, and *Esr1* RT-qPCR assays are listed, along with melting temperatures and amplicon sizes. All assays were designed using the online Genscript Real-time PCR Primer Design software (https://www.genscript.com/tools/real-time-pcr-tagman-primer-design-tool). Additional primers for the *Actb* and *18S* genes were adapted from (Dolinoy et al. 2010) and (La Salle et al. 2004), respectively.

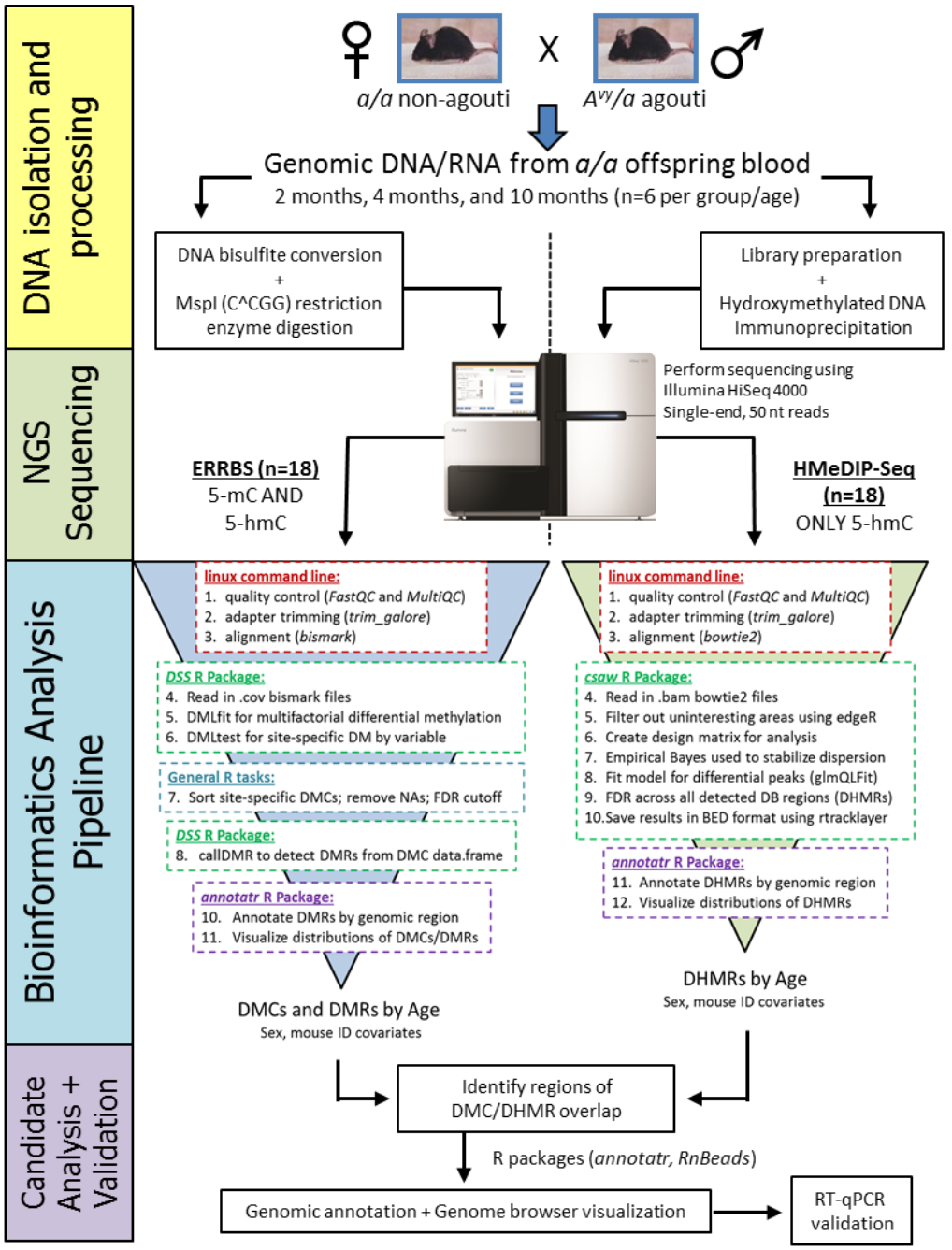


**Figure 4-1: Sequencing data collection and analysis workflow.** Genomic DNA was isolated from matched offspring blood samples at 2 months (n=6), 4 months (n=6), and 10 months of age (n=6). DNA samples were then split for separate, parallel processing steps specific to the ERRBS and HMeDIP-seq methods. All processed samples were amplified and sequenced on an Illumina HiSeq 4000 sequencer using single-end, 50 nt read length. Separate bioinformatics pipelines were used to analyze ERRBS and HMeDIP-seq data. Differentially methylated CpGs (DMCs) and regions (DMRs) were compared to differentially hydroxymethylated regions (DHMRs) for regions of chromosomal overlap. Regions of overlap were then annotated and visualized in the genome browser. The *Nfic* gene was validated using RT-qPCR on available RNA from the blood samples.

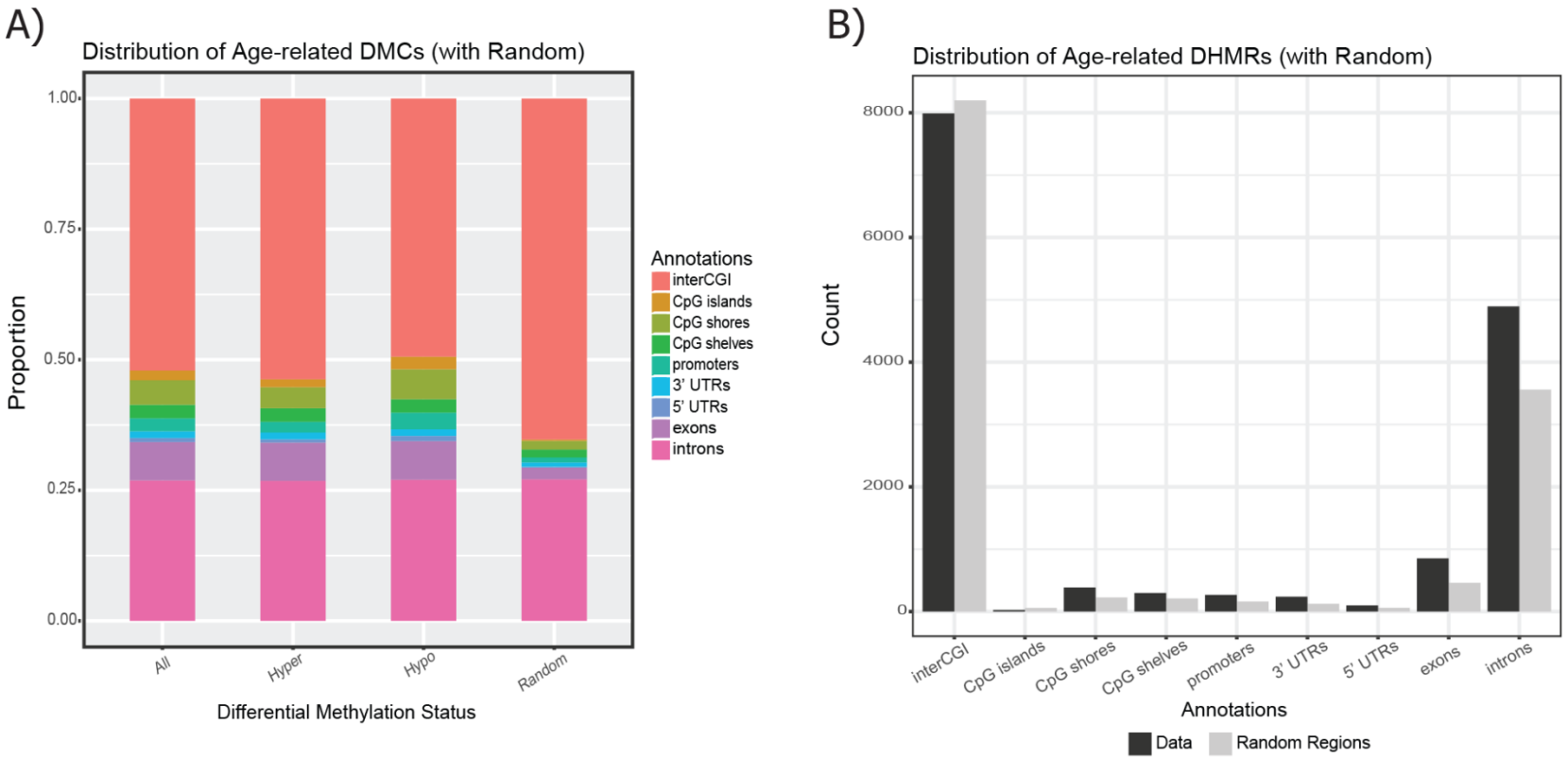


**Figure 4-2: Distributions of age-related DMCs and DHMRs compared to random.** Age-related DMCs and DHMRs were annotated to the mm10 genome using the *annotatr* package in R. Within *annotatr*, the randomize_regions function was used to create secondary, random distributions of annotated DMCs and DHMRs using the complete ERRBS and HMeDIP-seq data as background, respectively. Distributions of DMCs and DHMRs by genomic annotation were then plotted against the random distribution using the plot_annotation function. A) Compared to the random distribution, age-related DMCs (All, Hyper, and Hypo) were enriched at promoters, CpG islands, CpG shores, CpG shelves, promoters, 5' UTRs, and exons, but were depleted at interCGI regions. B) Compared to a random distribution, age-related DHMRs showed moderate enrichment at CpG shores, CpG shelves, promoters, 3'-UTRs, 5'-UTRs, exons, and introns, as well as mild depletion at interCGI regions and CpG islands.

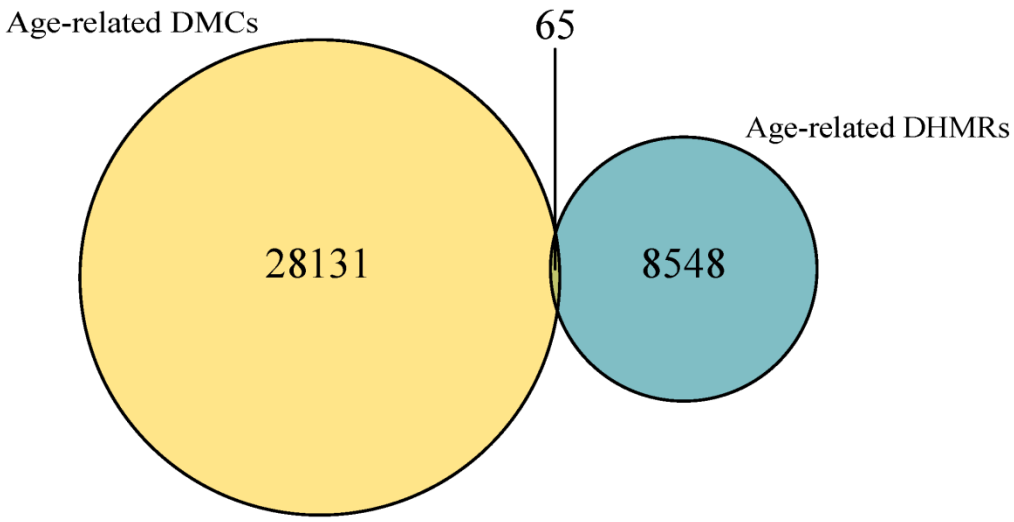


**Figure 4-3: Venn diagrams of intersecting age-related DMCs and DHMRs by chromosomal location.** The *bedtools* intercept function was used to test for overlap between DMCs and DHMRs by exact chromosomal location. Comparing age-related DMCs and DHMRs, we identified 65 regions that overlapped by chromosomal position. The age-related DMC and DHMR overlap sites annotated to 40 unique gene IDs. Of these 40 genes, three had multiple DMCs that overlapped a DHMR – *Fbln1*, *Ldlrad3*, and *Nfic*.

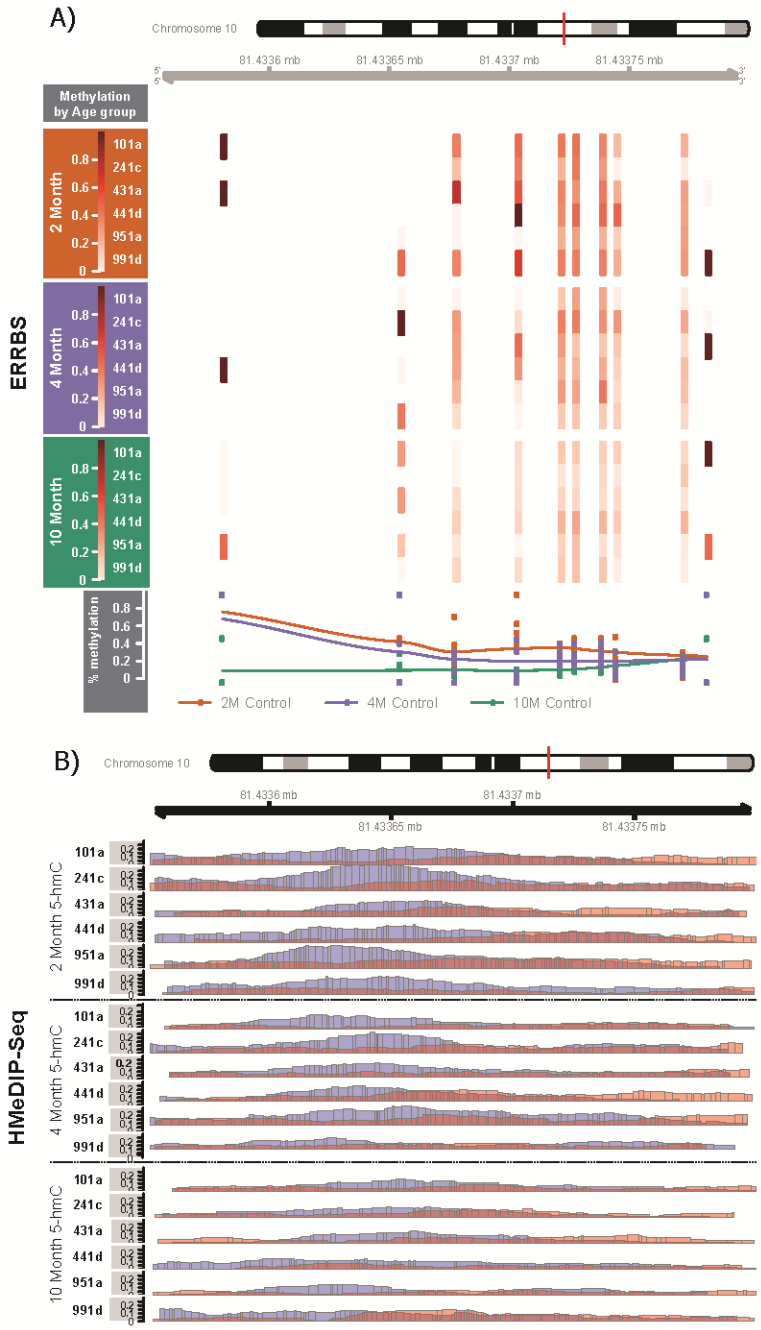


**Figure 4-4: ERRBS and HMeDIP-seq data for the *Nfic* gene DMR and DHMR overlap region.** (A) ERRBS and (B) HMeDIP-seq data at the identified *Nfic* DMC/DHMR overlap region (chr10: 81433551-81433800). 5-mC levels and 5-hmC peaks were visualized using the *Gviz*, *csaw*, and *RnBeads* R packages. 5-hmC and 5-mC levels at this overlap region both decrease with age in longitudinal mouse blood samples.

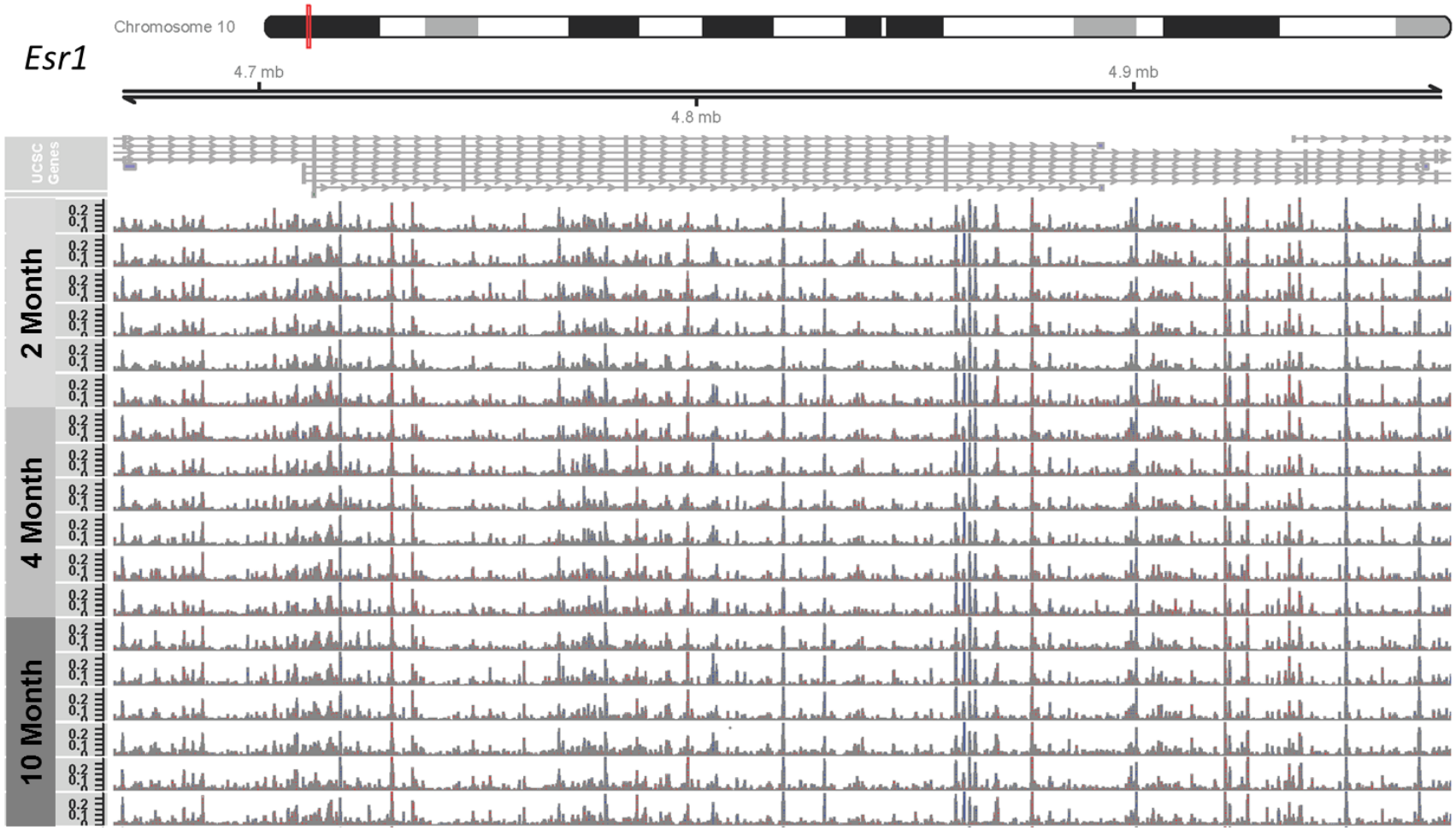


**Figure 4-5: 5-hmC peaks across the *Esr1* locus.** 5-hmC coverage was visualized across the Esr1 locus (chr10: 4666850-4972500) using the *csaw* R package. Region of visualization covers all age-related DMCs annotated to *Esr1*. As indicated by labels on the y-axis, data is shown for all 2 month (n=6), 4 month (n=6), and 10 month (n=6) blood samples. Data shows clear 5-hmC peaks along the entire *Esr1* locus, a pattern that is consistent across the life course. This data shows that 5-hmC content is under tight regulation at the *Esr1* locus.

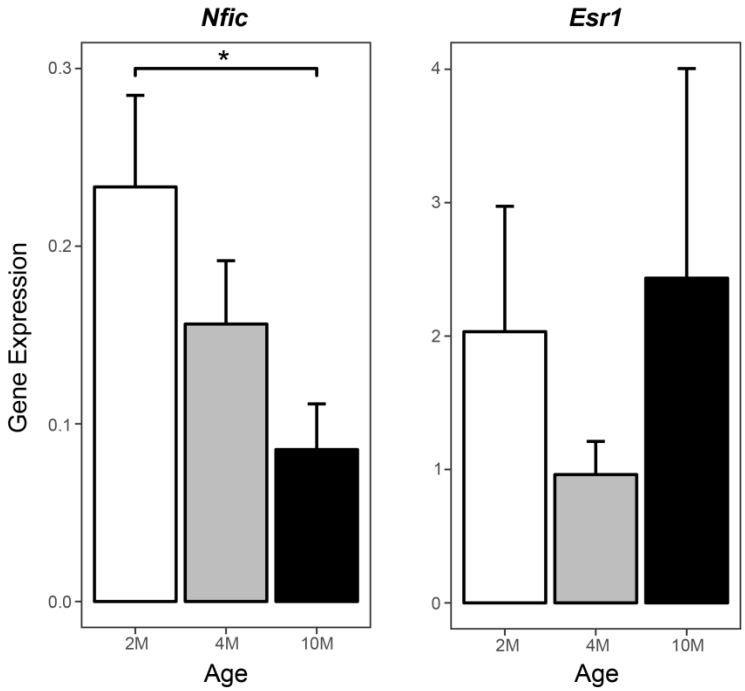


**Figure 4-6: RT-qPCR data for the *Nfic* and *Esr1* loci by age.** Based on DNA methylation results, RT-qPCR was used to investigate mRNA expression levels at the *Nfic* and *Esr1* genes. Three housekeeping genes – *Actb*, *18S*, and *Gapdh* – were included as internal controls in all RT-qPCR runs. In addition to housekeeping genes, an inter-plate calibrator control of brain cDNA was included for calculation of relative gene expression across multiple plates; all expression values are shown relative to this inter-plate calibrator. Expression levels were calculated following the $2^{-\Delta\Delta Ct}$ method. There was a significant decrease in mean *Nfic* expression between 2 and 10 month blood samples (p=0.04). *Esr1* expression did not significantly differ by age.

## 4.9 References


Akalin A, Kormaksson M, Li S, Garrett-Bakelman FE, Figueroa ME, Melnick A, et al. 2012. methylKit: a comprehensive R package for the analysis of genome-wide DNA methylation profiles. Genome Biol 13:R87; doi:10.1186/gb-2012-13-10-r87.

Assenov Y, Müller F, Lutsik P, Walter J, Lengauer T, Bock C. 2014. Comprehensive analysis of DNA methylation data with RnBeads. Nat. Methods 11:1138–1140; doi:10.1038/nmeth.3115.

Benjamini Y, Hochberg Y. 1995. Controlling the False Discovery Rate: A Practical and Powerful Approach to Multiple Testing. J. R. Stat. Soc. Ser. B 57:289–300; doi:10.2307/2346101.

Benjamini Y, Hochberg Y. 1997. Multiple Hypotheses Testing with Weights. Scand. J. Stat. 24:407–418; doi:10.1111/1467-9469.00072.

Bernal AJ, Jirtle RL. 2010. Epigenomic disruption: the effects of early developmental exposures. Birth Defects Res A Clin Mol Teratol 88:938–944; doi:10.1002/bdra.20685.

Booth MJ, Ost TWB, Beraldi D, Bell NM, Branco MR, Reik W, et al. 2013. Oxidative bisulfite sequencing of 5-methylcytosine and 5- hydroxymethylcytosine. Nat. Protoc. 8:1841–1851; doi:10.1038/nprot.2013.115.

Cancro MP, Hao Y, Scholz JL, Riley RL, Frasca D, Dunn-Walters DK, et al. 2009. B cells and aging: molecules and mechanisms. Trends Immunol. 30:313–318; doi:10.1016/j.it.2009.04.005.

Cavalcante RG, Patil S, Park Y, Rozek LS, Sartor MA. 2017. Integrating DNA Methylation and Hydroxymethylation Data with the Mint Pipeline. Cancer Res. 77:e27–e30; doi:10.1158/0008-5472.CAN-17-0330.

Cavalcante RG, Sartor MA. 2017. annotatr: genomic regions in context. Bioinformatics 33:2381–2383; doi:10.1093/bioinformatics/btx183.

Chaudhry AZ, Lyons GE, Gronostajski RM. 1997. Expression patterns of the four nuclear factor I genes during mouse embryogenesis indicate a potential role in development. Dev. Dyn. 208:313–325; doi:10.1002/(SICI)1097-0177(199703)208:3<313::AID-AJA3>3.0.CO;2-L.

Dolinoy DC, Weinhouse C, Jones TR, Rozek LS, Jirtle RL. 2010. Variable histone modifications at the A(vy) metastable epiallele. Epigenetics 5:637–44; doi:10.4161/epi.5.7.12892.

Edelmann S, Fahrner R, Malinka T, Song BH, Stroka D, Mermod N. 2015. Nuclear Factor I-C acts as a regulator of hepatocyte proliferation at the onset of liver regeneration. Liver Int. 35:1185–1194; doi:10.1111/liv.12697.

Egger G, Liang G, Aparicio A, Jones PA. 2004. Epigenetics in human disease and prospects for epigenetic therapy. Nature 429:457–463; doi:10.1038/nature02625.

Ehrlich M, Ehrlich KC. 2014. DNA cytosine methylation and hydroxymethylation at the borders. Epigenomics 6:563–6; doi:10.2217/epi.14.48.

Feng H, Conneely KN, Wu H. 2014. A Bayesian hierarchical model to detect differentially methylated loci from single nucleotide resolution sequencing data. Nucleic Acids Res. 42:1–11; doi:10.1093/nar/gku154.

Garrett-Bakelman FE, Sheridan CK, Kacmarczyk TJ, Ishii J, Betel D, Alonso A, et al. 2015. Enhanced reduced representation bisulfite sequencing for assessment of DNA methylation at base pair resolution. J Vis Exp e52246; doi:10.3791/52246.

Globisch D, Münzel M, Müller M, Michalakis S, Wagner M, Koch S, et al. 2010. Tissue distribution of 5-hydroxymethylcytosine and search for active demethylation intermediates. PLoS One 5:e15367; doi:10.1371/journal.pone.0015367.

Greco CM, Kunderfranco P, Rubino M, Larcher V, Carullo P, Anselmo A, et al. 2016. DNA hydroxymethylation controls cardiomyocyte gene expression in development and hypertrophy. Nat. Commun. 7:12418; doi:10.1038/ncomms12418.

Gronostajski RM. 2000. Roles of the NFI/CTF gene family in transcription and development. Gene 249: 31–45.

Hahn MA, Szabó PE, Pfeifer GP. 2014. 5-Hydroxymethylcytosine: a stable or transient DNA modification? Genomics 104:314–323; doi:10.1016/j.ygeno.2014.08.015.

Hahne F, Ivanek R. 2016. Visualizing Genomic Data Using Gviz and Bioconductor. In: *Methods in molecular biology (Clifton, N.J.)*. Vol. 1418 of. 335–351.

Harris L, Genovesi LA, Gronostajski RM, Wainwright BJ, Piper M. 2015. Nuclear factor one transcription factors: Divergent functions in developmental versus adult stem cell populations. Dev. Dyn. 244:227–238; doi:10.1002/dvdy.24182.

Hernandez Mora JR, Sanchez-Delgado M, Petazzi P, Moran S, Esteller M, Iglesias-Platas I, et al. 2017. Profiling of oxBS-450K 5-hydroxymethylcytosine in human placenta and brain reveals enrichment at imprinted loci. Epigenetics 00–00; doi:10.1080/15592294.2017.1344803.

Horvath S. 2013. DNA methylation age of human tissues and cell types. Genome Biol. 14:R115; doi:10.1186/gb-2013-14-10-r115.

Huang Y, Pastor WA, Shen Y, Tahiliani M, Liu DR, Rao A. 2010. The Behaviour of 5-Hydroxymethylcytosine in Bisulfite Sequencing. J. Liu, ed PLoS One 5:e8888; doi:10.1371/journal.pone.0008888.

Jones MJ, Goodman SJ, Kobor MS. 2015. DNA methylation and healthy human aging. Aging Cell 14:924–932; doi:10.1111/acel.12349.

Jung M, Pfeifer GP. 2015. Aging and DNA methylation. BMC Biol 13:7; doi:10.1186/s12915-015-0118-4.

Kochmanski J, Marchlewicz EH, Cavalcante RG, Perera BP, Sartor MA, Dolinoy DC. 2018. Longitudinal Effects of Developmental Bisphenol A Exposure on Epigenome-wide DNA Hydroxymethylation at Imprinted Loci in Mouse Blood. Env. Heal. Perspect (In revision).

Kochmanski J, Marchlewicz EH, Savidge M, Montrose L, Faulk C, Dolinoy DC. 2016. Longitudinal effects of developmental bisphenol A and variable diet exposures on epigenetic drift in mice. Reprod. Toxicol.; doi:10.1016/j.reprotox.2016.07.021.

Kochmanski J, Montrose L, Goodrich JM, Dolinoy DC. 2017. Environmental deflection: The impact of toxicant exposures on the aging epigenome. Toxicol. Sci. 156; doi:10.1093/toxsci/kfx005.

La Salle S, Mertineit C, Taketo T, Moens PB, Bestor TH, Trasler JM. 2004. Windows for sex-specific methylation marked by DNA methyltransferase expression profiles in mouse germ cells. Dev. Biol. 268:403–415; doi:10.1016/j.ydbio.2003.12.031.

Lee D-S, Choung H-W, Kim H-J, Gronostajski RM, Yang Y-I, Ryoo H-M, et al. 2014. NFI-C Regulates Osteoblast Differentiation via Control of Osterix Expression. Stem Cells 32:2467–2479; doi:10.1002/stem.1733.

Livak KJ, Schmittgen TD. 2001. Analysis of Relative Gene Expression Data Using Real-Time Quantitative PCR and the 2−ΔΔCT Method. Methods 25:402–408; doi:10.1006/meth.2001.1262.

Lokk K, Modhukur V, Rajashekar B, Märtens K, Mägi R, Kolde R, et al. 2014. DNA methylome profiling of human tissues identifies global and tissue-specific methylation patterns. Genome Biol. 15:3248; doi:10.1186/gb-2014-15-4-r54.

López V, Fernández AF, Fraga MF. 2017. The role of 5-hydroxymethylcytosine in development, aging and age-related diseases. Ageing Res. Rev. 37:28–38; doi:10.1016/J.ARR.2017.05.002.

Lun ATL, Smyth GK. 2016. csaw: a Bioconductor package for differential binding analysis of ChIP-seq data using sliding windows. Nucleic Acids Res. 44:e45–e45; doi:10.1093/nar/gkv1191.

Maegawa S, Hinkal G, Kim HS, Shen L, Zhang L, Zhang J, et al. 2010. Widespread and tissue specific age-related DNA methylation changes in mice. Genome Res 20:332–340; doi:10.1101/gr.096826.109.

Medvedeva YA, Khamis AM, Kulakovskiy I V, Ba-Alawi W, Bhuyan MS, Kawaji H, et al. 2014. Effects of cytosine methylation on transcription factor binding sites. BMC Genomics 15:119; doi:10.1186/1471-2164-15-119.

Mellén M, Ayata P, Dewell S, Kriaucionis S, Heintz N. 2012. MeCP2 binds to 5hmC enriched within active genes and accessible chromatin in the nervous system. Cell 151:1417–30; doi:10.1016/j.cell.2012.11.022.

Messerschmidt DM, Knowles BB, Solter D. 2014. DNA methylation dynamics during epigenetic reprogramming in the germline and preimplantation embryos. Genes Dev 28:812–828; doi:10.1101/gad.234294.113.

Moro-García MA, Alonso-Arias R, López-Larrea C. 2013. When aging reaches CD4+ T-cells: Phenotypic and functional changes. Front. Immunol. 4:1–12; doi:10.3389/fimmu.2013.00107.

National Research Council (US) Committee for the Update of the Guide for the Care and Use of Laboratory Animals. 2011.In: *Guide for the Care and Use of Laboratory Animals*. National Academies Press (U.S.):Washington, D.C.

Nestor CE, Ottaviano R, Reddington J, Sproul D, Reinhardt D, Dunican D, et al. 2012. Tissue type is a major modifier of the 5-hydroxymethylcytosine content of human genes. Genome Res 22:467–477; doi:10.1101/gr.126417.111.

Park Y, Wu H. 2016. Differential methylation analysis for BS-seq data under general experimental design. Bioinformatics 32:1446–1453; doi:10.1093/bioinformatics/btw026.

Reik W, Dean W, Walter J. 2001. Epigenetic reprogramming in mammalian development. Science (80-. ). 293:1089–1093; doi:10.1126/science.1063443.

Roh SY, Park J-C. 2017. The role of nuclear factor I-C in tooth and bone development. J. Korean Assoc. Oral Maxillofac. Surg. 43:63; doi:10.5125/jkaoms.2017.43.2.63.

Sérandour AA, Avner S, Oger F, Bizot M, Percevault F, Lucchetti-Miganeh C, et al. 2012. Dynamic hydroxymethylation of deoxyribonucleic acid marks differentiation-associated enhancers. Nucleic Acids Res. 40: 8255–65.

Shen L, Song CX, He C, Zhang Y. 2014. Mechanism and function of oxidative reversal of DNA and RNA methylation. Annu Rev Biochem 83:585–614; doi:10.1146/annurev-biochem-060713-035513.

Smallwood SA, Kelsey G. 2012. De novo DNA methylation: a germ cell perspective. Trends Genet 28:33–42; doi:10.1016/j.tig.2011.09.004.

Spruijt CG, Gnerlich F, Smits AH, Pfaffeneder T, Jansen PWTC, Bauer C, et al. 2013. Dynamic

readers for 5-(hydroxy)methylcytosine and its oxidized derivatives. Cell 152:1146–59; doi:10.1016/j.cell.2013.02.004.

Stroud H, Feng S, Kinney SM, Pradhan S, Jacobsen SE. 2011. 5-Hydroxymethylcytosine is associated with enhancers and gene bodies in human embryonic stem cells. Genome Biol. 12:R54; doi:10.1186/gb-2011-12-6-r54.

Tan L, Xiong L, Xu W, Wu F, Huang N, Xu Y, et al. 2013. Genome-wide comparison of DNA hydroxymethylation in mouse embryonic stem cells and neural progenitor cells by a new comparative hMeDIP-seq method. Nucleic Acids Res 41:e84; doi:10.1093/nar/gkt091.

Truong TP, Sakata-Yanagimoto M, Yamada M, Nagae G, Enami T, Nakamoto-Matsubara R, et al. 2015. Age-Dependent Decrease of DNA Hydroxymethylation in Human T Cells. J. Clin. Exp. Hematop. 55:1–6; doi:10.3960/jslrt.55.1.

Waterland RA, Jirtle RL. 2003. Transposable elements: targets for early nutritional effects on epigenetic gene regulation. Mol Cell Biol 23: 5293–5300.

Weinhouse C, Anderson OS, Bergin IL, Vandenbergh DJ, Gyekis JP, Dingman MA, et al. 2014. Dose-dependent incidence of hepatic tumors in adult mice following perinatal exposure to bisphenol A. Env. Heal. Perspect 122:485–491; doi:10.1289/ehp.1307449.

Welch RP, Lee C, Imbriano PM, Patil S, Weymouth TE, Smith RA, et al. 2014. ChIP-Enrich: gene set enrichment testing for ChIP-seq data. Nucleic Acids Res. 42:e105–e105; doi:10.1093/nar/gku463.

Wen L, Li X, Yan L, Tan Y, Li R, Zhao Y, et al. 2014. Whole-genome analysis of 5-hydroxymethylcytosine and 5-methylcytosine at base resolution in the human brain. Genome Biol 15:R49; doi:10.1186/gb-2014-15-3-r49.

Wu H, D'Alessio AC, Ito S, Wang Z, Cui K, Zhao K, et al. 2011. Genome-wide analysis of 5-hydroxymethylcytosine distribution reveals its dual function in transcriptional regulation in mouse embryonic stem cells. Genes Dev 25:679–684; doi:10.1101/gad.2036011.

Wu H, Wang C, Wu Z. 2013. A new shrinkage estimator for dispersion improves differential expression detection in RNA-seq data. Biostatistics 14:232–243; doi:10.1093/biostatistics/kxs033.

Wu H, Xu T, Feng H, Chen L, Li B, Yao B, et al. 2015. Detection of differentially methylated regions from whole-genome bisulfite sequencing data without replicates. Nucleic Acids Res. 43:1–9; doi:10.1093/nar/gkv715.

Xiong J, Jiang H-P, Peng C-Y, Deng Q-Y, Lan M-D, Zeng H, et al. 2015. DNA hydroxymethylation age of human blood determined by capillary hydrophilic-interaction liquid chromatography/mass spectrometry. Clin. Epigenetics 7:72; doi:10.1186/s13148-015-0109-x.

Zampieri M, Ciccarone F, Calabrese R, Franceschi C, Bürkle A, Caiafa P, et al. 2015. Reconfiguration of DNA methylation in aging. Mech. Ageing Dev. 151:60–70; doi:10.1016/j.mad.2015.02.002.

Ziller MJ, Hansen KD, Meissner A, Aryee MJ. 2014. Coverage recommendations for methylation analysis by whole-genome bisulfite sequencing. Nat. Methods 12:230–232; doi:10.1038/nmeth.3152.

# Chapter 5

## Neonatal DNA Methylation Patterns are Associated with Childhood Weight Status in the Healthy Families Project


### Abstract

Recent reports suggest that both cross-sectional DNA methylation and rates of age-related methylation are associated with obesity status, but it remains unclear whether levels of DNA methylation at various stages of childhood can be used to predict obesity likelihood. Using logistic regression, we tested whether neonatal bloodspot or childhood DNA methylation (12-24 months old (n=40), 3-5 years of age (n=40), or 10-12 years of age (n=52)) at several target gene regions predicted childhood obesity likelihood, as defined by weight-for-length (WFL) z-score at 12-14 mos. and body mass index (BMI) z-score at 3-5 and 10-12 years old. DNA methylation was quantified at a repetitive element (LINE-1), two imprinted genes (*IGF2, H19*), and four non-imprinted genes (*LEP*, *PPARA*, *ESR1*, *SREBF1*) related to growth and adiposity in children from the Healthy Families study. In 3-5 year olds, neonatal bloodspot LINE-1 methylation was negatively associated with obesity likelihood (OR= -0.40, p=0.04). There were also suggestive negative associations between bloodspot *IGF2* methylation and obesity likelihood in 12-24 month olds (OR= -0.24, p=0.07), 10-12 year olds (OR= -0.14, p=0.09), and when all age groups were combined (OR= -0.08, p=0.09). Across childhood age in matched blood samples, DNA methylation levels in blood significantly decreased ($p<0.05$) at LINE-1, *PPARA*, *ESR1*, *SREBF1*, *IGF2*, and *H19,* and significantly increased ($p<0.05$) at *LEP*. Our results suggest that age-related epigenetic changes occur at growth-related genes in the first decade of life, and that gene-specific neonatal bloodspot DNA methylation may be a useful biomarker for predicting obesity likelihood later in childhood.

## 5.1 Introduction

As a field of study, epigenetics refers to heritable and potentially reversible changes in an organism's gene regulation that occur independent of the DNA sequence. Epigenetic control mechanisms include chromatin modifications (e.g., histone tail acetylation), non-coding RNA interactions, and alterations to DNA (e.g., DNA methylation) (Bernal and Jirtle 2010; Egger et al. 2004). Previous studies have documented distinct, programmed waves of demethylation and *de novo* DNA methylation during fetal development, as well as evidence that these programmed events help regulate primordial germ cell proliferation and differentiation (Messerschmidt et al. 2014; Reik et al. 2001; Smallwood and Kelsey 2012). While developmental epigenetic events are typically under tight regulation, 5-methylcytosine (5-mC) levels have been shown to change in response to environmental factors during early development (Anderson et al. 2012; Bernal and Jirtle 2010; Manikkam et al. 2013), adolescence (Essex et al. 2013), and even adulthood (Tellez-Plaza et al. 2014; Wright et al. 2010). Given that DNA methylation is established during early development and sensitive to the environment, it has been proposed as a mechanism underlying the developmental origins of health and disease (DOHaD) hypothesis. DOHaD posits that developmental exposure to nutritional and environmental factors alters later-life susceptibility to chronic diseases (e.g., metabolic syndrome) by influencing developmental plasticity (Bateson et al. 2004; Heindel et al. 2015). This paradigm is supported by results from animal model exposure studies and human cohort epidemiological studies (Eriksson 2016; Hart et al. 2015; Heindel et al. 2015; Radford et al. 2014). Despite this rich literature, however, the biological mechanisms supporting the apparent delay between developmental exposure and later-life disease remain poorly characterized. Specifically, few studies have considered whether associations between DNA methylation and disease likelihood change as a function of age during sensitive periods in

early and mid-childhood. This project aims to shed light on the contribution of longitudinal childhood epigenetics to obesity in a human population.

Research suggests that prenatal nutrition can play an important role in establishment of the epigenome. For example, a recent intergenerational study in mice showed that in utero undernourishment leads to changes in the F1 adult male mouse methylome, as well as locus-specific alterations in F2 generation metabolism-related gene expression (Radford et al. 2014). Other animal studies indicate that high-fat-diet-induced obesity is associated with altered methylation in promoters of genes related to metabolism and obesity, including Leptin (*Lep*) and Peroxisome Proliferator-activated Receptor-α (*Ppara*) (Ge et al. 2014; Milagro et al. 2009). Genome-wide studies of the methylome have also noted both nutrient- and obesity-sensitive CpG sites throughout the epigenome, indicating that alterations in diet or adiposity can affect DNA methylation at specific genomic sites (Parle-McDermott and Ozaki 2011; Xu et al. 2013). Supplementing the available animal research, studies in human cohorts have shown that maternal differences in methyl donor intake are associated with altered DNA methylation in children at metastable epialleles (Dominguez-Salas et al. 2014) and target genes related to growth and metabolism (Pauwels et al. 2017). In addition, another recent human cohort study demonstrated associations between lower maternal intake of vitamin D and several adverse outcomes in children – impaired neurocognitive function at 10 years of age, greater risk of eating disorders during adolescence, and lower peak bone mass at 20 years of age (Hart et al. 2015). Based on these results, diet represents an important mediator of methylation, in that it has the potential to affect the epigenome throughout the life course.

In addition to the effects of diet, evidence also suggests that other lifestyle factors, including physical activity, can alter both gene expression levels (Huang et al. 2010; Lesniewski

et al. 2013; Lindholm et al. 2014) and site-specific DNA methylation (Barrès et al. 2012; Rönn et al. 2013). One recent study demonstrated that long-term endurance training is associated with significant changes in DNA methylation at specific enhancer regions across the genome (Lindholm et al. 2014), suggesting that physical activity may have long-term protective effects in the epigenome. Supporting this idea, a study in mice showed that induced maternal physical activity prevents high-fat-diet-induced offspring hypermethylation at the promoter of peroxisome proliferator-activated receptor γ coactivator-1α (Pgc-1α), a master regulator of metabolism (Laker et al. 2014). Together, the available data suggests that physical activity could be an important modifier of methylome establishment/upkeep.

While many DOHaD studies have focused on the association between developmental environment and a snapshot of the later-life epigenome, other recent studies have shown that the epigenome is dynamic with age in human twins (Fraga et al. 2005; Martino et al. 2013), non-twin human cohorts (Alisch et al. 2012; Heyn et al. 2012; Madrigano et al. 2012; Urdinguio et al. 2016; Wang et al. 2012), and rodent models (Maegawa et al. 2014; Spiers et al. 2016). Furthermore, reports indicate consistent patterns of DNA methylation with age -- higher gene-specific methylation (Teschendorff et al. 2013), lower global methylation (Issa 2014; Teschendorff et al. 2013), and bidirectional changes in methylation variability (Jones et al. 2015; Shah et al. 2014). In general, age has two types of effect on the epigenome – epigenetic drift, which refers to stochastic, bidirectional changes in epigenetic variability with age (Fraga et al. 2005; Jones et al. 2015; Teschendorff et al. 2013), and age-related methylation, which is defined as predictable, unidirectional changes in DNA methylation levels that occur with normal aging (Horvath 2013; Jung and Pfeifer 2015). Despite the establishment of these well-defined concepts

in adult populations, the patterns of epigenetic aging during childhood remain unclear, and could play an important role in early development of chronic diseases.

Expanding the literature on epigenetic aging, recent studies have suggested that rates of age-related methylation and epigenetic drift can be affected by environmental exposures. For example, mouse studies indicate that environmental exposure to lead (Pb), Western high-fat diet, or trichloroethylene (TCE) can modify the rates of either age-related methylation (Faulk et al. 2014; Kochmanski et al. 2016) or epigenetic drift (Gilbert et al. 2016), respectively. In an effort to describe a mechanism by which the environment could shape the aging epigenome, we recently introduced a new term – environmental deflection – that refers to any environment- or toxicant-mediated shift away from the baseline rate of age-related methylation or epigenetic drift within an organism (Kochmanski et al. 2017). Given that alterations in longitudinal epigenetic marks may facilitate long-term changes in gene regulation, environmental deflection could underlie the apparent delay between developmental exposure and biological effects later in life. In other words, alterations to the rates of age-related methylation may represent a mechanism underlying the DOHaD hypothesis.

Obesity is a well-documented risk factor for a number of chronic diseases, including heart disease, hypertension, various cancers, and type 2 diabetes (Dixon 2010). Rates of obesity continue to rise in the United States, but models using large numbers of BMI-associated genetic loci show that gene variants only explain 0.66-2.70% of BMI variation (Loos et al. 2017). This suggests that gene-environment interactions play an important role in the growing prevalence of obesity. Supporting this idea, reports suggest that both cross-sectional, gene-specific DNA methylation and rates of age-related methylation are associated with obesity status in humans (Almén et al. 2014; Horvath et al. 2014; Wahl et al. 2016). However, it remains to be seen

whether developmental programming of the epigenome at obesity-related genes is specifically associated with later-life obesity development. Here, we aim to shed light on this question by measuring longitudinal patterns of age-related DNA methylation at a number of obesity-related genes throughout childhood.

For this study, we examined DNA methylation levels at seven target gene regions – the LINE-1 repetitive element, *IGF2, H19, PPARA, LEP, ESR1,* and *SREBF1*. LINE-1, or long interspersed nuclear element 1, is a retrotransposon that comprises ~18% of the human genome (Rodić et al. 2013). Given its prevalence across the genome, LINE-1 can be used as a surrogate for global DNA methylation levels (Yang et al. 2004). Apart from LINE-1, all of the other interrogated genes play a role in metabolism, growth, or development. Insulin-like growth factor II (*IGF2*) and *H19* are well-characterized imprinted genes, in which parent-of-origin mono-allelic expression is involved in the regulation of body composition and growth (Huang et al. 2012; Lui et al. 2008; Soubry et al. 2013; St-Pierre et al. 2012). *PPARA* is a non-imprinted gene that encodes the peroxisome proliferator-activated receptor alpha (PPAR-α) protein, a nuclear receptor that regulates fatty acid metabolism (Lillycrop et al. 2008; Rees et al. 2008; Yoon 2009). *LEP* is a non-imprinted gene that encodes leptin, an adipokine involved in satiety signaling (Crujeiras et al. 2015; Lesseur et al. 2013). *ESR1* is a non-imprinted gene that encodes estrogen receptor alpha (ER-α), a transcription factor involved in regulation of energy homeostasis (Mauvais-Jarvis 2011). Lastly, *SREBF1* is a non-imprinted gene that encodes the Sterol regulatory element-binding transcription factor 1, a transcription factor involved in glucose metabolism and lipid homeostasis (Eberlé et al. 2004; Ferré and Foufelle 2007). Here, we test whether epigenetic modifications at these target genes are associated with obesity risk during childhood.

As described in detail elsewhere (Acharya et al. 2017), the University of Michigan Momentum Center Healthy Families (HF) Project is an interdisciplinary study that explores the obese phenotype among children in three age groups (12-24 months old (n=40), 3-5 years of age (n=40), or 10-12 years of age (n=52)) through measurements of weight status, biology, food environment, and parenting. As part of this project, longitudinal paired DNA methylation levels were quantified from neonatal bloodspots and capillary and venous blood draws in childhood. This study design allows for a comprehensive examination of associations between age, the epigenome, and obesity during childhood. Here, we tested three hypotheses: 1. DNA methylation at growth-related genes at birth and during childhood will be associated with obesity status; 2. growth-related genes will exhibit age-related DNA methylation in childhood; 3. rates of age-related methylation will differ by obesity status, childhood diet, physical activity, and/or age group.

In testing these hypotheses, we aim to identify early-life epigenetic biomarkers of childhood obesity onset, as well as determine whether age-related DNA methylation is occurring at obesity-related genes during the early stages of human life. Furthermore, we aim to test whether rates of age-related methylation vary by environmental factors throughout childhood. Combining these results, it is possible to assess the utility of the longitudinal methylome as a predictive tool for obesity risk during multiple stages of childhood.

## 5.2 Results

### *Summary statistics*

Mean weight-for-length (WFL) or BMI z-score and weight category distribution were not significantly different across the three age groups (**Table 5-1**). Child race/ethnicity was significantly different (p=0.013) in the toddler (12-24 months old) group compared to the total

population, but maternal education and child sex ratio were not significantly different by age group (**Table 5-1**).

***Associations between neonatal DNA methylation and childhood weight status***

First, logistic regression models were used to examine the relationship between neonatal bloodspot target gene DNA methylation and dichotomous obesity (Y/N). For the toddler group, no target genes demonstrated significant associations between bloodspot DNA methylation and obesity likelihood. However, in the preschool group, bloodspot LINE-1 methylation showed a significant negative association with obesity likelihood (log odds = -0.40, p=0.04) (**Figure 5-1**). In addition, preschool bloodspot *IGF2* methylation had a marginally significant negative association with obesity likelihood (log odds = -0.24, p=0.07). Matching this pattern, the school-aged group showed a marginally significant negative association between bloodspot *IGF2* methylation and obesity likelihood (log odds = -0.14, p=0.09). This negative marginal association between bloodspot *IGF2* methylation and log odds of obesity also held when all age groups were combined in a single model (log odds = -0.08, p=0.09) (**Figure 5-1**). No other investigated loci showed significant associations between bloodspot DNA methylation and log odds of obesity in the preschool or school-aged groups.

Separate from the logistic regression analysis, linear regression models were used to examine the relationship between bloodspot DNA methylation and continuous WFL or BMI z-score. For the toddler group, bloodspot *LEP* methylation showed a marginal negative association ($\beta$= -0.08, p=0.09) with WFL z-score, but no other investigated loci showed significant associations between bloodspot DNA methylation and WFL or BMI z-score in the toddler, preschool, or school-aged groups. This lack of significance also held true in models where all age groups were combined.

***Associations between childhood DNA methylation and childhood weight status***

Following up on the bloodspot DNA methylation results, simple logistic models were also used to determine whether childhood blood DNA methylation levels were associated with obesity likelihood. Just as in the bloodspot results, separate models were run for each age group. When combining all the age groups together into a single model, there was a marginally significant negative relationship between *LEP* methylation and obesity likelihood (log odds = -0.455, p=0.08) (**Figure 5-2**). In the preschool group alone, we also found a marginal negative association between blood *ESR1* methylation and obesity likelihood (log odds = -1.668, p=0.08) (**Figure 5-2**). However, both of these results are difficult to interpret due to the very low sample size of the childhood blood draws.

Given the difficulty in interpreting the logistic regression results, follow-up linear regression models were used to examine the relationship between childhood blood DNA methylation and continuous WFL or BMI z-score. In the preschool group, blood *PPARA* methylation showed a significant positive association with BMI z-score ($\beta$= 0.210, p=0.01) (**Figure 5-3**). While this result did not carry over to any of the other age groups, it is noteworthy that the preschool group had the largest childhood blood draw sample size. The remaining genetic loci did not demonstrate significant associations between DNA methylation and WFL or BMI z-score in any analysis.

***Age-related DNA methylation in matched samples***

Linear mixed effect (LME) models were used to model longitudinal patterns of age-related methylation for each target gene. Given that each age group contained different individuals, separate LME models were constructed for matched data in each age group (**Table 5-2**). Longitudinal changes in methylation reflect differences between neonatal bloodspot DNA

(birth) and blood draw (childhood). All genes were modeled using the mean of all included CpG sites. For all age groups, LINE-1, *H19*, *PPARA*, *LEP*, and *SREBF1* demonstrated significant age-related methylation (**Table 5-2**). In contrast, significance of age-related methylation at *IGF2* and *ESR1* differed by age, suggesting that patterns of age-related methylation are not static throughout childhood.

***Age-related DNA methylation by childhood age group***

To further test whether age-related methylation varied by recruited age group, an age*group interaction term was included in linear mixed effect models for each target gene. For most of the genes, the age*group interaction term was not significant. However, both *ESR1* ($\beta$=0.364; p=0.007) and LINE-1 ($\beta$=1.021; p=0.003) showed significant age*group interaction terms in the mixed models. At these genes, the slope of age-related methylation varied across the three age groups, showing a lower intensity of effect with age (**Figure 5-4**). This may reflect region-specific, controlled attenuation of age-related methylation that occurs throughout childhood.

***Effects of diet and physical activity on cross-sectional DNA methylation***

Cross-sectional linear regression models were used to test for associations between lifestyle factors – healthy eating index (HEI) score or moderate-to-vigorous physical activity per day (MVPA/day) – and target gene methylation later in life (Table S3). In the preschool group, there was a marginally significant negative relationship between MVPA/day and LEP methylation (p=0.06). In contrast, there was a marginally significant positive relationship between MVPA/day and LEP methylation in the school-aged children (p=0.07). There were no significant cross-sectional relationships between MVPA/day and target gene methylation in the

toddler group, and there were no significant cross-sectional relationships between HEI score and target gene methylation in any of the three age groups.

***Environmental deflection of age-related methylation***

Linear mixed effects models were used to examine environmental deflection of age-related methylation by obesity status (BMI/WFL z-score), physical activity (MVPA/day), and healthy eating index (HEI score). To test for environmental deflection by these environmental factors, age:environment interaction terms were added to the linear mixed effects models used to test for age-related methylation. To ensure model integrity, each of the included interaction terms – age:MVPA/day, age:HEI, and age:BMI/WFLz – were included in separate models. Overall, there were no consistent patterns of significant environmental deflection at any of the investigated genetic loci across all three time points. However, several target genes exhibited significant or marginally significant environmental deflection by BMI/WFL z-score, MVPA/day, or HEI (**Table 5-3**).

For the age:BMI/WFLz interaction term, there was no significant environmental deflection in the toddler group. In the preschool group, *PPARA* showed significant positive deflection of age-related methylation by BMI z-score (p=0.04) (**Figure 5-5**), but no other significant results were present. In the school-aged children, *SREBF1* showed significant negative environmental deflection of age-related methylation by BMI z-score (p=0.05), but no other target genes showed significant effects of BMI z-score.

For the age:MVPA/day interaction term, it was not possible to examine environmental deflection in the toddler group due to a lack of physical activity data. However, in the preschool group, *LEP* showed significant (p=0.02) positive deflection of age-related methylation by MVPA/day (**Figure 5-6**). No other significant results were present in the preschool age group. In

the school-aged children, *LEP* and *IGF2* showed significant (p=0.001) and marginally significant (p=0.09) negative environmental deflection of age-related methylation by MVPA/day. No other target genes showed significant environmental deflection by obesity status in the school-aged group.

For the age:HEI interaction term, there was no significant environmental deflection in the preschool or school-aged groups. In the toddler group, LEP demonstrated marginally significant negative environmental deflection of age-related methylation by HEI score (p=0.094), but no significant results were present.

## 5.3 Discussion

***Associations between DNA methylation and childhood weight status***

Neonatal bloodspot DNA methylation at the LINE-1 repetitive element and *IGF2* imprinted locus demonstrated significant and marginally significant negative associations with obesity likelihood in preschool children, respectively. These results, while not apparent in the other investigated loci, suggest that neonatal epigenetic biomarkers may be associated with childhood obesity. While these are only preliminary results from a small number of individuals, to our knowledge, this is the first time that neonatal bloodspot DNA methylation status has been linked to obesity likelihood in matched individuals during childhood.

The significant bloodspot locus, LINE-1, is an active retrotransposon that comprises ~18% of the human genome (Rodić et al. 2013). DNA methylation acts as a repressive mark at retrotransposons, blocking these repetitive elements from either duplicating in the genome or generating chimeric fusion transcripts (Slotkin and Martienssen 2007; Wang et al. 2016b). As a result, research indicates that decreases in LINE-1 methylation can increase retrotransposon activity, leading to a reduction in overall genomic stability (Rodić et al. 2013). While it's

possible that this mechanism could modify risk for obesity development in later childhood, LINE-1 is not protein-coding and has no direct involvement in human growth or development, making it difficult to determine the biological significance of specific changes in LINE-1 methylation in relation to obesity risk. However, separate from its intrinsic retrotransposon activity, LINE-1 methylation is prevalent enough in the genome that it also serves as a useful surrogate for global methylation levels (Yang et al. 2004). As such, the negative association between LINE-1 methylation and log odds of obesity in the preschool group may reflect a global link between lower DNA methylation and obesity likelihood during a specific phase of childhood.

Distinct from LINE-1, *IGF2* is an imprinted gene that encodes insulin-like growth factor II, a developmental growth factor that is active throughout life in humans (Chao and D'Amore 2008). As an imprinted gene, *IGF2* demonstrates parent-of-origin-dependent mono-allelic expression, a pattern at least partially controlled via differentially methylated regions (DMRs) (Chao and D'Amore 2008; Tobi et al. 2012). Allele-specific *IGF2* DMR methylation is established in the two waves of epigenomic reprogramming that occur during gametogenesis and early embryogenesis (Ishida and Moore 2013). The imprinted epigenetic marks at *IGF2* are then propagated throughout cellular replication and differentiation, providing life-long regulation of gene expression (Bartolomei and Ferguson-Smith 2011). Given this distinct pattern of programming, developmental changes in *IGF2* DMR imprinting could have long-lasting effects on *IGF2* expression, thereby altering growth and development. Recent studies support this idea, demonstrating associations between developmental *IGF2* DMR methylation and newborn growth indices; however, directionality of these effects varies by study, making interpretation difficult. For example, one study found a significant association between lower umbilical cord

blood *IGF2* DMR methylation and higher plasma IGF2 protein level, as well as a positive association between plasma IGF2 protein levels and birth weight (Hoyo et al. 2012). On the other hand, another study showed that greater placental *IGF2* DMR methylation was positively correlated with newborn length, head circumference, and weight (St-Pierre et al. 2012). Further complicating the issue, a third study found an association between higher cord blood *IGF2* DMR methylation and birth weight, but also showed that lower *IGF2* DMR methylation was associated with greater weight gain six months after birth (Bouwland-Both et al. 2013). These available cross-sectional data indicate that epigenetic programming of *IGF2* is associated with growth and development of newborns, and that directionality of this association is life stage-specific. Our results support this hypothesis, showing a positive link between lower bloodspot *IGF2* DNA methylation and higher obesity likelihood during specific stages of childhood. The consistency of this effect across multiple older age groups suggests that *IGF2* bloodspot methylation may be a meaningful biomarker of obesity risk in later childhood. To further validate this idea, this result must be replicated in a larger childhood obesity study.

In the cross-sectional blood draw DNA methylation models, *PPARA* promoter methylation showed a significant positive association with BMI z-score in the preschool children (**Figure 5-3**). *PPARA* encodes the peroxisome proliferator-activated receptor alpha (PPAR-α) protein, a nuclear receptor that regulates fatty acid metabolism (Yoon 2009). Greater expression of this gene leads to breakdown of fatty acids, potentially leading to reductions in dyslipidemia and obesity (Chung et al. 2016; Yoon 2009). As such, it is expected that higher methylation at the *PPARA* promoter would be associated with lower *PPARA* gene expression and an increased risk of obesity. The significant positive association between preschool *PPARA* promoter methylation and BMI z-score matches this expectation, suggesting that *PPARA* promoter

methylation may play a role in childhood obesity development. However, this result was not consistent across age groups, making interpretation of these data difficult. Future studies should further investigate the contribution of *PPARA* promoter methylation to obesity in children across multiple life stages.

In addition to *PPARA*, the *ESR1* and *LEP* loci each demonstrated marginally significant negative associations between childhood DNA methylation and log odds of obesity in a single age group. However, like the *PPARA* results, these trends were not stable across ages, making it difficult to interpret the data (**Figure 5-2**). Furthermore, childhood blood DNA methylation models showed greater variability in results compared to neonatal bloodspot models. This is likely due to the smaller sample size of the cross-sectional childhood blood draw samples compared to sourced bloodspots. Of particular note in the childhood DNA methylation models, *IGF2* and LINE-1 DNA methylation did not maintain the negative association with obesity likelihood seen in the neonatal bloodspots. This suggests that neonate DNA methylation levels at these loci, not cross-sectional DNA methylation, may be better predictors of later-life obesity risk. Based on our results, future studies investigating links between the epigenome and obesity should not only ensure large samples sizes, but also consider including neonatal bloodspot samples.

***Age-related methylation in matched samples***

A number of human cohort studies have examined the effect of age on the epigenome, with most of the available literature utilizing cross-sectional samples from pediatric or elderly populations (Alisch et al. 2012; Heyn et al. 2012; Madrigano et al. 2012; Wang et al. 2012). Here, we utilized matched bloodspot and blood samples from children in multiple age groups to investigate the effects of aging on the epigenome throughout different phases of childhood. We

found significant age-related methylation in all investigated genetic loci, with the directionality and magnitude of age effects varying by region. This matches previous studies, which have shown that the childhood methylome varies with age in a gene-specific fashion (Alisch et al. 2012; Urdinguio et al. 2016; Wang et al. 2012)**.** The directionality of age-related methylation was consistent across all three age groups for six out of the seven investigated loci, suggesting that aging effects during childhood are generally consistent at a given gene region.

It is noteworthy that age-related changes in DNA methylation were seen as early as 12-24 months old. This emphasizes the importance of considering age when interpreting DNA methylation data, suggesting that timing of sample collection during childhood could have a huge impact on how a study's results are interpreted. Supporting this idea, marginal associations between neonatal *IGF2* methylation and obesity likelihood disappeared in the 12-24 month old blood draw models, indicating that sample age can alter interpretation of the link between childhood DNA methylation and obesity risk. Based on these considerations, future studies should include longitudinal measurements of the childhood epigenome when testing for associations between DNA methylation and early-life disease risk.

***Age-related methylation by childhood age group***

Beyond demonstrating age-related methylation during childhood, we also showed that the magnitude of age-related methylation can vary by developmental stage. This is most apparent at LINE-1, *LEP*, and *ESR1*, where rates of age-related methylation significantly diminished with increasing age (**Figure 5-4**). These results indicate that rates of age-related methylation are not necessarily static during childhood, but may instead follow regulated trajectories. For example, the *ESR1* gene showed variable directionality of age-related methylation by age group, shifting from significant hypomethylation with age in preschool children to non-significant

hypermethylation with age in the school-aged children (**Figure 5-4**). The school-aged data were not unexpected, since previous studies in adult human colon tissue have demonstrated significant age-related hypermethylation at the *ESR1* promoter (Issa et al. 1994; Kaz et al. 2014). However, the shift from hypo- to hypermethylation with age indicates that childhood may be a period of particular epigenetic volatility at the *ESR1* promoter region. This idea matches evidence from previous studies, which show that patterns of age-related methylation are different during childhood and adulthood (Alisch et al. 2012; Simpkin et al. 2015), particularly at genes related to development (Acevedo et al. 2015; Urdinguio et al. 2016). Building on our results, future studies must not only capture cross-sectional measures of the epigenome early and late in life, but also characterize how longitudinal epigenetic marks vary during the child-to-adult transition. This would allow for improved identification of potential windows of epigenetic susceptibility.

***Environmental deflection of age-related methylation***

Continuous BMI/WFL z-score demonstrated significant environmental deflection of the *PPARA* and *SREBF1* gene regions in the preschool and school-aged children, respectively. In the preschool group, the age:BMIz interaction term was positive for the *PPARA* gene region. Given that our data show decreased *PPARA* DNA methylation throughout childhood, this result indicates that higher BMI is associated with weakened negative slope of age-related *PPARA* methylation in preschoolers. The *PPARA* pyrosequencing assay used in this study covers two CpG sites in the 5' promoter of the *PPARA* gene. *PPARA* encodes the peroxisome proliferator-activated receptor alpha (PPAR-α), a nuclear receptor that regulates fatty acid metabolism (Yoon 2009). Increased expression of this gene leads to breakdown of fatty acids, potentially leading to reductions in dyslipidemia and obesity (Chung et al. 2016; Yoon 2009). Given that increased DNA methylation in promoter regions is typically associated with decreased transcription

(Medvedeva et al. 2014), it is expected that decreased methylation at the *PPARA* promoter would be associated with an increase in *PPARA* gene expression and decreased adiposity. Working under this paradigm, negative age-related methylation at *PPARA* during childhood could reflect programmed, age-dependent increases in *PPARA* expression. When the slope of this decrease with age is moderated, the affected individual will have a weakened programmed response, potentially leading to decreased *PPARA* expression and obesity development later in childhood. Our results support this idea, showing that increased preschooler BMI z-score is associated with weakened negative rates of age-related methylation at the *PPARA* promoter.

The *SREBF1* pyrosequencing assay covers four CpG sites in the gene body of *SREBF1*, including one CpG site – Illumina 450k cg2747935 – that has shown associations with Vitamin B12 intake and BMI in previous epigenome-wide studies (Adaikalakoteswari et al. 2015; Wang et al. 2016a). In contrast to the *PPARA* results, *SREBF1* showed significant negative environmental deflection of age-related methylation by BMI z-score in the school-aged group. This is not unexpected, since the *SREBF1* gene encodes the SREBF-1c protein, an insulin-activated transcription factor involved in fatty acid synthesis and lipogenesis (Eberlé et al. 2004). Given its biological function, increased expression of *SREBF1* is expected to increase adiposity (Shimano 2009). Our data show decreased *SREBF1* DNA methylation with childhood age, suggesting that *SREBF1* expression and associated adiposity may increase with age. In addition to age effects, we also found a significant negative deflection of *SREBF1* methylation status by BMI z-score in school-aged children. While this result indicates that increased BMI may exacerbate the negative slope of *SREBF1* age-related methylation during childhood, the low sample size limits interpretability of deflection results.

For the most part, measured lifestyle factors – dietary recall and physical activity – did not significantly modify age-related methylation patterns. In all three age groups, HEI score showed no significant environmental deflection of age-related methylation, suggesting that diet quality may not alter the dynamics of longitudinal DNA methylation during childhood. However, the interpretability of this result depends largely on the inherent range of HEI scores present in our population. In this study population, the HEI score distributions for all ages approached normality, with the majority of scores falling near the mean for each age group (**Figure 5-7**). Given the small sample size of our cohort, our HEI score distributions did not adequately capture the far extremes of diet quality, where most effects are expected to occur. As such, an obesity cohort study measuring levels of specific nutrients may be more appropriate for determining whether diet can lead to environmental deflection of childhood age-related methylation patterns. Exploring this idea, a recent cross-sectional study in adult human colon tissue showed concurrent effects of age and specific nutrients – folate, vitamin D, and selenium – on DNA methylation levels at target genes (Tapp et al. 2013). However, while these results are intriguing, the study was non-longitudinal and failed to test for interactions between age and nutrient intake. To better determine the impact of specific nutrients on age-related methylation, future work in the field should consider matched, longitudinal study designs.

In contrast to HEI score, MVPA/day showed some significant environmental deflection of age-related methylation in the preschool and school-aged children. In both of these age groups, *LEP* showed a significant interaction between age and MVPA/day. However, these *LEP* interaction terms had opposing directionality across the age groups, shifting from positive to negative with increasing age. Assuming these opposing results are true positive, they may reflect changes in the effect of MVPA/day on rates of *LEP* age-related methylation during different

phases of childhood development. Although the mechanism behind this abrupt switch in deflection directionality remains unclear, it may be representative of physical activity dropping below some effect threshold in later childhood. Supporting the idea that physical activity could alter age-related methylation, previous research shows that physical activity can alter the adult epigenetic landscape through distinct alterations in either gene-specific (Nakajima et al. 2010; Zhang et al. 2015) or global methylation (White et al. 2013; Zhang et al. 2011). One study specifically addressed the idea that shifts in activity level could alter the course of age-related methylation, showing that an exercise intervention increased the rates of age-related methylation at the *ASC* gene in adult peripheral blood samples (Nakajima et al. 2010). In addition, a recent review of the literature concluded that physical activity leads to hypermethylation on a genome-wide scale (Yu and Irwin 2016). These findings support the positive age:MVPA interaction we found for *LEP* methylation in preschoolers, and further suggest a trend toward positive environmental deflection of DNA methylation by physical activity. Further investigation into physical activity-mediated environmental deflection at the genes related to growth and metabolism should be repeated in a larger cohort that includes a defined exercise regimen.

***Limitations and future directions***

Our study was unique in many ways, but the findings are limited by the small sample sizes in analyses with the neonatal bloodspots (n=40, n=40, n=52) and especially in analyses with matching blood samples at childhood (n=16, n=26, n=20). While we observed several significant ($p<0.05$) and marginally significant ($p<0.1$) associations between target gene DNA methylation and childhood obesity outcomes, none would withstand correction for multiple testing. Given the associations observed, we recommend future longitudinal studies with increased cohort size and longer follow-up across successive life stages. Follow-up studies

should also consider expanding beyond target gene pyrosequencing, instead measuring epigenome-wide DNA methylation from neonatal bloodspots. Using this approach, future studies could utilize the Horvath epigenetic clock algorithm to determine whether early-life exposures alter rates of epigenetic aging from birth to adulthood (Horvath 2013). This may lead to the identification of additional gene regions where bloodspot DNA methylation predicts either childhood or adulthood obesity likelihood, strengthening the utility of bloodspot epigenetics as a clinically relevant tool for chronic disease risk estimation.

Given the variability in DNA methylation levels by tissue, it remains to be seen whether the documented target gene age-related methylation in blood is consistent in other human tissues during childhood. Tissues of biological interest – i.e. liver, fat, muscle – may demonstrate significantly different associations between DNA methylation and age. Additionally, we did not correct for cellular heterogeneity over time, and the documented age-related methylation could be a reflection of shifting blood cell types with age. Future work should determine white blood cell percentage estimates from both neonatal bloodspots and childhood blood samples, then adjust for bias using a normalization method. Despite this uncertainty, there were some distinct advantages to using blood samples. First, they provided a matched tissue to retroactively collected neonatal bloodspots, allowing for direct measurement of intra-individual age-related methylation during childhood. In addition, blood is minimally invasive to collect from a cohort of children and was the best available biological sample for children in the Healthy Families project.

Expanding the utility of neonatal bloodspots, recent literature shows that it is possible to measure some exposures (e.g., lead, mercury) from dried bloodspot samples (Funk et al. 2013). As such, it is possible that future study designs could use neonatal bloodspots to examine the

effects of childhood exposure to environmental contaminants on age-related methylation and associated phenotypes. This type of paradigm would provide important insight into the temporality of exposure-mediated changes in DNA methylation, further teasing out whether epigenetic changes are a cause or effect of disease phenotypes. The utilization of neonatal bloodspots as research samples is an exciting new model for environmental epidemiology, and should be considered in future human cohort epigenetics studies.

## 5.4 Conclusions

We tested whether neonatal bloodspot DNA methylation and childhood DNA methylation (12-24 mos. old, 3-5 years of age, or 10-12 years of age) at several target gene regions was associated with childhood obesity status. DNA methylation was quantified at one repetitive element (LINE-1), two imprinted genes (*IGF2, H19*), and four non-imprinted genes (*LEP, PPARA, ESR1, SREBF1*) in children from the Healthy Families cohort. We demonstrated negative associations between bloodspot target gene DNA methylation and obesity likelihood in preschool children, suggesting that the neonatal methylome may be useful tool for estimating obesity risk in childhood. In addition, the use of both neonatal bloodspots and matched childhood blood samples allowed for a unique examination of early-life epigenetic patterns. During childhood, all seven investigated genetic loci demonstrated significant age-related methylation, with directionality of age effects varying by region. Environmental deflection of age-related methylation by BMI z-score, MVPA/day, and HEI was minimal, with only a few significant interactions. Associations between neonatal DNA methylation and obesity likelihood were diminished in later-life blood models, indicating that longitudinal studies are critical for effective interpretation of DNA methylation data during childhood. To improve the utility of these results, the dynamics of epigenome-wide bloodspot DNA methylation should be further evaluated in

larger cohorts that examine specific exposure to environmental chemicals or modified behaviors during childhood.

## 5.5 Methods

### *Healthy families study*

The HF project recruited 40 families with children 12-24 months old (toddlers), 40 families with children 3-5.99 years old (preschool), and 52 families with children 10-12.99 years old (school-aged) within 1-hour driving distance to Ann Arbor, MI. During a home visit by a research assistant, families provided survey data, child and parent anthropometry measurements, and written, informed consent. Questionnaires were used to assess sociodemographic characteristics, which included measures of maternal education, child race/ethnicity, and child sex. Each child was weighed to the nearest 0.1 kg using a Detecto Portable Scale Model (Detecto, Cat. #DR550C) and measured to the nearest 0.1 cm using a Seca 214 portable stadiometer (Seca, Prod. #213 1821 009). For toddlers, length was measured using a Seca 417 infantometer (Seca, Prod. # 417 1821 009). Each individual was weighed twice; if the two readings were inconsistent by more than 0.1 kg, the individual was weighed two more times. For the height and length measurement, the individual's position and posture were checked and the height/length measured twice; if the measurements differed by more than 0.5 cm, two more measurements were performed. Weight-for-length (WFL) or Body mass index (BMI) was then calculated. Separately, preschool and school-aged BMI z-score and toddler WFL z-score were derived using age- and sex-specific references from the US Centers for Disease Control (CDC) growth charts (Center for Health Statistics 2000). Per CDC recommendations, for preschool and school-age children, obese was categorized as a BMI $\geq$ 95th percentile, and overweight as a BMI $\geq$ 85th percentile and <95th percentile for age and sex (Defining Childhood Obesity 2016). For

toddlers, obese was categorized as a WFL ≥ 95th percentile and overweight ≥ 85th percentile and <95th percentile for age and sex. Institutional Review Board (IRB) approval was obtained for all research practices (HUM00079730).

***Neonatal bloodspots and blood collection***

Neonatal bloodspots (n=132) for each recruited child were sourced from the Michigan Neonatal Biobank (MNB). Consent was obtained from all recruited families prior to bloodspot retrieval. Michigan Department of Health and Human Services (MDHHS) and University of Michigan (UM) IRB approvals were obtained for the Healthy Families project (UM: HUM00079730), DNA isolations from neonatal bloodspots (MDHHS: 201311-04-EA), and DNA isolations from blood draw samples (UM: HUM00086182). Before retrieval, MNB neonatal bloodspots were stored at different temperatures depending upon their collection date. As such, the current age of each recruited child corresponded to the storage method for their bloodspot – toddler and preschooler bloodspots were stored at -20°C, school-aged children's bloodspots were stored at 4°C.Upon receiving the bloodspots, they were stored in their shipping bags at 4°C.

In addition to neonatal bloodspots, matched childhood blood samples were collected for recruited children by the Michigan Clinical Research Unit based on child assent (school-aged group)/parent consent (all ages). During this blood draw, 0.25-0.50 mL of blood (finger or heel poke) or 7 mL of blood (venous draw) were collected from the toddlers/preschoolers or school-aged children, respectively. Due to lack of consent, blood draw samples were only collected for approximately half of the recruited children (n=65). After collection, all blood draw samples were stored at -80°C.

***DNA isolation and bisulfite conversion***

DNA was isolated from neonatal bloodspots using a modified version of the Oragene QIAamp DNA Micro Kit (Qiagen, Cat. #56304). To maximize DNA yields from bloodspots, a number of changes were made to the standard QIAamp DNA Micro Kit protocol. First, isolations were performed on four 3mm bloodspot punches rather than the recommended three punches. Second, to account for the increase in sample punches, all protocol buffer volumes were scaled up by 33%. Third, to ensure complete digestion, the heated incubation step was increased from 1 hour to overnight. Fourth, the two vortex mixing steps were increased to 2 minutes and 5 minutes, respectively. Fifth, the elution buffer was heated to 56°C prior to use. Finally, the final elution step was repeated to maximize yield. Across all bloodspot samples, average DNA yield was 19.3 ng/µL (S.D. = 9.3 ng/µL) for 25 µL samples.

For the 12-24 mo. and 3-5 yr. age groups, DNA was isolated from blood samples using the Qiagen DNA Blood Mini Kit (Qiagen, Cat. #51104). For the 10-12 yr. group, DNA was isolated from blood samples using the Qiagen Flexigene Kit (Qiagen, Cat. #51206). DNA purity and yield was measured using a NanoDrop spectrophotometer. All isolated DNA was stored at -80°C prior to use.

Genomic DNA from all samples was bisulfite converted using the Zymo Research 96-well EZ-methylation kit (Zymo Research, Cat. #D5004). Depending on the total yield of each DNA sample, bisulfite conversion was carried out on 0.2-1 µg of genomic DNA. To amplify bisulfite converted DNA, polymerase chain reaction (PCR) was performed using HotStarTaq master mix (Qiagen, Cat. #203443), RNAse-free water, forward primer (9 pmol), and biotinylated reverse primer (9 pmol). Total PCR volume was 35 µL per sample, and gel electrophoresis was used to verify PCR product identity.

***Target gene pyrosequencing***

Upon successful DNA purification, bisulfite conversion, and PCR amplification, % DNA methylation was quantified for a panel of target genes using quantitative DNA pyrosequencing assays specific to each gene (**Table 5-4**). Methylation levels for all genes of interest were defined as the mean % methylation of all CpG sites in each gene's PCR amplicon. *SREBF1*, *PPARA*, *LEP*, *ESR1*, *H19*, and *IGF2* were chosen as a panel of target genes to explore based on their involvement in growth/development, obesity, and energy homeostasis. Long Interspersed Nucleotide Element 1 (LINE-1), a repetitive element spread throughout the human genome, was also included as a surrogate for global methylation levels (Martín-Núñez et al. 2014; Yang et al. 2004).

Quantification of DNA methylation levels was performed using the Qiagen Q96 PyroMark ID instrument (Qiagen). Percentage methylation at target CpG sites is calculated within the Pyromark software as the fraction of 5-methylcytosine (5-mC) among all cytosines (methylated and unmethylated). All samples were run in duplicate and mean methylation percentages were calculated as the mean of the duplicates. All pyrosequencing plates included 0%, 25%, 50%, 75%, and 100% methylation controls to ensure proper functioning of the instrument, and to provide baseline measures of methylation.

***Physical activity***

Physical activity was measured in preschool and school-aged children using an Actigraph (GT3X+, Pensacola, FL) accelerometer. Children were instructed to wear the accelerometer on an elastic belt at their hip for 7 consecutive days. To improve validity of included accelerometry data, participants who did not complete at least 4 days of valid recording, with at least 8 hours of measured activity, were removed prior to analysis. The 8 hour cutoff is below the standard 10

hour inclusion criteria, but was chosen in an effort to maximize sample size in this small study. Providing additional support for this choice, other recent studies have used 8 hour cutoffs when characterizing accelerometer data (Cain et al. 2013; Lockwood et al. 2016). At least one recorded weekend day was required for inclusion (Cain et al. 2013). Using the ActiLife software, accelerometer output was reduced into 1 minute epochs to classify data into three groups: moderate- to vigorous- intensity physical activity (MVPA/day; $min \cdot d^{-1}$), light intensity physical activity (LPA, $min \cdot d^{-1}$), and sedentary time (ST, $min \cdot d^{-1}$). Accelerometer data calibration was performed using previously established intensity cut points for children (Freedson et al. 2005). Physical activity data were not collected for toddlers.

***Dietary recall and healthy eating index***

Three separate, unannounced 24-hour dietary recalls (one weekend day, two weekdays) were completed with the parents of each enrolled child over the phone. Dietary recalls were completed according to the USDA Automated Multiple Pass Method (AMPM) (Blanton et al. 2006), and recorded using the Nutrition Data System for Research (NDSR) software (Tiro et al. 2013). During the phone call, parents were asked to recall exactly what their child ate/drank for the past 24 hours, and were provided with a Food Amounts Booklet to assist in portion size estimation. School-aged children were also sometimes asked recall questions by the staff directly to help clarify exact diet. Dietary recalls were broken down into specific nutrient and food group intakes using the Nutrition Data System for Research (NDSR) software (Tiro et al. 2013). According to guidelines established in the NDSR "Guide to Creating Variables Needed to Calculate Scores for Each Component of the Healthy Eating Index-2010 (HEI-2010)" (NDSR 2014), a Healthy Eating Index (HEI) score was then calculated for each meal (Guenther et al. 2014). All calculated HEI scores were based on serving size recommendations (per 1000 kcal)

from the Dietary Guidelines for Americans (McGuire 2011). Calculation of HEI was performed using an in-house SAS code, and the average of all three meal scores for each child was used as a final HEI score.

***Statistical analysis***

Simple summary statistics, including number of recruited individuals, sex ratios, and mean WFL or BMI z-score were calculated for each age group. For sex, child race/ethnicity, maternal education, and weight status category, a chi-squared test of equal proportions was computed to assess differences in distribution of sociodemographic characteristics across the three age groups. Analysis of variance (ANOVA) was used to test for significant differences in mean WFL or BMI z-score across the three age groups.

To test our first hypothesis, logistic regression models were used to examine the association between target gene bloodspot DNA methylation (% methylation) and obesity status (categorical outcome; obese vs. not obese) within each age group. As a secondary test of this association, linear regression models were used to examine the association between target gene bloodspot DNA methylation (% methylation) and continuous WFL or BMI z-score. This modeling approach was repeated to examine associations between blood draw DNA methylation at the same age and weight status.

For our second hypothesis, age-related methylation was measured as the absolute change in average DNA methylation for each gene from birth to follow-up in each of three age groups (toddler, preschool, school-aged**).** Linear mixed effect (LME) models were used to test for an association between percent DNA methylation and age at each gene region. Percent DNA methylation for all investigated loci was defined as the mean of all included CpG sites. Age, WFL or BMI z-score, and sex were included as explanatory variables in LME models. Linear

mixed models for each target region also included a paired individual factor to account for matched, within-individual data. Given that each age group contained different individuals, separate age-related methylation models were run for each group. All models were run using the *lme4* package in R 3.4.0 (http://www.r-project.org).

For the third hypothesis, childhood age group was delineated as a categorical variable. Using this new grouping variable, an age:group interaction term was included in the LME models to test for differences in age-related methylation slope by recruited age group. Environmental deflection of age-related methylation was tested using interaction terms between potential environmental modifiers and age in LME models. Interaction terms for age:BMI z-score, age:WFL z-score, age:HEI score, and age:MVPA/day were included in separate models to test the individual effects of each factor on age-related methylation.

Significance levels were set at $p \leq 0.05$ for all analyses. Results with $p \leq 0.10$ were considered suggestive of significance.

## 5.6 Funding

Data for this study were collected as a part of the Healthy Families Project, which was funded by the University of Michigan (UM) Momentum Center. The work was supported by the MCubed program at the University of Michigan; the Michigan Lifestage Environmental Exposures and Disease (M-LEEaD) NIEHS Core Center under grant P30 ES017885; and the UM NIEHS institutional Training Grant T32 ES007062.

## 5.7 Acknowledgements

We acknowledge the Michigan Neonatal Biobank for providing neonatal bloodspots.

## 5.8 Figures and Tables

| Variables | 12-24 months (n=40) | | 3-5 years (n=40) | | 10-12 years (n=52) | |
|---|---|---|---|---|---|---|
| | Mean | (SD) | Mean | (SD) | Mean | (SD) |
| **WFL or BMI z-score** | 0.32 | (0.94) | 0.38 | (1.06) | 0.24 | (1.28) |

| Variables | 12-24 months (n=40) | | 3-5 years (n=40) | | 10-12 years (n=52) | |
|---|---|---|---|---|---|---|
| | Count (n) | (%) | Count (n) | (%) | Count (n) | (%) |
| **Child Weight Class** | | | | | | |
| Underweight | 1 | (2.5) | 2 | (5) | 5 | (9.6) |
| Normal | 30 | (75) | 28 | (70) | 30 | (57.7) |
| Overweight | 6 | (15) | 6 | (15) | 10 | (19.2) |
| Obese | 3 | (7.5) | 4 | (10) | 7 | (13.5) |
| **Neonatal Bloodspots** | 40 | (100) | 40 | (100) | 52 | (100) |
| **Ancillary Blood Draws** | 19 | (47.5) | 26 | (65) | 20 | (38.5) |
| **Child Gender** | | | | | | |
| Male | 20 | (50) | 22 | (55) | 28 | (54) |
| Female | 20 | (50) | 18 | (45) | 24 | (46) |
| **Child Race*** | | | | | | |
| White | 24 | (60) | 31 | (77.5) | 38 | (73.1) |
| Black | 6 | (15) | 7 | (17.5) | 9 | (17.3) |
| American Indian or Alaska Native | 0 | (0) | 0 | (0) | 1 | (0) |
| Asian or Pacific Islander | 8 | (20) | 1 | (2.5) | 1 | (1.9) |
| Biracial | 2 | (5) | 1 | (2.5) | 3 | (5.7) |
| Other | 0 | (0) | 0 | (0) | 0 | (0) |
| **Child Ethnicity** | | | | | | |
| Hispanic or Latino | 4 | (10) | 2 | (5) | 2 | (3.8) |

| | | | | | | |
|---|---|---|---|---|---|---|
| Not hispanic or latino | 36 | (90) | 38 | (95) | 50 | (96.2) |
| **Maternal education** | | | | | | |
| Did not complete High School | 6 | (15) | 1 | (2.5) | 4 | (7.7) |
| Graduated High School | 4 | (10) | 2 | (5) | 9 | (17.3) |
| Completed GED | 1 | (2.5) | 0 | (0) | 1 | (1.9) |
| Have some college courses | 9 | (22.5) | 10 | (25) | 13 | (25) |
| Completed a 2-year degree | 7 | (17.5) | 6 | (15) | 7 | (13.4) |
| Completed a 4-year degree | 13 | (32.5) | 21 | (52.5) | 18 | (34.6) |

**Table 5-1: Summary statistics for Healthy Families cohort**. A total of n=132 bloodspots for children in three age groups were sourced from the Michigan Neonatal Biobank. At visits during childhood, anthropometry data were collected. ANOVA was used to compare mean WFL or BMI z-score across age groups. A chi-squared test of equal proportions was used to test for significant differences in categorical variable proportions by age group. WFL z-score, BMI z-score, and distribution of weight categories were not significantly different by age; child race was significantly different by age group.* = p-value < 0.05.

| Toddler Age-related Methylation | | | | | |
|---|---|---|---|---|---|
| **Gene** | **N** | **Mean Bloodspot % Methylation (SE)** | **Mean 12-24 month old % Methylation (SE)** | **Methylation by Age - Beta coefficient†** | **p-value** |
| LINE-1 | 18 | 80.44 (0.89) | 77.99 (0.23) | -2.431 | 0.011* |
| *IGF2* | 18 | 49.10 (1.43) | 47.93 (0.59) | -1.147 | 0.310 |
| *H19* | 18 | 58.14 (1.36) | 52.37 (0.56) | -5.774 | <0.001* |
| *PPARA* | 18 | 18.29 (0.88) | 14.45 (0.67) | -3.852 | 0.001* |
| *LEP* | 18 | 21.9 (0.69) | 26.93 (0.63) | 5.020 | <0.001* |
| *ESR1* | 18 | 4.96 (0.23) | 4.40 (0.18) | -0.582 | 0.052 |
| *SREBF1* | 13 | 50.52 (2.47) | 41.42 (2.91) | -11.750 | 0.005* |
| **Preschool Age-related Methylation** | | | | | |
| **Gene** | **N** | **Mean Bloodspot % Methylation (SE)** | **Mean 3-5 year old % Methylation (SE)** | **Methylation by Age - Beta coefficient†** | **p-value** |
| LINE-1 | 25 | 82.15 (0.66) | 77.68 (0.23) | -2.058 | <0.001* |
| *IGF2* | 25 | 50.98 (0.91) | 47.06 (0.50) | -1.865 | <0.001* |
| *H19* | 25 | 61.92 (1.39) | 52.36 (0.45) | -4.652 | <0.001* |
| *PPARA* | 23 | 21.62 (0.74) | 12.58 (0.49) | -4.890 | <0.001* |
| *LEP* | 23 | 22.05 (1/19) | 28.59 (0.65) | 3.297 | <0.001* |
| *ESR1* | 23 | 5.42 (0.28) | 4.54 (0.18) | -0.430 | 0.008* |
| *SREBF1* | 22 | 47.85 (1.49) | 37.89 (1.65) | -5.306 | <0.001* |
| **School-Aged Age-related Methylation** | | | | | |
| **Gene** | **N** | **Mean Bloodspot % Methylation (SE)** | **Mean 10-12 year old % Methylation (SE)** | **Methylation by Age - Beta coefficient†** | **p-value** |
| LINE-1 | 17 | 81.95 (0.73) | 79.69 (0.49) | -0.843 | 0.018* |
| *IGF2* | 16 | 49.34 (1.71) | 45.30 (0.48) | -1.779 | 0.013* |
| *H19* | 16 | 63.23 (3.51) | 52.81 (0.59) | -4.683 | 0.002* |
| *PPARA* | 16 | 19.98 (2.04) | 10.06 (0.47) | -3.607 | 0.002* |
| *LEP* | 13 | 19.52 (2.27) | 27.68 (0.74) | 2.184 | 0.047* |
| *ESR1* | 15 | 4.71 (0.29) | 5.08 (0.17) | 0.120 | 0.337 |
| *SREBF1* | 12 | 51.11 (2.08) | 36.38 (1.55) | -5.305 | <0.001* |

**Table 5-2: Age-related methylation separated by gene region and age group.** The three sections of the table show target gene age-related methylation for the separate age groups. WFL or BMI z-score and sex were included as covariates in all models. Linear mixed models included a paired factor to account for matched, within-individual effects. Separate models were run for each gene; beta coefficients and associated p-values for age from each model are reported. † = Beta coefficient for age predictor in linear mixed model; * = $p<0.05$.

| Toddler | | Environmental Deflection | | | | | |
|---|---|---|---|---|---|---|---|
| **Gene** | **N** | **Age:BMIz - Beta coefficient†** | **p-value** | **Age:MVPA - Beta coefficient†** | **p-value** | **Age:HEI - Beta coefficient†** | **p-value** |
| LINE-1 | 36 | -0.457 | 0.551 | N/A | N/A | 0.036 | 0.671 |
| *IGF2* | 36 | -0.369 | 0.708 | N/A | N/A | -0.110 | 0.335 |
| *H19* | 37 | 0.434 | 0.726 | N/A | N/A | -0.037 | 0.786 |
| *PPARA* | 36 | 0.500 | 0.591 | N/A | N/A | -0.041 | 0.694 |
| *LEP* | 36 | 0.764 | 0.353 | N/A | N/A | -0.151 | **0.094^** |
| *ESR1* | 36 | -0.113 | 0.683 | N/A | N/A | 0.015 | 0.596 |
| *SREBF1* | 26 | -1.198 | 0.687 | N/A | N/A | 0.084 | 0.793 |
| **Preschool** | | **Environmental Deflection** | | | | | |
| **Gene** | **N** | **Age:BMIz - Beta coefficient†** | **p-value** | **Age:MVPA - Beta coefficient†** | **p-value** | **Age:HEI - Beta coefficient†** | **p-value** |
| LINE-1 | 50 | 0.277 | 0.456 | -0.005 | 0.739 | 0.044 | 0.123 |
| *IGF2* | 50 | 0.293 | 0.528 | -0.005 | 0.782 | 0.007 | 0.854 |
| *H19* | 50 | -0.202 | 0.807 | -0.019 | 0.565 | 0.059 | 0.352 |
| *PPARA* | 47 | 0.771 | **0.042*** | -0.008 | 0.606 | 0.025 | 0.423 |
| *LEP* | 46 | -0.176 | 0.639 | 0.033 | **0.016*** | 0.024 | 0.402 |
| *ESR1* | 46 | 0.006 | 0.970 | 0.005 | 0.480 | -0.007 | 0.548 |
| *SREBF1* | 44 | 0.867 | 0.367 | -0.006 | 0.896 | 0.030 | 0.738 |
| **School-Aged Children** | | **Environmental Deflection** | | | | | |
| **Gene** | **N** | **Age:BMIz - Beta coefficient†** | **p-value** | **Age:MVPA - Beta coefficient†** | **p-value** | **Age:HEI - Beta coefficient†** | **p-value** |
| LINE-1 | 35 | 0.040 | 0.863 | -0.002 | 0.905 | 0.040 | 0.331 |
| *IGF2* | 33 | 0.026 | 0.950 | -0.047 | **0.093^** | 0.107 | 0.209 |
| *H19* | 33 | 0.020 | 0.977 | -0.056 | 0.363 | 0.012 | 0.919 |
| *PPARA* | 32 | -0.437 | 0.517 | -0.080 | 0.510 | -0.080 | 0.510 |
| *LEP* | 27 | -0.231 | 0.733 | -0.180 | **0.001*** | 0.186 | 0.125 |
| *ESR1* | 31 | -0.076 | 0.470 | -0.011 | 0.202 | -0.009 | 0.637 |
| *SREBF1* | 25 | -1.248 | **0.050*** | -0.031 | 0.576 | -0.036 | 0.768 |

**Table 5-3: Environmental deflection of age-related DNA methylation.** Environmental deflection was investigated for each separate age group using interaction terms between age and environmental predictors of interest. Linear mixed models included a paired factor to account for matched, within-individual effects, and sex was included as a covariate in all models. Separate models were run for each gene; beta coefficients and associated p-values for interaction terms from separate models are reported. † = Beta coefficient for age:environment interaction terms in LME models that control for gender and id random effect; * = $p<0.05$; ^ = $p<0.10$.

| Assay | LINE-1 | *IGF2*[1] | *H19*[1] | *PPARA* | *LEP*[2] | *ESR1* | *SREBF1*[3] |
|---|---|---|---|---|---|---|---|
| **Location (hg19)** | Repetitive Element | chr11: 2169499; chr11: 2169515; chr11: 2169518 | chr11: 2024254; chr11: 2024257; chr11: 2024259; chr11: 2024261 | chr22: 46545064; chr22: 46545083 | chr7: 127881127; chr7: 127881129; chr7:12788113 | chr6: 152128834; chr6: 152128841; chr6: 152128845; chr6: 152128868 | chr17: 17723203; chr17: 17723288; chr17: 17723297; chr17: 17723305 |
| **Forward PCR Primer** | 5'-TTGAGTTAGGTGTGGGATATAGTT-3' | 5'-GGAGGGGGTTTATTTTTTTAGGAAG-3' | 5'-TTTGTTGATTTTATTAAGGGAG-3' | 5'-GGAGGTTTTTATGAGGATGTAGTT-3' | 5'-GAGTTTTTGGAGGGATATTAAGGAT-3' | 5'-GTTGGAGGTTAGGGAGTTTAGGA-3' | 5'-TTTGTTTGGGTTTTGATGTAAATGTA-3' |
| **Reverse PCR Primer** | 5'-[Biotin]-CAAAAAATCAAAAAATTCCCTTTCC-3' | 5'-[Biotin]-AACCCCAACAAAAACCACTAAACAC-3' | 5'-[Biotin]-CTATAAATAAACCCCAACCAAAC-3' | 5'-[Biotin]-ACACATATTAACCAACAATAACTATCAT-3' | 5'-[Biotin]-CAAAATTATATAAAACCCTATAACCTACCA-3' | 5'-[Biotin]-CTAACCCCCACCCTACCCC-3' | 5'-[Biotin]-ATTCAACTCCACCCCTATATTAAACTAC-3' |
| **Sequencing Primer** | 5'-AGGTGTGGATATAGT-3' | 5'-GGGGTTTATTTTTTTAGGA-3' | 5'-GTGTGGAATTAGAAGT-3' | 5'-GGATGTGGTTGTTTG-3' | 5'-GGGAGGTATTTAAGGG-3'; 5'-GGGAGGGGAGGGAGTTGG-3' | 5'-GGTTAGGGAGTTTAGGAG-3' | 5'-GTATTGGTTTTAAGTTAGGTT-3' |
| **Sequence to Analyze** | TTYGTGGTGYGTYGTTTTTTAAGTYGGTTTGAAAAG | AGTATAGTTAYGTYGTTTTTTATTGGTTTYGTTAAGTAGA | GGTYGYGYGGYGGTAGTGTAGGTTTATATATTATAGTT | TATATTTTAYGAGATATGTAGGATATTAYGTGTATAGGTTATTTTATAAATTTTGAAATAA | TGYGYGYGTGGTTTTTGGHG | TTGGYGGAGGGYGTTYGTTTTGGGATTGTATTTGTTTTYGT | TTTAGTGYGAGGTTGYGTTTATTTYGGTAATAAGTATATTAGGATTGTTAGTAATAGGGTATTTTAAGTAGTYGAGTGGAGTTTTAGTTTTTAAAGTTTG |
| **Amplicon Length (bp)** | ~150 bp | 93 | 145 | 198 | 383 | 119 | 293 |
| **Annealing Temperature (°C)** | 55 | 55 | 51 | 54.5 | 52 | 58/56* | 56 |
| **Number of Cycles** | 48 | 50 | 50 | 48 | 50 | 15/29* | 44 |
| **Number of CpG Sites** | 4 | 3 | 4 | 2 | 3 | 4 | 4 |

**Table 5-4: Pyrosequencing primer sequences and PCR conditions.** Pyrosequencing primer sequences and PCR conditions. Information for each assay, including genomic location (individual CpGs analyzed), primer sequences (5'-3'), sequence to analyze, amplicon length, annealing temperature, number of cycles, and number of CpG sites measured. Touchdown PCR was used for *ESR1* assay, as indicated by the multiple temperatures and cycle numbers. [1]Assay adapted from Hoyo et al., 2012; [2]Assay adapted from Lesseur et al., 2013; [3]Assay adapted from Adaikalakoteswari et al., 2016.

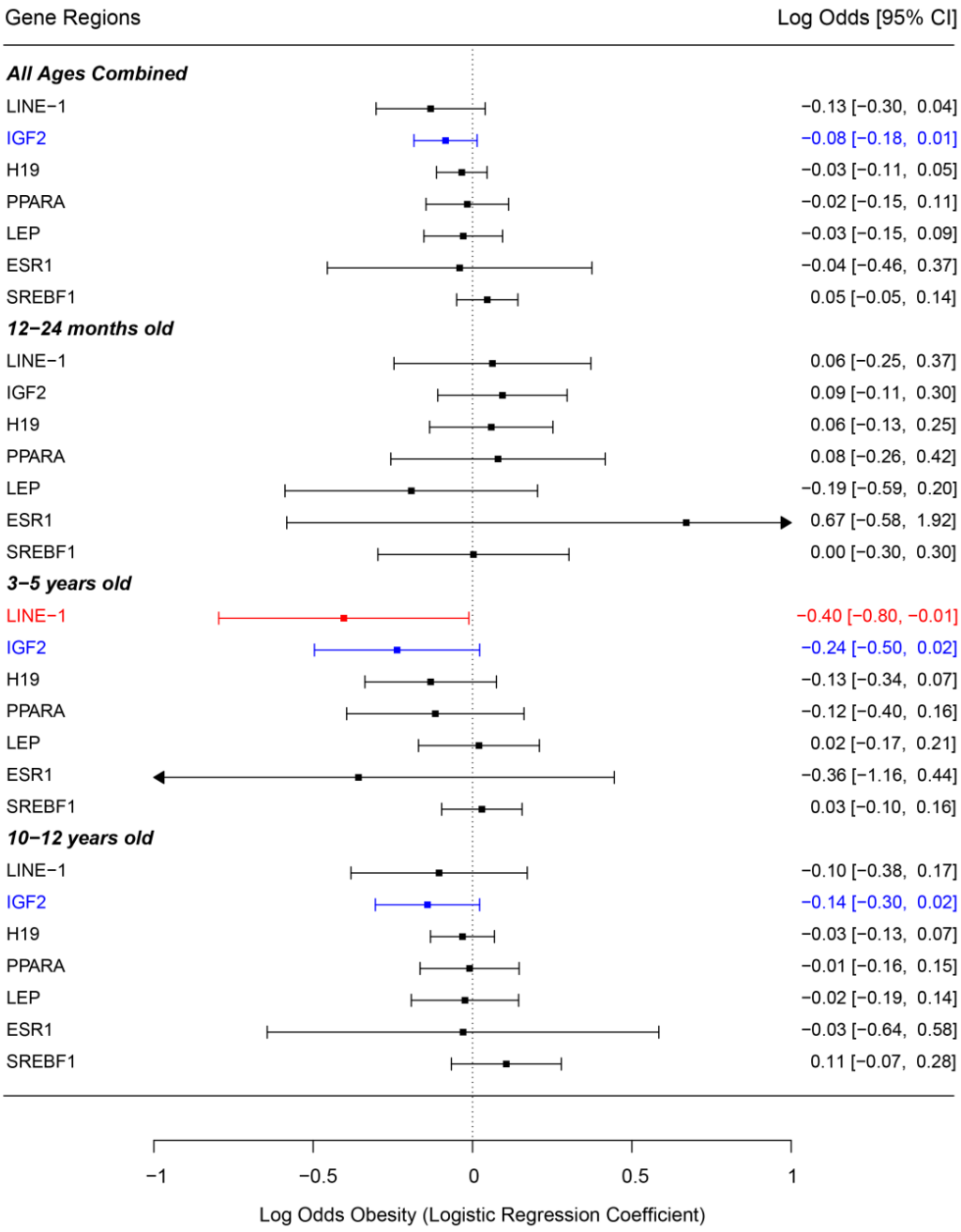


**Figure 5-1: Associations between bloodspot DNA methylation and log odds of obesity (Y/N).** Forest plot of logistic regression models examining associations between neonatal bloodspot DNA methylation at investigated target genes and log odds of obesity. Logistic regression coefficients are represented as log odds of obesity in the right column. The left column shows how the obesity outcome was grouped by age in the regression models. It also lists all target genes included in analyses. Associations that approach significance ($p<0.10$) are indicated in blue, and significant ($p<0.05$) associations are indicated in red. Arrows indicate that confidence interval extends beyond the scale of the plot.

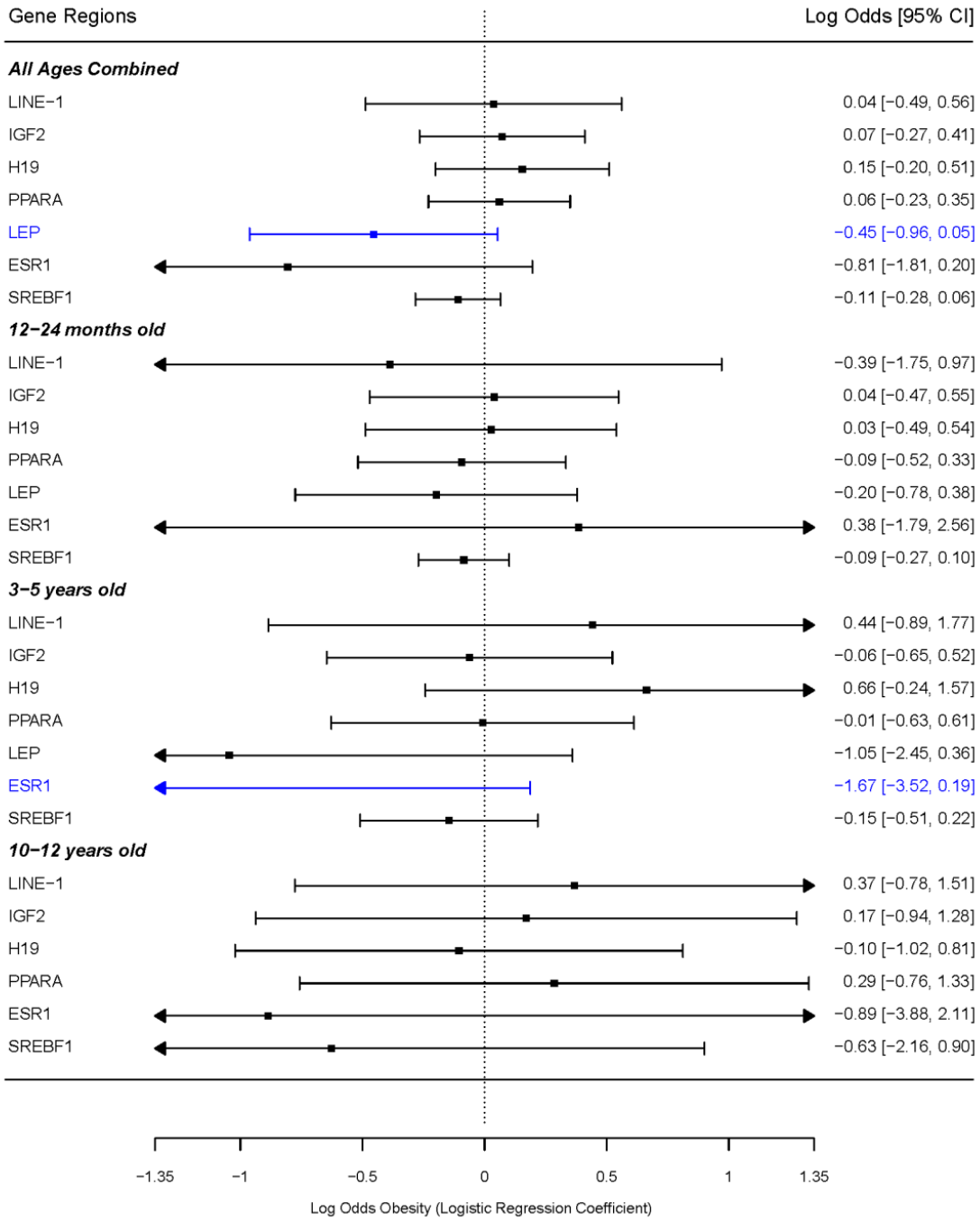


**Figure 5-2: Associations between childhood blood DNA methylation and log odds obesity (Y/N)**. Forest plot of obesity likelihood by childhood blood draw DNA methylation at investigated target genes. Logistic regression coefficients are represented as log odds of obesity in the right column. The left column shows how the obesity likelihood outcome was grouped by age in the regression models. It also lists all of the target gene methylation predictors included in bloodspot logistic regression models. For the 10-12 year old age group, no *LEP* methylation data was available for obese individuals. Trends that approach significance ($p<0.10$) are indicated in blue.

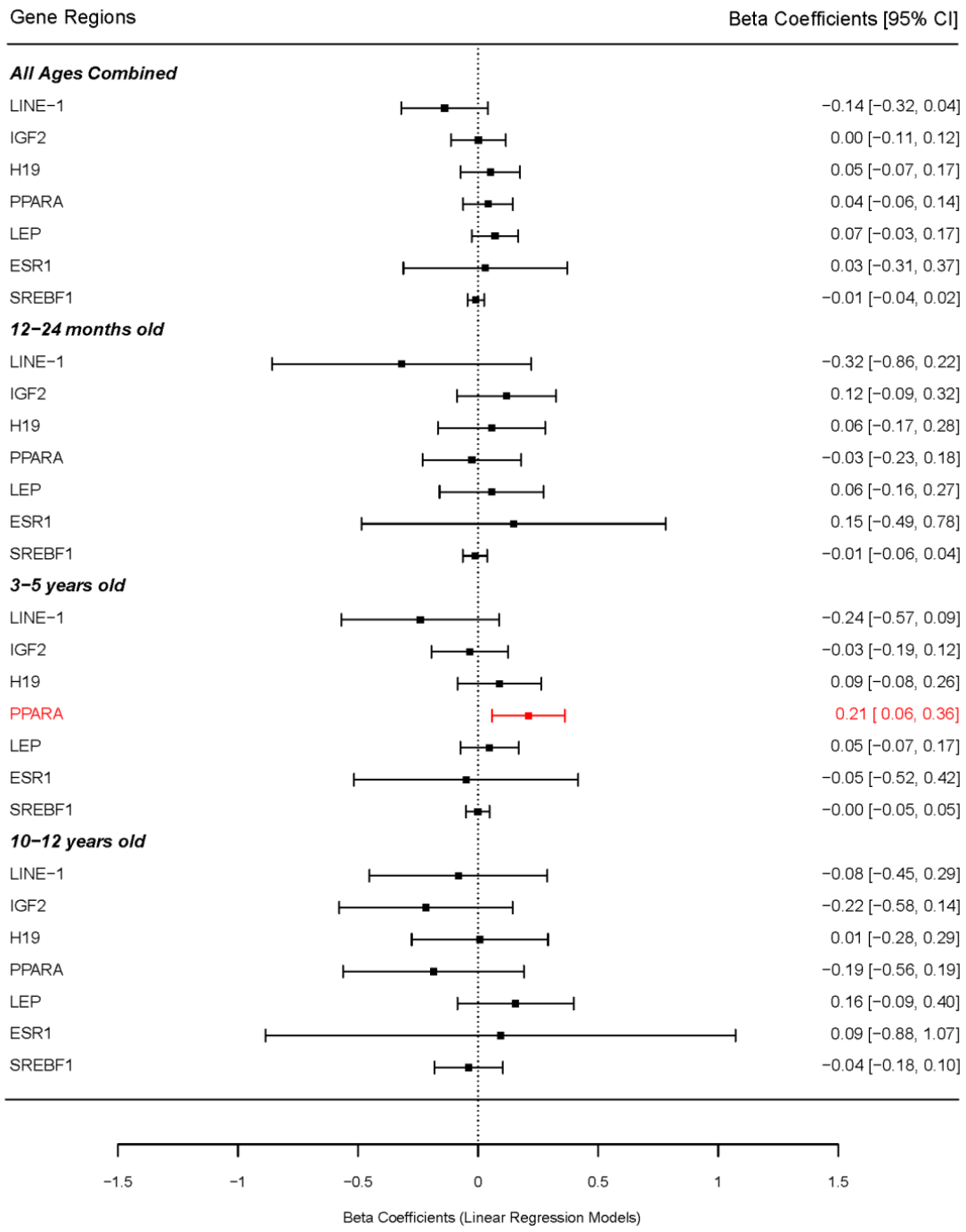


**Figure 5-3: Associations between childhood blood DNA methylation and WFL or BMI z-score.** Forest plot of continuous WFL or BMI z-score by childhood blood draw DNA methylation at investigated target genes. Linear regression coefficients are shown in the right column. The left column shows how the regression models were grouped by age. It also lists all of the target gene methylation predictors included in blood logistic regression models. Significant positive association between PPARA blood DNA methylation and WFL or BMI z-score ($p<0.05$) is indicated in red.

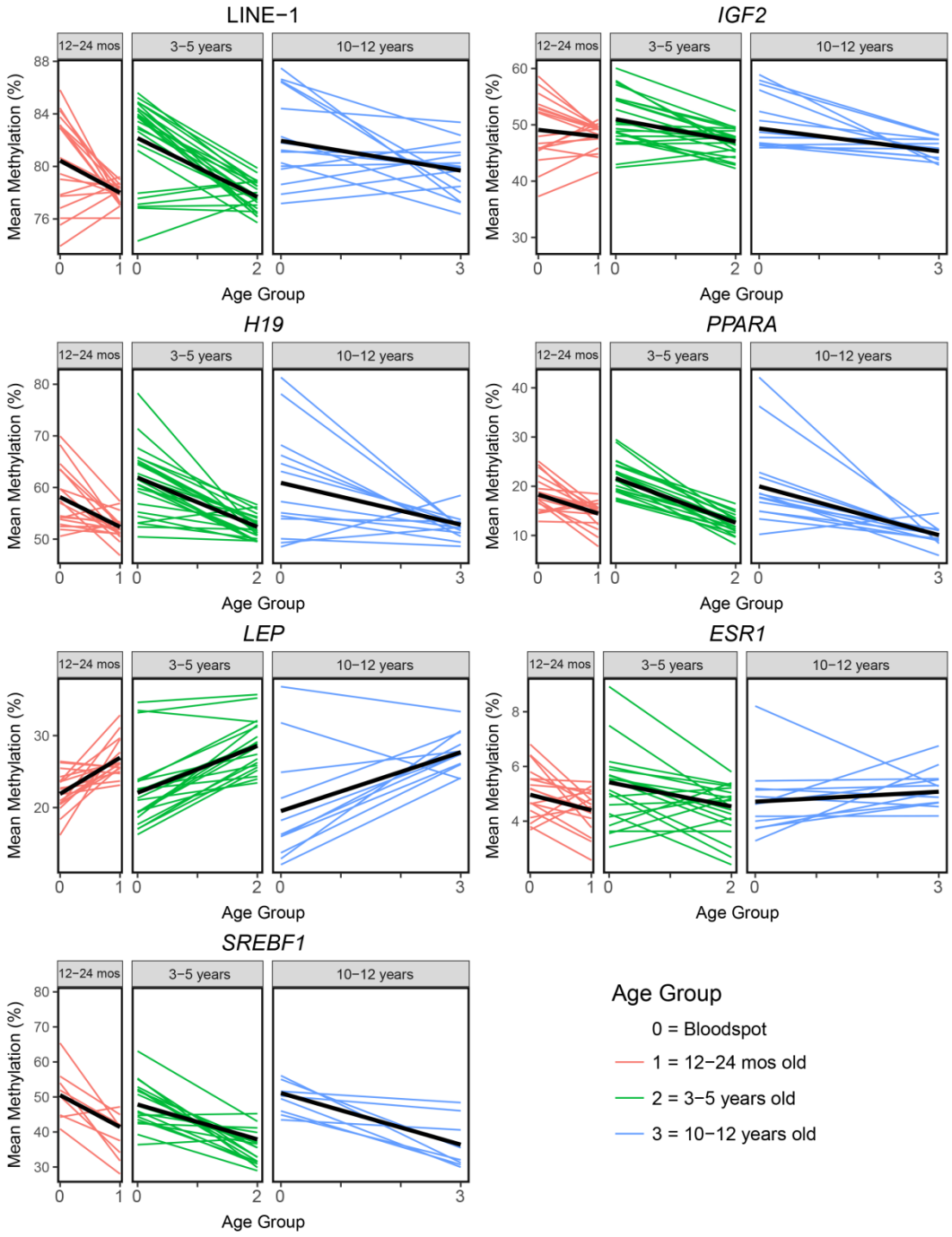


**Figure 5-4: Age-related methylation at seven target loci by age group.** Spaghetti plots are used to visualize age-related methylation for all individuals at each gene region. The three separate age groups are represented in different boxes, as well as by different colors. Thick black lines correspond to linear regression lines for association between age and mean methylation at each gene region. Age groups are indicated as 0, 1, 2, and 3, which correspond to bloodspot (time=0) and follow-up at one of three age groups – 12-24 months old (time=1), 3-5 years old (time=2), and 10-12 years old (time=3). All seven target genes demonstrated significant ($p<0.05$) age-related methylation between birth and at least one follow-up age.

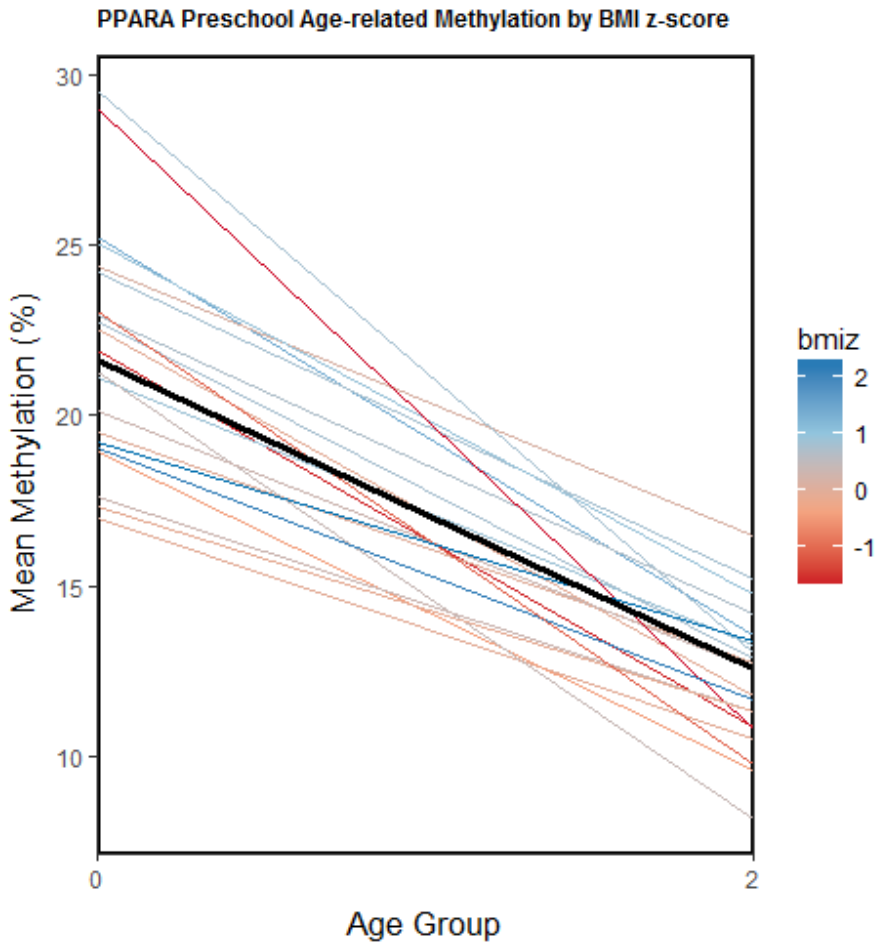


**Figure 5-5: Environmental deflection of preschool *PPARA* age-related DNA methylation by BMI z-score.** Line plot of longitudinal *PPARA* DNA methylation from neonatal bloodspot (age group = 0) to preschool (age group = 2). BMI z-score is indicated on a colored scale, with blue representing higher z-score and red representing lower z-score. In the preschool group, *PPARA* showed significant positive deflection of age-related methylation by BMI z-score (p=0.04). The thick black line is the best-fit regression slope of DNA methylation over time for all individuals combined. Going from low BMI z-score (red) to high BMI z-score (blue), individuals had increased slopes of age-related methylation at the *PPARA* gene. This result was only present in the preschool age group.

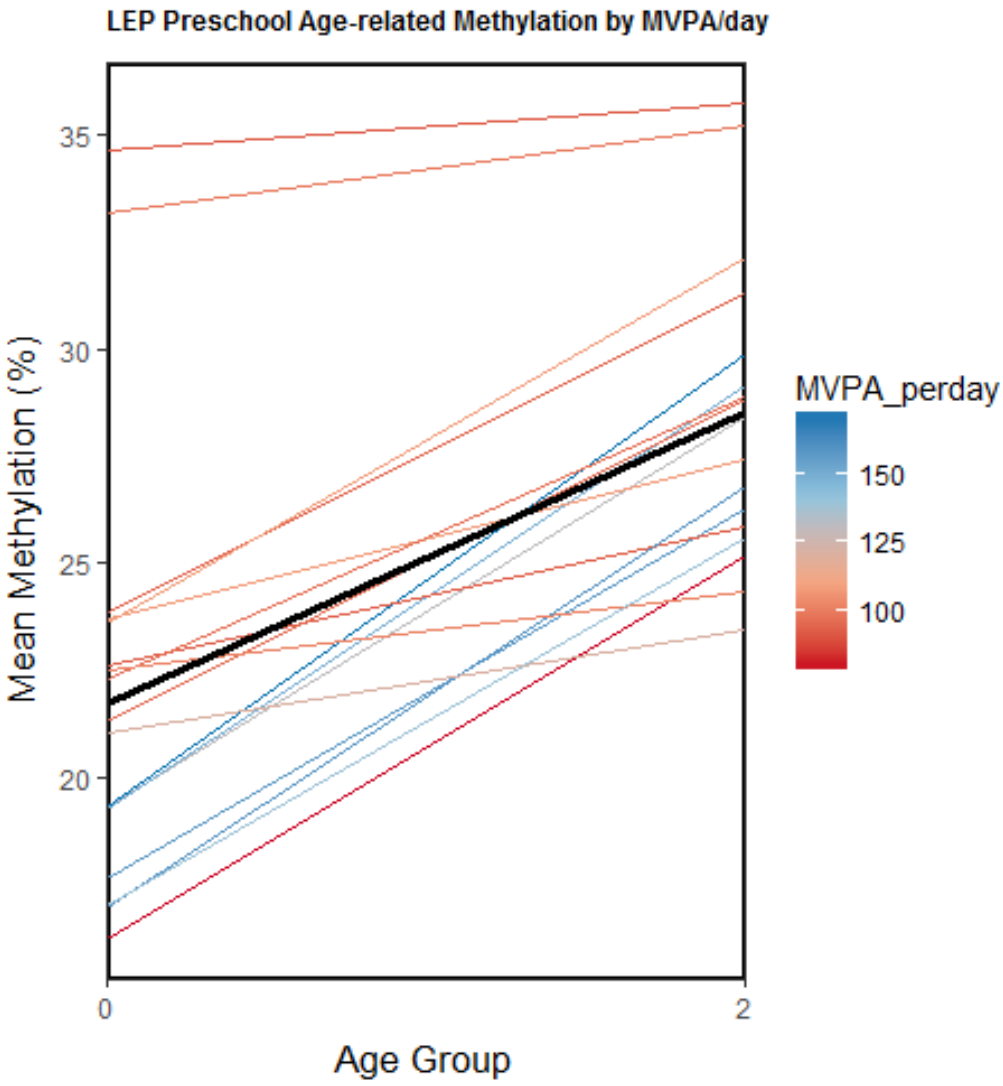


**Figure 5-6: Environmental deflection of preschool *LEP* age-related DNA methylation by MVPA/day**. Line plot of longitudinal *LEP* DNA methylation from neonatal bloodspot (age group = 0) to preschool (age group = 2). MVPA/day is indicated on a colored scale, with blue representing higher activity counts and red representing lower activity counts. In the preschool group, *LEP* showed significant positive deflection of age-related methylation by MVPA/day (p=0.02). The thick black line is the best-fit regression slope of DNA methylation over time for all individuals combined. Going from low MVPA/day (red) to high MVPA/day (blue), individuals had increased slopes of age-related methylation at the *LEP* gene. This result was only present in the preschool age group.

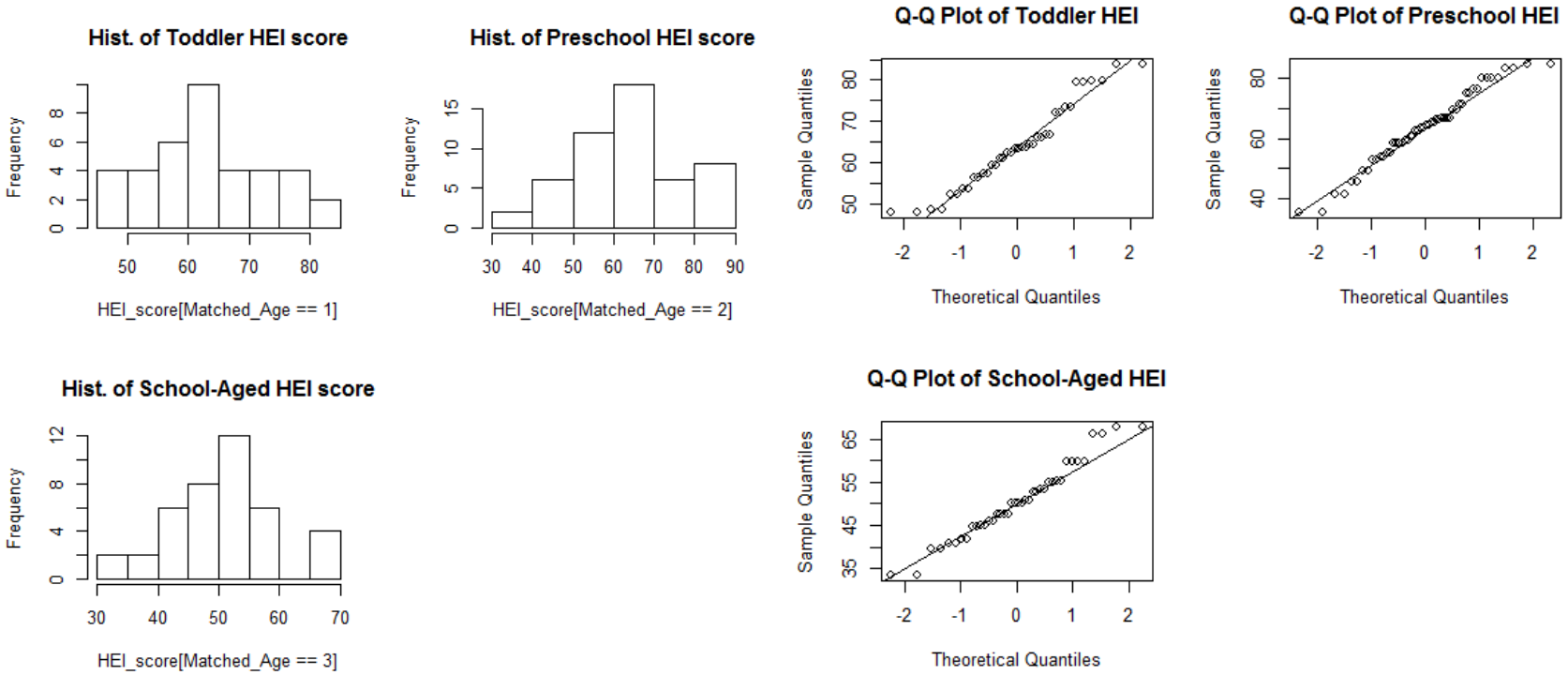


**Figure 5-7: Histograms and Q-Q plots of HEI score distributions**. Histograms and Q-Q plots demonstrate general normality of HEI score data for each separate age group. Low sample size was available at the high and low end of HEI score range, meaning HEI score distributions did not adequately capture the far extremes of diet quality.

## 5.9 References


Acevedo N, Reinius LE, Vitezic M, Fortino V, Söderhäll C, Honkanen H, et al. 2015. Age-associated DNA methylation changes in immune genes, histone modifiers and chromatin remodeling factors within 5 years after birth in human blood leukocytes. Clin. Epigenetics 7:34; doi:10.1186/s13148-015-0064-6.

Acharya Y, Norton EC, Lumeng JC. 2017. The Effect of Financial Compensation on Willingness to Supply a Child?s Blood Sample: A Randomized Controlled Trial. Eval. Health Prof. 16327871770956; doi:10.1177/0163278717709563.

Adaikalakoteswari A, Finer S, Voyias PD, McCarthy CM, Vatish M, Moore J, et al. 2015. Vitamin B12 insufficiency induces cholesterol biosynthesis by limiting s-adenosylmethionine and modulating the methylation of SREBF1 and LDLR genes. Clin. Epigenetics 7:14; doi:10.1186/s13148-015-0046-8.

Alisch RS, Barwick BG, Chopra P, Myrick LK, Satten GA, Conneely KN, et al. 2012. Age-associated DNA methylation in pediatric populations. Genome Res 22:623–632; doi:10.1101/gr.125187.111.

Almén MS, Nilsson EK, Jacobsson JA, Kalnina I, Klovins J, Fredriksson R, et al. 2014. Genome-wide analysis reveals DNA methylation markers that vary with both age and obesity. Gene 548:61–67; doi:10.1016/j.gene.2014.07.009.

Anderson OS, Sant KE, Dolinoy DC. 2012. Nutrition and epigenetics: an interplay of dietary methyl donors, one-carbon metabolism and DNA methylation. J Nutr Biochem 23:853–859; doi:10.1016/j.jnutbio.2012.03.003.

Barrès R, Yan J, Egan B, Treebak JT, Rasmussen M, Fritz T, et al. 2012. Acute exercise remodels promoter methylation in human skeletal muscle. Cell Metab 15:405–411; doi:10.1016/j.cmet.2012.01.001.

Bartolomei MS, Ferguson-Smith AC. 2011. Mammalian genomic imprinting. Cold Spring Harb. Perspect. Biol. 3; doi:10.1101/cshperspect.a002592.

Bateson P, Barker D, Clutton-Brock T, Deb D, D'Udine B, Foley RA, et al. 2004. Developmental plasticity and human health. Nature 430:419–421; doi:10.1038/nature02725.

Bernal AJ, Jirtle RL. 2010. Epigenomic disruption: the effects of early developmental exposures. Birth Defects Res A Clin Mol Teratol 88:938–944; doi:10.1002/bdra.20685.

Blanton CA, Moshfegh AJ, Baer DJ, Kretsch MJ. 2006. The USDA Automated Multiple-Pass Method accurately estimates group total energy and nutrient intake. J Nutr 136: 2594–2599.

Bouwland-Both MI, van Mil NH, Stolk L, Eilers PHC, Verbiest MMPJ, Heijmans BT, et al. 2013. DNA methylation of IGF2DMR and H19 is associated with fetal and infant growth:

the generation R study. PLoS One 8:e81731; doi:10.1371/journal.pone.0081731.

Cain KL, Sallis JF, Conway TL, Van Dyck D, Calhoon L. 2013. Using accelerometers in youth physical activity studies: a review of methods. J. Phys. Act. Health 10: 437–50.

Center for Health Statistics N. 2000. Vital and Health Statistics, Series 11, No. 246 (5/2002)--updated 6/30/2010.

Chao W, D'Amore PA. 2008. IGF2: epigenetic regulation and role in development and disease. Cytokine Growth Factor Rev. 19:111–20; doi:10.1016/j.cytogfr.2008.01.005.

Chung S, Kim YJ, Yang SJ, Lee Y, Lee M. 2016. Nutrigenomic Functions of PPARs in Obesogenic Environments. PPAR Res. 2016:1–17; doi:10.1155/2016/4794576.

Crujeiras AB, Carreira MC, Cabia B, Andrade S, Amil M, Casanueva FF. 2015. Leptin resistance in obesity: An epigenetic landscape. Life Sci. 140:57–63; doi:10.1016/j.lfs.2015.05.003.

Defining Childhood Obesity. 2016. Centers Dis. Control Prev. Available: https://www.cdc.gov/obesity/childhood/defining.html [accessed 11 August 2017].

Dixon JB. 2010. The effect of obesity on health outcomes. Mol. Cell. Endocrinol. 316:104–108; doi:10.1016/j.mce.2009.07.008.

Dominguez-Salas P, Moore SE, Baker MS, Bergen AW, Cox SE, Dyer RA, et al. 2014. Maternal nutrition at conception modulates DNA methylation of human metastable epialleles. Nat. Commun. 5:3746; doi:10.1038/ncomms4746.

Eberlé D, Hegarty B, Bossard P, Ferré P, Foufelle F. 2004. SREBP transcription factors: master regulators of lipid homeostasis. Biochimie 86:839–848; doi:10.1016/j.biochi.2004.09.018.

Egger G, Liang G, Aparicio A, Jones PA. 2004. Epigenetics in human disease and prospects for epigenetic therapy. Nature 429:457–463; doi:10.1038/nature02625.

Eriksson JG. 2016. Developmental Origins of Health and Disease – from a small body size at birth to epigenetics. Ann. Med. 48:456–467; doi:10.1080/07853890.2016.1193786.

Essex MJ, Boyce WT, Hertzman C, Lam LL, Armstrong JM, Neumann SM, et al. 2013. Epigenetic vestiges of early developmental adversity: childhood stress exposure and DNA methylation in adolescence. Child Dev 84:58–75; doi:10.1111/j.1467-8624.2011.01641.x.

Faulk C, Liu K, Barks A, Goodrich JM, Dolinoy DC. 2014. Longitudinal epigenetic drift in mice perinatally exposed to lead. Epigenetics 9:934–941; doi:10.4161/epi.29024.

Ferré P, Foufelle F. 2007. SREBP-1c transcription factor and lipid homeostasis: clinical perspective. Horm. Res. 68:72–82; doi:10.1159/000100426.

Fraga MF, Ballestar E, Paz MF, Ropero S, Setien F, Ballestar ML, et al. 2005. Epigenetic differences arise during the lifetime of monozygotic twins. Proc Natl Acad Sci U S A 102:10604–10609; doi:10.1073/pnas.0500398102.

Freedson P, Pober D, Janz KF. 2005. Calibration of accelerometer output for children. Med. Sci. Sports Exerc. 37: S523-30.

Funk WE, McGee JK, Olshan AF, Ghio AJ. 2013. Quantification of arsenic, lead, mercury and cadmium in newborn dried blood spots. Biomarkers 18:174–177; doi:10.3109/1354750X.2012.750379.

Ge ZJ, Luo SM, Lin F, Liang QX, Huang L, Wei YC, et al. 2014. DNA methylation in oocytes and liver of female mice and their offspring: effects of high-fat-diet-induced obesity. Env. Heal. Perspect 122:159–164; doi:10.1289/ehp.1307047.

Gilbert KM, Blossom SJ, Erickson SW, Reisfeld B, Zurlinden TJ, Broadfoot B, et al. 2016. Chronic exposure to water pollutant trichloroethylene increased epigenetic drift in CD4(+) T cells. Epigenomics 8:633–649; doi:10.2217/epi-2015-0018.

Guenther PM, Kirkpatrick SI, Reedy J, Krebs-Smith SM, Buckman DW, Dodd KW, et al. 2014. The Healthy Eating Index-2010 is a valid and reliable measure of diet quality according to the 2010 Dietary Guidelines for Americans. J. Nutr. 144:399–407; doi:10.3945/jn.113.183079.

Hart PH, Lucas RM, Walsh JP, Zosky GR, Whitehouse AJO, Zhu K, et al. 2015. Vitamin D in Fetal Development: Findings From a Birth Cohort Study. Pediatrics 135.

Heindel JJ, Balbus J, Birnbaum L, Brune-Drisse MN, Grandjean P, Gray K, et al. 2015. Developmental Origins of Health and Disease: Integrating Environmental Influences. Endocrinology 156:3416–3421; doi:10.1210/EN.2015-1394.

Heyn H, Li N, Ferreira HJ, Moran S, Pisano DG, Gomez A, et al. 2012. Distinct DNA methylomes of newborns and centenarians. Proc. Natl. Acad. Sci. 109:10522–10527; doi:10.1073/pnas.1120658109.

Horvath S. 2013. DNA methylation age of human tissues and cell types. Genome Biol. 14:R115; doi:10.1186/gb-2013-14-10-r115.

Horvath S, Erhart W, Brosch M, Ammerpohl O, von Schönfels W, Ahrens M, et al. 2014. Obesity accelerates epigenetic aging of human liver. Proc. Natl. Acad. Sci. U. S. A. 111:15538–43; doi:10.1073/pnas.1412759111.

Hoyo C, Fortner K, Murtha AP, Schildkraut JM, Soubry A, Demark-Wahnefried W, et al. 2012. Association of cord blood methylation fractions at imprinted insulin-like growth factor 2 (IGF2), plasma IGF2, and birth weight. Cancer Causes Control 23:635–45;

doi:10.1007/s10552-012-9932-y.

Huang P, Li S, Shao M, Qi Q, Zhao F, You J, et al. 2010. Calorie restriction and endurance exercise share potent anti-inflammatory function in adipose tissues in ameliorating diet-induced obesity and insulin resistance in mice. Nutr Metab 7:59; doi:10.1186/1743-7075-7-59.

Huang R-C, Galati JC, Burrows S, Beilin LJ, Li X, Pennell CE, et al. 2012. DNA methylation of the IGF2/H19 imprinting control region and adiposity distribution in young adults. Clin. Epigenetics 4:21; doi:10.1186/1868-7083-4-21.

Ishida M, Moore GE. 2013. The role of imprinted genes in humans. Mol. Aspects Med. 34:826–840; doi:10.1016/j.mam.2012.06.009.

Issa J-PJ, Ottaviano YL, Celano P, Hamilton SR, Davidson NE, Baylin SB. 1994. Methylation of the oestrogen receptor CpG island links ageing and neoplasia in human colon. Nat. Genet. 7:536–540; doi:10.1038/ng0894-536.

Issa JP. 2014. Aging and epigenetic drift: a vicious cycle. J Clin Invest 124:24–29; doi:10.1172/JCI69735.

Jones MJ, Goodman SJ, Kobor MS. 2015. DNA methylation and healthy human aging. Aging Cell 14:924–932; doi:10.1111/acel.12349.

Jung M, Pfeifer GP. 2015. Aging and DNA methylation. BMC Biol 13:7; doi:10.1186/s12915-015-0118-4.

Kaz AM, Wong C-J, Dzieciatkowski S, Luo Y, Schoen RE, Grady WM. 2014. Patterns of DNA methylation in the normal colon vary by anatomical location, gender, and age. Epigenetics 9:492–502; doi:10.4161/epi.27650.

Kochmanski J, Marchlewicz EH, Savidge M, Montrose L, Faulk C, Dolinoy DC. 2016. Longitudinal effects of developmental bisphenol A and variable diet exposures on epigenetic drift in mice. Reprod. Toxicol.; doi:10.1016/j.reprotox.2016.07.021.

Kochmanski J, Montrose L, Goodrich JM, Dolinoy DC. 2017. Environmental Deflection: The Impact of Toxicant Exposures on the Aging Epigenome. Toxicol. Sci. 156:kfx005; doi:10.1093/toxsci/kfx005.

Laker RC, Lillard TS, Okutsu M, Zhang M, Hoehn KL, Connelly JJ, et al. 2014. Exercise prevents maternal high-fat diet-induced hypermethylation of the Pgc-1α gene and age-dependent metabolic dysfunction in the offspring. Diabetes 63:1605–1611; doi:10.2337/db13-1614.

Lesniewski LA, Zigler ML, Durrant JR, Nowlan MJ, Folian BJ, Donato AJ, et al. 2013. Aging compounds western diet-associated large artery endothelial dysfunction in mice: prevention

by voluntary aerobic exercise. Exp Gerontol 48:1218–1225; doi:10.1016/j.exger.2013.08.001.

Lesseur C, Armstrong DA, Paquette AG, Koestler DC, Padbury JF, Marsit CJ. 2013. Tissue-specific Leptin promoter DNA methylation is associated with maternal and infant perinatal factors. Mol. Cell. Endocrinol. 381:160–167; doi:10.1016/j.mce.2013.07.024.

Lillycrop KA, Phillips ES, Torrens C, Hanson MA, Jackson AA, Burdge GC. 2008. Feeding pregnant rats a protein-restricted diet persistently alters the methylation of specific cytosines in the hepatic PPAR alpha promoter of the offspring. Br J Nutr 100:278–282; doi:10.1017/S0007114507894438.

Lindholm ME, Marabita F, Gomez-Cabrero D, Rundqvist H, Ekström TJ, Tegnér J, et al. 2014. An integrative analysis reveals coordinated reprogramming of the epigenome and the transcriptome in human skeletal muscle after training. Epigenetics 9:1557–1569; doi:10.4161/15592294.2014.982445.

Lockwood J, Jeffery A, Schwartz A, Manlhiot C, Schneiderman JE, McCrindle BW, et al. 2016. Comparison of a physical activity recall questionnaire with accelerometry in children and adolescents with obesity: a pilot study. Pediatr. Obes.; doi:10.1111/ijpo.12172.

Loos RJF, Cecile A, Janssens JW. 2017. Perspective Predicting Polygenic Obesity Using Genetic Information.; doi:10.1016/j.cmet.2017.02.013.

Lui JC, Finkielstain GP, Barnes KM, Baron J. 2008. An imprinted gene network that controls mammalian somatic growth is down-regulated during postnatal growth deceleration in multiple organs. Am J Physiol Regul Integr Comp Physiol 295:R189-96; doi:10.1152/ajpregu.00182.2008.

Madrigano J, Baccarelli AA, Mittleman MA, Sparrow D, Vokonas PS, Tarantini L, et al. 2012. Aging and epigenetics: Longitudinal changes in gene-specific DNA methylation. Epigenetics 7:63–70; doi:10.4161/epi.7.1.18749.

Maegawa S, Gough SM, Watanabe-Okochi N, Lu Y, Zhang N, Castoro RJ, et al. 2014. Age-related epigenetic drift in the pathogenesis of MDS and AML. Genome Res 24:580–591; doi:10.1101/gr.157529.113.

Manikkam M, Tracey R, Guerrero-Bosagna C, Skinner MK. 2013. Plastics derived endocrine disruptors (BPA, DEHP and DBP) induce epigenetic transgenerational inheritance of obesity, reproductive disease and sperm epimutations. PLoS One 8:e55387; doi:10.1371/journal.pone.0055387.

Martín-Núñez GM, Cabrera-Mulero R, Rubio-Martín E, Rojo-Martínez G, Olveira G, Valdés S, et al. 2014. Methylation levels of the SCD1 gene promoter and LINE-1 repeat region are associated with weight change: An intervention study. Mol. Nutr. Food Res. 58:1528–1536; doi:10.1002/mnfr.201400079.

Martino D, Loke YJ, Gordon L, Ollikainen M, Cruickshank MN, Saffery R, et al. 2013. Longitudinal, genome-scale analysis of DNA methylation in twins from birth to 18 months of age reveals rapid epigenetic change in early life and pair-specific effects of discordance. Genome Biol 14:R42; doi:10.1186/gb-2013-14-5-r42.

Mauvais-Jarvis F. 2011. Estrogen and androgen receptors: regulators of fuel homeostasis and emerging targets for diabetes and obesity. Trends Endocrinol. Metab. 22:24–33; doi:10.1016/j.tem.2010.10.002.

McGuire S. 2011. U.S. Department of Agriculture and U.S. Department of Health and Human Services, Dietary Guidelines for Americans, 2010. 7th Edition, Washington, DC: U.S. Government Printing Office, January 2011. Adv. Nutr. 2:293–4; doi:10.3945/an.111.000430.

Medvedeva YA, Khamis AM, Kulakovskiy I V, Ba-Alawi W, Bhuyan MS, Kawaji H, et al. 2014. Effects of cytosine methylation on transcription factor binding sites. BMC Genomics 15:119; doi:10.1186/1471-2164-15-119.

Messerschmidt DM, Knowles BB, Solter D. 2014. DNA methylation dynamics during epigenetic reprogramming in the germline and preimplantation embryos. Genes Dev 28:812–828; doi:10.1101/gad.234294.113.

Milagro FI, Campión J, García-Díaz DF, Goyenechea E, Paternain L, Martínez JA. 2009. High fat diet-induced obesity modifies the methylation pattern of leptin promoter in rats. J Physiol Biochem 65: 1–9.

Nakajima K, Takeoka M, Mori M, Hashimoto S, Sakurai A, Nose H, et al. 2010. Exercise Effects on Methylation of *ASC* Gene. Int. J. Sports Med. 31:671–675; doi:10.1055/s-0029-1246140.

NDSR. 2014. Guide to Creating Variables Needed to Calculate Scores for Each Component of the Healthy Eating Index-2010 (HEI-2010).

Parle-McDermott A, Ozaki M. 2011. The impact of nutrition on differential methylated regions of the genome. Adv Nutr 2:463–471; doi:10.3945/an.111.001008.

Pauwels S, Ghosh M, Duca RC, Bekaert B, Freson K, Huybrechts I, et al. 2017. Maternal intake of methyl-group donors affects DNA methylation of metabolic genes in infants. Clin. Epigenetics 9:16; doi:10.1186/s13148-017-0321-y.

Radford EJ, Ito M, Shi H, Corish JA, Yamazawa K, Isganaitis E, et al. 2014. In utero undernourishment perturbs the adult sperm methylome and intergenerational metabolism. Science (80-. ). 345:1255903–1255903; doi:10.1126/science.1255903.

Rees WD, McNeil CJ, Maloney CA. 2008. The Roles of PPARs in the Fetal Origins of

Metabolic Health and Disease. PPAR Res 2008:459030; doi:10.1155/2008/459030.

Reik W, Dean W, Walter J. 2001. Epigenetic reprogramming in mammalian development. Science (80-. ). 293:1089–1093; doi:10.1126/science.1063443.

Rodić N, Burns KH, Vallot C, Castoro R, Chung W. 2013. Long Interspersed Element–1 (LINE-1): Passenger or Driver in Human Neoplasms? S.M. Rosenberg, ed PLoS Genet. 9:e1003402; doi:10.1371/journal.pgen.1003402.

Rönn T, Volkov P, Davegårdh C, Dayeh T, Hall E, Olsson AH, et al. 2013. A six months exercise intervention influences the genome-wide DNA methylation pattern in human adipose tissue. PLoS Genet 9:e1003572; doi:10.1371/journal.pgen.1003572.

Shah S, McRae AF, Marioni RE, Harris SE, Gibson J, Henders AK, et al. 2014. Genetic and environmental exposures constrain epigenetic drift over the human life course. Genome Res 24:1725–1733; doi:10.1101/gr.176933.114.

Shimano H. 2009. SREBPs: physiology and pathophysiology of the SREBP family. FEBS J. 276:616–621; doi:10.1111/j.1742-4658.2008.06806.x.

Simpkin AJ, Suderman M, Gaunt TR, Lyttleton O, McArdle WL, Ring SM, et al. 2015. Longitudinal analysis of DNA methylation associated with birth weight and gestational age. Hum. Mol. Genet. 24:3752–63; doi:10.1093/hmg/ddv119.

Slotkin RK, Martienssen R. 2007. Transposable elements and the epigenetic regulation of the genome. Nat. Rev. Genet. 8:272–285; doi:10.1038/nrg2072.

Smallwood SA, Kelsey G. 2012. De novo DNA methylation: a germ cell perspective. Trends Genet 28:33–42; doi:10.1016/j.tig.2011.09.004.

Soubry A, Schildkraut JM, Murtha A, Wang F, Huang Z, Bernal A, et al. 2013. Paternal obesity is associated with IGF2 hypomethylation in newborns: results from a Newborn Epigenetics Study (NEST) cohort. BMC Med 11:29; doi:10.1186/1741-7015-11-29.

Spiers H, Hannon E, Wells S, Williams B, Fernandes C, Mill J. 2016. Age-associated changes in DNA methylation across multiple tissues in an inbred mouse model. Mech Ageing Dev 154:20–23; doi:10.1016/j.mad.2016.02.001.

St-Pierre J, Hivert M-F, Perron P, Poirier P, Guay S-P, Brisson D, et al. 2012. IGF2 DNA methylation is a modulator of newborn's fetal growth and development. Epigenetics 7:1125–1132; doi:10.4161/epi.21855.

Tapp HS, Commane DM, Bradburn DM, Arasaradnam R, Mathers JC, Johnson IT, et al. 2013. Nutritional factors and gender influence age-related DNA methylation in the human rectal mucosa. Aging Cell 12:148–55; doi:10.1111/acel.12030.

Tellez-Plaza M, Tang WY, Shang Y, Umans JG, Francesconi KA, Goessler W, et al. 2014. Association of global DNA methylation and global DNA hydroxymethylation with metals and other exposures in human blood DNA samples. Env. Heal. Perspect 122:946–954; doi:10.1289/ehp.1306674.

Teschendorff AE, West J, Beck S. 2013. Age-associated epigenetic drift: implications, and a case of epigenetic thrift? Hum Mol Genet 22:R7–R15; doi:10.1093/hmg/ddt375.

Tiro J, Lee SJC, Lipshultz SE, Miller TL, Wilkinson JD, Mestre MA, et al. 2013. Nutrition Data System for Research (NDSR). In: *Encyclopedia of Behavioral Medicine*. Springer New York:New York, NY. 1348–1350.

Tobi EW, Slagboom PE, van Dongen J, Kremer D, Stein AD, Putter H, et al. 2012. Prenatal Famine and Genetic Variation Are Independently and Additively Associated with DNA Methylation at Regulatory Loci within IGF2/H19. F. Lyko, ed PLoS One 7:e37933; doi:10.1371/journal.pone.0037933.

Urdinguio RG, Torró MI, Bayón GF, Álvarez-Pitti J, Fernández AF, Redon P, et al. 2016. Longitudinal study of DNA methylation during the first 5 years of life. J. Transl. Med. 14:160; doi:10.1186/s12967-016-0913-x.

Wahl S, Drong A, Lehne B, Loh M, Scott WR, Kunze S, et al. 2016. Epigenome-wide association study of body mass index, and the adverse outcomes of adiposity. Nature 541:81–86; doi:10.1038/nature20784.

Wang B, Gao W, Li J, Yu C, Cao W, Lv J, et al. 2016a. Methylation loci associated with body mass index, waist circumference, and waist-to-hip ratio in Chinese adults: an epigenome-wide analysis. Lancet 388:S21; doi:10.1016/S0140-6736(16)31948-1.

Wang D, Liu X, Zhou Y, Xie H, Hong X, Tsai H-J, et al. 2012. Individual variation and longitudinal pattern of genome-wide DNA methylation from birth to the first two years of life. Epigenetics 7:594–605; doi:10.4161/epi.20117.

Wang T, Santos JH, Feng J, Fargo DC, Shen L, Riadi G, et al. 2016b. A Novel Analytical Strategy to Identify Fusion Transcripts between Repetitive Elements and Protein Coding-Exons Using RNA-Seq. P. Ortinski, ed PLoS One 11:e0159028; doi:10.1371/journal.pone.0159028.

White AJ, Sandler DP, Bolick SCE, Xu Z, Taylor JA, DeRoo LA. 2013. Recreational and household physical activity at different time points and DNA global methylation. Eur. J. Cancer 49:2199–2206; doi:10.1016/j.ejca.2013.02.013.

Wright RO, Schwartz J, Wright RJ, Bollati V, Tarantini L, Park SK, et al. 2010. Biomarkers of lead exposure and DNA methylation within retrotransposons. Env. Heal. Perspect 118:790–795; doi:10.1289/ehp.0901429.

Xu X, Su S, Barnes VA, De Miguel C, Pollock J, Ownby D, et al. 2013. A genome-wide methylation study on obesity. Epigenetics 8:522–533; doi:10.4161/epi.24506.

Yang AS, Estécio MRH, Doshi K, Kondo Y, Tajara EH, Issa J-PJ. 2004. A simple method for estimating global DNA methylation using bisulfite PCR of repetitive DNA elements. Nucleic Acids Res. 32:e38; doi:10.1093/nar/gnh032.

Yoon M. 2009. The role of PPARα in lipid metabolism and obesity: Focusing on the effects of estrogen on PPARα actions. Pharmacol. Res. 60:151–159; doi:10.1016/j.phrs.2009.02.004.

Yu H, Irwin ML. 2016. Effects of Physical Activity on DNA Methylation and Associations with Breast Cancer. Springer International Publishing. 251–264.

Zhang FF, Cardarelli R, Carroll J, Zhang S, Fulda KG, Gonzalez K, et al. 2011. Physical activity and global genomic DNA methylation in a cancer-free population. Epigenetics 6: 293–299.

Zhang Y, Hashimoto S, Fujii C, Hida S, Ito K, Matsumura T, et al. 2015. NFκB2 Gene as a Novel Candidate that Epigenetically Responds to Interval Walking Training. Int. J. Sports Med. 36:769–775; doi:10.1055/s-0035-1547221.

# Chapter 6

# Conclusion

## 6.1 Dissertation Objectives

The overall goal of this dissertation was to improve understanding of the epigenetic mechanisms driving the developmental origins of health and disease (DOHaD) hypothesis (Bateson et al. 2004; Heindel et al. 2015). Specifically, we aimed to determine whether epigenetic aging, the changes that occur in the epigenome with age, contribute to later-life disease development. In an effort to answer this question, we tested whether early-life exposure to specific environmental factors alters long-term regulation of the epigenome, as had been suggested in previous human (Horvath et al. 2014; Shah et al. 2014; van Dongen et al. 2016; Zannas et al. 2015) and animal model (Faulk et al. 2014; Gilbert et al. 2016; Kochmanski et al. 2016) studies. To examine the effects of perinatal environmental exposures on longitudinal epigenetic patterns, we exposed mice to bishenol A (BPA) and/or Western high-fat diet (WHFD) throughout the perinatal period, then measured longitudinal DNA methylation from blood and tail tissues. Both BPA and HFD have shown cross-sectional effects on the epigenome (Anderson et al. 2012; Yoon et al. 2017), but their effects on epigenetic aging were unclear prior to this dissertation.

To describe the effects of the perinatal environment on epigenetic aging, we first developed a formal conceptual framework – environmental deflection (Kochmanski et al. 2017). This concept, which refers to environment-mediated shifts in the aging epigenome, was tested in each part of this dissertation. In the first chapter, we hypothesized that early-life exposure to the

endocrine-disrupting chemical BPA would result in altered epigenetic aging in a mouse model, as measured via longitudinal DNA methylation levels across multiple mouse tissues. Secondarily, it was hypothesized that the effects of BPA on murine epigenetic aging would be mitigated by increased physical activity and exacerbated by co-exposure to WHFD. In the fifth chapter, utilizing samples from a children's cohort, it was hypothesized that physical activity and diet would also modify rates of epigenetic aging in a human population, and that long-term changes in age-related methylation would be associated with obesity status. Human results were used in an attempt to improve the clinical significance of our animal model data.

While the concept of environmental deflection cut through all aspects of this dissertation, there were also several experimental questions unique to each chapter. For example, in chapter 1, we compared the aging epigenome between two tissues – tail and blood – testing for tissue-specific differences in the effects of perinatal exposures. In chapter 2, we examined epigenome-wide 5-mC and 5-hmC levels based on BPA exposure, testing whether exposure modified establishment and long-term regulation of multiple epigenetic marks. Finally, in chapter 3, we included a disease outcome of interest – obesity. Recent research indicates that obesity is associated with cross-sectional measures of the epigenome (Almén et al. 2014; Wahl et al. 2016), but little has done to test whether obesity modifies rates of epigenetic aging during childhood. In the third chapter, matched neonatal bloodspots and blood draw samples were used to test whether obesity was associated with changes in the aging epigenome during the early phases of life. Despite these chapter-specific questions, all of the additional experiments fed into a single goal – to determine the contribution of epigenetic aging to the DOHaD paradigm.

## 6.2 Summary of Dissertation Findings

Contrary to our initial hypothesis, we did not find any significant effects of BPA exposure on age-related methylation at target genes in mice. These results suggest that BPA may not deflect epigenetic aging in mice. Despite the negative findings for BPA, we demonstrated significant effects of WHFD on age-related methylation at target genes related to growth and development in mouse tail and blood tissues. These data support the environmental deflection paradigm, showing that perinatal exposure to an altered diet can alter epigenetic aging across multiple murine tissues.

On a genome-wide scale, we found some evidence for environmental deflection of 5-mC levels in mouse blood by BPA exposure, but no evidence for BPA-induced deflection of 5-hmC. These inconsistent results may be the byproduct of differences in data structure and analysis methods for 5-hmC and 5-mC, but they could also reflect differences in the effects of environmental factors on these separate epigenetic marks. Despite the unclear environmental epigenome-wide deflection results, we did identify twelve BPA-related DHMRs annotated to murine imprinted genes. While this result was not predicted, it fits with previous data showing that developmental BPA exposure can alter the epigenome (Anderson et al. 2012; Susiarjo et al. 2013). Providing support for the functional relevance of these 5-hmC findings, we showed BPA-related gene expression across the life-course at the imprinted *Gnas* locus. The exact mechanism of action for BPA's effect on 5-hmC remains unclear, but we hypothesize that it may be a byproduct of oxidative stress induction by BPA, as has been shown in previous research (Gassman 2017). In addition to the effects of BPA exposure, we also identified a region upstream of the *Nfic* gene that showed simultaneous age-related decreases in 5-mC and 5-hmC levels. Following up on these results, we showed that *Nfic* expression significantly decreased

with age, suggesting that epigenetic aging may have functional effects. Further investigation into the biological outcomes of epigenetic aging will require additional measurements of longitudinal gene expression.

In humans, we found some evidence for environmental deflection of age-related methylation by physical activity-related energy expenditure, but no environmental deflection by healthy eating index, a measure of diet quality. This latter result was unexpected given the clear effects of WHFD on age-related methylation in the mouse exposure study. This inconsistency between species could reflect difficulties in accurately measuring human diet, differences in follow-up time-scale used for the two species, or the fact that humans have a number of uncharacterized environmental factors that were not considered in our analyses. Examining the mouse and human results as a whole, the target genes analyzed in both mice and humans – *IGF2/Igf2*, *H19*, *ESR1/Esr1*, and LINE-1 did not display any consistent, cross-species patterns of environmental deflection by environmental factors. This lack of consistency may be a byproduct of biological differences in humans and mice, species that show clear divergences in both genetic sequence and regulatory control (Yue et al. 2014). However, interpretation of our human findings is also limited by a small sample size; a larger cohort may show effects of environment on epigenetic aging that better correspond to the mouse data. Despite these inter-species inconsistencies, we did show evidence for environmental deflection by environmental factors in both species, suggesting that this is a shared epigenetic phenomenon in multiple mammal species.

While the mouse exposure study results differed from our human cohort, longitudinal mouse model studies still provide a number of experimental benefits for investigating the aging epigenome. For one, mice advance to adulthood at a rapid pace, reaching full maturation at

approximately postnatal day 60 (Brust et al. 2015); this allows for a relatively fast examination of the entire life-course. Second, in addition to their short lifespan, mice also have closed environments with controlled diets and chemical exposures. Third, our mouse colony is a genetically invariant in-bred strain, which eliminates genetic heterogeneity. Combines, these benefits remove much of the variability and confounding present in human cohort studies, allowing for longitudinal experimental designs that examine the effects of an isolated exposure early in life. This would be difficult, if not impossible, to achieve in human cohorts, even using large samples sizes and sophisticated statistical models.

## 6.3 Significance of Findings

Despite multiple public health initiatives aimed at improving metabolic health in the U.S., obesity rates have continued to climb over the past few decades, reaching 39.8% in 2015-2016 (Hales et al. 2017). Of particular concern, obesity is associated with a number of chronic diseases, including heart disease, hypertension, some cancers, and type 2 diabetes (Dixon 2010). Based on these negative health effects, the estimated annual medical cost of obesity in the U.S. is $149.4 billion in 2014 U.S. dollars (Kim and Basu 2016). Previous research has shown that the best predictors of adult obesity are obesity during childhood or a family history of obesity (Loos and Janssens 2017), results that seem to suggest a critical role for genetics in determining obesity status. However, reviews of this subject have shown that BMI-associated genetic variants only explain 0.66-2.70% of BMI variation , concluding that the available genetic information does not accurately predict risk of obesity (Loos and Janssens 2017). Genetics-based models fail to capture the essential role of the environment – including diet, behavior, and chemical exposures – in shaping obesity risk. As such, biomarkers of the developmental environment, including the

neonatal epigenome, have the potential to provide important information about chronic disease risk through adulthood.

In the last two decades, Bisphenol A has been the subject of a vast amount of research, as well as significant public concern. Exposure to BPA is near ubiquitous in the U.S. population (Calafat et al. 2008), and it is found in a number of consumer goods, including plastic bottles, canned food liners, and some paper products (Cooper et al. 2011). Worries about the safety of BPA are largely based on evidence indicating that it is an endocrine disrupting chemical, meaning BPA can interfere with normal hormone synthesis, metabolism, or function (Diamanti-Kandarakis et al. 2009). Specifically, research has shown that BPA is an estrogen-mimicking chemical that can activate growth-related transcription factors and bind to nuclear receptors involved in cell growth/maturation (Krüger et al. 2008; Sui et al. 2012). In addition to its activity as an EDC, previous work has reported BPA-induced oxidative stress (Gassman 2017), as well as associations between BPA exposure and metabolic disorders (Alonso-Magdalena et al. 2015; Carwile and Michels 2011; Ko et al. 2014). However, as a result of contradictory results showing sex-specific links between BPA exposure and a lean phenotype in mice (Anderson et al. 2013; van Esterik et al. 2014), the exact human health effects of BPA exposure remain controversial. In an effort to better determine the mechanism of action for BPA, recent studies have investigated the epigenetic effects of BPA exposure, showing that developmental BPA exposure can alter global, genome-wide, and gene promoter-specific methylation in mouse models (Anderson et al. 2012; Singh and Li 2012; Susiarjo et al. 2013). However, these studies failed to distinguish the effects of BPA exposure on 5-mC and 5-hmC, separate epigenetic marks that can have opposing associations with gene transcription (Hahn et al. 2014; Wu et al. 2011). Here, we followed up on previous studies, showing that genome-wide 5-hmC was altered by BPA exposure, with specific

effects taking place at a number of imprinted genes. Given their tight regulation during development and involvement in growth-related biological pathways (Bartolomei and Ferguson-Smith 2011), modified regulation of imprinted genes has the potential to adversely impact long-term health. As such, our results showing longitudinal BPA-related differential hydroxymethylation at imprinted genes may represent a epigenetic mechanism by which BPA impacts health throughout the life-course.

Typical toxicology studies examine the effects of a single chemical exposure at multiple doses in an animal model. While these types of studies are useful for identifying specific functional outcomes of exposure, they do not consider whether diet and/or behavioral factors modify the effects of exposure. Normal human environments are a mélange of behaviors, diet, and chemical exposures, so examining the effect of an isolated chemical exposure has only limited applicability to the human condition. Here, in an effort to determine how chemical exposures interact with other environmental variables, we integrated changes in diet quality and physical activity into our longitudinal models. This is particularly important in the field of toxicoepigenetics since previous studies have demonstrated significant associations between the epigenome and developmental high-fat diet or physical activity (Dudley et al. 2011; Laker et al. 2014; Marco et al. 2013; Xu et al. 2017). Results from this dissertation showed that diet and/or physical activity modified rates of age-related methylation at specific genes related growth and development, but failed to show an interaction between diet/physical activity and BPA exposure. In addition, the effects of WHFD were greater than BPA in all measures of target gene DNA methylation in our mouse model, suggesting that developmental diet may have a larger effect on the methylome than perinatal BPA exposure. These data suggest that the epigenetic effects of WHFD and BPA are separate phenomena, and may work through separate biological pathways.

However, it is also possible that the effects of BPA were simply washed out by WHFD in the combined exposure group, and that these two exposures could still interact with one another in a "two-hit" exposure design. That is, early life exposure to BPA could set the epigenome in a poised state, making it more vulnerable to later-life environmental challenges, including WHFD. This paradigm of epigenetic dormancy is supported by recent research (Chamorro-Garcia et al. 2017), suggesting that future studies should focus on dietary and chemical exposures that are staggered throughout life, not necessarily simultaneous during development.

## 6.4 Strengths and Limitations

This dissertation has a number of strengths that set it apart from traditional toxicology research. First, it utilizes the toxicoepigenetics framework, examining the effects of environmental exposures on epigenetic marks, a biological mechanism thought to play an important role in the developmental origins of disease. Second, we integrated data from modern sequencing technologies, allowing for a wide examination of the effects of environmental factors on the epigenome. Third, from the dissertation's inception, we planned to include both mouse and human data in an effort to increase translatability of results. To ensure comparability of data across species, we used the same data collection and analysis methods for mouse and human DNA methylation results.

Older toxicoepigenetics studies followed a simple, two-step experimental design: 1. maternal exposure to toxicant; 2. cross-sectional measure of offspring epigenome at sacrifice. This study design is effective at identifying dichotomous effects of exposure on the epigenome compared to control, but fails to consider how exposure alters long-term regulation of the genome. Eschewing the typical cross-sectional approach used in previous toxicoepigenetics studies, we used longitudinal data to examine the effects of developmental dietary exposures on

the aging epigenome. As a result, this dissertation aims to expand on a growing question in the field: can early-life toxicant exposures alter rates of epigenetic aging?

Although very similar statistical methods were applied to both mouse and human data in this dissertation, several differences in study design and scope between the animal and human projects make the results difficult to compare between species. First, the human data was only collected during childhood, meaning measures of age-related methylation from our human cohort only represented the early phases of life. In contrast, our mouse studies followed the animals throughout life – PND21 to 10 months of age – thereby capturing the early phases of adulthood when chronic disease is expected to develop. Second, the environment of the recruited human cohort was not controlled, meaning background exposures to various environmental factors may be confounding the human methylation data. In contrast, the murine environment was carefully controlled, with dietary exposures representing the only difference between groups of mice. This allows for a reduction in background noise from environmental factors, and may explain the increased significance found in our mouse data. Third, the mice used in this study come from an in-bred, genetically invariant colony, while the recruited humans come from a heterogeneous population. This means that the mouse data, while less variable, may not be representative of a real-world population. As such, the mouse experiments should be repeated in different strains of mice to determine whether exposure effects are specific to our mouse colony.

Sample sizes were limited in both the mouse and human portions of this dissertation. For the mouse exposure study, group sizes were selected based on power calculations performed for previous longitudinal mouse studies performed in the Dolinoy Lab. Nevertheless, larger group sizes would have improved analyses, particularly the environmental deflection interaction terms in linear mixed models. Due to increased environmental variability and population heterogeneity,

small sample size is an even greater concern in the human cohort. Fitting with this idea, interaction term fidelity broke down in the smallest batches of childhood human pyrosequencing data. Increasing the sample size of recruited human cohorts would improve statistical modeling of environmental deflection.

Given how recently epigenetic aging has emerged as a topic of research interest, precise differences in how aging alters the epigenome in mice and humans remain unclear. Despite similarities in the underlying mechanisms of aging, research shows that mice and humans have marked differences in their metabolic stability throughout life (Demetrius 2006). Metabolic stability, which refers to the ability of an organism's metabolic network to maintain normal redox balances in response to changes in enzymatic processes, is essential for maintaining homeostasis, thereby slowing the aging process. Mice have lower metabolic stability than humans, and are therefore expected to show decreased ability to offset the effects of aging (Demetrius 2006). As such, it is also possible that both epigenetic aging and environmental deflection are distinct in mice and humans. Additional cross-species comparisons are needed to test this idea.

## 6.5 Future Directions

This dissertation attempted to integrate data from a mouse exposure study and a human cohort to investigate the contribution of toxicant-mediated environmental deflection to the obese phenotype. Unfortunately, while we found a number of significant results, interpretation of the data was limited by a number of experimental limitations. As a result, we did not definitively determine whether environmental deflection is a mechanism underlying chronic disease development. Despite this, the available data are suggestive in many ways, and pave the way for additional studies.

While it is difficult to directly compare the human and mouse data generated in this dissertation project, the available analyses suggest that the environment plays a role in shaping the aging epigenome in both species. Following up on these results, future studies should investigate whether specific environmental exposures – i.e. endocrine disrupting chemicals, pesticides, metals – have consistent effects on epigenetic aging in both humans and animal models. Studies should also examine the effects of exposure on long-term phenotype. This could be achieved through longitudinal measurements of body composition, RT-qPCR for gene expression, or physical analysis of additional tissues for pathological responses to exposure. Only with this type of combined approach will it be possible to determine the phenotypic consequences of environmental deflection.

In this dissertation, we showed that BPA exposure modified establishment of 5-hmC at a number of imprinted genes in a mouse blood. As a result of epigenetic control mechanisms, imprinted genes exhibit monoallelic, parent-of-origin-specific gene expression during development (Bartolomei and Ferguson-Smith 2011; Das et al. 2009). Research shows that imprinting control regions (ICRs) are not demethylated during post-fertilization reprogramming (Arnaud 2010; Kelsey and Feil 2012; Kim et al. 2017; Pidsley et al. 2012; Smallwood and Kelsey 2012), making imprinted genes important potential targets of developmental exposures (Haycock and Ramsay 2009; Heijmans et al. 2008; Nye et al. 2015; Susiarjo et al. 2013). While a number of studies have examined 5-mC levels at murine imprinted genes, this is the first report of differential 5-hmC levels at imprinted genes in mouse blood. Given the novelty of this finding, this result should be tested in additional murine tissues, as well as human cohorts.

For the human cohort, we isolated DNA from neonatal bloodspots and used DNA methylation levels from these samples as a baseline epigenome. The goal of this project was to

determine whether or not the measured neonatal DNA methylation was associated with obesity. However, the sample size of obese children from our cohort was quite small, making this relationship difficult to model. Additionally, we only measured DNA methylation at a few target genes related to growth and development. Moving forward, cohort size should be increased and data should be expanded to an epigenome-wide scale using sequencing technologies. In this way, it would be possible to determine whether the obesity phenotype is associated with neonatal DNA methylation. As an ultimate goal, future studies should examine whether it is possible to predict obesity risk from epigenetic biomarkers measured at birth. This would be a valuable clinical tool for identifying at-risk individuals prior to disease development.

## 6.6 Conclusion

In this dissertation, we showed that diet and physical activity have the potential to alter rates of age-related methylation throughout the life-course. These data support the environmental deflection paradigm that was described during the course of this project, showing that the environment can alter not only the cross-sectional measures of the epigenome, but also epigenetic aging. Separately, we showed that both age and BPA exposure can alter murine DNA hydroxymethylation, a secondary regulatory mark in the epigenome. The findings from this dissertation are relevant to the growing field of toxicoepigenetics, and help shed light on the mechanisms underpinning the developmental origins of health and disease hypothesis (**Figure 6-1**). In an attempt to increase the clinical relevance of the mouse results, environmental deflection by physical activity and diet quality was also tested in a human cohort. While exact directionality of results varied by organism, our data support the idea that the aging epigenome is sensitive to environmental cues. These results emphasize the importance of longitudinal study design in toxicoepigenetics research, and suggest that environmental factors play a key role in the

developmental origins of adult disease. This idea has important implications for public health policies related to chronic disease prevention, including chemical regulations, dietary suggestions, and exercise recommendations.

## 6.7 Figures and Tables

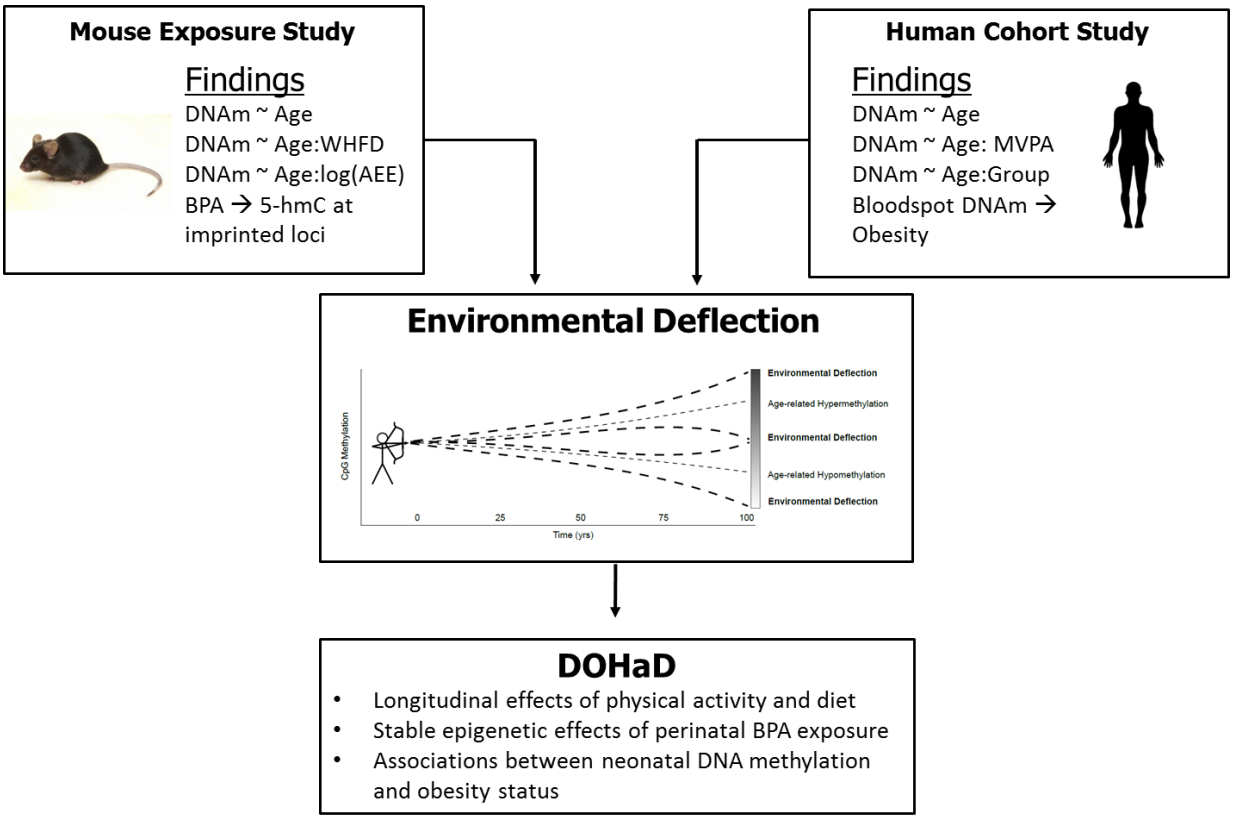


**Figure 6-1: Synthesis of dissertation findings as they relate to the DOHaD hypothesis.** Age-related methylation was documented in both the mouse exposure study and the human cohort study. In mice, Western high-fat diet (WHFD) and activity-related energy expenditure (AEE) altered rates of epigenetic aging. Also in mice, BPA exposure had a long-term effect on 5-hmC levels at imprinted loci. In humans, moderate-to-vigorous physical activity (MVPA) levels altered gene-specific epigenetic aging, Childhood age group also altered rates of age-related methylation at several gene regions, indicating that epigenetic aging is dynamic throughout the life course. Also in humans, gene-specific neonatal bloodspot DNA methylation was associated with obesity likelihood in childhood. Combined, our data support the idea that the aging epigenome is sensitive to environmental cues, and that environmental deflection may play a role in the developmental origins of health and disease.

## 6.8 References


Almén MS, Nilsson EK, Jacobsson JA, Kalnina I, Klovins J, Fredriksson R, et al. 2014. Genome-wide analysis reveals DNA methylation markers that vary with both age and obesity. Gene 548:61–67; doi:10.1016/j.gene.2014.07.009.

Alonso-Magdalena P, Quesada I, Nadal Á. 2015. Prenatal Exposure to BPA and Offspring Outcomes: The Diabesogenic Behavior of BPA. Dose. Response. 13:1559325815590395; doi:10.1177/1559325815590395.

Anderson OS, Nahar MS, Faulk C, Jones TR, Liao C, Kannan K, et al. 2012. Epigenetic responses following maternal dietary exposure to physiologically relevant levels of bisphenol A. Environ. Mol. Mutagen. 53:334–342; doi:10.1002/em.21692.

Anderson OS, Peterson KE, Sanchez BN, Zhang Z, Mancuso P, Dolinoy DC. 2013. Perinatal bisphenol A exposure promotes hyperactivity, lean body composition, and hormonal responses across the murine life course. FASEB J 27:1784–1792; doi:10.1096/fj.12-223545.

Arnaud P. 2010. Genomic imprinting in germ cells: imprints are under control. Reproduction 140:411–423; doi:10.1530/REP-10-0173.

Bartolomei MS, Ferguson-Smith AC. 2011. Mammalian genomic imprinting. Cold Spring Harb. Perspect. Biol. 3; doi:10.1101/cshperspect.a002592.

Bateson P, Barker D, Clutton-Brock T, Deb D, D'Udine B, Foley RA, et al. 2004. Developmental plasticity and human health. Nature 430:419–421; doi:10.1038/nature02725.

Brust V, Schindler PM, Lewejohann L. 2015. Lifetime development of behavioural phenotype in the house mouse (Mus musculus). Front. Zool. 12 Suppl 1:S17; doi:10.1186/1742-9994-12-S1-S17.

Calafat AM, Ye X, Wong LY, Reidy JA, Needham LL. 2008. Exposure of the U.S. population to bisphenol A and 4-tertiary-octylphenol: 2003-2004. Env. Heal. Perspect 116:39–44; doi:10.1289/ehp.10753.

Carwile JL, Michels KB. 2011. Urinary bisphenol A and obesity: NHANES 2003–2006. Environ. Res. 111:825–830; doi:10.1016/j.envres.2011.05.014.

Chamorro-Garcia R, Diaz-Castillo C, Shoucri BM, Käch H, Leavitt R, Shioda T, et al. 2017. Ancestral perinatal obesogen exposure results in a transgenerational thrifty phenotype in mice. Nat. Commun. 8:2012; doi:10.1038/s41467-017-01944-z.

Cooper JE, Kendig EL, Belcher SM. 2011. Assessment of bisphenol A released from reusable plastic, aluminium and stainless steel water bottles. Chemosphere 85:943–7; doi:10.1016/j.chemosphere.2011.06.060.

Das R, Hampton DD, Jirtle RL. 2009. Imprinting evolution and human health. Mamm. Genome 20:563–572; doi:10.1007/s00335-009-9229-y.

Demetrius L. 2006. Aging in Mouse and Human Systems: A Comparative Study. Ann. N. Y. Acad. Sci. 1067:66–82; doi:10.1196/annals.1354.010.

Diamanti-Kandarakis E, Bourguignon J-P, Giudice LC, Hauser R, Prins GS, Soto AM, et al. 2009. Endocrine-disrupting chemicals: an Endocrine Society scientific statement. Endocr. Rev. 30:293–342; doi:10.1210/er.2009-0002.

Dixon JB. 2010. The effect of obesity on health outcomes. Mol. Cell. Endocrinol. 316:104–108; doi:10.1016/j.mce.2009.07.008.

Dudley KJ, Sloboda DM, Connor KL, Beltrand J, Vickers MH. 2011. Offspring of Mothers Fed a High Fat Diet Display Hepatic Cell Cycle Inhibition and Associated Changes in Gene Expression and DNA Methylation. A. Wutz, ed PLoS One 6:e21662; doi:10.1371/journal.pone.0021662.

Faulk C, Liu K, Barks A, Goodrich JM, Dolinoy DC. 2014. Longitudinal epigenetic drift in mice perinatally exposed to lead. Epigenetics 9:934–941; doi:10.4161/epi.29024.

Gassman NR. 2017. Induction of oxidative stress by bisphenol A and its pleiotropic effects. Environ. Mol. Mutagen. 58:60–71; doi:10.1002/em.22072.

Gilbert KM, Blossom SJ, Erickson SW, Reisfeld B, Zurlinden TJ, Broadfoot B, et al. 2016. Chronic exposure to water pollutant trichloroethylene increased epigenetic drift in CD4(+) T cells. Epigenomics 8:633–649; doi:10.2217/epi-2015-0018.

Hahn MA, Szabo PE, Pfeifer GP. 2014. 5-Hydroxymethylcytosine: a stable or transient DNA modification? Genomics 104:314–323; doi:10.1016/j.ygeno.2014.08.015.

Hales CM, Carroll MD, Fryar CD, Ogden CL. 2017. Prevalence of Obesity Among Adults and Youth: United States, 2015–2016 Key findings Data from the National Health and Nutrition Examination Survey. NCHS Data Brief.

Haycock PC, Ramsay M. 2009. Exposure of Mouse Embryos to Ethanol During Preimplantation Development: Effect on DNA Methylation in the H19 Imprinting Control Region1. Biol. Reprod. 81:618–627; doi:10.1095/biolreprod.108.074682.

Heijmans BT, Tobi EW, Stein AD, Putter H, Blauw GJ, Susser ES, et al. 2008. Persistent epigenetic differences associated with prenatal exposure to famine in humans. Proc. Natl. Acad. Sci. U. S. A. 105:17046–9; doi:10.1073/pnas.0806560105.

Heindel JJ, Balbus J, Birnbaum L, Brune-Drisse MN, Grandjean P, Gray K, et al. 2015. Developmental Origins of Health and Disease: Integrating Environmental Influences. Endocrinology 156:3416–3421; doi:10.1210/EN.2015-1394.

Horvath S, Erhart W, Brosch M, Ammerpohl O, von Schönfels W, Ahrens M, et al. 2014. Obesity accelerates epigenetic aging of human liver. Proc. Natl. Acad. Sci. U. S. A. 111:15538–43; doi:10.1073/pnas.1412759111.

Kelsey G, Feil R. 2012. New insights into establishment and maintenance of DNA methylation imprints in mammals. Philos. Trans. R. Soc. B Biol. Sci. 368:20110336–20110336; doi:10.1098/rstb.2011.0336.

Kim DD, Basu A. 2016. Estimating the Medical Care Costs of Obesity in the United States: Systematic Review, Meta-Analysis, and Empirical Analysis. Value Heal. 19:602–613; doi:10.1016/j.jval.2016.02.008.

Kim J, He H, Kim H. 2017. Inversion of the imprinting control region of the Peg3 domain. Y. Yu, ed PLoS One 12:e0181591; doi:10.1371/journal.pone.0181591.

Ko A, Hwang M-S, Park J-H, Kang H-S, Lee H-S, Hong J-H. 2014. Association between Urinary Bisphenol A and Waist Circumference in Korean Adults. Toxicol. Res. 30:39–44; doi:10.5487/TR.2014.30.1.039.

Kochmanski J, Marchlewicz EH, Savidge M, Montrose L, Faulk C, Dolinoy DC. 2016. Longitudinal effects of developmental bisphenol A and variable diet exposures on epigenetic drift in mice. Reprod. Toxicol.; doi:10.1016/j.reprotox.2016.07.021.

Kochmanski J, Montrose L, Goodrich JM, Dolinoy DC. 2017. Environmental Deflection: The Impact of Toxicant Exposures on the Aging Epigenome. Toxicol. Sci. 156:kfx005; doi:10.1093/toxsci/kfx005.

Krüger T, Long M, Bonefeld-Jørgensen EC. 2008. Plastic components affect the activation of the aryl hydrocarbon and the androgen receptor. Toxicology 246:112–123; doi:10.1016/j.tox.2007.12.028.

Laker RC, Lillard TS, Okutsu M, Zhang M, Hoehn KL, Connelly JJ, et al. 2014. Exercise prevents maternal high-fat diet-induced hypermethylation of the Pgc-1α gene and age-dependent metabolic dysfunction in the offspring. Diabetes 63:1605–1611; doi:10.2337/db13-1614.

Loos RJF, Janssens ACJW. 2017. Predicting Polygenic Obesity Using Genetic Information. Cell Metab. 25:535–543; doi:10.1016/j.cmet.2017.02.013.

Marco A, Kisliouk T, Weller A, Meiri N. 2013. High fat diet induces hypermethylation of the hypothalamic Pomc promoter and obesity in post-weaning rats. Psychoneuroendocrinology 38:2844–2853; doi:10.1016/j.psyneuen.2013.07.011.

Nye MD, Hoyo C, Murphy SK. 2015. In vitro lead exposure changes DNA methylation and expression of IGF2 and PEG1/MEST. Toxicol. In Vitro 29:544–50;

doi:10.1016/j.tiv.2015.01.002.

Pidsley R, Fernandes C, Viana J, Paya-Cano JL, Liu L, Smith RG, et al. 2012. DNA methylation at the Igf2/H19 imprinting control region is associated with cerebellum mass in outbred mice. Mol. Brain 5:42; doi:10.1186/1756-6606-5-42.

Shah S, McRae AF, Marioni RE, Harris SE, Gibson J, Henders AK, et al. 2014. Genetic and environmental exposures constrain epigenetic drift over the human life course. Genome Res 24:1725–1733; doi:10.1101/gr.176933.114.

Singh S, Li SS. 2012. Epigenetic effects of environmental chemicals bisphenol a and phthalates. Int J Mol Sci 13:10143–10153; doi:10.3390/ijms130810143.

Smallwood SA, Kelsey G. 2012. De novo DNA methylation: a germ cell perspective. Trends Genet 28:33–42; doi:10.1016/j.tig.2011.09.004.

Sui Y, Ai N, Park SH, Rios-Pilier J, Perkins JT, Welsh WJ, et al. 2012. Bisphenol A and its analogues activate human pregnane X receptor. Env. Heal. Perspect 120:399–405; doi:10.1289/ehp.1104426.

Susiarjo M, Sasson I, Mesaros C, Bartolomei MS. 2013. Bisphenol A Exposure Disrupts Genomic Imprinting in the Mouse. G. Kelsey, ed PLoS Genet. 9:e1003401; doi:10.1371/journal.pgen.1003401.

van Dongen J, Nivard MG, Willemsen G, Hottenga JJ, Helmer Q, Dolan C V, et al. 2016. Genetic and environmental influences interact with age and sex in shaping the human methylome. Nat Commun 7:11115; doi:10.1038/ncomms11115.

van Esterik JCJ, Dollé MET, Lamoree MH, van Leeuwen SPJ, Hamers T, Legler J, et al. 2014. Programming of metabolic effects in C57BL/6JxFVB mice by exposure to bisphenol A during gestation and lactation. Toxicology 321:40–52; doi:10.1016/j.tox.2014.04.001.

Wahl S, Drong A, Lehne B, Loh M, Scott WR, Kunze S, et al. 2016. Epigenome-wide association study of body mass index, and the adverse outcomes of adiposity. Nature 541:81–86; doi:10.1038/nature20784.

Wu H, D'Alessio AC, Ito S, Wang Z, Cui K, Zhao K, et al. 2011. Genome-wide analysis of 5-hydroxymethylcytosine distribution reveals its dual function in transcriptional regulation in mouse embryonic stem cells. Genes Dev 25:679–684; doi:10.1101/gad.2036011.

Xu WH, Wu H, Xia WL, Lan H, Wang Y, Zhang Y, et al. 2017. Physical exercise before pregnancy helps the development of mouse embryos produced in vitro. Mitochondrion 34:36–42; doi:10.1016/j.mito.2016.12.004.

Yoon A, Tammen SA, Park S, Han SN, Choi S-W. 2017. Genome-wide hepatic DNA methylation changes in high-fat diet-induced obese mice. Nutr. Res. Pract. 11:105–113;

doi:10.4162/nrp.2017.11.2.105.

Yue F, Cheng Y, Breschi A, Vierstra J, Wu W, Ryba T, et al. 2014. A comparative encyclopedia of DNA elements in the mouse genome. Nature 515:355–64; doi:10.1038/nature13992.

Zannas AS, Arloth J, Carrillo-Roa T, Iurato S, Röh S, Ressler KJ, et al. 2015. Lifetime stress accelerates epigenetic aging in an urban, African American cohort: relevance of glucocorticoid signaling. Genome Biol 16:266; doi:10.1186/s13059-015-0828-5.